frontiers

RESEARCH TOPICS

THERAPEUTIC TARGETING OF CIRCULATING TUMOR CELLS

Hosted by
Michael R. King

frontiers in ONCOLOGY

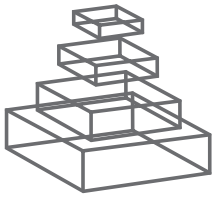

frontiers

Cover image provided by Ibbl sarl, Lausanne CH

ISSN 1664-8714
ISBN 978-2-88919-089-8
DOI 10.3389/978-2-88919-089-8

ABOUT FRONTIERS

Frontiers is more than just an open-access publisher of scholarly articles: it is a pioneering approach to the world of academia, radically improving the way scholarly research is managed. The grand vision of Frontiers is a world where all people have an equal opportunity to seek, share and generate knowledge. Frontiers provides immediate and permanent online open access to all its publications, but this alone is not enough to realize our grand goals.

FRONTIERS JOURNAL SERIES

The Frontiers Journal Series is a multi-tier and interdisciplinary set of open-access, online journals, promising a paradigm shift from the current review, selection and dissemination processes in academic publishing.
All Frontiers journals are driven by researchers for researchers; therefore, they constitute a service to the scholarly community. At the same time, the Frontiers Journal Series operates on a revolutionary invention, the tiered publishing system, initially addressing specific communities of scholars, and gradually climbing up to broader public understanding, thus serving the interests of the lay society, too.

DEDICATION TO QUALITY

Each Frontiers article is a landmark of the highest quality, thanks to genuinely collaborative interactions between authors and review editors, who include some of the world's best academicians. Research must be certified by peers before entering a stream of knowledge that may eventually reach the public - and shape society; therefore, Frontiers only applies the most rigorous and unbiased reviews.
Frontiers revolutionizes research publishing by freely delivering the most outstanding research, evaluated with no bias from both the academic and social point of view.
By applying the most advanced information technologies, Frontiers is catapulting scholarly publishing into a new generation.

WHAT ARE FRONTIERS RESEARCH TOPICS?

Frontiers Research Topics are very popular trademarks of the Frontiers Journals Series: they are collections of at least ten articles, all centered on a particular subject. With their unique mix of varied contributions from Original Research to Review Articles, Frontiers Research Topics unify the most influential researchers, the latest key findings and historical advances in a hot research area!
Find out more on how to host your own Frontiers Research Topic or contribute to one as an author by contacting the Frontiers Editorial Office: researchtopics@frontiersin.org

THERAPEUTIC TARGETING OF CIRCULATING TUMOR CELLS

Hosted By:
Michael R. King, Cornell University, USA

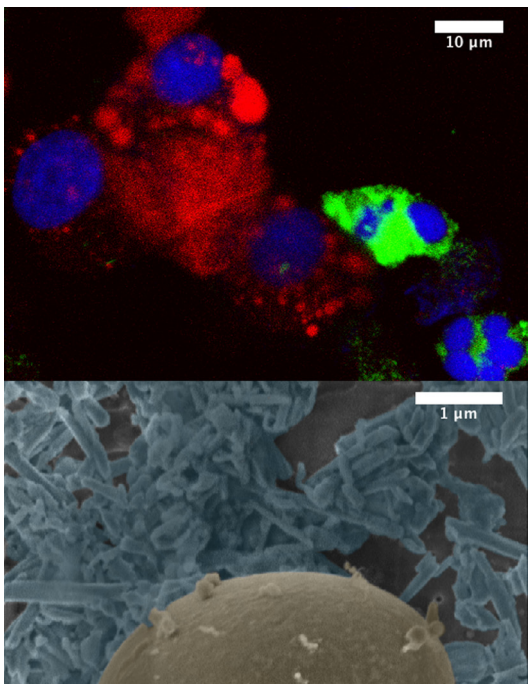

Image by Andrew D. Hughes

There has been increased interest in circulating tumor cells (CTC), as a diagnostic readout of disease progression, and a tool for personalized medicine. The next generation of therapy for metastatic cancer may well involve neutralizing CTC as a means to prevent metastasis. In this topic we focus on recent research exploring this concept.

Table of Contents

frontiers in ONCOLOGY

EDITORIAL
published: 29 November 2012
doi: 10.3389/fonc.2012.00184

Rolling in the deep: therapeutic targeting of circulating tumor cells

Michael R. King*

Department of Biomedical Engineering, Cornell University, Ithaca, NY, USA
**Correspondence: mrk93@cornell.edu*

Edited by:
Yisong Wang, National Institute of Health, USA

Reviewed by:
Yisong Wang, National Institute of Health, USA

Circulating tumor cells (CTCs). What exactly are these cells that we liken to "finding a needle in a haystack?" CTCs originate from a primary tumor, are often but not always of epithelial phenotype, and are dispersed in the peripheral circulation among millions of (somewhat smaller) leukocytes per milliliter and billions of red blood cells. They can and do interact with the proteins and formed elements of blood. They are the subject of rapidly increasing interest in research and clinical diagnostics. But are they the same cells that initiate metastases? Recent improvements to animal models of bloodborne metastasis have begun to elucidate the physical determinants of tissue tropism in metastasis. One thing for certain is that CTC count is now recognized as a strong predictor of patient survival in many cancers, such as those originating from breast and prostate. This Special Topic of Frontiers of Oncology attempts to address some of the important questions surrounding CTCs: what are these cells, how may we study and target them therapeutically, and what secrets they may hold in controlling and combating cancer metastasis.

Eleven of the 15 papers in this Special Topic come from investigators of the collaborative network of Physical Science-Oncology Centers established in 2009 by the US National Cancer Institute. These 12 centers across the United States bring together biologists, clinicians, physical scientists, and engineers to develop innovative new ways to understand and fight cancer. The specific centers represented here include: the Cornell University Center on the Microenvironment and Metastasis; the Center for Transport Oncophysics of the Methodist Hospital Research Institute; the Moffitt Cancer Center Physical Science-Oncology Center; the 4DB Center of Scripps Research Institute; and the Dana-Farber Cancer Institute Physical Science-Oncology Center.

The papers in this Special Topic can be categorized into one of three parts. In the first part, therapies directed toward CTCs in the bloodstream, and the responses of CTCs to cancer therapies, are considered. This subject is broadly reviewed by Greene et al. (2012) and then reviewed in the context of cancer stem cells by Faltas (2012). Li and King (2012) discuss cell adhesion receptors and how they can be targeted to neutralize CTCs. Liesveld (2012) discusses the targeting of myelogenous leukemia stem cells in the bloodstream, and Paolo Decuzzi and coworkers present data on the adhesion response of a model CTC cell line to curcumin treatment (Palange et al., 2012).

The second group of papers focuses on the basic science of CTCs, and how we might expect them to behave while in the circulation. Geng et al. (2012) show that the breast cancer biomarker MUC1 can act as a simultaneous adhesion counter-receptor for both endothelial E-selectin and ICAM-1, and they present a new model for the metastatic adhesion cascade paradigm. Burdick et al. (2012) consider not only the adhesion characteristics of CTCs to E-selectin, but propose that surface ligand expression may signal phenotypic changes of cancer stem cells. Rejniak (2012) presents a computational model that can be used to simulate the shear-induced deformation of CTCs in the bloodstream. In a pair of related papers, Tormoen et al. (2012b) pose the question of whether CTCs play a role in coagulation and thrombosis in the bloodstream, and then Lee et al. (2012) describe their theoretical model of procoagulant CTCs under flow.

The third and final part of this special issue is focused on the characterization of patient CTCs, including new methods dedicated to this goal. Another contribution from Tormoen et al. (2012a) presents new coagulation factor probes for the identification of procoagulant CTCs. Diamond et al. (2012) describe their characterization of prostate cancer CTCs isolated from patient blood. Garcia-Villa et al. (2012) measured the γ-H2AX levels in CTCs obtained from patients undergoing chemotherapy. Finally, a pair of papers from McCarty and coworkers describes the application of precise image analysis methods to measure the density and volume of patient CTCs in ovarian (Phillips et al., 2012b) and breast cancer (Phillips et al., 2012a), including a comparison with properties measured for normal blood cells.

The images featured on page 2 of this E-book, provided by Andrew Hughes of Cornell University, show viable CTCs isolated from a pancreatic cancer patient (upper image). The epithelial cancer cells stain positive for cytokeratin (red), and negative for the leukocyte marker CD45 (green), and show characteristically large nuclei stained in blue. The lower scanning electron micrograph shows a human leukocyte resting on a layer of halloysite nanotubes; these cells are unable to spread onto halloysite which enables efficient isolation of patient CTCs. This research is described in the lead paper by Greene et al. (2012).

REFERENCES

Burdick, M. M., Henson, K. A., Delgadillo, L. F., Choi, Y. E., Goetz, D. J., Tees, D. F. J., et al. (2012). Expression of E-selectin ligands on circulating tumor cells: cross-regulation with cancer stem cell regulatory pathways? *Front. Oncol.* 2:103. doi: 10.3389/fonc.2012.00103

Diamond, E., Lee, G. Y., Akhtar, N. H., Kirby, B. J., Giannakakou, P., Tagawa, S. T., et al. (2012). Isolation and characterization of circulating tumor cells in prostate cancer. *Front. Oncol.* 2:131. doi: 10.3389/fonc.2012.00131

Faltas, B. (2012). Cornering metastases: therapeutic targeting of circulating tumor cells and stem cells. *Front. Oncol.* 2:68. doi: 10.3389/fonc.2012.00068

Garcia-Villa, A., Balasubramanian, P., Miller, B. L., Lustberg, M. B., Ramaswamy, B., and Chalmers, J. J. (2012). Assessment of γ-H2AX levels in circulating tumor cells from patients receiving chemotherapy. *Front. Oncol.* 2:128. doi: 10.3389/fonc.2012.00128

Geng, Y., Yeh, K., Takatani, T., and King, M. R. (2012). Three to tango: MUC1 as a ligand for both E-selectin and ICAM-1 in the breast cancer metastatic cascade. *Front. Oncol.* 2:76. doi: 10.3389/fonc.2012.00076

Greene, B. T., Hughes, A. D., and King, M. R. (2012). Circulating tumor cells: the substrate of personalized medicine? *Front. Oncol.* 2:69. doi: 10.3389/fonc.2012.00069

Lee, A. M., Tormoen, G. W., Kanso, E., McCarty, O. J. T., and Newton, P. K. (2012). Modeling and simulation of procoagulant circulating tumor cells in flow. *Front. Oncol.* 2:108. doi: 10.3389/fonc.2012.00108

Li, J., and King, M. R. (2012). Adhesion receptors as therapeutic targets for circulating tumor cells. *Front. Oncol.* 2:79. doi: 10.3389/fonc.2012.00079

Liesveld, J. (2012). Targeting myelogenous leukemia stem cells: role of the circulation. *Front. Oncol.* 2:86. doi: 10.3389/fonc.2012.00086

Palange, A. L., Di Mascolo, D., Singh, J., De Franceschi, M. S., Carallo, C., Gnasso, A., et al. (2012). Modulating the vascular behavior of metastatic breast cancer cells by curcumin treatment. *Front. Oncol.* 2:161. doi: 10.3389/fonc.2012.00161

Phillips, K. G., Kolatkar, A., Rees, K. J., Rigg, R., Marrinucci, D., Luttgen, M., et al. (2012a). Quantification of cellular volume and sub-cellular density fluctuations: comparison of normal peripheral blood cells and circulating tumor cells identified in a breast cancer patient. *Front. Oncol.* 2:96. doi: 10.3389/fonc.2012.00096

Phillips, K. G., Velasco, C. R., Li, J., Kolatkar, A., Luttgen, M., Bethel, K., et al. (2012b). Optical quantification of cellular mass, volume, and density of circulating tumor cells identified in an ovarian cancer patient. *Front. Oncol.* 2:72. doi: 10.3389/fonc.2012.00072

Rejniak, K. A. (2012). Investigating dynamical deformations of tumor cells in circulation: predictions from a theoretical model. *Front. Oncol.* 2:111. doi: 10.3389/fonc.2012.00111

Tormoen, G. W., Cianchetti, F. A., Bock, P. E., and McCarty, O. J. T. (2012a). Development of coagulation factor probes for the identification of procoagulant circulating tumor cells. *Front. Oncol.* 2:110. doi: 10.3389/fonc.2012.00110

Tormoen, G. W., Haley, K. M., Levine, R. L., and McCarty, O. J. T. (2012b). Do circulating tumor cells play a role in coagulation and thrombosis? *Front. Oncol.* 2:115. doi: 10.3389/fonc.2012.00115

Received: 11 November 2012; accepted: 14 November 2012; published online: 29 November 2012.

*Citation: King MR (2012) Rolling in the deep: therapeutic targeting of circulating tumor cells. Front. Oncol. **2**:184. doi: 10.3389/fonc.2012.00184*

This article was submitted to Frontiers in Cancer Molecular Targets and Therapeutics, a specialty of Frontiers in Oncology.

frontiers in ONCOLOGY

REVIEW ARTICLE
published: 02 July 2012
doi: 10.3389/fonc.2012.00069

Circulating tumor cells: the substrate of personalized medicine?

Bryan T. Greene[1,2]*†, Andrew D. Hughes[3]† and Michael R. King[3]

[1] *BioCytics, Inc., Huntersville, NC, USA*
[2] *Carolina BioOncology Institute, PLLC, Huntersville, NC, USA*
[3] *Department of Biomedical Engineering, Cornell University, Ithaca, NY, USA*

Edited by:
Michael R. King, Cornell University, USA

Reviewed by:
Justin Lathia, Lerner Research Institute, USA
Kuldeepsinh Prabhudattsinh Rana, Consulting, India
Sujata Kumari Bhatia, Harvard University, USA

****Correspondence:***
Bryan T. Greene, BioCytics, Inc., 9801 W. Kincey Avenue, Suite 145, Huntersville, NC 28078, USA.
e-mail: bryan.greene@biocytics.com

†Bryan T. Greene and Andrew D. Hughes have contributed equally to this work.

Circulating tumor cells (CTCs) are believed to be responsible for the development of metastatic disease. Over the last several years there has been a great interest in understanding the biology of CTCs to understand metastasis, as well as for the development of companion diagnostics to predict patient response to anti-cancer targeted therapies. Understanding CTC biology requires innovative technologies for the isolation of these rare cells. Here we review several methods for the detection, capture, and analysis of CTCs and also provide insight on improvements for CTC capture amenable to cellular therapy applications.

Keywords: circulating tumor cells, leukapheresis, leukopak, selectins, EpCAM

INTRODUCTION

At its basic definition, cancer is the uncontrolled growth of cells in the body. Over the past several decades, our understanding of cancer has greatly improved and it is now clear that while the basic definition of cancer holds true, cancer is an extremely complex disease composed of various molecular alterations and phenotypic changes. The vast majority of cancer deaths occur due to metastasis of the primary tumor to distant sites via circulating tumor cells (CTCs) in the circulation. CTCs are extremely rare. Over the past 5–10 years, various methodologies and platforms have been developed to isolate CTCs for further characterization and molecular analyses. The emergence of these technologies have spurred a great interest in CTCs and researchers and clinicians are realizing the importance of CTCs in cancer biology as well as their use in cancer diagnosis and therapy.

While the potential of using CTCs to guide patient treatment remains promising, the rate-limiting step for widespread use of CTCs in the clinic remains the lack of robust and high-throughput technologies for isolation of these rare cells. In fact, in most cases, most CTC isolation platforms isolate a few to several hundred CTCs, rendering the functional characterization of these cells extremely difficult (Maheswaran and Haber, 2010). This review is not intended to be an exhaustive description of all CTC isolation technologies (for further reading, see Hughes and King, 2012), but instead will provide a historical framework for CTC isolation and then focus on current "state of the art" for isolation of viable CTCs and their potential use in cell therapy.

CTC ISOLATION: FINDING A NEEDLE IN A HAYSTACK

CTCs IN THE CLINIC: HISTORICAL PERSPECTIVE

Great interest in the CTC field was ignited by the introduction of the CellSearch system (Allard et al., 2004). The CellSearch system (Veridex, Raritan, NJ, USA) was FDA cleared in January 2004 as a prognostic tool for identifying and counting CTCs in a blood sample to predict progression-free and overall survival in patients with metastatic breast cancer. In 2007 and 2008, the CellSearch system was cleared as an aid for monitoring metastatic colorectal and prostate cancer patients, respectively. The CellSearch system, like many other platforms, relies on the expressed surface ligand epithelial cellular adhesion molecule (EpCAM) and immunomagnetic capture to isolate CTCs. CTCs are subsequently stained and quantified using an antibody against cytokeratins. Contaminating leukocytes are identified using an antibody against CD45. CTCs are defined as cytokeratin positive and CD45 negative.

The CellSearch system made possible, for the first time, the capture of CTCs in a standardized and highly reproducible fashion within a clinical context. Our group was one of the first to offer the CellSearch test and to date we have performed approximately 1,500 CellSearch CTC tests on blood from over 150 metastatic cancer patients. Our data from this aggregate of patients (*unpublished*) is consistent with an earlier study showing that a significant fraction of blood samples tested using the CellSearch system lacked CTCs (Allard et al., 2004). In addition, CTC outputs from the CellSearch system typically have low yield and purity (Allard et al., 2004).

NEXT GENERATION CTC CAPTURE PLATFORMS

Since the introduction of the CellSearch system, several groups have invested significant time and resources in developing newer CTC isolation technologies that overcome the barriers to widespread clinical use associated with the CellSearch system, namely low yield, low purity, and low throughput. These include methodologies that isolate CTCs based on size or other physical properties (Muller et al., 2005; Wulfing et al., 2006; Mohamed et al., 2009; Tan et al., 2009). For example, the MagSweeper uses a slowly rotating magnetic stir bar coated with antibodies against EpCAM to capture CTCs from unfractionated blood samples, thus improving throughput due to the elimination of sample preparation steps (Talasaz et al., 2009). Recent work has used the MagSweeper to enrich CTCs from patient samples, which were then individually evaluated for expression levels of 87 genes using a microfluidic-based qRT-PCR technique. A high degree of expression heterogeneity was observed between CTCs, with generally high expression levels of epithelial-to-mesenchymal transition (EMT)-related genes such as TGFβ1, vimentin, and CXCR4 (Powell et al., 2012). Additionally, comparison of four breast cancer cell lines and the isolated primary CTCs showed particularly disparate expression profiles, suggesting that cancer cell lines are of dubious utility as a model for CTC research.

The CTC-chip and herringbone (HB)-chip use antibody-coated microfluidic devices for capture of $EpCAM^+$ CTCs from unprocessed whole blood (Nagrath et al., 2007; Maheswaran et al., 2008; Stott et al., 2010a). The HB-chip is more amenable to manufacturing for high-throughput applications and CTCs captured on the device are of sufficiently high purity and yield to be interrogated for molecular alterations (Stott et al., 2010b). A recent observation has been the capture of clusters of CTCs, called circulating tumor microemboli (CTM), from several prostate and lung cancer patients using the HB-chip (Stott et al., 2010a). Capture of CTM has also been observed using a slide-based high definition CTC (HD-CTC) imaging platform (Cho et al., 2012). Indeed, in a recent study using the "HD-CTC assay" on samples from 68 patients with metastatic breast, prostate, or pancreatic cancer, clusters of two or more CTCs were identified in 88% of patients (Marrinucci et al., 2012). Interestingly, we have made similar observations from samples processed on the CellSearch system (**Figure 1**). It is unclear what the clinical significance of these CTC clusters is, although a notable hypothesis suggests that these clusters may serve as a potential mechanism to prevent anoikis thereby enhancing metastatic potential (Zhang et al., 2008).

The HD-CTC technique is notable in that CTCs in a sample of blood are enriched only by erythrocyte lysis, and then automated scanning is used to identify CTCs based on fluorescent probes. This is important because the only underlying assumption is that CTCs will not lyse along with erythrocytes in ammonium chloride solution, which is reasonable. Many other CTC isolation techniques rely on specific surface markers, such as EpCAM for positive selection or CD45 for negative selection. It has been shown that EpCAM, while widely expressed across cancer types, is not universally expressed (Went et al., 2004). Thus CTC capture based on surface marker expression induces a bias of unknown consequence. Currently, the HD-CTC technique identifies CTCs based on cytokeratin expression and CD45 absence, which imposes another bias in that cancer cells that undergo EMT may not produce cytokeratin (Marrinucci et al., 2012). However, the platform is amenable to the use of alternate probes that are more universal. A significant challenge remains for identifying a universal biomarker for CTCs.

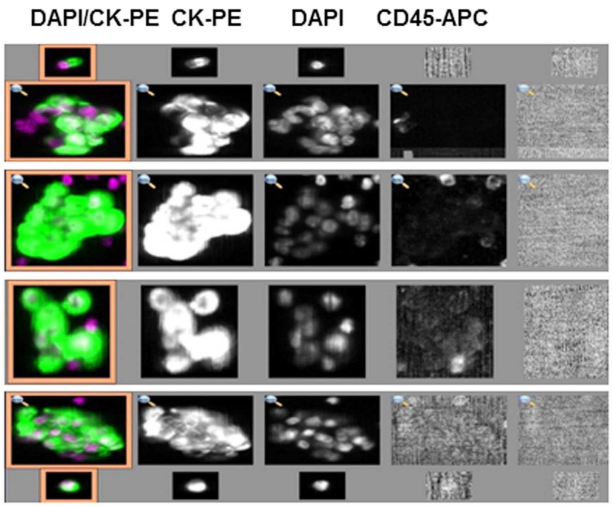

FIGURE 1 | Circulating tumor cell clusters captured from a breast cancer patient using the CellSearch system. (CK, cytokeratin; PE, phycoerythrin; APC, allophycocyanin; DAPI, 4′,6-diamidino-2-phenylindole).

Alternate approaches to CTC isolation are currently in development, based on the generally held observation that CTCs are larger than leukocytes, by processing cell samples through a filter. A commercially available version, Isolation by Size of Epithelial/Trophoblastic Tumor cells, or ISET (RareCell Diagnostics), works by simultaneously lysing erythrocytes and fixing remaining cells in paraformaldehyde, and then perfusing the sample through a polycarbonate filter with 8 μm pores. CTCs thus remain on the filter, which can be stored prior to analysis of captured CTCs. Capture sensitivity has been reported to be one CTC per milliliter of blood (Vona et al., 2000). CTCs have been analyzed by *in situ* immunohistochemistry as well as real-time RT-PCR (Pinzani et al., 2006; Krebs et al., 2012). Interestingly, a recent study found CTM in 43% of patients studied, and evaluation by Ki67 immunohistochemistry showed that captured CTC were proliferative while CTM were not (Krebs et al., 2012).

An alternative form of filtration device uses a parylene membrane that allows for formation of pores of controlled size and shape. In a proof of concept study, a device was constructed to process whole blood and ∼90% recovery was achieved with spiked samples (Zheng et al., 2007). A promising aspect of this device is that the filtration was performed within minutes, showing a higher throughput than most microfluidic methods. An integrated electrode system allows for *in situ* electrolysis of captured cells to facilitate rapid harvesting of genetic material. More recently, this parylene filter system has been used to capture CTCs from patient samples (Lin et al., 2010).

Our group has developed a technique for capturing CTCs based on their ability to adhere to endothelium during extravasation

(Hughes et al., 2012a,b). This technique relies on the binding of CTCs to microtubes coated with a combination of E-selectin protein and epithelial specific antibodies absorbed to an immobilized nanotube layer and perfused under flow. Selectin-mediated capture mimics the normal and malignant process of cell adhesion to blood vessels during metastasis and suggests that CTCs captured using this approach may be more invasive and have undergone EMT to some degree. The CTCs captured by this approach remain viable and can be cultured short term to potentiate subsequent analysis. A halloysite nanotube coating enables >50% purity. It is interesting to note that in general more CTCs were isolated and identified using the selectin-based technique compared to CellSearch on ostensibly identical samples (i.e., two tubes were drawn from each patient and processed by either technique in parallel; **Figure 2**). Indeed, 7 of 12 patient samples were positive for CTCs using CellSearch, while 12 of 12 were positive using our device. Other techniques have similarly found significant discord when using CellSearch on parallel samples; generally more CTCs are found, suggesting that CellSearch neglects to identify many CTCs and has a tendency to report false negatives (Lin et al., 2010; Kirby et al., 2012; Krebs et al., 2012; Marrinucci et al., 2012).

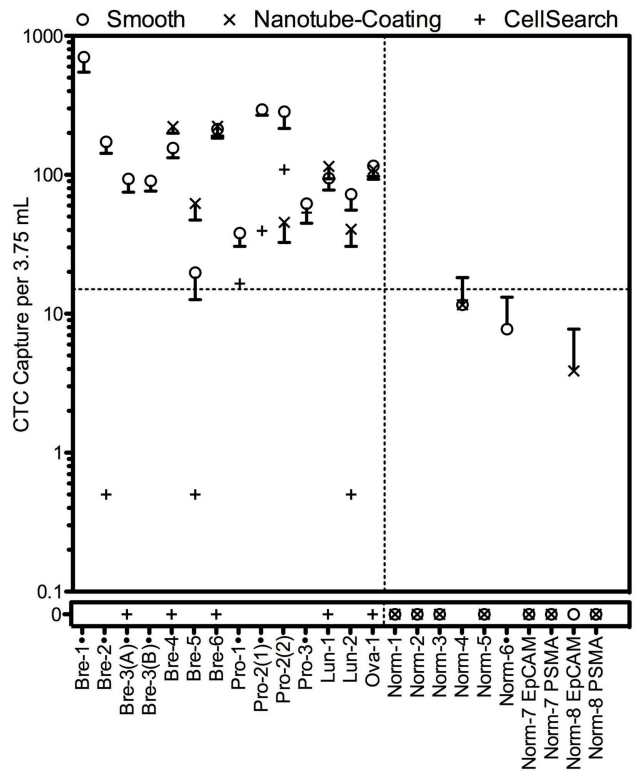

FIGURE 2 | Circulating tumor cell capture using the selectin-functionalized microtube device compared to CTC capture of identical samples using CellSearch. The microtube device was prepared with or without a halloysite nanotube coating. Figure from Hughes and King (2012).

THERAPEUTIC APPLICATIONS OF CTCs

The molecular characterization of CTCs may provide opportunities for therapeutic targeting of CTCs or real-time monitoring of targeted anti-cancer agents (Leversha et al., 2009; Punnoose et al., 2010). Maheswaran et al. (2008) identified mutations in epidermal growth factor receptor (EGFR) in CTCs from lung cancer patients and showed that after continued anti-EGFR therapy, a resistance-associated EGFR mutation emerged. In a separate study using multicolor flow cytometry to rapidly detect and analyze CTCs following erythrocyte lysis, researchers monitored the expression of EGFR in its phosphorylated and unphosphorylated states during the time in which patients were being treated with different therapies for squamous cell carcinoma of the head and neck (SCCHN). The researchers found interesting correlations between different treatment combinations, CTC counts, and EGFR activation (Tinhofer et al., 2012).

Using multiple CTC isolation platforms, several groups have examined Her-2 expression on CTCs and shown in some cases discordance of Her-2 expression between the primary tumor and CTCs (Hayes et al., 2002; Meng et al., 2004; Punnoose et al., 2010; Riethdorf et al., 2010). It follows that if CTCs do not express the same markers as the primary tumor cells, then drugs chosen based on primary tumor markers will be ineffective against CTCs and the secondary tumors they seed. Comprehensive molecular profiling of CTCs in the clinic remains hampered by the low yield and low throughput of most CTC platforms.

The idea of harvesting CTCs from a patient and then studying these CTCs to rapidly determine the best possible treatment for that patient is compelling. The feasibility of such a scheme has been demonstrated to some degree using the geometrically enhanced differential immunocapture (GEDI) device, which is akin to the CTC-chip developed by Toner and colleagues (Nagrath et al., 2007) with altered micropost arrangements to promote collisions with CTCs based on size (Gleghorn et al., 2010). In the most recent study using this device, CTCs were captured within the chip and then treated with different chemotherapeutics *in situ* to assay drug susceptibility (Kirby et al., 2012).

Cellular therapy has recently emerged as a promising approach for treatment of malignancy. Tumor infiltrating lymphocytes or gene-engineered T cells have been used with some success in metastatic cancer patients (Restifo et al., 2012). Provenge is the first active cellular therapy approved by the Food and Drug administration for the treatment of prostate cancer (Wesley et al., 2012). Provenge is manufactured by culturing a patient's peripheral blood mononuclear cells (PBMNCs) and antigen presenting cells with the tumor-associated antigen prostatic acid phosphatase and granulocyte-macrophage colony stimulating factor. Treatment consists of three infusions at approximately 2-week intervals. Provenge is the first autologous anti-cancer cell therapy shown to provide a survival advantage (Wesley et al., 2012).

One intriguing possibility is the *ex vivo* manipulation of CTCs for cellular therapy of cancer. The rate-limiting step in this approach is the low yield associated with many CTC platforms. In theory, if enough CTCs could be obtained and expanded, they could be used as a platform for the development of personalized tumor immunotherapy. An alternative approach for increasing

the amount of CTCs collected from patients is through leukapheresis (**Figure 3**). Leukapheresis is a laboratory procedure in which white blood cells (WBCs or PBMNCs) or peripheral blood stem cells (PBSCs) are separated from blood. During leukapheresis, a patient's blood is passed through a machine that removes the WBCs or PBSCs and then returns the balance of blood back to the patient. This process usually takes 3 or 4 h to filter the entire blood supply (approximately 4–6 l). Collected PBSCs may be used in autologous PBSC transplants to "rescue" the immune system and blood-forming cells of cancer patients following high-dose chemotherapy (Montgomery and Cottler-Fox, 2007). Leukapheresis is common in the stem cell transplant setting for treatment of lymphomas, multiple myeloma, and some solid tumors. The cell therapy Provenge uses leukapheresis to obtain PBMNCs and antigen presenting cells for further manipulation (Wesley et al., 2012).

The product of leukapheresis, termed a leukopak, may also contain CTCs. In theory, one may be able to increase the CTC yield by filtering the entire blood supply, thereby capturing every CTC in the body as opposed to the 0.1–0.2% that would be present in a 7.5-ml blood sample. An increase in CTC yield would improve the diagnostic utility of CTCs and potentially facilitate *in vitro* drug screens on CTCs to predict patient response. Our own group has a Western IRB approved protocol and informed consent for performing leukapheresis on cancer patients in a private, community based, Phase I oncology clinic. In a recent proof of concept study, Eifler et al. (2011) showed using spike-in experiments that isolation of CTCs via leukapheresis followed by elutriation to separate cells based on size, is feasible. Using fluorescence activated cell sorting (FACS) the authors showed high recovery of CaOV-3 cells spiked into leukopaks obtained from healthy volunteers (Eifler et al., 2011). Importantly, no tumor cell events were observed from leukopaks that had not been spiked with tumor cells. Interestingly, analysis by flow cytometry also revealed a $CD45^+$ and $EpCAM^+$ dual positive population of cells that occurred at the highest frequency in the leukopak, and decreased with increasing elutriation fraction. B-lymphocytes were associated with EpCAM binding suggesting that leukocyte lineage specific markers should be used in negative depletion strategies prior to CTC capture, rather than CD45 which could bias results (Eifler et al., 2011).

Following elutriation, CTCs were further captured using FACS or EpCAM-coupled magnetic beads (Eifler et al., 2011). Immunomagnetic bead adsorption recovered 10% of tumor cells with a median purity of 3.5% (Eifler et al., 2011). EpCAM-coupled magnetic bead isolation of CTCs from leukopaks is not ideal, in part because of the cost associated with using such a large amount of EpCAM antibody.

More recently, several groups are further exploring the potential of leukapheresis/apheresis for use in CTC isolation. Stratmann et al. (2012) obtained blood samples and buffy coat by apheresis from breast and pancreatic patients (non-metastatic and metastatic). These samples were then processed using several CTC technologies. Importantly, all methods were able to detect CTCs in buffy coat from both non-metastatic and metastatic cancer patients and newer CTC isolation platforms (i.e., filer based, etc.) showed in general a better yield of CTCs in comparison to CellSearch. In an additional study, Stoecklein et al. (2012) showed in breast cancer patients that higher CTC detection frequencies and numbers could be obtained using leukapheresis products as compared to matched peripheral blood samples from the same patient. Moreover, captured CTCs were amendable to comparative genomic hybridization (Stoecklein et al., 2012). Taken together, these results show the exciting opportunity and potential of using leukapheresis for CTC isolation. Clearly, newer technologies that can accommodate large blood volumes are needed for CTC isolation following leukapheresis to be used widespread in the clinic. In future studies, our group is planning to investigate the feasibility of processing large volumes using the selectin-based approach.

One of the more ambitious approaches to the incorporation of CTCs in the design of new cancer therapies is to consider CTCs as a target for therapy. This is promising considering that 90% of cancer deaths are caused by metastasis (Wittekind and Neid, 2005). The disruption of cancer cell dissemination would thus represent a powerful therapeutic strategy. Photoacoustic flow cytometry has been developed in recent years that allows for the detection and ablation of CTCs *in vivo*. This technology functions by shining a laser through the skin into a vessel that is up to 3 mm deep and detecting the acoustic vibrations that result from the absorption of laser light by target nanoparticles (Zharov et al., 2007). The most direct application of this technology is for the detection of circulating melanoma cells, capitalizing on their endogenous expression of melanin nanoparticles for detection (Nedosekin et al., 2011). Increasing the incident laser energy can lead to the generation of heat by the vibrating nanoparticles to a sufficient degree that

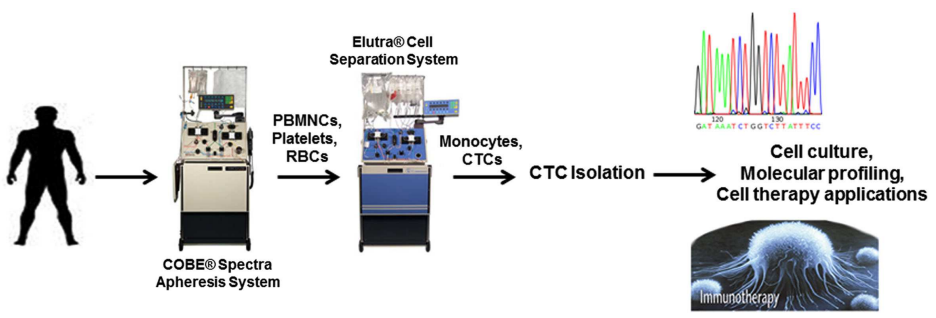

FIGURE 3 | Illustration showing potential applications of CTCs following isolation after leukapheresis.

the flowing melanin-containing cells are ablated (Galanzha et al., 2009b). This technology can be applied to less photo-distinct CTCs using targeted gold nanoparticles, for example to target CD44 to detect and eradicate cancer stem cells (Galanzha et al., 2009a).

Our group has proposed the idea of a shunt device that can be implanted into the vasculature to capture and eradicate CTCs *in vivo*. This device is composed of a selectin-functionalized microtube that will induce the rolling of CTCs along the luminal surface. In one realization of this device, the microtube lumen is co-functionalized with tumor necrosis factor-related apoptosis-inducing ligand (TRAIL, also known as Apo2) that signals cell death to cancer cells via the caspase pathway. A validation study *in vitro* achieved a 30% kill rate of cancer cells without compromising leukocyte viability (Rana et al., 2009). Ongoing studies are evaluating the benefits of manipulating the nanoscale topography of the luminal surface to achieve greater CTC eradication. An alternate version of this device is a microtube shunt that is functionalized with a halloysite nanotube coating which is then coated with targeted liposomes. Liposomes containing the anti-cancer drug doxorubicin are coated with polyethylene glycol (PEG) and E-selectin. Thus flowing cancer cells roll on the selectin-coated liposomes, and we have shown that these liposomes remain on the cell surface and are internalized (Mitchell et al., 2012).

CONCLUSION

The true potential of CTCs has yet to be realized because of limits in technology used to capture these cells and our lack of a complete understanding of metastasis. This is complicated by the fact that our understanding of CTCs is subject to the techniques available to identify and isolate CTCs, and the biases inherent to them. Nevertheless, progress has been made to advance the state of knowledge and probe the use of CTCs in more active roles than simply enumeration. CTCs have the potential to serve as a readily accessible, transparent window into an individual's disease. The ideal device is one that can be used at the point of care to quickly harvest CTCs and make them available for subsequent analyses. One may envision how such a scheme would produce personalized cancer therapies by allowing clinicians to evaluate susceptibilities in the laboratory, and create tailored therapies for each individual. There are myriad possibilities if CTCs can be isolated at high-throughput and purity without bias.

ACKNOWLEDGMENTS

This work was funded by National Institutes of Health, Grant No. CA143876 (Michael R. King), by a National Science Foundation Graduate Research Fellowship (Andrew D. Hughes), and by BioCytics, Inc. (Bryan T. Greene).

REFERENCES

Allard, W. J., Matera, J., Miller, M. C., Repollet, M., Connelly, M. C., Rao, C., Tibbe, A. G., Uhr, J. W., and Terstappen, L. W. (2004). Tumor cells circulate in the peripheral blood of all major carcinomas but not in healthy subjects or patients with nonmalignant diseases. *Clin. Cancer Res.* 10, 6897–6904.

Cho, E. H., Wendel, M., Luttgen, M., Yoshioka, C., Marrinucci, D., Lazar, D., Schram, E., Nieva, J., Bazhenova, L., Morgan, A., Ko, A. H., Korn, W. M., Kolatkar, A., Bethel, K., and Kuhn, P. (2012). Characterization of circulating tumor cell aggregates identified in patients with epithelial tumors. *Phys. Biol.* 9, 016001.

Eifler, R. L., Lind, J., Falkenhagen, D., Weber, V., Fischer, M. B., and Zeillinger, R. (2011). Enrichment of circulating tumor cells from a large blood volume using leukapheresis and elutriation: proof of concept. *Cytometry B Clin. Cytom.* 80, 100–111.

Galanzha, E. I., Kim, J. W., and Zharov, V. P. (2009a). Nanotechnology-based molecular photoacoustic and photothermal flow cytometry platform for in-vivo detection and killing of circulating cancer stem cells. *J. Biophotonics* 2, 725–735.

Galanzha, E. I., Shashkov, E. V., Spring, P. M., Suen, J. Y., and Zharov, V. P. (2009b). In vivo, noninvasive, label-free detection and eradication of circulating metastatic melanoma cells using two-color photoacoustic flow cytometry with a diode laser. *Cancer Res.* 69, 7926–7934.

Gleghorn, J. P., Pratt, E. D., Denning, D., Liu, H., Bander, N. H., Tagawa, S. T., Nanus, D. M., Giannakakou, P. A., and Kirby, B. J. (2010). Capture of circulating tumor cells from whole blood of prostate cancer patients using geometrically enhanced differential immunocapture (GEDI) and a prostate-specific antibody. *Lab. Chip* 10, 27–29.

Hayes, D. F., Walker, T. M., Singh, B., Vitetta, E. S., Uhr, J. W., Gross, S., Rao, C., Doyle, G. V., and Terstappen, L. W. (2002). Monitoring expression of HER-2 on circulating epithelial cells in patients with advanced breast cancer. *Int. J. Oncol.* 21, 1111–1117.

Hughes, A. D., and King, M. R. (2012). Nanobiotechnology for the capture and manipulation of circulating tumor cells. *Wiley Interdiscip. Rev. Nanomed. Nanobiotechnol.* 4, 291–309.

Hughes, A. D., Mattison, J., Western, L. T., Powderly, J. D., Greene, B. T., and King, M. R. (2012a). Microtube device for selectin-mediated capture of viable circulating tumor cells from blood. *Clin. Chem.* 58, 846–853.

Hughes, A. D., Mattison, J., Powderly, J. D., Greene, B. T., and King, M. R. (2012b). Rapid isolation of viable circulating tumor cells from patient blood samples. *J. Vis. Exp.* 64, e4248.

Kirby, B. J., Jodari, M., Loftus, M. S., Gakhar, G., Pratt, E. D., Chanel-Vos, C., Gleghorn, J. P., Santana, S. M., Liu, H., Smith, J. P., Navarro, V. N., Tagawa, S. T., Bander, N. H., Nanus, D. M., and Giannakakou, P. (2012). Functional characterization of circulating tumor cells with a prostate-cancer-specific microfluidic device. *PLoS ONE* 7, e35976. doi: 10.1371/journal.pone.0035976

Krebs, M. G., Hou, J. M., Sloane, R., Lancashire, L., Priest, L., Nonaka, D., Ward, T. H., Backen, A., Clack, G., Hughes, A., Ranson, M., Blackhall, F. H., and Dive, C. (2012). Analysis of circulating tumor cells in patients with non-small cell lung cancer using epithelial marker-dependent and -independent approaches. *J. Thorac. Oncol.* 7, 306–315.

Leversha, M. A., Han, J., Asgari, Z., Danila, D. C., Lin, O., Gonzalez-Espinoza, R., Anand, A., Lilja, H., Heller, G., Fleisher, M., and Scher, H. I. (2009). Fluorescence in situ hybridization analysis of circulating tumor cells in metastatic prostate cancer. *Clin. Cancer Res.* 15, 2091–2097.

Lin, H. K., Zheng, S. Y., Williams, A. J., Balic, M., Groshen, S., Scher, H. I., Fleisher, M., Stadler, W., Datar, R. H., Tai, Y. C., and Cote, R. J. (2010). Portable filter-based microdevice for detection and characterization of circulating tumor cells. *Clin. Cancer Res.* 16, 5011–5018.

Maheswaran, S., and Haber, D. A. (2010). Circulating tumor cells: a window into cancer biology and metastasis. *Curr. Opin. Genet. Dev.* 20, 96–99.

Maheswaran, S., Sequist, L. V., Nagrath, S., Ulkus, L., Brannigan, B., Collura, C. V., Inserra, E., Diederichs, S., Iafrate, A. J., Bell, D. W., Digumarthy, S., Muzikansky, A., Irimia, D., Settleman, J., Tompkins, R. G., Lynch, T. J., Toner, M., and Haber, D. A. (2008). Detection of mutations in EGFR in circulating lung-cancer cells. *N. Engl. J. Med.* 359, 366–377.

Marrinucci, D., Bethel, K., Kolatkar, A., Luttgen, M. S., Malchiodi, M., Baehring, F., Voigt, K., Lazar, D., Nieva, J., Bazhenova, L., Ko, A. H., Korn, W. M., Schram, E., Coward, M., Yang, X., Metzner, T., Lamy, R., Honnatti, M., Yoshioka, C., Kunken, J., Petrova, Y., Sok, D., Nelson, D., and Kuhn, P. (2012). Fluid biopsy in patients with metastatic prostate, pancreatic and breast cancers. *Phys. Biol.* 9, 016003.

Meng, S., Tripathy, D., Shete, S., Ashfaq, R., Haley, B., Perkins, S., Beitsch, P., Khan, A., Euhus, D., Osborne, C., Frenkel, E., Hoover, S., Leitch, M., Clifford, E., Vitetta, E., Morrison, L., Herlyn, D., Terstappen, L. W., Fleming, T., Fehm, T., Tucker, T., Lane, N., Wang, J., and Uhr, J. (2004). HER-2 gene amplification can be acquired as breast cancer progresses. *Proc. Natl. Acad. Sci. U.S.A.* 101, 9393–9398.

Mitchell, M. J., Chen, C. S., Ponmudi, V., Hughes, A. D., and King, M. R. (2012). E-selectin liposomal and nanotube-targeted delivery of doxorubicin to circulating tumor cells. *J. Control Release* 160, 609–617.

Mohamed, H., Murray, M., Turner, J. N., and Caggana, M. (2009). Isolation of tumor cells using size and deformation. *J. Chromatogr. A* 1216, 8289–8295.

Montgomery, M., and Cottler-Fox, M. (2007). Mobilization and collection of autologous hematopoietic progenitor/stem cells. *Clin. Adv. Hematol. Oncol.* 5, 127–136.

Muller, V., Stahmann, N., Riethdorf, S., Rau, T., Zabel, T., Goetz, A., Janicke, F., and Pantel, K. (2005). Circulating tumor cells in breast cancer: correlation to bone marrow micrometastases, heterogeneous response to systemic therapy and low proliferative activity. *Clin. Cancer Res.* 11, 3678–3685.

Nagrath, S., Sequist, L. V., Maheswaran, S., Bell, D. W., Irimia, D., Ulkus, L., Smith, M. R., Kwak, E. L., Digumarthy, S., Muzikansky, A., Ryan, P., Balis, U. J., Tompkins, R. G., Haber, D. A., and Toner, M. (2007). Isolation of rare circulating tumour cells in cancer patients by microchip technology. *Nature* 450, 1235–1239.

Nedosekin, D. A., Sarimollaoglu, M., Ye, J. H., Galanzha, E. I., and Zharov, V. P. (2011). In vivo ultra-fast photoacoustic flow cytometry of circulating human melanoma cells using near-infrared high-pulse rate lasers. *Cytometry* 79A, 825–833.

Pinzani, P., Salvadori, B., Simi, L., Bianchi, S., Distante, V., Cataliotti, L., Pazzagli, M., and Orlando, C. (2006). Isolation by size of epithelial tumor cells in peripheral blood of patients with breast cancer: correlation with real-time reverse transcriptase-polymerase chain reaction results and feasibility of molecular analysis by laser microdissection. *Hum. Pathol.* 37, 711–718.

Powell, A. A., Talasaz, A. H., Zhang, H., Coram, M. A., Reddy, A., Deng, G., Telli, M. L., Advani, R. H., Carlson, R. W., Mollick, J. A., Sheth, S., Kurian, A. W., Ford, J. M., Stockdale, F. E., Quake, S. R., Pease, R. F., Mindrinos, M. N., Bhanot, G., Dairkee, S. H., Davis, R. W., and Jeffrey, S. S. (2012). Single cell profiling of circulating tumor cells: transcriptional heterogeneity and diversity from breast cancer cell lines. *PLoS ONE* 7, e33788. doi: 10.1371/journal.pone.0033788

Punnoose, E. A., Atwal, S. K., Spoerke, J. M., Savage, H., Pandita, A., Yeh, R. F., Pirzkall, A., Fine, B. M., Amler, L. C., Chen, D. S., and Lackner, M. R. (2010). Molecular biomarker analyses using circulating tumor cells. *PLoS ONE* 5, e12517. doi: 10.1371/journal.pone.0012517

Rana, K., Liesveld, J. L., and King, M. R. (2009). Delivery of apoptotic signal to rolling cancer cells: a novel biomimetic technique using immobilized TRAIL and E-selectin. *Biotechnol. Bioeng.* 102, 1692–1702.

Restifo, N. P., Dudley, M. E., and Rosenberg, S. A. (2012). Adoptive immunotherapy for cancer: harnessing the T cell response. *Nat. Rev. Immunol.* 12, 269–281.

Riethdorf, S., Muller, V., Zhang, L., Rau, T., Loibl, S., Komor, M., Roller, M., Huober, J., Fehm, T., Schrader, I., Hilfrich, J., Holms, F., Tesch, H., Eidtmann, H., Untch, M., Von Minckwitz, G., and Pantel, K. (2010). Detection and HER2 expression of circulating tumor cells: prospective monitoring in breast cancer patients treated in the neoadjuvant GeparQuattro trial. *Clin. Cancer Res.* 16, 2634–2645.

Stoecklein, N. H., Niederacher, D., Topp, S. A., Fohrding, L. Z., Vay, C., Knoefel, W. T., Kasprowicz, N. S., Hepp, P. G., Mohrmann, S., Janni, W., Stratmann, A., Krahn, T., Honisch, E., Raba, K., and Fischer, J. C. (2012). Effect of leukapheresis on efficient CTC enrichment for comprehensive molecular characterization and clinical diagnostics. *J. Clin. Oncol.* 30(Suppl.), abstr. e21020.

Stott, S. L., Hsu, C. H., Tsukrov, D. I., Yu, M., Miyamoto, D. T., Waltman, B. A., Rothenberg, S. M., Shah, A. M., Smas, M. E., Korir, G. K., Floyd, F. P. Jr., Gilman, A. J., Lord, J. B., Winokur, D., Springer, S., Irimia, D., Nagrath, S., Sequist, L. V., Lee, R. J., Isselbacher, K. J., Maheswaran, S., Haber, D. A., and Toner, M. (2010a). Isolation of circulating tumor cells using a microvortex-generating herringbone-chip. *Proc. Natl. Acad. Sci. U.S.A.* 107, 18392–18397.

Stott, S. L., Lee, R. J., Nagrath, S., Yu, M., Miyamoto, D. T., Ulkus, L., Inserra, E. J., Ulman, M., Springer, S., Nakamura, Z., Moore, A. L., Tsukrov, D. I., Kempner, M. E., Dahl, D. M., Wu, C. L., Iafrate, A. J., Smith, M. R., Tompkins, R. G., Sequist, L. V., Toner, M., Haber, D. A., and Maheswaran, S. (2010b). Isolation and characterization of circulating tumor cells from patients with localized and metastatic prostate cancer. *Sci. Transl. Med.* 2, 25ra23.

Stratmann, A., Fischer, J. C., Niederacher, D., Raba, K., Schmitz, A., Kim, P. S., Singh, S., Stoecklein, N. H., and Krahn, T. (2012). A comprehensive comparision of circulating tumor cell capturing technologies by apheresis of cancer patients. *J. Clin. Oncol.* 30(Suppl.), abstr. e21017.

Talasaz, A. H., Powell, A. A., Huber, D. E., Berbee, J. G., Roh, K. H., Yu, W., Xiao, W., Davis, M. M., Pease, R. F., Mindrinos, M. N., Jeffrey, S. S., and Davis, R. W. (2009). Isolating highly enriched populations of circulating epithelial cells and other rare cells from blood using a magnetic sweeper device. *Proc. Natl. Acad. Sci. U.S.A.* 106, 3970–3975.

Tan, S. J., Yobas, L., Lee, G. Y., Ong, C. N., and Lim, C. T. (2009). Microdevice for the isolation and enumeration of cancer cells from blood. *Biomed. Microdevices* 11, 883–892.

Tinhofer, I., Hristozova, T., Stromberger, C., Keilhoiz, U., and Budach, V. (2012). Monitoring of circulating tumor cells and their expression of EGFR/phospho-EGFR during combined radiotherapy regimens in locally advanced squamous cell carcinoma of the head and neck. *Int. J. Radiat. Oncol. Biol. Phys.* [Epub ahead of print].

Vona, G., Sabile, A., Louha, M., Sitruk, V., Romana, S., Schutze, K., Capron, F., Franco, D., Pazzagli, M., Vekemans, M., Lacour, B., Brechot, C., and Paterlini-Brechot, P. (2000). Isolation by size of epithelial tumor cells – a new method for the immunomorphological and molecular characterization of circulating tumor cells. *Am. J. Pathol.* 156, 57–63.

Went, P. T., Lugli, A., Meier, S., Bundi, M., Mirlacher, M., Sauter, G., and Dirnhofer, S. (2004). Frequent EpCam protein expression in human carcinomas. *Hum. Pathol.* 35, 122–128.

Wesley, J., Whitmore, J., Trager, J., and Sheikh, N. (2012). An overview of sipuleucel-T: autologous cellular immunotherapy for prostate cancer. *Hum. Vaccin. Immunother.* 8, 520–527.

Wittekind, C., and Neid, M. (2005). Cancer invasion and metastasis. *Oncology* 69(Suppl. 1), 14–16.

Wulfing, P., Borchard, J., Buerger, H., Heidl, S., Zanker, K. S., Kiesel, L., and Brandt, B. (2006). HER2-positive circulating tumor cells indicate poor clinical outcome in stage I to III breast cancer patients. *Clin. Cancer Res.* 12, 1715–1720.

Zhang, Z., Han, L., Cao, L., Liang, X., Liu, Y., Liu, H., Du, J., Qu, Z., Zhu, C., Liu, S., Li, H., and Sun, W. (2008). Aggregation formation mediated anoikis resistance of BEL7402 hepatoma cells. *Folia Histochem. Cytobiol.* 46, 331–336.

Zharov, V. P., Galanzha, E. I., Shashkov, E. V., Kim, J. W., Khlebtsov, N. G., and Tuchin, V. V. (2007). Photoacoustic flow cytometry: principle and application for real-time detection of circulating single nanoparticles, pathogens, and contrast dyes in vivo. *J. Biomed. Opt.* 12, 051503.

Zheng, S., Lin, H., Liu, J. Q., Balic, M., Datar, R., Cote, R. J., and Tai, Y. C. (2007). Membrane microfilter device for selective capture, electrolysis and genomic analysis of human circulating tumor cells. *J. Chromatogr. A* 1162, 154–161.

Conflict of Interest Statement: The authors declare that the research was conducted in the absence of any commercial or financial relationships that could be construed as a potential conflict of interest.

Received: 01 June 2012; accepted: 13 June 2012; published online: 02 July 2012.
Citation: Greene BT, Hughes AD and King MR (2012) Circulating tumor cells: the substrate of personalized medicine? Front. Oncol. ***2****:69. doi: 10.3389/fonc.2012.00069*
This article was submitted to Frontiers in Cancer Molecular Targets and Therapeutics, a specialty of Frontiers in Oncology.

frontiers in ONCOLOGY

MINI REVIEW ARTICLE
published: 03 July 2012
doi: 10.3389/fonc.2012.00068

Cornering metastases: therapeutic targeting of circulating tumor cells and stem cells

Bishoy Faltas*

Division of Hematology and Medical Oncology, Weill Cornell Medical College, New York, NY, USA

Edited by:
Michael R. King, Cornell University, USA

Reviewed by:
Michael R. King, Cornell University, USA
Jiahe Li, Cornell University, USA

****Correspondence:***
Bishoy Faltas, Division of Hematology and Medical Oncology, Weill Cornell Medical College, New York, NY 10065, USA. e-mail: beshoyso@yahoo.com

The last decade has witnessed an evolution of our understanding of the biology of the metastatic cascade. Recent insights into the metastatic process show that it is complex, dynamic, and multi-directional. This process starts at a very early stage in the natural history of solid tumor growth leading to early development of metastases that grow in parallel with the primary tumor. The role of stem cells in perpetuating cancer metastases is increasingly becoming more evident. At the same time, there is a growing recognition of the crucial role circulating tumor cells (CTCs) play in the development of metastases. These insights have laid the biological foundations for therapeutic targeting of CTCs, a promising area of research that aims to reduce cancer morbidity and mortality by preventing the development of metastases at a very early stage. The hematogenous transport phase of the metastatic cascade provides critical access to CTCs for therapeutic targeting aiming to interrupt the metastatic process. Recent advances in the fields of nanotechnology and microfluidics have led to the development of several devices for *in vivo* targeting of CTC during transit in the circulation. Selectin-coated tubes that target cell adhesion molecules, immuno-magnetic separators, and *in vivo* photo-acoustic flow cytometers are currently being developed for this purpose. On the pharmacological front, several pharmacological and immunological agents targeting cancer stem cells are currently being developed. Such agents may ultimately prove to be effective against circulating tumor stem cells (CTSCs). Although still in its infancy, therapeutic targeting of CTCs and CTSCs offers an unprecedented opportunity to prevent the development of metastasis and potentially alter the natural history of cancer. By rendering cancer a "local" disease, these approaches could lead to major reductions in metastasis-related morbidity and mortality.

Keywords: circulating tumor cells, cancer stem cell, epithelial–mesenchymal transition, immuno-magnetic separation, selectin ligands, targeted therapy, metastasis

THE BIOLOGY OF THE METASTATIC CASCADE

The metastatic spread of cancer is the main cause of morbidity and mortality in cancer patients (Duffy et al., 2008). The development of metastases from solid tumors is a complex multi-step process and is one of the most enigmatic aspects of cancer biology. Recently, studies using *in vivo* vital microscopy have shed more light on the physiology of the metastasis. These studies show a metastatic process that proceeds in a pre-determined cascade comprising the following steps: neoangiogenesis, *trans*-endothelial migration, entry into the blood stream (intravasation), transport through the vasculature followed by extravasation, and ultimately resulting in colonization and growth at distant sites (Chambers et al., 1995; Morris et al., 1997; **Figure 1**).

Although the biology of the metastatic process is not fully understood, new insights are emerging from recently discovered metastatic phenomena. For instance, it was previously believed that the development of metastases is a late event that occurs only after primary tumors reach a certain critical mass (the linear-progression model). Recent evidence indicates that tumor cells disseminate at a relatively early stage of the natural history of tumor growth. This leads to parallel growth of metastasis along with primary tumor growth (the parallel-progression model; Klein, 2009). Similarly, metastatic spread has been classically viewed as a unidirectional process with dissemination of cancer cells occurring only from primary tumors to form secondary metastases. On the contrary, recent experimental evidence points toward a new paradigm where cancer progress is a multi-directional process in which tumor cells are capable of self-seeding the primary tumor (Kim et al., 2009; Comen et al., 2011).

The metastatic process is selective and inefficient with many cancer cells initially gaining access to the circulation but only a few ultimately succeeding in proliferating as distant metastases (Wong et al., 2001). In fact, it is estimated that only 1% of micro-metastases eventually thrive as macro-metastases (Wittekind and Neid, 2005). Despite this relative metastatic inefficiency, the absolute magnitude of metastatic spread is enormous and represents the primary cause of cancer morbidity and mortality (Wittekind and Neid, 2005; Chaffer and Weinberg, 2011).

THERAPEUTIC TARGETING OF THE METASTATIC CASCADE

Despite the tremendous toll of metastases on human mortality and morbidity, the development of preventive anti-metastatic therapies has been slow and often hampered by the lack of understanding of the biology of the metastatic cascade (Mina and

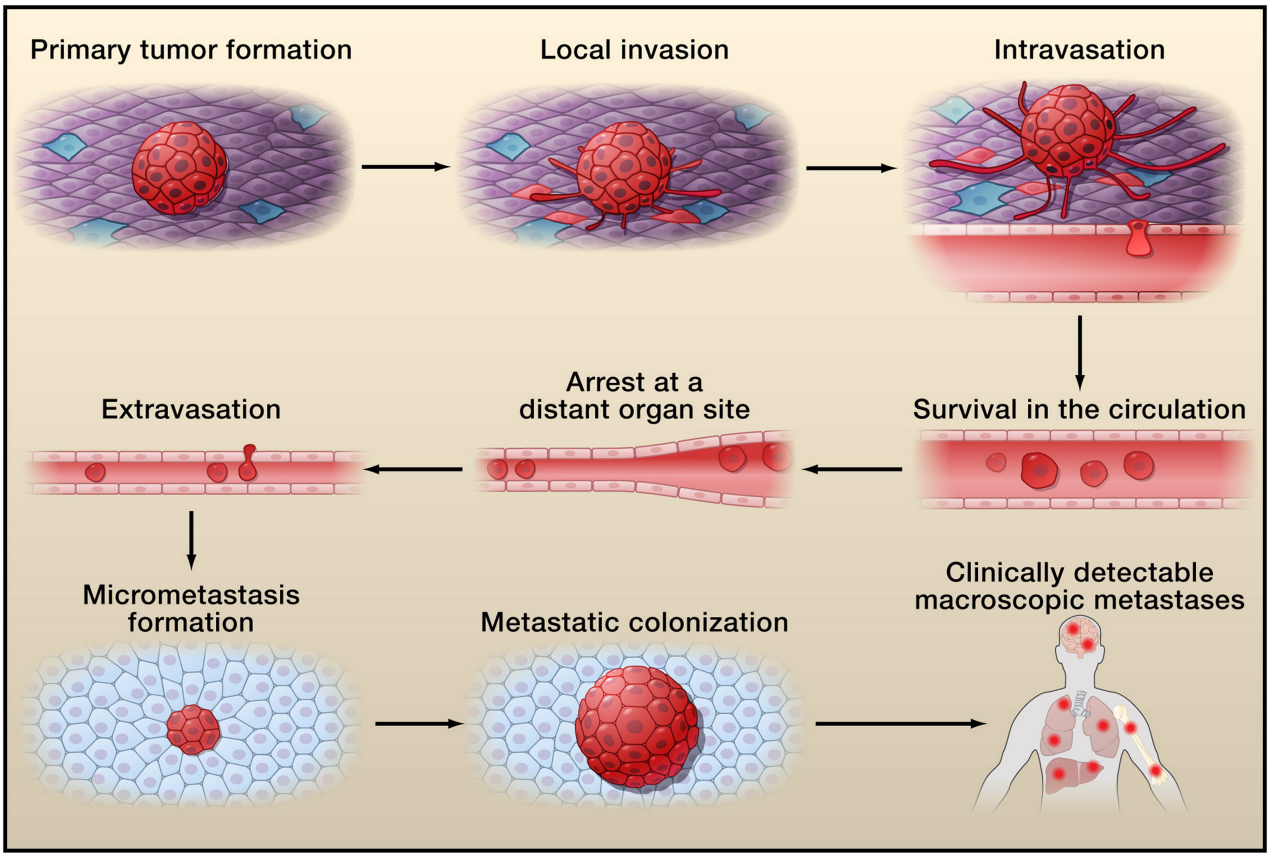

FIGURE 1 | The invasion–metastasis cascade. Tumor cells exit their primary sites of growth (local invasion, intravasation), translocate systemically (survival in the circulation, arrest at a distant organ site, extravasation), and adapt to survive in distant tissues (micro-metastasis formation, metastatic colonization). Adapted with permission from Valastyan and Weinberg (2011).

Sledge, 2011). Most currently developed anti-metastatic therapy strategies target the final steps of the metastatic cascade such as extravasated dormant cancer cells in the metastatic niche thus missing the opportunity to interrupt metastases development at earlier stages (Chambers et al., 2000; MacDonald et al., 2002). Targeting earlier "up-stream" events in the metastatic cascade is likely to be more effective in preventing metastases from developing with greater yield in reducing or even eliminating their devastating clinical impact. The hematogenous transport phase of cancer cells presents a particularly attractive opportunity for therapeutic targeting for multiple reasons; first, it occurs early enough to provide a rational up-stream target for strategies aiming to reduce or completely prevent the development of distant metastases. Secondly, hematogenous transport represents the final common pathway of metastatic spread, even for tumors initially spreading through lymphatics which eventually inter-connect with the circulatory system (Sleeman et al., 2011). Finally, the transport phase is relatively accessible to a variety of pharmacological and mechanical targeting interventions.

CIRCULATING TUMOR CELLS AS THERAPEUTIC TARGETS

Circulating tumor cells (CTCs) are cancer cells that detach from the primary tumor and enter the bloodstream. Several systems have been developed for isolation and characterization of CTCs from blood samples including the FDA approved CellSearch® platform (Hughes and King, 2012; Yu et al., 2011). Using these platforms, CTCs have been isolated from blood samples of patients with a variety of tumors including head and neck (Nichols et al., 2011), breast (Swaby and Cristofanilli, 2011), lung (O'Flaherty et al., 2011), colorectal, gastric, pancreatic (Takeuchi and Kitagawa, 2010), renal cell, urinary bladder, and prostate cancers (Kruck et al., 2011). Recent studies show significant correlation between higher CTC counts and shorter overall survival in patients with metastatic breast, lung, and prostate carcinomas (Cristofanilli et al., 2004; Miller et al., 2010). These studies support a critical role for CTCs in tumor progression and metastases. As a result, it is now hypothesized that targeting CTCs during their hematogenous transport could lead to effective interruption of the metastatic cascade and ultimately, reduction of cancer morbidity and mortality (Faltas, 2010).

CIRCULATING TUMOR STEM CELLS AND EPITHELIAL–MESENCHYMAL TRANSITION

Circulating tumor cells occur in heterogeneous populations with pronounced differences in their metastatic potential. Some CTC populations undergo a transformative process called

epithelial–mesenchymal transition (EMT) that leads to acquisition of enhanced migratory and invasive properties (Bonnomet et al., 2010). Cells undergoing EMT also acquire cancer stem cell (CSC)-like characteristics including the capacity for self-renewal, re-differentiation, dormancy, active DNA repair, drug resistance, and resistance to apoptosis leading to resistance to chemotherapeutic agents (Monteiro and Fodde, 2010; Chaffer and Weinberg, 2011). These CTCs possessing stem cell like characteristics will be referred to in this review as circulating tumor stem cells (CTSCs). Because of these unique characteristics, CTSCs are considered high-value targets for anti-metastatic therapies. Unfortunately, the biology of this unique subset of cells is not fully understood, posing a challenge to precise identification of cell populations most likely to initiate metastases in distant organs or those that are most difficult to eliminate using existing chemotherapeutic approaches (Faltas et al., 2011). Several markers have been proposed to identify CTSCs including CD133, a glycoprotein expressed on hematopoietic progenitors. In one study, real-time reverse-transcriptase polymerase chain reaction was used to detect mRNA of CD133 as a marker for CTSCs in patients with colorectal cancer. This study demonstrated the prognostic significance of a combined carcinoembryonic antigen (CEA)/cytokeratin (CK)/CD133 pattern but not for CD133 alone in patients with Dukes' B and C colorectal carcinoma (Iinuma et al., 2011). A marker "profile" that combines markers predicting poor clinical outcomes, resistance to chemotherapy, or susceptibility to apoptosis evasion (CD26, epidermal growth factor receptor, myeloid leukemia cell differentiation protein Mcl-1, and Ki-67) with the stem cell marker CD133 is currently under investigation. This approach is expected to result in improved ability to detect and target genuinely metastatic CTSC phenotypes (Faltas et al., 2011).

APPROACHES FOR THERAPEUTIC TARGETING OF CIRCULATING TUMOR CELLS AND CIRCULATING TUMOR STEM CELLS

Improved understanding of metastatic biology has laid the biological foundations for therapeutic targeting of CTCs and CTSCs. **Table 1** summarizes important concepts in metastatic biology and their implications for therapeutic targeting. *In vivo* therapeutic targeting of CTCs and CTSCs to interrupt the transport phase of the metastatic cascade and subsequent development of metastasis is in itself, a novel concept (Hughes and King, 2012) and variety of targeting approaches are currently under development.

Table 1 | Emerging concepts in metastatic biology and their implications for therapeutic targeting.

Biological concept	Implications for therapeutic targeting	Reference
• Metastasis progresses in a sequence of events. • Each step in the metastatic cascade is considered rate-limiting.	Interrupting the hematogenous transport step can potentially interrupt the entire cascade.	Chambers et al. (1995), Morris et al. (1997)
• The parallel-progression model of metastatic tumors.	Early targeting of CTC can eliminate early development of micro-metastases. Anti-metastatic therapies may need to be eliminated in conjunction with therapy for primary tumors.	Klein (2009)
• Self-seeding of primary tumor.	Therapeutic targeting of CTC even after the development of secondary metastases may still alter the natural history of the disease.	Kim et al. (2009), Comen et al. (2011)
• Hematogenous transport represents the final common pathway of metastatic spread.	Hematogenous transport is a rational therapeutic target to prevent the development of metastases.	Sleeman et al. (2011)
• Hematogenous spread is an early event in the metastatic cascade.	The hematogenous transport phase provides a unique therapeutic window for targeting an "up-stream" event in the metastatic cascade.	Faltas (2010)
• Circulating tumor cells (CTCs) predict survival of patients with metastatic cancers.	Targeting circulating tumor cells could potentially prolong survival of cancer patients.	Cristofanilli et al. (2004), Miller et al. (2010)
• Circulating tumor stem cells (CTSCs) capacity for self-renewal, re-differentiation, dormancy, active DNA repair, drug resistance, and resistance to apoptosis.	CTSCs are considered high-value targets for anti-metastatic therapies. Better profiling of CTSCs could have profound implications for therapeutic targeting.	Faltas et al. (2011)
• CTCs can undergo a transformative process called epithelial–mesenchymal transition (EMT) that leads to the acquisition of enhanced migratory and invasive properties.	Cell signaling pathways affecting regulation of EMT are attractive therapeutic targets for anti-metastatic therapies. On the other hand EMT can alter surface marker expression leading to decreased efficacy of anti-metastatic therapies targeting specific epithelial surface markers.	Aalaoui-Jamali et al. (2011)

PHARMACOLOGICAL AND IMMUNOLOGICAL TARGETING APPROACHES

Pharmacological targeting depends primarily on the identification of suitable molecular targets which are over-expressed and critically important for CTCs' survival and function. CTSC subsets are high-value targets because of their aggressive invasive and proliferative characteristics and their resistance to traditional chemotherapeutic agents. Current therapeutic approaches focusing on targeting CSCs in primary tumors could be extended to target CTSCs that express the same therapeutic targets.

Targeting surface receptors expressed preferentially in CSCs is one promising approach that could potentially be extended to CTSCs. In a study of human breast cancer xenografts in Swiss nude mice, an antibody targeting CD44, a surface marker expressed on CSCs, was found to reduce tumor growth and to prevent relapse after chemotherapy (Marangoni et al., 2009). In another study, targeting CD44 with short interfering RNA (siRNA) resulted in suppression of human colon cancer xenografts (Subramaniam et al., 2007). Investigators have also developed a fusion protein (dCD133KDEL) targeting CD 133, another CSC marker expressed by several human cancer cells (LaBarge and Bissell, 2008; Wang et al., 2008; Faltas et al., 2011). The fusion protein resulted in significant tumor reduction in a xenotransplant model of CD133+ human head and neck cancer (Waldron et al., 2011).

Epithelial cell adhesion molecule (EpCAM) is another interesting therapeutic target (Armstrong and Eck, 2003). It is frequently expressed on CSCs from breast, colon, pancreas, and prostate tumors (Gires et al., 2009). EpCAM is also expressed on CTCs but not on blood cells. This preferential expression is the basis of many diagnostic assays used to isolate CTCs from the bloodstream (Liljefors et al., 2005; Yu et al., 2011). Clinical trials using anti-EpCAM monoclonal antibodies slowed progression and prolonged survival in patient with metastatic colorectal carcinoma (Liljefors et al., 2005).

As mentioned earlier; CTSCs can arise through the EMT process (Bonnomet et al., 2010). Hence, signaling pathways affecting the regulation of EMT are attractive therapeutic targets for anti-metastatic therapies. Inhibitors of PAR6A, Notch1, Hedgehog, Wnt, integrins, polycomb repressive complex 1 (PRC1) protein, Bmi-1, claudin, tyrosine kinase, and Rho GTPases have been reported to block EMT and a few select agents are undergoing early clinical trials (Aalaoui-Jamali et al., 2011).

In the future, a better understanding and profiling of shared characteristics between CTCs, CTSCs, and CSCs in different tumor subtypes will allow extension of the CSC targeting approaches mentioned above toward the design of specific anti-CTSC therapies. More clinical trials need to be designed to assess the impact of targeted pharmacological approaches against CTCs and CTSCs that aim to reduce metastases. These trials should include biomarker endpoints such CTC and CTSC counts and characteristics as well as survival endpoints to assess the full clinical impact of hindering metastasis development and to guide further drug development.

IN VIVO DEVICE-BASED TARGETING APPROACHES

Devices designed to target CTCs and CTSCs *in vivo* can be either intra-corporeal or extra-corporeal. Intra-corporeal devices such as indwelling vascular devices (Faltas, 2010) and shunts (Wojciechowski et al., 2008) have the potential to continuously screen the entire circulation for CTC and CTSCs. This could theoretically improve the absolute magnitude of capture and ultimately result in greater improvements in clinical outcomes. On the other hand, intra-corporeal devices are susceptible to infection, clotting, and other physiological and anatomical design limitations (Faltas, 2010). Alternatively, extra-corporeal devices could isolate and destroy cancerous cells before returning the purged blood to the systemic circulation. Such design avoids many of the limitations inherent to intra-corporeal devices achieving higher capture efficiency per pass. However, the potential increase in capture efficiency per pass may be offset by limited contact time between the device and the circulation because extra-corporeal devices can only be used intermittently leaving periods of unopposed CTC dissemination. Some of these devices could also function as "theranostic" devices that simultaneously monitor CTC counts and analyze their biological characteristics while purging the circulation from CTCs. The resulting data could have prognostic as well as, predictive implications.

Circulating tumor cells and CTSCs can be isolated by targeting cell adhesion molecules expressed on their surfaces. One approach utilizes a vascular shunt functionalized with E-selectin to induce CTCs to adhere to and roll over the shunt's internal surface functionalized with immobilized TNF-related apoptosis-inducing ligand (TRAIL) molecules. This device resulted in apoptosis of 30% of CTCs after 1 h of rolling exposure (Rana et al., 2009). In another study, a P-selectin based vascular shunt functionalized with nanoscale liposomes containing siRNA was successful in delivering siRNA into leukemic cells inducing inhibition of target gene expression (Huang and King, 2009). The same approach can be extended to deliver siRNA into CTCs (Hughes and King, 2012).

Immuno-magnetic separation is another promising strategy that utilizes magnetic nano or micro-particles tagged with antibodies targeting surface receptors expressed by CTC/CTSC populations of interest followed by application of a magnetic field to capture cell-magnetic particle complexes. This principle is utilized by the CellSearch® diagnostic device approved for *ex vivo* separation of EpCAM+ CTCs in peripheral blood samples. The same concept is currently under development for *in vivo* applications. In one study aiming to prevent direct metastatic spread of ovarian cancer inside the peritoneal cavity, researchers used super-paramagnetic nanoparticles conjugated to a peptide targeting the EphA2 receptor expressed by ovarian cancer cells. The application of an external magnetic field resulted in cell capture from a flow stream *in vitro* and from the peritoneal cavity of experimental mice *in vivo* (Scarberry et al., 2008, 2010). In another study mice receiving this treatment were found to have tumor progression 10.77-times slower than that in the control group (Scarberry et al., 2011). The investigators envision the extension of this concept to produce a "dialysis-like" treatment that removes malignant cells from the body. This could potentially result in improved long-term survival of ovarian cancer patients (Scarberry et al., 2008).

On a parallel front, an extra-corporeal microfluidic immunomagnetic blood-cleansing device has been developed to treat sepsis. The device uses magnetic micro-beads coated with polyclonal

antibodies to bind *Candida albicans* in the blood. Bead–fungi complexes were then subjected to a continuous magnetic gradient that enabled uninterrupted high throughput separation of fungi from whole blood. A multiplexed version of the device achieved over 80% clearance of fungi from contaminated blood at a flow rate of 20 ml/h in a single pass. The same technology can also be adapted to purge the blood from CTCs (Lee, 2009; Yung et al., 2009).

In vivo photo-acoustic flow cytometry is another emerging CTC separation technology. In one variant, melanin nanoparticles that naturally occur in melanoma CTCs were exposed to photons from a laser. The nanoparticles absorbed the photons generating heat energy that lysed CTCs while simultaneously expanding to produce acoustic waves detectable by an ultrasound transducer (Weight et al., 2006; Hughes and King, 2012). The same technique was applied to capture breast cancer CTCs using magnetic nanoparticles functionalized to target urokinase plasminogen activator, a receptor commonly expressed on breast CTCs. This was followed by photo-acoustic detection using gold-plated carbon nanotubes conjugated with folic acid as a second contrast agent (Galanzha et al., 2009a). In another study, photo-acoustic detection was used to target CD44+ CTSCs in a mouse model of human breast cancer (Galanzha et al., 2009b).

CHALLENGES FACING THERAPEUTIC TARGETING OF CTC AND CTSCs

Several challenges currently face CTC/CTSC therapeutic targeting efforts. CTCs are rare in the general circulation relative to other blood elements thus requiring ultra-efficient targeting. Pharmacological agents designed to target CTC/CTSCs need to achieve high selectivity while maintaining acceptable clinical toxicity, an important and sometimes an elusive goal. Furthermore, incomplete characterization and profiling of CTC populations hinders efforts to selectively target CTC subsets that are most likely to develop into metastases. CTSCs are emerging as a potentially high-value CTC subset but are still poorly defined and incompletely profiled to date (Faltas et al., 2011). Whereas a number of pharmacologic agents that target CSCs are under development (Aalaoui-Jamali et al., 2011), little is known regarding their specific effectiveness against CTSCs.

Device-based approaches face unique challenges of their own. While pre-clinical models have demonstrated proof of concept, many technical and biocompatibility issues need to be resolved before these devices reach clinical trials in humans. Such devices need to reach a certain threshold of capture efficiency while maintaining physiologic blood flow to prevent thrombosis or tumor seeding of the device (Faltas, 2010). Thromboembolic complications are to be anticipated with the use of such devices and while these complications can be prevented or managed with concomitant use of anticoagulants, this introduces significant bleeding risks that may decrease the overall clinical benefit. Bloodstream infection related to indwelling vascular devices is another serious clinical problem that could potentially complicate clinical adoption of such technology. Approaches utilizing functionalized surfaces face challenges related to bio-fouling by plasma proteins and blood elements that alter the biological activity of such functionalized surfaces (Hughes and King, 2012). Systems utilizing magnetic nanoparticles will require more robust data on the potential long-term toxicity of these particles when used *in vivo* (Scheinberg et al., 2010). Using animal-derived antibodies to isolate CTCs in humans could potentially induce hypersensitivity reactions and while humanized antibodies can be synthesized, they are generally more expensive.

CONCLUSION

Recent insights into the biology of the metastasis have improved our understanding of the metastatic cascade and potential therapeutic targets. These insights have laid the biological foundations for therapeutic targeting of CTCs, a promising area of research that aims to reduce cancer morbidity and mortality by preventing the development of metastases at a very early stage. Studies reveal a multi-step metastatic process that is complex, dynamic, and multi-directional. Metastatic cancer cells disseminate very early in the course of solid tumor growth forming metastases that grow in parallel with the primary tumor. The crucial role of CTCs and CTSCs in initiating and perpetuating metastases is increasingly being recognized. Despite challenges facing precise identification of CTSCs, they are likely to emerge as attractive therapeutic targets because of their stem cell like properties. Several pharmacological and immunological CSC targeting agents are being developed that may eventually prove effective against CTSCs sharing the same biological characteristics.

The hematogenous transport phase of the metastatic cascade provides critical access to CTCs and CTSCs that permits therapeutic targeting. Recent advances in the fields of nanotechnology and microfluidics have led to the development of several devices for *in vivo* targeting of CTC during transit in the circulation. Selectin-coated tubes that target cell adhesion molecules, immuno-magnetic separators, and *in vivo* photo-acoustic flow cytometers are currently being developed for this purpose. While pre-clinical models are showing promising preliminary results, several technical and biocompatibility issues need to be resolved before these devices could reach clinical trials on humans.

Although still in its infancy, therapeutic targeting of CTCs and CTSCs offers an unprecedented opportunity to prevent the development of metastasis and potentially alter the natural history of cancer. More research is needed to expedite the translation of these promising technologies to clinical therapies. By rendering cancer a "local" disease, these approaches could lead to major reductions in metastasis-related morbidity and mortality.

ACKNOWLEDGMENT

The author would like to thank Paul L. Bernstein, MD for his critical review of the manuscript.

REFERENCES

Aalaoui-Jamali, M., Bijian, K., and Batist, G. (2011). Emerging drug discovery approaches for selective targeting of "precursor" metastatic breast cancer cells: highlights and perspectives. *Am. J. Transl. Res.* 3, 434–444.

Armstrong, A., and Eck, S. L. (2003). EpCAM: a new therapeutic target for an old cancer antigen. *Cancer Biol. Ther.* 2, 320–326.

Bonnomet, A., Brysse, A., Tachsidis, A., Waltham, M., Thompson, E. W., Polette, M., and Gilles, C. (2010). Epithelial-to-mesenchymal

transitions and circulating tumor cells. *J. Mammary Gland Biol. Neoplasia* 15, 261–273.

Chaffer, C. L., and Weinberg, R. A. (2011). A perspective on cancer cell metastasis. *Science* 331, 1559–1564.

Chambers, A. F., MacDonald, I. C., Schmidt, E. E., Koop, S., Morris, V. L., Khokha, R., and Groom, A. C. (1995). Steps in tumor metastasis: new concepts from intravital videomicroscopy. *Cancer Metastasis Rev.* 14, 279–301.

Chambers, A. F., MacDonald, I. C., Schmidt, E. E., Morris, V. L., and Groom, A. C. (2000). Clinical targets for anti-metastasis therapy. *Adv. Cancer Res.* 79, 91–121.

Comen, E., Norton, L., and Massague, J. (2011). Clinical implications of cancer self-seeding. *Nat. Rev. Clin. Oncol.* 8, 369–377.

Cristofanilli, M., Budd, G. T., Ellis, M. J., Stopeck, A., Matera, J., Miller, M. C., Reuben, J. M., Doyle, G. V., Allard, W. J., Terstappen, L. W., and Hayes, D. F. (2004). Circulating tumor cells, disease progression, and survival in metastatic breast cancer. *N. Engl. J. Med.* 351, 781–791.

Duffy, M. J., McGowan, P. M., and Gallagher, W. M. (2008). Cancer invasion and metastasis: changing views. *J. Pathol.* 214, 283–293.

Faltas, B. (2010). Targeting hematogenous spread of circulating tumor cells by a chemotactic drug-eluting IVC filter to prevent pulmonary and systemic metastasis. *Med. Hypotheses* 74, 668–669.

Faltas, B., Zeidan, A., Peters, K., Das, A., Joudeh, J., Navaraj, A., Dolloff, N. G., Harvey, H. A., Jiang, Y., Allen, J. E., Dicker, D. T., and El Deiry, W. S. (2011). Identifying circulating tumor stem cells that matter: the key to prognostication and therapeutic targeting. *J. Clin. Oncol.* 29, 2946–2947; author reply 2947–2948.

Galanzha, E. I., Shashkov, E. V., Kelly, T., Kim, J. W., Yang, L., and Zharov, V. P. (2009a). In vivo magnetic enrichment and multiplex photoacoustic detection of circulating tumour cells. *Nat. Nanotechnol.* 4, 855–860.

Galanzha, E. I., Kim, J. W., and Zharov, V. P. (2009b). Nanotechnology-based molecular photoacoustic and photothermal flow cytometry platform for in-vivo detection and killing of circulating cancer stem cells. *J. Biophotonics* 2, 725–735.

Gires, O., Klein, C. A., and Baeuerle, P. A. (2009). On the abundance of EpCAM on cancer stem cells. *Nat. Rev. Cancer* 9, 143; author reply 143.

Huang, Z., and King, M. R. (2009). An immobilized nanoparticle-based platform for efficient gene knockdown of targeted cells in the circulation. *Gene Ther.* 16, 1271–1282.

Hughes, A. D., and King, M. R. (2012). Nanobiotechnology for the capture and manipulation of circulating tumor cells. *Wiley Interdiscip. Rev. Nanomed. Nanobiotechnol.* 4, 291–309.

Iinuma, H., Watanabe, T., Mimori, K., Adachi, M., Hayashi, N., Tamura, J., Matsuda, K., Fukushima, R., Okinaga, K., Sasako, M., and Mori, M. (2011). Clinical significance of circulating tumor cells, including cancer stem-like cells, in peripheral blood for recurrence and prognosis in patients with dukes' stage B and C colorectal cancer. *J. Clin. Oncol.* 29, 1547–1555.

Kim, M. Y., Oskarsson, T., Acharyya, S., Nguyen, D. X., Zhang, X. H., Norton, L., and Massague, J. (2009). Tumor self-seeding by circulating cancer cells. *Cell* 139, 1315–1326.

Klein, C. A. (2009). Parallel progression of primary tumours and metastases. *Nat. Rev. Cancer* 9, 302–312.

Kruck, S., Gakis, G., and Stenzl, A. (2011). Disseminated and circulating tumor cells for monitoring chemotherapy in urological tumors. *Anticancer Res.* 31, 2053–2057.

LaBarge, M. A., and Bissell, M. J. (2008). Is CD133 a marker of metastatic colon cancer stem cells? *J. Clin. Invest.* 118, 2021–2024.

Lee, A. A. (2009). Cutting edge: microfluidic-micromagnetic blood cleansing device. *Lab Chip* 9, 1167.

Liljefors, M., Nilsson, B., Fagerberg, J., Ragnhammar, P., Mellstedt, H., and Frodin, J. E. (2005). Clinical effects of a chimeric anti-EpCAM monoclonal antibody in combination with granulocyte-macrophage colony-stimulating factor in patients with metastatic colorectal carcinoma. *Int. J. Oncol.* 26, 1581–1589.

MacDonald, I. C., Groom, A. C., and Chambers, A. F. (2002). Cancer spread and micrometastasis development: quantitative approaches for in vivo models. *Bioessays* 24, 885–893.

Marangoni, E., Lecomte, N., Durand, L., de Pinieux, G., Decaudin, D., Chomienne, C., Smadja-Joffe, F., and Poupon, M. F. (2009). CD44 targeting reduces tumour growth and prevents post-chemotherapy relapse of human breast cancers xenografts. *Br. J. Cancer* 100, 918–922.

Miller, M. C., Doyle, G. V., and Terstappen, L. W. (2010). Significance of circulating tumor cells detected by the CellSearch system in patients with metastatic breast colorectal and prostate cancer. *J. Oncol.* 2010, 617421.

Mina, L. A., and Sledge, G. W. Jr. (2011). Rethinking the metastatic cascade as a therapeutic target. *Nat. Rev. Clin. Oncol.* 8, 325–332.

Monteiro, J., and Fodde, R. (2010). Cancer stemness and metastasis: therapeutic consequences and perspectives. *Eur. J. Cancer* 46, 1198–1203.

Morris, V. L., Schmidt, E. E., MacDonald, I. C., Groom, A. C., and Chambers, A. F. (1997). Sequential steps in hematogenous metastasis of cancer cells studied by in vivo videomicroscopy. *Invasion Metastasis* 17, 281–296.

Nichols, A. C., Lowes, L. E., Szeto, C. C., Basmaji, J., Dhaliwal, S., Chapeskie, C., Todorovic, B., Read, N., Venkatesan, V., Hammond, A., Palma, D. A., Winquist, E., Ernst, S., Fung, K., Franklin, J. H., Yoo, J., Koropatnick, J., Mymryk, J. S., Barrett, J. W., and Allan, A. L. (2011). Detection of circulating tumor cells in advanced head and neck cancer using the cellsearch system. *Head Neck*. doi: 10.1002/hed.21941 [Epub ahead of print].

O'Flaherty, J. D., Gray, S., O'Leary, J. J., Blackhall, F. H., and O'Byrne, K. J. (2011). Circulating tumour cells, their role in metastasis and their clinical utility in lung cancer. *Lung Cancer* 76, 19–25.

Rana, K., Liesveld, J. L., and King, M. R. (2009). Delivery of apoptotic signal to rolling cancer cells: a novel biomimetic technique using immobilized TRAIL and E-selectin. *Biotechnol. Bioeng.* 102, 1692–1702.

Scarberry, K. E., Dickerson, E. B., McDonald, J. F., and Zhang, Z. J. (2008). Magnetic nanoparticle-peptide conjugates for in vitro and in vivo targeting and extraction of cancer cells. *J. Am. Chem. Soc.* 130, 10258–10262.

Scarberry, K. E., Dickerson, E. B., Zhang, Z. J., Benigno, B. B., and McDonald, J. F. (2010). Selective removal of ovarian cancer cells from human ascites fluid using magnetic nanoparticles. *Nanomed. Nanotechnol. Biol. Med.* 6, 399–408.

Scarberry, K. E., Mezencev, R., and McDonald, J. F. (2011). Targeted removal of migratory tumor cells by functionalized magnetic nanoparticles impedes metastasis and tumor progression. *Nanomedicine (Lond.)* 6, 69–78.

Scheinberg, D. A., Villa, C. H., Escorcia, F. E., and McDevitt, M. R. (2010). Conscripts of the infinite armada: systemic cancer therapy using nanomaterials. *Nat. Rev. Clin. Oncol.* 7, 266–276.

Sleeman, J. P., Nazarenko, I., and Thiele, W. (2011). Do all roads lead to Rome? routes to metastasis development. *Int. J. Cancer* 128, 2511–2526.

Subramaniam, V., Vincent, I. R., Gilakjan, M., and Jothy, S. (2007). Suppression of human colon cancer tumors in nude mice by siRNA CD44 gene therapy. *Exp. Mol. Pathol.* 83, 332–340.

Swaby, R. F., and Cristofanilli, M. (2011). Circulating tumor cells in breast cancer: a tool whose time has come of age. *BMC Med.* 9, 43. doi: 10.1186/1741-7015-9-43

Takeuchi, H., and Kitagawa, Y. (2010). Circulating tumor cells in gastrointestinal cancer. *J. Hepatobiliary Pancreat. Sci.* 17, 577–582.

Valastyan, S., and Weinberg, R. A. (2011). Tumor metastasis: molecular insights and evolving paradigms. *Cell* 147, 275–292.

Waldron, N. N., Kaufman, D. S., Oh, S., Inde, Z., Hexum, M. K., Ohlfest, J. R., and Vallera, D. A. (2011). Targeting tumor-initiating cancer cells with dCD133KDEL shows impressive tumor reductions in a xenotransplant model of human head and neck cancer. *Mol. Cancer Ther.* 10, 1829–1838.

Wang, J., Sakariassen, P. O., Tsinkalovsky, O., Immervoll, H., Boe, S. O., Svendsen, A., Prestegarden, L., Røsland, G., Thorsen, F., Stuhr, L., Molven, A., Bjerkvig, R., and Enger, P. Ø. (2008). CD133 negative glioma cells form tumors in nude rats and give rise to CD133 positive cells. *Int. J. Cancer* 122, 761–768.

Weight, R. M., Viator, J. A., Dale, P. S., Caldwell, C. W., and Lisle, A. E. (2006). Photoacoustic detection of metastatic melanoma cells in the human circulatory system. *Opt. Lett.* 31, 2998–3000.

Wittekind, C., and Neid, M. (2005). Cancer invasion and metastasis. *Oncology* 69(Suppl. 1), 14–16.

Wojciechowski, J. C., Narasipura, S. D., Charles, N., Mickelsen, D., Rana, K., Blair, M. L., and King, M. R. (2008). Capture and enrichment of CD34-positive haematopoietic stem and progenitor cells from blood circulation using P-selectin in an implantable device. *Br. J. Haematol.* 140, 673–681.

Wong, C. W., Lee, A., Shientag, L., Yu, J., Dong, Y., Kao, G., Al-Mehdi, A. B., Bernhard, E. J., and Muschel, R. J. (2001). Apoptosis: an early event in metastatic inefficiency. *Cancer Res.* 61, 333–338.

Yu, M., Stott, S., Toner, M., Maheswaran, S., and Haber, D. A. (2011). Circulating tumor cells: approaches to isolation and characterization. *J. Cell Biol.* 192, 373–382.

Yung, C. W., Fiering, J., Mueller, A. J., and Ingber, D. E. (2009). Micromagnetic-microfluidic blood cleansing device. *Lab Chip* 9, 1171–1177.

Conflict of Interest Statement: The author declares that the research was conducted in the absence of any commercial or financial relationships that could be construed as a potential conflict of interest.

Received: 01 June 2012; paper pending published: 11 June 2012; accepted: 12 June 2012; published online: 03 July 2012.

*Citation: Faltas B (2012) Cornering metastases: therapeutic targeting of circulating tumor cells and stem cells. Front. Oncol. **2**:68. doi: 10.3389/fonc.2012.00068*

This article was submitted to Frontiers in Cancer Molecular Targets and Therapeutics, a specialty of Frontiers in Oncology.

frontiers in ONCOLOGY

REVIEW ARTICLE
published: 24 July 2012
doi: 10.3389/fonc.2012.00079

Adhesion receptors as therapeutic targets for circulating tumor cells

Jiahe Li and Michael R. King*

Department of Biomedical Engineering, Cornell University, Ithaca, NY, USA

Edited by:
Silvia Giordano, University of Torino, Italy

Reviewed by:
Maria Felice Brizzi, University of Torino, Italy
Guido Serini, University of Torino School of Medicine, Italy

***Correspondence:**
Michael R. King, Department of Biomedical Engineering, Cornell University, 205 Weill Hall, Ithaca, NY 14853, USA.
e-mail: mike.king@cornell.edu

Metastasis contributes to >90% of cancer-associated mortality. Though primary tumors can be removed by surgical resection or chemo/radiotherapy, metastatic disease is a great challenge to treatment due to its systemic nature. As metastatic "seeds," circulating tumor cells (CTCs) are believed to be responsible for dissemination from a primary tumor to anatomically distant organs. Despite the possibility of physical trapping of CTCs in microvessels, recent advances have provided insights into the involvement of a variety of adhesion molecules on CTCs. Such adhesion molecules facilitate direct interaction with the endothelium in specific tissues or indirectly through leukocytes. Importantly, significant progress has been made in understanding how these receptors confer enhanced invasion and survival advantage during hematogenous circulation of CTCs through recruitment of macrophages, neutrophils, platelets, and other cells. This review highlights the identification of novel adhesion molecules and how blocking their function can compromise successful seeding and colonization of CTCs in new microenvironment. Encouraged by existing diagnostic tools to identify and isolate CTCs, strategic targeting of these adhesion molecules to deliver conventional chemotherapeutics or novel apoptotic signals is discussed for the neutralization of CTCs in the circulation.

Keywords: adhesion, receptors, CTCs, cancer therapy

INTRODUCTION

Circulating tumor cells (CTCs) are cells that leave a primary tumor and circulate in the blood. More than a century ago the Australian physician Thomas Ashworth first observed CTCs in the blood of a patient with metastatic cancer. He hypothesized that "the cancer itself being seen in the blood may tend to throw some light upon the mode of origin of multiple tumors existing in the same person." In the past decade, advancing technologies to detect and isolate CTCs have provided unique fluid biopsy information for prognosis, management of chemotherapy dosing and timing as well as monitoring the development of drug resistance over time (Nagrath et al., 2007; Lowes et al., 2011; Scher et al., 2011). Driven by these technologies, numerous clinical studies performed for breast, colon, prostate, and other epithelial cancers establish a clear connection between average CTC counts and overall survival rate before and during treatment (Cristofanilli et al., 2004, 2005; Hou et al., 2009; Criscitiello et al., 2010; Yalcin et al., 2010; Danila et al., 2011; Lianidou and Markou, 2011).

In contrast to the rapid development of tools for CTC detection and isolation, effective therapies that directly remove CTCs from the blood circulation are still underexplored. This is probably attributable to our limited understanding of the heterogeneity of CTCs: in most studies, CTCs are defined as being positive for epithelial cell adhesion molecule (EpCAM+) and cytokeratin 8, 18, or 19 (CK+) and negative for CD45 (CD45−) (Allard et al., 2004). However, almost a third of patients with advanced breast, colorectal, and prostate cancers have CTCs that do not meet these criteria (Coumans et al., 2010). Despite the heterogeneity of CTC markers, some studies have shown that cancer stem cell (CSC) or stem-like cell (CSC-like) markers are frequently expressed by CTCs (Aktas et al., 2009; Theodoropoulos et al., 2010; Iinuma et al., 2011; Toloudi et al., 2011; Kasimir-Bauer et al., 2012; Wang et al., 2012). Such features are especially relevant for targeting CTCs as CSCs are believed to represent a subpopulation of cancer cells that drive the growth and progression of metastatic cancers (Ghiaur et al., 2012; Vermeulen et al., 2012).

The presence of CTCs in the circulation can in part explain a clinical observation that the removal of a primary tumor is often followed with distant metastasis and/or local recurrence. For example, it was estimated that 20–50% patients first diagnosed with primary breast cancer eventually developed metastatic disease in the past (Lu et al., 2009). In the case of hepatocellular carcinoma (HCC), liver transplantation is the best treatment for early-stage patients. Unfortunately, every year around 10% of recipients develop post-transplant HCC recurrence, which leads to death in almost all patients (Toso et al., 2011). To understand the molecular mechanism, Kim and colleagues developed a tumor self-seeding mouse model whereby the local recurrence mediated by CTCs was investigated using human colorectal, melanoma, and breast cancer cells. They found that tumor-derived IL-6 and IL-8 served as CTC attractants whereas the seeder CTCs highly expressed invasion-associated genes (*MMP1*, *FSCN1*, and *CXCL1*) to promote infiltration (Kim et al., 2009). This finding highlights a highly orchestrated process of local recurrence mediated by CTCs.

CTCs play a predominant role in the metastases to distant organs. In the blood circulation, CTCs are subject to a multitude of stresses including anchorage-dependent survival signaling,

immuno-surveilance, and shear stress. For example, CTCs are deprived of integrin-dependent adhesion to extracellular matrix (ECM) components in comparison to nontransformed cells. Whereas such loss of anchorage induces apoptosis (anoikis) in normal cell types, CTCs are particularly resistant to anoikis by promoting PI3K/Akt proliferation signaling and expression of anti-apoptotic proteins such as BCL2 (Frisch and Ruoslahti, 1997; Guo and Giancotti, 2004). Notably, numerous research has demonstrated that CTCs do not mobilize in the circulation alone. Instead, through heterotypic interactions with endothelial cells and different types of haemopotoeic cells, CTCs acquire the potential to metastasize to distant organs (**Figure 1**). Therefore, such receptor-mediated adhesion can provide a unique opportunity for neutralizing CTCs either through the blockade of receptors or receptor-targeted drug delivery.

THE BIOLOGY OF SELECTIN-MEDIATED HEMATOGENOUS METASTASIS

Selectins are transmembrane glycoproteins which were initially found to bind specific glycoproteins on leukocytes. Three structurally related adhesion molecules, L-, E-, and P-selectin are composed of an N-terminal C-type lectin domain which confers specific, Ca^{2+}-dependent carbohydrate-binding activity. It is followed by an epidermal growth factor (EGF)-like domain, a variable number of short consensus repeats domains (2, 6, and 9 for L-, E-, and P-selectin, respectively), a single-pass transmembrane domain and a short intracellular C-terminal tail (Ley, 2003). Despite structural similarity, the three selectins have distinct tissue-specific expression and binding kinetics. L-selectin is constitutively expressed on the surface of almost all types of leukocytes and is cleaved from the cell surface upon activation with a variety of cytokines and chemokines (Grailer et al., 2009). In contrast, the expression of E- and P-selectin is inducible on vascular endothelial cells during inflammation. Whereas E-selectin depends on de novo mRNA synthesis, P-selectin is stored in Weibel-Palade bodies of endothelial cells. Additionally, platelets express P-selectin which translocates from α-granules upon platelet activation (Larsen et al., 1992).

The role of selectins in mediating the rolling and trafficking of neutrophils and monocytes to inflammation sites has been well studied. More recently, it has been proposed that CTCs adopt similar strategies to facilitate their initial entrapment in the vessels and subsequent extravasation. Köhler and colleagues provided the first *in vivo* evidence that E- and P-selectin are essential for colorectal cancer metastasis. They generated a transgenic immuno-compromised mouse with E- and P-selectin doubly knocked out. Compared to wild-type mice, the double knockout mice with subcutaneously implanted colon cancer cells showed lung metastases reduced in number by 84% (Kohler et al., 2010). In agreement with earlier *in vitro* studies, a model was proposed in which the sialylated fucosylated glycans decorated on transmembrane proteins or specific lipids of CTCs mediate the rolling and adhesion to selectin-expressing endothelial cells. The role of selectin ligands in mediating the hematogenous metastasis of CTCs has been reviewed extensively elsewhere (Konstantopoulos and Thomas, 2009; Geng et al., 2012). However, this section focuses on therapeutic interventions of selectin binding that have been explored for the prevention of metastasis.

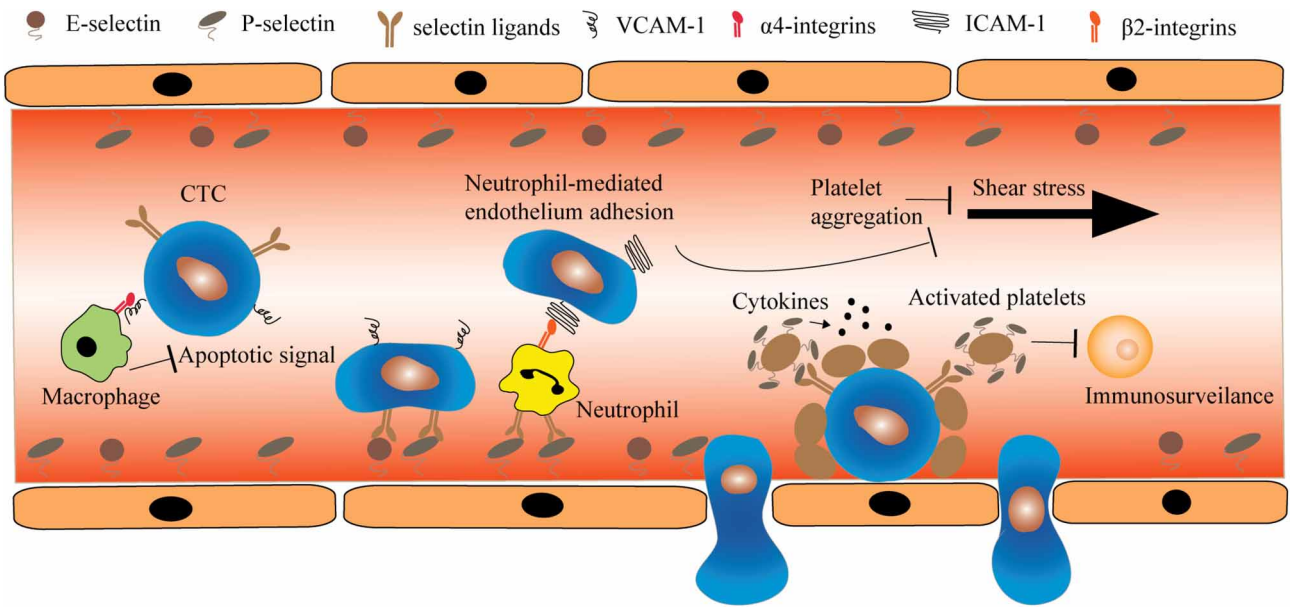

FIGURE 1 | The heterotypic cell interactions between CTCs and haemopotoeic cells in the circulation. Macrophages interact with CTCs via α4-integrin-VCAM-1 ligation and transmit anti-apoptotic signal such as TRAIL to CTCs. In contrast, certain CTCs deficient for selectin ligands can roll and adhere to endothelial cells through heterotypic interaction with neutrophils. This interaction is mediated by β2-integrin and ICAM-1 expressed on neutrophils and CTCs, respectively. Additionally, CTCs can locally induce platelet aggregation. The deposition of platelets on CTCs prevents the damage caused by shear stress and immuno-surveillance.

CARBOHYDRATE-BASED INHIBITORS

Given that all three selectins recognize sialylated fucosylated glycans such as sLe^x, the sLe^x analogs have been shown to significantly prevent neutrophil accumulation and myocardial necrosis after ischemia and reperfusion in animal models (Buerke et al., 1994; Lefer et al., 1994; Zacharowski et al., 1999). This implies that the same analogs may be potent inhibitors for reducing CTC adhesion to endothelium. Shirota and colleagues investigated the inhibitory effect of a sLe^x analog, GSC-150 on hepatic metastasis of human colon carcinoma in nude mice. They found that liver metastases were significantly attenuated when cancer cells were co-administered with GSC-150 (Shirota et al., 2001). In addition to sLe^x analogs, novel disaccharides have been generated which function as competitive substrate inhibitors for glycotransferases involved in the synthesis of sLe^x. To this end, a disaccharide compound was able to inhibit sLe^x formation in human monocytic leukemia cells, U937. Its therapeutic effect was further studied in Lewis lung carcinoma *in vivo* where the experimental metastasis was significantly reduced through the decreased expression of sLe^x (Brown et al., 2009). Nevertheless, strategies to abrogate sLe^x-selectin interaction must be considered carefully. Given the turnover rate of selectins or glycotransferases, such carbohydrates may not have a long-lasting inhibitory effect. Moreover, as sLe^x is essential for directing neutrophils and lymphocytes to inflamed tissues, the chronic exposure to sLe^x analogs or metabolic inhibitors can interfere with the normal inflammatory response. Therefore, investigations on the cellular sLe^x synthesis that differentiate CTCs from leukocytes may provide more specific targeting of CTCs while reducing side effects.

GENE SILENCING OF FUCOSYLTRANSFERASES IN CTCs

As the key determinants of selectin ligands, sLe^x and sLe^a are synthesized in the Golgi compartments by sequential actions of N-acetylglucosaminyl-, galactosyl-, sialyl-, and fucosyltransferases. Of note is the terminal step of transferring fucose to N-acetylglucosamine catalyzed by a family of fucosyltransferase genes (Hennet, 2002). At least nine *FUT* genes have been identified in the human genome among which *FUT*3, 4, 6, and 7 have been well characterized. They are redundant in the synthesis of sialyl lewis carbohydrates but display cell type-specific expression. FUT4 and FUT7 are mainly expressed in blood cell lineages and play a key role in the selectin ligand-mediated migration of leukocytes during the inflammatory response (Weninger et al., 2000). In contrast, FUT3 and FUT6 are more associated with the progression of cancers, including breast (Matsuura et al., 1998; Ding and Zheng, 2004), prostate (Barthel et al., 2008), lung (Ogawa et al., 1996), liver (Wang et al., 2003), and gastric cancer (Petretti et al., 1999). To exploit the therapeutic potential of targeting fucosyltransferases, our laboratory first confirmed that hematopoietic cell lines (HL60 and KG1a) predominantly express FUT4 and FUT7 whereas prostate cancer cell line MDA PCa2b mainly expresses FUT3. Next, siRNA against FUT3 reduced sLe^x expression on prostate cancer cells and significantly inhibited cell rolling and adhesion to a E-selectin-functionalized surface under physiological flow. In addition, the siRNA was able to impair cell growth which may not be directly associated with sLe^x. In fact, two recent studies revealed that the overexpression of FUT4 and FUT6 promoted cell growth by elevating intracellular Akt phosphorylation and suppressing the cyclin-dependent kinase inhibitor p21 in epidermoid carcinoma and HCC cells, respectively, (Yang et al., 2010; Guo et al., 2012). Therefore, silencing FUTs via siRNA can simultaneously inhibit the adhesion and clonal expansion of CTCs in the blood circulation. To apply this strategy *in vivo*, P-selectin-based liposome nanoparticles recently developed in our laboratory can be used to encapsulate siRNAs against FUTs (Huang and King, 2009). Although P-selectin recognizes both circulating leukocytes and CTCs, siRNAs against FUTs exclusively expressed in CTCs provide additional targeting specificity.

THERAPEUTIC ABROGATION OF CTC-HEMATOPOIETIC CELL INTERACTION

It is estimated that less than 0.01% of CTCs shed from a primary tumor can survive to produce clinically relevant metastases (Joyce and Pollard, 2009). This suggests that the process of metastasis by CTCs is largely inefficient. Whereas the mechanisms underlying such high rates of attrition remain poorly understood, recent studies identified two important cell adhesion molecules involved in the physical interactions of CTCs with hematopoietic cells: vascular cell adhesion molecule-1 (VCAM-1) and intercellular adhesion molecule-1 (ICAM-1). Such interactions facilitate CTCs in several aspects: (1) survival in the circulation, (2) initial arrest and subsequent extravasation, and (3) eventual growth into overt metastasis (Chambers et al., 2002).

The transmembrane protein VCAM-1 was originally thought to be presented exclusively on endothelial cells in response to tumor necrosis factor-alpha (TNF-α) and interleukin-1 (IL-1) during inflammation (Coussens and Werb, 2002). It binds to the leukocyte integrins α4β1 and α4β7 on circulating monocytes, granulocytes, and lymphocytes (Osborn et al., 1989; Elices et al., 1990). However, aberrant expression of VCAM-1 was found to be one of 18 signature genes associated with lung metastasis of breast cancer in both experimental mouse models and patients (Minn et al., 2005). Chen and colleagues found that VCAM-1 on breast cancer CTCs tethered to metastasis-associated macrophages which express α4-integrins. Clustering of VCAM-1 on CTCs induces Akt activation and protects CTCs from proapoptotic cytokines such as TNF-related apoptosis-inducing ligand (TRAIL). Notably, either silencing VCAM-1 expression by siRNA or blocking antibody against α4-integrins abolished the pro-survival effect of VCAM-1 (Chen et al., 2011). In addition, VCAM-1 was also recently found to be associated with bone metastasis in breast cancer. Prior to this study, a bone-metastatic gene signature including *CXCR4*, *IL11*, *CTGF*, *MMP1,* and *OPN* was identified through the reiterative selection of human breast cancer cells MDA-MB-231 in immuno-compromised mice (Kang et al., 2003). However, by studying a subpopulation of MDA-MB-231 which experienced a long dormancy prior to bone metastasis, Lu and colleagues discovered that the aberrant expression of VCAM-1 engaged α4-integrins on monocytic osteoclast progenitors to promote the local osteolytic activity in bone (Lu et al., 2011). This mouse study was further corroborated by comparing VCAM-1 levels between clinical early and late recurrences of bone

metastases. Higher VCAM-1 was significantly associated with early relapse (Wang et al., 2005).

Like VCAM-1, ICAM-1 is another cell surface glycoprotein which is typically expressed on endothelial cells in response to TNF-α or IL-1 in inflammation. However, the constitutive expression of ICAM-1 on CTCs was found to promote tumor cell transendothelial migration in melanoma (Huh et al., 2010), pancreatic (Roland et al., 2010), and breast cancers (Wu et al., 2001). To understand this mechanism, *in vitro* biophysical studies demonstrated that under physiological shear stress ICAM-1 on melanoma CTCs promotes the heterotypic interaction with neutrophils by engaging β2-integrins (CD11a and CD11b) (Hoskins and Dong, 2006; Liang et al., 2008). Moreover, as neutrophils have selectin ligands, such heterotypic interaction facilitates the adhesion and extravasation of melanoma CTCs which otherwise bind inefficiently to the endothelium (Slattery and Dong, 2003; Liang et al., 2005). Later, our laboratory studied the physical mechanisms of retinoblastoma metastasis. Whereas human RB cell lines RB143 and WERI-Rb27 do not express E-selectin ligands, they can be recruited to an E-selectin-coated surface through attachment to activated neutrophils. This interaction is also mediated by ICAM-1: β2-integrin (Geng et al., 2010). To test the involvement of this heterotypic interaction *in vivo*, Jin Huh and colleagues compared the lung metastases of human melanoma cells injected alone or in combination with human neutrophils (Huh et al., 2010). They found that human neutrophils enhanced CTCs retention in the lung by three-fold. To dissect the molecular mechanism, the cytokine interleukin-8 (IL-8) was found to be a key determinant expressed by melanoma cells to attract neutrophils. IL-8 secretion increased β2-integrin levels on neutrophils and heterotypic aggregation between ICAM-1-positive CTCs and neutrophils. Importantly, siRNA against IL-8 impaired transendothelial migration and lung metastasis by ∼50%. In addition to targeting IL-8 as a therapeutic approach, it is possible that blocking antibodies against ICAM-1 or β2-integrins may be also effective (Rosette et al., 2005).

PLATELETS AGGRAVATE CTC METASTASIS

Platelets are anuclear cytoplasmic bodies released from megakaryocytes in the bone marrow. It is estimated that one liter of blood contains about 400 billion circulating platelets. The primary role of platelets is to maintain haemostasis. This is initiated via platelet activation which results in adhesion and release of a multitude of bioactive factors from platelet granules. In addition to haemostatic regulation, platelets have long been believed to play a critical role in cancer metastasis through the enhancement of CTC survival and adhesion to the endothelium in the circulation. The involvement of platelets in cancer was first recorded in the mid-nineteenth century by the French clinician Armand Trousseau. He diagnosed patients with migratory thrombophlebitis caused by an occult visceral carcinoma (Gupta and Massague, 2004). In fact, preclinical studies in genetic knockout mice provide evidence that upon immediate entry into the circulation, tissue factor highly expressed by CTCs can signal downstream through FVIIa and FXa to activate a coagulation cascade leading to thrombin generation, fibrin deposition, and platelet aggregation around CTCs (Camerer et al., 2004; Kasthuri et al., 2009; Liu et al., 2011). Such a "platelet cloak" is known to initially trap tumor cells in microvessels (Borsig et al., 2001).

Several mechanisms of platelets in promoting CTC survival have been proposed based on preclinical experiments in mice using a variety of mouse and human carcinoma cell lines. Aggregation of platelets around CTCs protect against immune-mediated clearance of CTCs largely mediated by natural killer (NK) cells. The potential of CTCs to induce platelet aggregation correlates with their enhanced metastatic potential. Bernhard Nieswandt and colleagues demonstrated for the first time that platelets directly impair NK lysis of tumor cells *in vitro* and *in vivo*. In a mouse model of experimental metastasis, they found that tumor seeding in the lung was reduced when platelets were depleted from the host (Nieswandt et al., 1999). Further studies reveal that CTC evasion of NK cells is not merely attributed to physical shielding of platelets. NK cell activity is guided by the principles of "missing-self" and "induced-self," which imply that cells lacking expression of MHC class I (missing-self) and/or a stress-induced expression of ligands for activating NK receptors (induced-self) are preferentially recognized and eliminated (Moretta and Moretta, 2004; Lanier, 2005). While CTCs are often associated with lack of MHC class I, platelets can disrupt "missing self" recognition of NK cells by grafting MHC I class onto CTCs (Placke et al., 2012). Furthermore, platelet-derived transforming growth factor β (TGF-β) can downregualte the activating immunoreceptor NK group 2, member D (NKG2D) on NK cells (Kopp et al., 2009).

THERAPEUTIC INTERVENTION OF PLATELET ADHESION TO CTCs

As the blood clotting pathway contributes to platelet adhesion to CTCs, a variety of anticoagulation agents have been tested either alone or together with conventional cancer drugs in preclinical mouse models. Using an experimental metastasis mouse model, Amirkhosravi and colleagues found that the intravenous injection of recombinant mouse tissue factor pathway inhibitor (TFPI) immediately before inoculation of tumor cells reduced metastasis by 83% (Amirkhosravi et al., 2002, 2007). Similarly, Cilostazol, a selective inhibitor of phosphodiesterase 3 with anticoagulatory and profibrinolytic effects completely abolished the complex formation of 4T1 tumor cells in the presence of activated platelets *in vitro*. In a spontaneous model of mouse 4T1 breast cancer, the injection of Cilostazol six hours before tumor inoculation reduced pulmonary metastasis by 55%. As platelet aggregation and adhesion to CTCs enhance their survival in the blood circulation, abrogation of the coagulation cascade renders CTCs susceptible to cancer drugs. Wenzel and colleagues invented dual liposomes simultaneously containing the hemostatic inhibitor dipyridamole and the anticancer drug perifosine. The liposomes caused a 90% reduction in the number of lung metastases in a mouse experimental metastasis model (Wenzel et al., 2010).

Despite the fact that anticoagulants hold promise for the prevention of metastasis, they may impair the normal hemostatic function of platelets in the presence of bleeding. Platelet intervention therapies against metastasis must exhibit certain specificity for tumor cell-platelet interactions. Therefore, direct inhibition of platelet adhesion to CTCs may minimize the cardiovascular side effect of anticoagulants. To this goal, heparin and chemically

modified heparins have been shown to attenuate the metastasis of human colon carcinoma in a mouse xenograft model (Koenig et al., 1998; Stevenson et al., 2005; Hostettler et al., 2007). The anti-metastatic effect of heparin was initially believed to associate with its anticoagulant activity. Later it was found that competitive binding of heparin to P-selectin on activated platelets abolishes interaction with P-selectin ligands such as sialylated fucosylated mucins expressed on human colon carcinoma cells (Wei et al., 2004; Stevenson et al., 2005; Hostettler et al., 2007; Lee et al., 2008). As the anticoagulant activity of heparin is undesirable in the context of blocking CTC-platelet interactions, polysaccharides isolated from certain sea plants and fungi have shown enhanced inhibition of P-selectin binding without anticoagulant effect. A fucosylated chondroitin sulfate (FucCS) from sea cucumber is 4–8 fold more potent than heparin in the inhibition of LS180 carcinoma cell attachment to immobilized P- and L-selectin. Moreover, administration of FucCS 30 min prior to mouse colon carcinoma MC-38 injection is associated with 2-fold CTC-platelet aggregates than heparin in the mouse lung. Long-term experiment reveals that FuCS significantly reduced lung metastatic foci by 80% compared to saline control (Borsig et al., 2007).

THERAPEUTIC BLOCKAGE OF PLATELET SIGNALING TO CTCs

Certain CTCs express epithelial markers such as EpCAM and cytokeratins, suggesting that the epithelial-mesenchymal transition (EMT) is not necessarily required for CTCs to access the blood circulation. Instead, a transient contact between platelets and CTCs in the blood circulation is sufficient to induce an EMT gene signature and invasive behavior primarily through the platelet-secreted transforming growth factor-β1 (TGF-β1) (Labelle et al., 2011). Recently, a small molecule inhibitor, SD-208, has been shown to block the TGF-β receptor I kinase (TβRI) activity. SD-208 successfully prevented the development of TGF-β-induced bone metastases and decreased the progression of established osteolytic lesions in a melanoma mouse model (Mohammad et al., 2011). Therefore, SD-208 possibly represents a viable therapeutic to inhibit platelet-derived TGF-β signaling. In addition to TGF-β, platelet α-granules store abundant proangiogenic factors including vascular endothelial growth factor (VEGF), basic fibroblast growth factor (bFGF), EGF, platelet-derived growth factor (PDGF) and insulin-like growth factor-1 and -2 (IGF-1 and -2) (Sierko and Wojtukiewicz, 2007). Given that inhibitors for the proangiogenic factors or their counter-receptors are available as cancer drugs in the treatment of solid tumors (Roberts et al., 2005; Moreira et al., 2007; Weroha and Haluska, 2008), it is possible that such inhibitors can be used as adjuvant therapies in the context of targeting CTCs.

NOVEL SELECTIN-BASED TARGETING DRUG DELIVERY TO CTCs

Over the past several years, our laboratory has developed a biomimetic approach to isolate CTCs using a selectin-immobilized microtube device (Hughes and King, 2010; Hughes et al., 2012a,b). Two factors are responsible for the efficient capture of CTCs by this device. First, the ability of selectins to mediate the rapid tethering and rolling of leukocytes or CTCs under shear is attributed to the fast kinetics between selectins and selectin ligands (Lawrence and Springer, 1991; Wild et al., 2001). The fact that cells can be enriched under flow conditions significantly enhances the sample processing rate. Second, the microtube allows for the margination of CTCs toward the wall to interact with immobilized selectins. This margination effect has been well characterized when leukocytes circulate in a flow-dependent interaction with red blood cells (Bagge et al., 1983; Goldsmith and Spain, 1984; Iadocicco et al., 2002).

Inspired by isolating CTCs under flow conditions, we translated the device to a unique drug delivery platform whereby the immobilization of drug molecules on the surface creates a high localized concentration. One device immobilizes E-selectin-conjugated liposomes onto the surface of a blood-compatible microrenathane (MRE) tube. After encapsulating doxorubicin (DOX), the liposomes could specifically capture cells from the flow and efficiently deliver DOX into adherent cells. Moreover, a halloysite nanotube (HNT)-coated surface further enhanced the targeting and killing of cancer cells (**Figures 2A,B**), which was attributed to the increased surface area for both E-selectin and DOX.

To provide more specificity to CTCs, two additional approaches have been pursued by our laboratory. One approach was to functionalize the microtube surface with both E-selectin and antibodies against epithelial markers such as EpCAM. Such additional antibodies were able to discriminate between leukocytes and CTCs when cells roll on the surface (Hughes et al., 2012a). The second approach was to replace DOX with molecules that are tumor-specific, such as TRAIL. TRAIL holds promise as a tumor-specific therapeutic as it selectively induces an apoptotic signal by binding to death receptors on the cell surface (Koschny et al., 2007; Wang, 2008). To this end, our lab developed a death receptor-mediated apoptosis device to deliver apoptosis signal to captured CTCs (**Figure 3A**). Notably, with TRAIL and E-selectin on the surface, one hour of rolling exposure was sufficient to kill 30% of leukemia cells (HL60) whereas the viability of normal mononuclear cells was not affected (**Figures 3B,C**) (Rana et al., 2009, 2012).

CONCLUDING REMARKS

In haematogenous metastasis, a primary tumor sheds CTCs into the blood circulation which comprise a population of carcinoma cells that can exhibit CSC or CSC-like features. Two hypotheses have been proposed regarding how CTCs establish the initial contact with endothelial cells prior to metastasis. The physical trapping hypothesis is based on the fact that the luminal diameter of capillaries is ∼8 μm while the diameter of CTCs ranges from 20 to 30 μm. Thus, CTCs can be simply mechanically trapped in the capillary bed during their first pass through the circulation (Valastyan and Weinberg, 2011). However, the findings that certain CTCs display organ-specific tropism (e.g., bone metastases in breast and prostate cancer) challenge this hypothesis (Kang et al., 2003; Barthel et al., 2008). In fact, by displaying selectin ligands on their surface, CTCs in certain cancers acquire the ability to roll and adhere to the endothelium and subsequently exit from the circulation. The identification of selectin-dependent

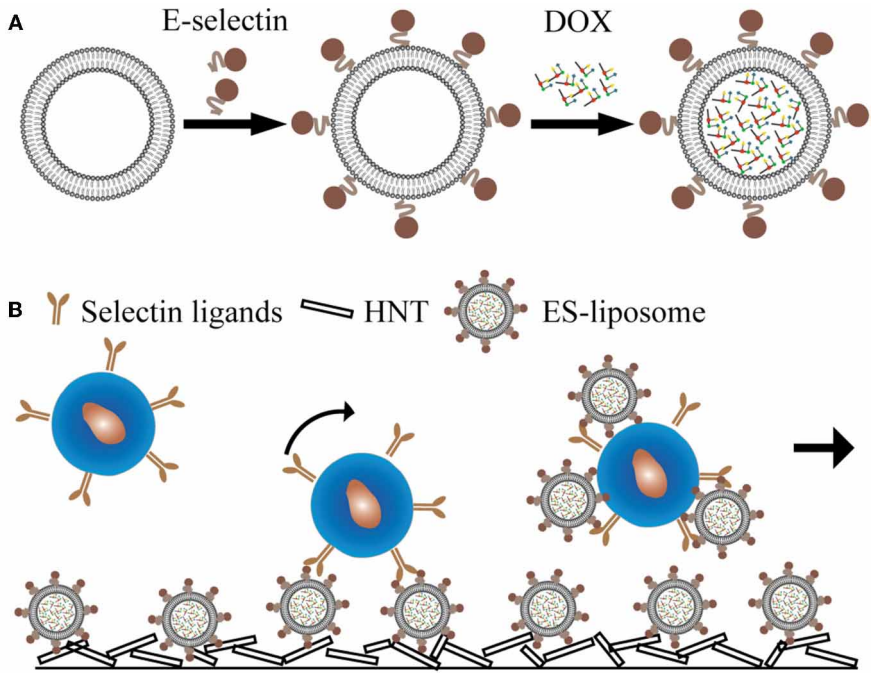

FIGURE 2 | E-selectin liposomal and nanotube-targeted delivery of doxorubicin to CTCs. (A) Schematic of E-selectin-coated liposome encapsulating doxorubicin (DOX). **(B)** Schematic of a microtube device for delivering DOX to captured CTCs.

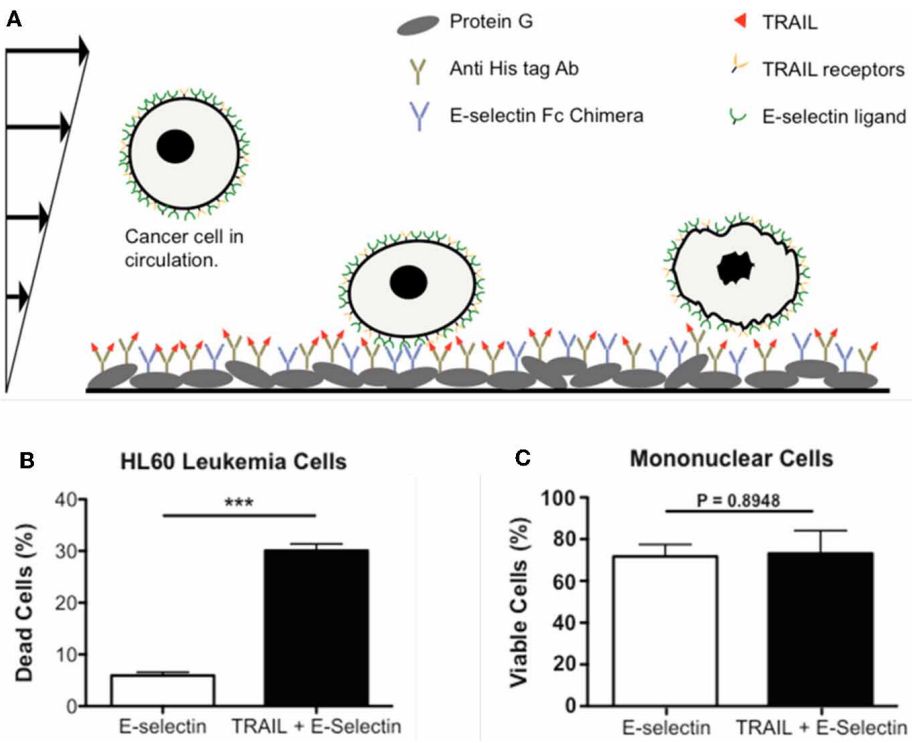

FIGURE 3 | Delivery of apoptotic signal to rolling cancer cells. **(A)** Schematic of a biomimetic device for inducing apoptosis in CTCs using E-selectin and TRAIL. **(B)** HL60 leukemic cells are eliminated by approximately 30% following perfusion through a device coated with both E-selectin and TRAIL. **(C)** Viability of normal mononuclear cells is not affected by the TRAIL-coating, confirming the specificity of TRAIL for malignant cells. **(A–C)** are reproduced from Rana et al., 2009 with permission. Rana et al., 2009 is Copyright 2008 Wiley Periodicals, Inc.).

metastasis has made it possible to develop a range of antagonists against selectins or selectin ligands. Such antagonists have proven efficient in reducing experimental metastases in many mouse cancer models. However, they may impair the selectin-dependent trafficking of leukocytes to inflamed areas during the normal inflammatory response. The gene silencing of specific FUTs may confer specificity to CTCs as different FUTs have been shown to differentially express in CTCs versus leukocytes (Yin et al., 2010). Nevertheless, the CTC-endothelium interaction alone is not sufficient for CTCs to overcome damages incurred by hemodynamic shear forces and immuno-surveillance. The survival of CTCs in the blood circulation also depends on the interactions with haemopoetic cells such as macrophages, neutrophils, and platelets which require distinct adhesion receptors. Though the abrogation of individual adhesion receptors has shown promising results in a variety of mouse cancer models, it may be clinically relevant to develop a cocktail therapy which simultaneously targets multiple interactions between CTCs and other cell types.

ACKNOWLEDGMENTS

This work was supported by NIH Grant No. CA143876 to Michael R. King.

REFERENCES

Aktas, B., Tewes, M., Fehm, T., Hauch, S., Kimmig, R., and Kasimir-Bauer, S. (2009). Stem cell and epithelial-mesenchymal transition markers are frequently overexpressed in circulating tumor cells of metastatic breast cancer patients. *Breast Cancer Res.* 11, R46.

Allard, W. J., Matera, J., Miller, M. C., Repollet, M., Connelly, M. C., Rao, C., Tibbe, A. G., Uhr, J. W., and Terstappen, L. W. (2004). Tumor cells circulate in the peripheral blood of all major carcinomas but not in healthy subjects or patients with nonmalignant diseases. *Clin. Cancer Res.* 10, 6897–6904.

Amirkhosravi, A., Meyer, T., Amaya, M., Davila, M., Mousa, S. A., Robson, T., and Francis, J. L. (2007). The role of tissue factor pathway inhibitor in tumor growth and metastasis. *Semin. Thromb. Hemost.* 33, 643–652.

Amirkhosravi, A., Meyer, T., Chang, J. Y., Amaya, M., Siddiqui, F., Desai, H., and Francis, J. L. (2002). Tissue factor pathway inhibitor reduces experimental lung metastasis of B16 melanoma. *Thromb. Haemost.* 87, 930–936.

Bagge, U., Blixt, A., and Strid, K. G. (1983). The initiation of post-capillary margination of leukocytes: studies *in vitro* on the influence of erythrocyte concentration and flow velocity. *Int. J. Microcirc. Clin. Exp.* 2, 215–227.

Barthel, S. R., Gavino, J. D., Wiese, G. K., Jaynes, J. M., Siddiqui, J., and Dimitroff, C. J. (2008). Analysis of glycosyltransferase expression in metastatic prostate cancer cells capable of rolling activity on microvascular endothelial (E)-selectin. *Glycobiology* 18, 806–817.

Borsig, L., Wang, L., Cavalcante, M. C., Cardilo-Reis, L., Ferreira, P. L., Mourao, P. A., Esko, J. D., and Pavao, M. S. (2007). Selectin blocking activity of a fucosylated chondroitin sulfate glycosaminoglycan from sea cucumber. Effect on tumor metastasis and neutrophil recruitment. *J. Biol. Chem.* 282, 14984–14991.

Borsig, L., Wong, R., Feramisco, J., Nadeau, D. R., Varki, N. M., and Varki, A. (2001). Heparin and cancer revisited: mechanistic connections involving platelets, P-selectin, carcinoma mucins, and tumor metastasis. *Proc. Natl. Acad. Sci. U.S.A.* 98, 3352–3357.

Brown, J. R., Yang, F., Sinha, A., Ramakrishnan, B., Tor, Y., Qasba, P. K., and Esko, J. D. (2009). Deoxygenated disaccharide analogs as specific inhibitors of beta1-4-galactosyltransferase 1 and selectin-mediated tumor metastasis. *J. Biol. Chem.* 284, 4952–4959.

Buerke, M., Weyrich, A. S., Zheng, Z., Gaeta, F. C., Forrest, M. J., and Lefer, A. M. (1994). Sialyl Lewisx-containing oligosaccharide attenuates myocardial reperfusion injury in cats. *J. Clin. Invest.* 93, 1140–1148.

Camerer, E., Qazi, A. A., Duong, D. N., Cornelissen, I., Advincula, R., and Coughlin, S. R. (2004). Platelets, protease-activated receptors, and fibrinogen in hematogenous metastasis. *Blood* 104, 397–401.

Chambers, A. F., Groom, A. C., and Macdonald, I. C. (2002). Dissemination and growth of cancer cells in metastatic sites. *Nat. Rev. Cancer* 2, 563–572.

Chen, Q., Zhang, X. H., and Massague, J. (2011). Macrophage binding to receptor VCAM-1 transmits survival signals in breast cancer cells that invade the lungs. *Cancer Cell* 20, 538–549.

Coumans, F. A., Doggen, C. J., Attard, G., De Bono, J. S., and Terstappen, L. W. (2010). All circulating EpCAM+CK+CD45- objects predict overall survival in castration-resistant prostate cancer. *Ann. Oncol.* 21, 1851–1857.

Coussens, L. M., and Werb, Z. (2002). Inflammation and cancer. *Nature* 420, 860–867.

Criscitiello, C., Sotiriou, C., and Ignatiadis, M. (2010). Circulating tumor cells and emerging blood biomarkers in breast cancer. *Curr. Opin. Oncol.* 22, 552–558.

Cristofanilli, M., Budd, G. T., Ellis, M. J., Stopeck, A., Matera, J., Miller, M. C., Reuben, J. M., Doyle, G. V., Allard, W. J., Terstappen, L. W., and Hayes, D. F. (2004). Circulating tumor cells, disease progression, and survival in metastatic breast cancer. *N. Engl. J. Med.* 351, 781–791.

Cristofanilli, M., Hayes, D. F., Budd, G. T., Ellis, M. J., Stopeck, A., Reuben, J. M., Doyle, G. V., Matera, J., Allard, W. J., Miller, M. C., Fritsche, H. A., Hortobagyi, G. N., and Terstappen, L. W. (2005). Circulating tumor cells: a novel prognostic factor for newly diagnosed metastatic breast cancer. *J. Clin. Oncol.* 23, 1420–1430.

Danila, D. C., Fleisher, M., and Scher, H. I. (2011). Circulating tumor cells as biomarkers in prostate cancer. *Clin. Cancer Res.* 17, 3903–3912.

Ding, K. F., and Zheng, S. (2004). [Study on relationship of fucosyltransferase gene types in breast cancer with metastasis and prognosis]. *Zhonghua Wai Ke Za Zhi* 42, 546–550.

Elices, M. J., Osborn, L., Takada, Y., Crouse, C., Luhowskyj, S., Hemler, M. E., and Lobb, R. R. (1990). VCAM-1 on activated endothelium interacts with the leukocyte integrin VLA-4 at a site distinct from the VLA-4/fibronectin binding site. *Cell* 60, 577–584.

Frisch, S. M., and Ruoslahti, E. (1997). Integrins and anoikis. *Curr. Opin. Cell Biol.* 9, 701–706.

Geng, Y., Marshall, J. R., and King, M. R. (2012). Glycomechanics of the metastatic cascade: tumor cell-endothelial cell interactions in the circulation. *Ann. Biomed. Eng.* 40, 790–805.

Geng, Y., Narasipura, S., Seigel, G. M., and King, M. R. (2010). Vascular recruitment of human retinoblastoma cells by multi-cellular adhesive interactions with circulating leukocytes. *Cell. Mol. Bioeng.* 3, 361–368.

Ghiaur, G., Gerber, J. M., Matsui, W., and Jones, R. J. (2012). Cancer stem cells: relevance to clinical transplantation. *Curr. Opin. Oncol.* 24, 170–175.

Goldsmith, H. L., and Spain, S. (1984). Margination of leukocytes in blood flow through small tubes. *Microvasc. Res.* 27, 204–222.

Grailer, J. J., Kodera, M., and Steeber, D. A. (2009). L-selectin: role in regulating homeostasis and cutaneous inflammation. *J. Dermatol. Sci.* 56, 141–147.

Guo, Q., Guo, B., Wang, Y., Wu, J., Jiang, W., Zhao, S., Qiao, S., and Wu, Y. (2012). Functional analysis of alpha1, 3/4-fucosyltransferase VI in human hepatocellular carcinoma cells. *Biochem. Biophys. Res. Commun.* 417, 311–317.

Guo, W., and Giancotti, F. G. (2004). Integrin signalling during tumour progression. *Nat. Rev. Mol. Cell Biol.* 5, 816–826.

Gupta, G. P., and Massague, J. (2004). Platelets and metastasis revisited: a novel fatty link. *J. Clin. Invest.* 114, 1691–1693.

Hennet, T. (2002). The galactosyltransferase family. *Cell. Mol. Life Sci.* 59, 1081–1095.

Hoskins, M. H., and Dong, C. (2006). Kinetics analysis of binding between melanoma cells and neutrophils. *Mol. Cell. Biomech.* 3, 79–87.

Hostettler, N., Naggi, A., Torri, G., Ishai-Michaeli, R., Casu, B., Vlodavsky, I., and Borsig, L. (2007). P-selectin- and heparanase-dependent antimetastatic activity of non-anticoagulant heparins. *FASEB J.* 21, 3562–3572.

Hou, J. M., Greystoke, A., Lancashire, L., Cummings, J., Ward, T., Board,

R., Amir, E., Hughes, S., Krebs, M., Hughes, A., Ranson, M., Lorigan, P., Dive, C., and Blackhall, F. H. (2009). Evaluation of circulating tumor cells and serological cell death biomarkers in small cell lung cancer patients undergoing chemotherapy. *Am. J. Pathol.* 175, 808–816.

Huang, Z., and King, M. R. (2009). An immobilized nanoparticle-based platform for efficient gene knockdown of targeted cells in the circulation. *Gene Ther.* 16, 1271–1282.

Hughes, A. D., and King, M. R. (2010). Use of naturally occurring halloysite nanotubes for enhanced capture of flowing cells. *Langmuir* 26, 12155–12164.

Hughes, A. D., Mattison, J., Western, L. T., Powderly, J. D., Greene, B. T., and King, M. R. (2012a). Microtube device for selectin-mediated capture of viable circulating tumor cells from blood. *Clin. Chem.* 58, 846–853.

Hughes, A. D., Mattison, J., Powderly, J. D., Greene, B. T., and King, M. R. (2012b). Rapid isolation of viable circulating tumor cells from patient blood samples. *J. Vis. Exp.* pii: 4248.

Huh, S. J., Liang, S., Sharma, A., Dong, C., and Robertson, G. P. (2010). Transiently entrapped circulating tumor cells interact with neutrophils to facilitate lung metastasis development. *Cancer Res.* 70, 6071–6082.

Iadocicco, K., Monteiro, L. H., and Chaui-Berlinck, J. G. (2002). A theoretical model for estimating the margination constant of leukocytes. *BMC Physiol.* 2, 3.

Iinuma, H., Watanabe, T., Mimori, K., Adachi, M., Hayashi, N., Tamura, J., Matsuda, K., Fukushima, R., Okinaga, K., Sasako, M., and Mori, M. (2011). Clinical significance of circulating tumor cells, including cancer stem-like cells, in peripheral blood for recurrence and prognosis in patients with Dukes' stage B and C colorectal cancer. *J. Clin. Oncol.* 29, 1547–1555.

Joyce, J. A., and Pollard, J. W. (2009). Microenvironmental regulation of metastasis. *Nat. Rev. Cancer* 9, 239–252.

Kang, Y., Siegel, P. M., Shu, W., Drobnjak, M., Kakonen, S. M., Cordon-Cardo, C., Guise, T. A., and Massague, J. (2003). A multigenic program mediating breast cancer metastasis to bone. *Cancer Cell* 3, 537–549.

Kasimir-Bauer, S., Hoffmann, O., Wallwiener, D., Kimmig, R., and Fehm, T. (2012). Expression of stem cell and epithelial-mesenchymal transition markers in primary breast cancer patients with circulating tumor cells. *Breast Cancer Res.* 14, R15.

Kasthuri, R. S., Taubman, M. B., and Mackman, N. (2009). Role of tissue factor in cancer. *J. Clin. Oncol.* 27, 4834–4838.

Kim, M. Y., Oskarsson, T., Acharyya, S., Nguyen, D. X., Zhang, X. H., Norton, L., and Massague, J. (2009). Tumor self-seeding by circulating cancer cells. *Cell* 139, 1315–1326.

Koenig, A., Norgard-Sumnicht, K., Linhardt, R., and Varki, A. (1998). Differential interactions of heparin and heparan sulfate glycosaminoglycans with the selectins. Implications for the use of unfractionated and low molecular weight heparins as therapeutic agents. *J. Clin. Invest.* 101, 877–889.

Kohler, S., Ullrich, S., Richter, U., and Schumacher, U. (2010). E-/P-selectins and colon carcinoma metastasis: first *in vivo* evidence for their crucial role in a clinically relevant model of spontaneous metastasis formation in the lung. *Br. J. Cancer* 102, 602–609.

Konstantopoulos, K., and Thomas, S. N. (2009). Cancer cells in transit: the vascular interactions of tumor cells. *Annu. Rev. Biomed. Eng.* 11, 177–202.

Kopp, H. G., Placke, T., and Salih, H. R. (2009). Platelet-derived transforming growth factor-beta down-regulates NKG2D thereby inhibiting natural killer cell antitumor reactivity. *Cancer Res.* 69, 7775–7783.

Koschny, R., Walczak, H., and Ganten, T. M. (2007). The promise of TRAIL–potential and risks of a novel anticancer therapy. *J. Mol. Med. (Berl.)* 85, 923–935.

Labelle, M., Begum, S., and Hynes, R. O. (2011). Direct signaling between platelets and cancer cells induces an epithelial-mesenchymal-like transition and promotes metastasis. *Cancer Cell* 20, 576–590.

Lanier, L. L. (2005). NK cell recognition. *Annu. Rev. Immunol.* 23, 225–274.

Larsen, G. R., Sako, D., Ahern, T. J., Shaffer, M., Erban, J., Sajer, S. A., Gibson, R. M., Wagner, D. D., Furie, B. C., and Furie, B. (1992). P-selectin and E-selectin. Distinct but overlapping leukocyte ligand specificities. *J. Biol. Chem.* 267, 11104–11110.

Lawrence, M. B., and Springer, T. A. (1991). Leukocytes roll on a selectin at physiologic flow rates: distinction from and prerequisite for adhesion through integrins. *Cell* 65, 859–873.

Lee, D. Y., Park, K., Kim, S. K., Park, R. W., Kwon, I. C., Kim, S. Y., and Byun, Y. (2008). Antimetastatic effect of an orally active heparin derivative on experimentally induced metastasis. *Clin. Cancer Res.* 14, 2841–2849.

Lefer, D. J., Flynn, D. M., Phillips, M. L., Ratcliffe, M., and Buda, A. J. (1994). A novel sialyl LewisX analog attenuates neutrophil accumulation and myocardial necrosis after ischemia and reperfusion. *Circulation* 90, 2390–2401.

Ley, K. (2003). The role of selectins in inflammation and disease. *Trends Mol. Med.* 9, 263–268.

Liang, S., Fu, C., Wagner, D., Guo, H., Zhan, D., Dong, C., and Long, M. (2008). Two-dimensional kinetics of beta 2-integrin and ICAM-1 bindings between neutrophils and melanoma cells in a shear flow. *Am. J. Physiol. Cell Physiol.* 294, C743–C753.

Liang, S., Slattery, M. J., and Dong, C. (2005). Shear stress and shear rate differentially affect the multi-step process of leukocyte-facilitated melanoma adhesion. *Exp. Cell Res.* 310, 282–292.

Lianidou, E. S., and Markou, A. (2011). Circulating tumor cells as emerging tumor biomarkers in breast cancer. *Clin. Chem. Lab. Med.* 49, 1579–1590.

Liu, Y., Jiang, P., Capkova, K., Xue, D., Ye, L., Sinha, S. C., Mackman, N., Janda, K. D., and Liu, C. (2011). Tissue factor-activated coagulation cascade in the tumor microenvironment is critical for tumor progression and an effective target for therapy. *Cancer Res.* 71, 6492–6502.

Lowes, L. E., Goodale, D., Keeney, M., and Allan, A. L. (2011). Image cytometry analysis of circulating tumor cells. *Methods Cell Biol.* 102, 261–290.

Lu, J., Steeg, P. S., Price, J. E., Krishnamurthy, S., Mani, S. A., Reuben, J., Cristofanilli, M., Dontu, G., Bidaut, L., Valero, V., Hortobagyi, G. N., and Yu, D. (2009). Breast cancer metastasis: challenges and opportunities. *Cancer Res.* 69, 4951–4953.

Lu, X., Mu, E., Wei, Y., Riethdorf, S., Yang, Q., Yuan, M., Yan, J., Hua, Y., Tiede, B. J., Haffty, B. G., Pantel, K., Massague, J., and Kang, Y. (2011). VCAM-1 promotes osteolytic expansion of indolent bone micrometastasis of breast cancer by engaging alpha4beta1-positive osteoclast progenitors. *Cancer Cell* 20, 701–714.

Matsuura, N., Narita, T., Hiraiwa, N., Hiraiwa, M., Murai, H., Iwase, T., Funahashi, H., Imai, T., Takagi, H., and Kannagi, R. (1998). Gene expression of fucosyl- and sialyltransferases which synthesize sialyl Lewisx, the carbohydrate ligands for E-selectin, in human breast cancer. *Int. J. Oncol.* 12, 1157–1164.

Minn, A. J., Gupta, G. P., Siegel, P. M., Bos, P. D., Shu, W., Giri, D. D., Viale, A., Olshen, A. B., Gerald, W. L., and Massague, J. (2005). Genes that mediate breast cancer metastasis to lung. *Nature* 436, 518–524.

Mohammad, K. S., Javelaud, D., Fournier, P. G., Niewolna, M., McKenna, C. R., Peng, X. H., Duong, V., Dunn, L. K., Mauviel, A., and Guise, T. A. (2011). TGF-beta-RI kinase inhibitor SD-208 reduces the development and progression of melanoma bone metastases. *Cancer Res.* 71, 175–184.

Moreira, I. S., Fernandes, P. A., and Ramos, M. J. (2007). Vascular endothelial growth factor (VEGF) inhibition–a critical review. *Anticancer Agents Med. Chem.* 7, 223–245.

Moretta, L., and Moretta, A. (2004). Unravelling natural killer cell function: triggering and inhibitory human NK receptors. *EMBO J.* 23, 255–259.

Nagrath, S., Sequist, L. V., Maheswaran, S., Bell, D. W., Irimia, D., Ulkus, L., Smith, M. R., Kwak, E. L., Digumarthy, S., Muzikansky, A., Ryan, P., Balis, U. J., Tompkins, R. G., Haber, D. A., and Toner, M. (2007). Isolation of rare circulating tumour cells in cancer patients by microchip technology. *Nature* 450, 1235–1239.

Nieswandt, B., Hafner, M., Echtenacher, B., and Mannel, D. N. (1999). Lysis of tumor cells by natural killer cells in mice is impeded by platelets. *Cancer Res.* 59, 1295–1300.

Ogawa, J., Inoue, H., and Koide, S. (1996). Expression of alpha-1, 3-fucosyltransferase type IV and VII genes is related to poor prognosis in lung cancer. *Cancer Res.* 56, 325–329.

Osborn, L., Hession, C., Tizard, R., Vassallo, C., Luhowskyj, S., Chi-Rosso, G., and Lobb, R. (1989). Direct expression cloning of vascular cell adhesion molecule 1, a cytokine-induced endothelial protein that binds to lymphocytes. *Cell* 59, 1203–1211.

Petretti, T., Schulze, B., Schlag, P. M., and Kemmner, W. (1999). Altered mRNA expression of glycosyltransferases in human gastric carcinomas. *Biochim. Biophys. Acta* 1428, 209–218.

Placke, T., Orgel, M., Schaller, M., Jung, G., Rammensee, H. G., Kopp, H. G., and Salih, H. R. (2012). Platelet-derived MHC class I confers a pseudonormal phenotype to cancer cells that subverts the antitumor reactivity of natural killer immune cells. *Cancer Res.* 72, 440–448.

Rana, K., Liesveld, J. L., and King, M. R. (2009). Delivery of apoptotic signal to rolling cancer cells: a novel biomimetic technique using immobilized TRAIL and E-selectin. *Biotechnol. Bioeng.* 102, 1692–1702.

Rana, K., Reinhart-King, C. A., and King, M. R. (2012). Inducing apoptosis in rolling cancer cells: a combined therapy with aspirin and immobilized TRAIL and E-selectin. *Mol. Pharm.* doi: 10.1021/mp300073j. [Epub ahead of print].

Roberts, W. G., Whalen, P. M., Soderstrom, E., Moraski, G., Lyssikatos, J. P., Wang, H. F., Cooper, B., Baker, D. A., Savage, D., Dalvie, D., Atherton, J. A., Ralston, S., Szewc, R., Kath, J. C., Lin, J., Soderstrom, C., Tkalcevic, G., Cohen, B. D., Pollack, V., Barth, W., Hungerford, W., and Ung, E. (2005). Antiangiogenic and antitumor activity of a selective PDGFR tyrosine kinase inhibitor, CP-673, 451. *Cancer Res.* 65, 957–966.

Roland, C. L., Dineen, S. P., Toombs, J. E., Carbon, J. G., Smith, C. W., Brekken, R. A., and Barnett, C. C. Jr. (2010). Tumor-derived intercellular adhesion molecule-1 mediates tumor-associated leukocyte infiltration in orthotopic pancreatic xenografts. *Exp. Biol. Med. (Maywood)* 235, 263–270.

Rosette, C., Roth, R. B., Oeth, P., Braun, A., Kammerer, S., Ekblom, J., and Denissenko, M. F. (2005). Role of ICAM1 in invasion of human breast cancer cells. *Carcinogenesis* 26, 943–950.

Scher, H. I., Morris, M. J., Basch, E., and Heller, G. (2011). End points and outcomes in castration-resistant prostate cancer: from clinical trials to clinical practice. *J. Clin. Oncol.* 29, 3695–3704.

Shirota, K., Kato, Y., Irimura, T., Kondo, H., and Sugiyama, Y. (2001). Anti-metastatic effect of the sialyl Lewis-X analog GSC-150 on the human colon carcinoma derived cell line KM12-HX in the mouse. *Biol. Pharm. Bull.* 24, 316–319.

Sierko, E., and Wojtukiewicz, M. Z. (2007). Inhibition of platelet function: does it offer a chance of better cancer progression control? *Semin. Thromb. Hemost.* 33, 712–721.

Slattery, M. J., and Dong, C. (2003). Neutrophils influence melanoma adhesion and migration under flow conditions. *Int. J. Cancer* 106, 713–722.

Stevenson, J. L., Choi, S. H., and Varki, A. (2005). Differential metastasis inhibition by clinically relevant levels of heparins–correlation with selectin inhibition, not antithrombotic activity. *Clin. Cancer Res.* 11, 7003–7011.

Theodoropoulos, P. A., Polioudaki, H., Agelaki, S., Kallergi, G., Saridaki, Z., Mavroudis, D., and Georgoulias, V. (2010). Circulating tumor cells with a putative stem cell phenotype in peripheral blood of patients with breast cancer. *Cancer Lett.* 288, 99–106.

Toloudi, M., Apostolou, P., Chatziioannou, M., and Papasotiriou, I. (2011). Correlation between cancer stem cells and circulating tumor cells and their value. *Case Rep. Oncol.* 4, 44–54.

Toso, C., Mentha, G., and Majno, P. (2011). Liver transplantation for hepatocellular carcinoma: five steps to prevent recurrence. *Am. J. Transplant.* 11, 2031–2035.

Valastyan, S., and Weinberg, R. A. (2011). Tumor metastasis: molecular insights and evolving paradigms. *Cell* 147, 275–292.

Vermeulen, L., De Sousa E Melo, F., Richel, D. J., and Medema, J. P. (2012). The developing cancer stem-cell model: clinical challenges and opportunities. *Lancet Oncol.* 13, e83–e89.

Wang, J., Cao, M. G., You, C. Z., Wang, C. L., Liu, S. L., Kai, C., and Dou, J. (2012). A preliminary investigation of the relationship between circulating tumor cells and cancer stem cells in patients with breast cancer. *Cell. Mol. Biol. (Noisy-le-grand)* 58(Suppl.), OL1641–OL1645.

Wang, S. (2008). The promise of cancer therapeutics targeting the TNF-related apoptosis-inducing ligand and TRAIL receptor pathway. *Oncogene* 27, 6207–6215.

Wang, Q. Y., Wu, S. L., Chen, J. H., Liu, F., and Chen, H. L. (2003). Expressions of Lewis antigens in human non-small cell pulmonary cancer and primary liver cancer with different pathological conditions. *J. Exp. Clin. Cancer Res.* 22, 431–440.

Wang, Y., Klijn, J. G., Zhang, Y., Sieuwerts, A. M., Look, M. P., Yang, F., Talantov, D., Timmermans, M., Meijer-Van Gelder, M. E., Yu, J., Jatkoe, T., Berns, E. M., Atkins, D., and Foekens, J. A. (2005). Gene-expression profiles to predict distant metastasis of lymph-node-negative primary breast cancer. *Lancet* 365, 671–679.

Wei, M., Tai, G., Gao, Y., Li, N., Huang, B., Zhou, Y., Hao, S., and Zeng, X. (2004). Modified heparin inhibits P-selectin-mediated cell adhesion of human colon carcinoma cells to immobilized platelets under dynamic flow conditions. *J. Biol. Chem.* 279, 29202–29210.

Weninger, W., Ulfman, L. H., Cheng, G., Souchkova, N., Quackenbush, E. J., Lowe, J. B., and Von Andrian, U. H. (2000). Specialized contributions by alpha(1,3)-fucosyltransferase-IV and FucT-VII during leukocyte rolling in dermal microvessels. *Immunity* 12, 665–676.

Wenzel, J., Zeisig, R., Haider, W., Habedank, S., and Fichtner, I. (2010). Inhibition of pulmonary metastasis in a human MT3 breast cancer xenograft model by dual liposomes preventing intravasal fibrin clot formation. *Breast Cancer Res. Treat.* 121, 13–22.

Weroha, S. J., and Haluska, P. (2008). IGF-1 receptor inhibitors in clinical trials–early lessons. *J. Mammary Gland Biol. Neoplasia* 13, 471–483.

Wild, M. K., Huang, M. C., Schulze-Horsel, U., Van Der Merwe, P. A., and Vestweber, D. (2001). Affinity, kinetics, and thermodynamics of E-selectin binding to E-selectin ligand-1. *J. Biol. Chem.* 276, 31602–31612.

Wu, Q. D., Wang, J. H., Condron, C., Bouchier-Hayes, D., and Redmond, H. P. (2001). Human neutrophils facilitate tumor cell transendothelial migration. *Am. J. Physiol. Cell Physiol.* 280, C814–C822.

Yalcin, S., Kilickap, S., Portakal, O., Arslan, C., Hascelik, G., and Kutluk, T. (2010). Determination of circulating tumor cells for detection of colorectal cancer progression or recurrence. *Hepatogastroenterology* 57, 1395–1398.

Yang, X. S., Liu, S., Liu, Y. J., Liu, J. W., Liu, T. J., Wang, X. Q., and Yan, Q. (2010). Overexpression of fucosyltransferase IV promotes A431 cell proliferation through activating MAPK and PI3K/Akt signaling pathways. *J. Cell. Physiol.* 225, 612–619.

Yin, X., Rana, K., Ponmudi, V., and King, M. R. (2010). Knockdown of fucosyltransferase III disrupts the adhesion of circulating cancer cells to E-selectin without affecting hematopoietic cell adhesion. *Carbohydr. Res.* 345, 2334–2342.

Zacharowski, K., Otto, M., Hafner, G., Marsh, H. C. Jr., and Thiemermann, C. (1999). Reduction of myocardial infarct size with sCR1sLe(x), an alternatively glycosylated form of human soluble complement receptor type 1 (sCR1), possessing sialyl Lewis x. *Br. J. Pharmacol.* 128, 945–952.

Conflict of Interest Statement: Michael R. King is a scientific advisor of CellTraffix, Inc. Jiahe Li has no commercial or financial relationships that could be construed as a potential conflict of interest.

Received: 29 May 2012; accepted: 07 July 2012; published online: 24 July 2012.
*Citation: Li J and King MR (2012) Adhesion receptors as therapeutic targets for circulating tumor cells. Front. Oncol. **2**:79. doi: 10.3389/fonc.2012.00079*
This article was submitted to Frontiers in Cancer Molecular Targets and Therapeutics, a specialty of Frontiers in Oncology.

frontiers in ONCOLOGY

REVIEW ARTICLE
published: 02 August 2012
doi: 10.3389/fonc.2012.00086

Targeting myelogenous leukemia stem cells: role of the circulation

Jane Liesveld*

Hematology/Oncology Division, University of Rochester, Rochester, NY, USA

Edited by:
Michael R. King, Cornell University, USA

Reviewed by:
Joel Wojciechowski, Balance Engineering LLC, USA
Srinivas Narasipura, Rush University, USA

****Correspondence:***
Jane Liesveld, Hematology/Oncology Division, University of Rochester, Box 704, 601 Elmwood Avenue, Rochester, NY, USA.
e-mail: jane_liesveld@urmc.rochester.edu

Unlike stem cells from solid tumors, the stem cells which initiate myelogenous leukemias arise in marrow, an organ with a unique circulation which allows ready access of leukemia cells, including leukemia stem cells (LSCs), to the vasculature. This poses unique problems in the targeting of LSCs since these cells are found circulating in the majority of leukemia cases at diagnosis and are usually not detectable during remission states. Because most cases of leukemia relapse, it is suggested that LSCs remain quiescent in the marrow until they eventually proliferate and circulate again. This indicates that effective targeting of LSCs must occur not only in peripheral circulation but in the micro-circulation of the marrow. Targeting such interactions may overcome cell adhesion-mediated treatment resistance, other multi-drug resistance mechanisms, and opportunities for clonal evolution in the marrow environment. Targeting selectins and integrins, signal transduction mediators, and chemokine/cytokine networks in the marrow micro-circulation may aid in abrogating leukemia-initiating stem cells which contribute to disease relapse. LSCs possess surface antigen profiles and signal transduction activation profiles which may allow differential targeting as compared with normal hematopoietic stem cells.

Keywords: leukemia stem cells, antibody, signal transduction, vascular interactions, targeting

DEFINING THE LEUKEMIA STEM CELL AND ITS IMPORTANCE

Myeloid leukemias are a group of disorders arising in marrow and often involving blood which are characterized by overproduction of immature leukocytes or terminally differentiated cells as in chronic myelogenous leukemia (CML). In this review, we will focus on acute leukemias where impairment of differentiation is found. Most therapies available to treat acute myelogenous leukemia target leukemia blast cells which are in general a later progenitor/precursor cell no longer capable of self-renewal and multipotential differentiation. Only about 0.01% of normal marrow cells are hematopoietic stem cells (HSCs), and what the actual leukemia stem cell (LSC) number is at a typical new diagnosis of acute myeloid leukemia (AML) is not known. Also, it is not known if mutations which are associated with AML arise in normal stem cells or in more differentiated cell types which then acquire stem-like features (Misaghian et al., 2009). Leukemia stem cells are defined functionally as cells which are able to engraft in immunocompromised mice, but it is possible that xenotransplantation underestimates the numbers and types of stem cells due to the presence of a foreign microenvironment (Adams and Strasser, 2008). The concept that a LSC which is a counterpart to a normal HSC exists has been considered for many decades, but thus far the implications that such a cell has in the manifestation and therapy of acute myelogenous leukemia have remained controversial.

The cellular origin of AML remains unclear, with ongoing controversy as to whether it arises from a transformed true HSC with multipotential self-renewal capacity or in a more mature progenitor cell. Most AML cells do not possess the properties of self-renewal and multipotency. This has led to the concept of stem cell heterogeneity (Nguyen et al., 2012; Walter et al., 2012). Some leukemias may arise at the level of pluripotent $CD33^-$ precursors, some may have an initial mutation in a pluripotent HSC with a collaborating mutation such as a core binding factor mutation occurring later, or some may arise at the level of a committed myeloid precursor as is the case in acute promyelocytic leukemia. Both the mutation(s) leading to a leukemic state and the cell of origin of the mutation are thought to have prognostic bearing (Walter et al., 2012). The LSC may not always be a rare population of quiescent cells. The phenotype, frequency, and functional properties of these cells may also change during disease progression (Mather, 2012; Nguyen et al., 2012).

Bonnet and Dick (1997) found that only leukemic blasts with the immature cell-surface phenotype characterized by CD34 expression with lack of CD38 expression were capable of transferring AML to immunodeficient mice; severe combined immunodeficiency (SCID) mice. This seemed consistent with a cancer stem cell (CSC) hypothesis which suggests that tumors are maintained by a small population of stem cell-like cancer cells which have the capability for indefinite self-renewal (Lapidot et al., 1994). Subsequently, some leukemia-initiating cells (L-ICs) have been found in the CD34 negative marrow fractions (Taussig et al., 2010). Also, LSCs have a hierarchy defined by length of repopulating potential in serial immune deficient mice transplantations defined as short- and long-term potential (Sarry et al., 2011). Those with long-term potential are thought to be quiescent (outside of active cell cycle) and express high levels of the multi-drug resistance phenotype, MDR-1, indicating ability to efflux cytotoxic drugs (Krause and van Etten, 2007). There is also evidence that pathways involved in proliferation of primitive cells such as Hox, hedgehog, notch, and

Wnt are all involved in the maintenance and proliferation of the LSC (reviewed in Krause and van Etten, 2007).

While the $CD34^+CD38^-$ cells are clonal as based on cytogenetics, fluorescence *in situ* hybridization (FISH), and reverse transcriptase polymerase chain reaction (RT-PCR) in some cases, normal $CD34^+CD38^-$ cells are also capable of engrafting NOD/SCID mice and must be distinguished from their leukemic counterparts in the course of functional assays. If a multipotential $CD34^+CD38^-$ stem cell is the cell of origin for acute leukemia, it is not known why the lymphoid phenotype is suppressed after transformation. Satoh and Ogata (2006) have postulated that myeloid HSCs with minimal lymphopoietic potential may be the site of transformation in AML and could be a target to eliminate the LSC in many cases.

The LSC is best defined functionally by its ability to recapitulate leukemia faithfully in immunocompromised mice. This requires not only homing and engraftment potential to the murine microenvironment but ability to express the phenotype of the original AML in terms of surface phenotype and of clonal markers such as chromosome translocations or deletions or of other abnormal molecular markers such as nucleophosmin-1, Flt3–ITD expression, or Ras mutations. Unfortunately, only about 50% of AML cases have clonal chromosome markers to allow easy distinction, but other aberrant leukemic cell phenotypes can sometimes allow the distinction of normal vs. leukemia human $CD45^+$ cells to be made by flow cytometry or by mutation analysis by PCR or sequencing. Detecting the presence of human $CD45^+$ cells is not sufficient as normal HSCs are also able to engraft immunodeficient mice, so documentation of the leukemic nature of the engrafting cells is required. *In vivo* L-IC and HSC assays are important to measure functional stem cell capability and to measure effectiveness of therapies against L-ICs as has been determined with a compound kinetin riboside which has potential therapeutic efficacy and preferential effects against LSCs as compared with normal HSCs (McDermott et al., 2012). Some AML do not engraft immune deficient mice, and it is thought that murine engraftment could represent proliferative potential of the leukemic cells or could simply reflect ability to interact with the murine microenvironment (Risueno et al., 2011). Targeting LSCs is thought to be of importance since the burden of LSCs at diagnosis has prognostic significance. Patients whose blasts at diagnosis fail to engraft NOD/SCID mice at high cell doses have superior long-term survival (Pearce et al., 2006).

Knowing which "stem cell" to target therapeutically in AML is difficult, however, since relapse may occur in a founder clone, a recurring subclone, or in a novel stem cell clone (Walter et al., 2012). Not only do controversies exist about how to identify a LSC but also about whether such a stem cell must be eliminated in order to effectively treat the leukemia (Kelly et al., 2007; Majeti, 2011). The possibility that stem cell-like components of tumors may change phenotype rapidly and reversibly also makes study of these cells difficult (Mather, 2012). Because of the heterogeneity in the phenotype of LSCs, surface antigen phenotype is inadequate as a means of isolation. High expression of aldehyde dehydrogenase (ALDH) activity in conjunction with CD34 has been found to delineate an L-IC (Ran et al., 2012). The frequency of aldehyde bright cells in the marrow at time of initial diagnosis is an independent prognostic factor predicting overall survival (Ran et al., 2012). It has also been shown that in a majority of AML cases, two subsets with progenitor immunophenotype coexist, and both have LSC activity and are hierarchically patterned (Goarden et al., 2011).

That the stem cell model has clinical significance in AML is suggested by studies such as one which showed that the percentage of $CD34^+CD38^-$ LSCs at the time of diagnosis correlated with the duration of relapse-free survival in 92 patients (van Rhenen et al., 2005). Those with >3.5% AML LSCs had a median relapse-free survival of 5.6 months vs. those with <3.5% who had a median relapse-free survival of 16 months. The presence of a $CD34^+CD38^-$ ALDH intermediate population has been shown to correlate with minimal residual disease (MRD) and subsequent relapse and to be able to distinguish LSCs from normal stem cells which are aldehyde high expressors (Gerber et al., 2012). Overall, LSC frequency is thought to be an important component of MRD (Buccisano et al., 2012).

ASSAYING THE LSC

The LSC can be assayed by flow cytometry and immunophenotype, but given the vagaries and lack of standardization of this technique, it is most accurately assayed by its ability to engraft immune deficient mice, although as noted above, there are both quantitative and qualitative problems with those assays (Mather, 2012). The L-IC is able to recapitulate the phenotype of the original leukemia when transplanted into NOD/SCID mice and then to be secondarily transplanted to another sublethally irradiated mouse. The NOD/SCID xenograft has no B or T cells, and leukemia engraftment is often quite low and requires transplantation of thousands of cells. In the NOD/SCID/IL-2Rγ−/− (NSG) species, NK cells are also deficient and as few as 100 cells will transplant the leukemia (Ishikawa et al., 2005). ALDH has been utilized as a marker of LSCs, and *in vitro* long-term culture assays have been reported to identify an L-IC (Sutherland et al., 2001).

Initially, it was thought that the LSC resided in the $CD34^+CD38^-$ compartment, but many anti-CD38 antibodies, including those utilized in the original isolation of LSCs inhibit engraftment of $CD34^+CD38^+$ leukemia cells through an Fc-dependent mechanism (Taussig et al., 2008). Blockade of Fc receptors can result in engraftment of $CD38^+$ AML cells, suggesting that $CD38^+$ fractions may contain LSCs (Taussig et al., 2008). Also, in some AML cases with nucleophosmin mutation, the L-ICs reside in the CD34 negative fraction (Taussig et al., 2010). **Table 1** illustrates some of the characteristics of AML stem cells as contrasted with normal HSCs.

MEANS TO TARGET LSCs

TARGETING CELL-SURFACE MOLECULES ON LSCs

One means of isolating and potentially targeting LSCs would be to target cell-surface molecules on the cell surface which are selectively or differentially expressed relative to normal tissue, in this case the normal HSC. Such antibodies could be expressed on differentiated normal cells but not on normal HSCs. LSCs lack Thy-1 (CD90) and c-kit (CD117), both found on normal HSCs, but they possess CD123, CD33, and C-type lectin-like molecule-1 (CLL-1).

Table 1 | Sample characteristics of leukemia vs. normal stem cells.

	LSC	HSC
Frequency	Usually rare	Rare
Cell cycle status	Quiescent	Quiescent
MDR-1 expression	+	+
CD34 expression	+	+
CD38 expression	Sometimes	−
HLA-DR expression	−	−
CD71 expression	−	−
CD33 expression	− (Usually)	−
CD117 expression	−	+
CD90 expression	−	+
CD123 expression	+	− (Usually)
Aldehyde dehydrogenase expression	+ But intermediate	+ (Bright)

LSC, leukemia stem cell; HSC, hematopoietic stem cell; MDR, multi-drug resistance.

CD96, CD45, CD32, and CD25 have been shown to be preferentially expressed on AML stem cells as compared with normal HSCs (reviewed in Majeti et al., 2009). CD90 is expressed by normal but not AML stem cells (Baum et al., 1992). LSCs do not express human leukocyte antigen (HLA)-DR or CD71 (Blair et al., 1998). Many of these antigens are expressed on the cell surface, allowing stem cell targeting throughout the circulation without specific delivery requirements.

ANTIGENS USED IN TARGETING AML LSCs

CD33

CD33 is a sialylated protein expressed on normal cells with myelomonocytic differentiation, AML blasts, and some LSC populations. Numerous antibodies to CD33 have been developed for clinical use, including gemtuzumab ozogamicin, a recombinant humanized anti-CD33 conjugated with calicheamicin (Hamann et al., 2002). This conjugate induced remission in relapsed AML, most cases being $CD33^+$, but it also had some activity in $CD33^-$ cases probably due in large part to the calicheamicin effects (Jawad et al., 2010; Pollard et al., 2012). It was also able to eliminate promyelocytes in cases of acute promyelocytic leukemia. While not studied directly, it was thought to differentially kill leukemia cells and possibly LSCs, but prolonged cytopenias also suggested in some cases that it was expressed on normal HSCs as well (Walter et al., 2012). Gemtuzumab ozogamicin (anti-CD33 conjugated with calicheamicin) was approved for the treatment of relapsed AML in elderly patients. Because CD33 is also expressed on endothelial cells of certain vascular beds, toxicities such as sinusoidal obstructive syndrome of liver occurred in some cases (McDonald, 2002), leading to eventual voluntary withdrawal of this conjugated antibody from the market. It is still being utilized in clinical trial settings, however, so future studies may be able to discern its effects on LSCs in states of MRD and other therapeutic settings in leukemia (Castaigne et al., 2012). Other antibody conjugates are also under development (Walter et al., 2012).

CD33 is a relatively hard molecule to target due to relatively low antigen expression (about 104 CD33 molecules/cell) and slow conjugate internalization (Walter et al., 2012). In CML, it has been found (Hermann et al., 2012b) that $CD34^+CD38^-CD123^+$ cells expressed significantly higher levels of CD33 compared to normal $CD34^+CD38^-$ stem cells. Levels of CD33 mRNA were also higher. Gemtuzumab ozogamicin inhibited these in long-term culture initiating cell assays, but no mention was made of inhibition of engraftment in NOD/SCID mice, however.

CD123

CD123 is the high-affinity interleukin-3 receptor alpha chain. While it is differentially expressed on leukemia vs. normal stem cells (Jordan et al., 2000), cord blood may express CD123 positive progenitors. CD123 has been targeted for clinical use with a diphtheria toxin–IL-3 fusion protein (Kuo et al., 2009) and numerous additional means to target CD123 have been developed. Jin et al. (2009) reported on a monoclonal antibody, 7G3 which targets CD123. It was able to reduce AML-LSC engraftment and improve murine survival in models of pre-established leukemia where the antibody showed reduced AML burden in the marrow and periphery as well as impaired secondary transplantation after 7G3 exposure, indicating that LSCs had been inhibited. Stein et al. (2009) used single chain Fv antibody fragments specific for CD123 designed to specifically target LSCs. This binding created two cell death inducing molecules; one being immunotoxic through truncation with a pseudomonas exotoxin and the other targeted to the low-affinity Fcγ receptor III (CD16). This construct was able to generate potent lysis of MOLM-143, and SKNO-1 cells in ADCC reactions. None of the CD123 targeted agents have had significant clinical development to date.

C-type lectin-like molecule 1

This molecule has been found to be expressed on $CD34^+CD38^-$ AML cells. Its expression tracked with clinical remission or relapse. It was not found on $CD34^+CD38^-$ cells from normal marrow or on cells regenerating post-chemotherapy (van Rhenen et al., 2007). Zhang et al. (2011) have developed nanoparticles covalently decorated with CLL-1 targeting peptides. These are loaded with daunorubicin which is then internalized to LSCs but not to normal HSCs. Other antibody means of targeting CLL-1 are also under development (Zhao et al., 2010).

CD96

CD96 is a member of the immune globulin superfamily. It is normally found on T-lymphocytes. It is thought to be LSC-specific as it is found on most $CD34^+CD38^-$ AML cells whereas it is only expressed weakly in the normal counterparts (Hosen et al., 2007). When leukemic cells were separated into CD96 positive and negative cells, only positive cells engrafted Rag-deficient mice, suggesting that this may be an LSC-specific therapeutic target.

Anti-PR1/HLA-A2 T-cell receptor

Antibodies against PR1 induce complement-dependent cytotoxicity against AML progenitor cells. PR1 is a HLA-A2 restricted leukemia-associated peptide from proteinase 3 (P3) and neutrophil elastase (NE) recognized by anti-PR1-specific cytotoxic

T lymphocytes which can contribute to cytogenetic remission of AML. These cells cause specific lysis of AML, including LSCs (Sergeeva et al., 2011).

CD44

The CD44-6v isoform is differentially expressed by AML progenitor cells. An activating CD44-specific antibody was able to eradicate AML but not normal cord blood and normal adult marrow engraftment in NOD/SCID mice (Jin et al., 2006). *In vivo*, the effect of this antibody, H9 was limited to situations with a lower burden of disease (Jin et al., 2006).

CD32

This antigen has been reported by Saito et al. (2010) to be differentially expressed on the AML stem cell. It recognizes the FcRIIa low-affinity receptor and as such is expressed on monocytes and other effectors of ADCC as well.

CD25

Saito et al. (2010) also described this on the AML stem cell. Either CD32 or CD25 or both were expressed in 32/61 (53%) of patients in AML LSCs which were able to initiate AML and were cell–cycle quiescent and chemotherapy resistant *in vivo*.

CD47

CD47 is a ligand to SIRP-alpha (signal regulatory protein-alpha). Its expression sends a "don't eat me" message to phagocytic cells. Blocking antibodies to CD47 enabled phagocytosis of human AML LSCs but not normal LSCs (Jaiswal et al., 2009). This antibody has been found effective in a treatment model where NSG mice were transplanted with LSCs. After 8–12 weeks the mice were treated with control IgG or blocking antibodies to CD47. The antibodies to CD47 resulted in rapid clearance of AML in blood and also of marrow LSCs. There was absence of leukemia in secondary recipients (Majeti et al., 2009). CD47 is expressed on many tissues, and it may be more effective with chemotherapy or with mobilizing agents to facilitate phagocytosis in the peripheral circulation (Majeti et al., 2009).

SUMMARY OF ANTIBODY TARGETING

While antibodies have been developed to target differentially expressed surface markers on AML vs. normal cells, none of these have had significant impact on disease outcomes to date. In part, this may be due to lack of complete specificity, inadequate targeting, toxicities due to non-specificity, antigen modulation, and subsequent resistance, or other as yet undiscovered mechanisms. Despite its removal from the market in the United States, the anti-CD33 antibody with which most experience developed, gemtuzumab ozogamicin, has recently been tested in low doses during induction and consolidation chemotherapy for AML and has been found to result in superior overall and disease-free survival when used in combination with chemotherapy (Castaigne et al., 2012). LSC frequency or MRD was not measured as part of the study, so whether this relates to stem cell targeting or other mechanisms of leukemia suppression remains uncertain.

TARGETING SIGNALING PATHWAYS IN LSCs WITH SMALL MOLECULE INHIBITORS

One approach to eliminating the LSC would be to target pathways regulating stem cell self-renewal, particularly if these are differentially expressed in LSCs vs. HSCs (Rasheed et al., 2011). For example, inhibitors of Wnt have been examined in CML (Baghdadi et al., 2012) and notch inhibitors have been examined in ALL, but these are also toxic to normal HSCs in some cases, indicating a need to find selective inhibitors or relatively selective inhibitors for LSCs (Guzman and Jordan, 2004; Mikkola et al., 2010). Heat shock protein inhibitors have been found to be inhibitory to AML progenitor cells, but whether those represent true stem cells is uncertain (Hermann et al., 2012a).

PI3K/AKT/mTOR PATHWAY

The PI3K/AKT/mTOR pathway is activated in the majority of AML cases, but the effects of inhibiting this pathway on LSC frequency have not been described in detail (Mikkola et al., 2010). In mice, when PTEN, normally a suppressor of the PI3K/AKT/mTOR pathway is depleted, normal HSCs are depleted, but L-ICs are expanded (Lee et al., 2010). The mTOR inhibitor, rapamycin, blocks this. The depletion of Pten-deficient HSCs was not caused by oxidative stress (Peng et al., 2010).

Altman et al. (2011) have found that dual targeting of mTORC1 and mTORC2 results in potent suppressive effects on primitive leukemic progenitors from AML patients. Inhibition of the mTOR catalytic site with OSI-027, a dual mTORC1/mTORC2 inhibitor, resulted in suppression of mTORC2 and mTORC1 complexes and elicited a much more potent anti-leukemic response than selective mTORC1 targeting with rapamycin. Whether these inhibitors act at a true stem cell level remains unclear.

NF-κB pathway

NF-κB has been found to be active in most AML stem cells but not in normal lineage negative progenitors (Jordan et al., 2006). The proteasome inhibitor, MG-132, inhibited NF-κB activation through stabilization of its cellular inhibitor, IκB and was able to induce apoptosis in $CD34^{+}CD38^{-}$ AML cells while sparing normal progenitors. Since that report, other inhibitors of NF-κB such as bortezomib or specific inhibitors of IκB kinase which phosphorylate and inactivate IκB have been developed and have been reported to be inhibitory to AML progenitor cells (Frelin et al., 2005). The drug parthenolide has IKB-Iκκ inhibitory activity and is able to induce apoptosis in AML cells coincident with NF-κB inhibition, p53 activation, and induction of reactive oxygen species (Neelakantan et al., 2009).

Tyrosine kinase inhibitors

These have been utilized primarily to target bcr/abl, the driving mechanism in CML. While most bcr/abl inhibitors such as imatinib mesylate, nilotinib, and dasatinib eradicate most CML cells, they are ineffective against a reservoir of quiescent LSCs (Baghdadi et al., 2012). Inhibition of the Wnt/beta-catenin, hedgehog, and histone deacetylases has been shown to have potential to inhibit the CML stem cell.

Hedgehog/smoothened pathway

Hedgehog signaling is essential for maintenance of CSCs (Zhao et al., 2009). Loss of smoothened, an essential component of the Hedgehog pathway, impairs HSC renewal and decreases induction of CML by bcr/abl. Inhibition of hedgehog by cyclopamine inhibited the propagation of CML. In contrast, hedgehog signaling is not required for adult murine HSC function and hematopoiesis (Su et al., 2012). Its role in an AML LSC is not well worked out yet, but inhibitors of the Wnt and Shh signaling pathway cause less apoptosis in normal vs. leukemic HSCs (Hofmann et al., 2009).

Oxidative stress pathways

While states of low oxidative stress are thought to aid in maintenance of stem cell quiescence, CSCs may be susceptible to agents which induce oxidative stress. In fact, excessive production of ROS or a deficiency in antioxidant pathways has been noted in acute leukemias (Hole et al., 2011). This has not been studied systematically as a means of differential LSC targeting.

TARGETING VASCULAR INTERACTIONS

Since LSCs as well as their blast progeny can be isolated from the vasculature in which they circulate, it is likely that exploitation of LSC–vascular interactions would have greater impact on targeting these stem cells than would be the case in other cancers where the stem cells do not routinely circulate except at times of active metastasizing. Furthermore, the LSC arises in the marrow microenvironment, an organ that is very vascular, again suggesting a potential role for targeting leukemia/vascular interactions. In the marrow, LSCs interact with cells, cell matrix, and soluble factors in the microenvironmental niche (Konopleva and Jordan, 2011). In mice, the microenvironmental niche has been characterized as vascular and osteoblastic, but whether such distinct niches exist in human marrow is uncertain. When leukemia cells enter the blood, they must traverse the endothelial cells lining the marrow sinusoids which comprise the vascular niche, and when they return to the marrow, they are engaged by selectins for rolling on the endothelial layer after which they attach via integrins or other adhesins. Thereafter, they transmigrate the endothelial barrier before again lodging in the marrow niche.

Role of endothelial cells

As noted above, when LSCs and other AML cells home to marrow or egress marrow to the peripheral circulation, they must traverse an endothelial monolayer. These form an intact lining of marrow sinusoidal vessels. The homing process involves rolling on selectin surfaces, engaging integrin or other adhesion receptors, transmigrating the endothelial layer, and lodging in the marrow hematopoietic niche. Chemotherapy resistant AML stem cells are thought to engraft with the marrow endosteal region (Ishikawa et al., 2004). Stem cell interactions with the niche can therefore theoretically be disrupted at each of these steps with possible impact on survival, proliferation, and function.

Sipkins et al. (2005), using intravital microscopy showed that NALM-6, an ALL cell line, engrafted in microvascular domains in the marrow. Colmone et al. (2008) demonstrated that the NALM-6 cells actively disrupted normal vascular niches for transplanted human $CD34^+$ cells and caused normal $CD34^+$ cells to leave their niches and to engraft in alternative niches. Targeting the supportive function of the vascular niche in marrow and circulation may therefore have inhibitory activity against LSCs. Whether this will have a differential effect as compared with normal stem cells remains uncertain.

Targeting vascular endothelial growth factor (VEGF) and its receptor, VEGFR2 (KDR) may inhibit both AML cells and endothelial cell proliferation as both possess these receptors (Ziegler et al., 1999). Marrow vascularity is increased in AML, and targeting this vasculature may decrease AML proliferation. The role of specific angiopoietins such as basic fibroblast growth factor or transforming growth factor-beta has not been examined as related to AML stem cell survival, but this might also represent pathways which might be targeted to decrease proliferation of AML cells (Folkman, 2001). It has also been demonstrated that leukemia cells secrete factors which can enhance endothelial cell proliferation which in turn can stimulate leukemia cell proliferation and survival (Veiga et al., 2006). Targeting endothelial cells via inhibition of the angiopoietin–Tie2 axis (Schliemann et al., 2007) or via combretastatins (Petit et al., 2008) might also inhibit leukemia cell proliferation, but specificity for LSCs has not been determined.

CXCL12 and CXCR4

The CXCL12–CXCR4 chemokine–chemokine receptor axis is involved in AML stem cell interaction with the marrow as is also the case with normal HSCs. CXCR4 is expressed on primary leukemic cells, and high expression is a negative prognostic factor (Rombouts et al., 2004). Treatment with the CXCR4 antagonist, plerixafor, has been found to increase sensitivity of Flt-3 mutated AML cells to the FLT3 inhibitor, sorafenib and to induce the mobilization of AML cells into the peripheral blood (Zeng et al., 2009). It is uncertain whether there is preferential mobilization of LSCs vs. normal progenitors and bulk AML cells.

Anti-VLA-4 and anti-VCAM

The integrin–integrin receptor pair of very late antigen-4 and vascular cell adhesion molecule-1 is involved in retention of AML cells in marrow. AML blasts with higher CD49d expression have a poorer prognosis (Matsunaga et al., 2003), but the function of very late-antigen-4 as measured by binding of soluble VCAM-1 may be associated with improved overall survival of patients (Becker et al., 2009). Interactions between VLA-4 and fibronectin or VCAM may modulate chemotherapy response. How this impacts AML stem cells remains uncertain. Targeting other integrin-linked pathways may also inhibit AML stem cells (Muranyi et al., 2010).

Role of CD44

CD44 is a glycoprotein which binds to hyaluronan, selectins, and osteopontin and has pleiotropic functions in organogenesis, cell homing, and migration (Krause et al., 2006). High levels of the molecule on AML cells are associated with higher relapse rates (Quere' et al., 2011). The anti-CD44 antibody, H90 targets LSCs in human AML through niche disruption and with evidence of LSC differentiation and loss of LSC self-renewal capacity as compared with effects on normal HSCs. Jin et al. (2006) found that using an activating monoclonal antibody to CD44, leukemic repopulation

of NOD/SCID mice was markedly reduced probably due to interference with transport to the stem cell-supportive niches. Since CD44 is ubiquitously expressed, it is not known if the differential effects on LSCs are due to alternative splicing or other reasons.

Role of hypoxia

The marrow microenvironment in AML is relatively hypoxic (Fiegl et al., 2009). Under normoxic conditions, it has been found (Wang et al., 2011) that HIF-1α signaling was selectively activated in the stem cells of murine lymphoma and human AML. HIF-1α shRNA and HIF-1α inhibitors abrogated the colony-forming unit (CFU activity) of human CSCs. The inhibitor echinomycin eradicated serially transplantable human AML cells in xenogeneic models by preferential elimination of leukemic-/cancer-specific stem cells. The increased HIF-1 activity in cancer stem cells was seen in both hypoxic and normoxic states. Rakicidin A is another compound which may target a hypoxic microenvironment (Yamazaki et al., 2007).

Role of selectins

Leukemic stem cells express sialylated carbohydrate ligands on their surfaces that adhere to selectin proteins found on endothelial cells. In marrow vascular beds, these selectins are constitutively expressed. Immobilized selectin protein can be utilized as a targeting mechanism for cells under flow and can capture some LSCs. Mitchell et al. (2012) have utilized targeted liposomal doxorubicin (L-DXR) functionalized with recombinant human E-selectin and polyethylene glycol. Normal leukocytes exposed to these molecules demonstrated minimal cell death, whereas leukemia cells could be targeted. This mechanism was effective either in suspension or immobilized onto microtubular devices. P-selectin coated microtubules have been found to enrich for some hematopoietic progenitors from marrow through differential rolling (Narasipura et al., 2008), and this observation may allow delivery of cytotoxics to cancer cells (Rana et al., 2009), but whether this will have a differential effect on LSCs vs. other leukemia progenitors is still unclear.

ROLE OF CELL CYCLE IN THE VASCULAR NICHE

Chemotherapy agents used to treat leukemia kill cells that are in active cell cycle but spare LSCs which are in a quiescent state in the marrow endosteal niche. Like normal stem cells, LSCs are predominately in a quiescent state which allows avoidance of stem cell exhaustion and minimization of risk of oncogenic events. Those LSCs located more centrally in the marrow cavity have a higher likelihood of being in active cell cycle (Doan and Chute, 2012). Attempts have been made to use agents such as granulocyte colony stimulating factor to cause LSCs to cycle, disrupting them from their vascular niche and increasing their sensitivity to agents such as cytarabine (Mikkola et al., 2010). Such efforts have not had great therapeutic impacts, however (Pabst et al., 2012).

SUMMARY

The LSC, like its normal stem cell counterpart, lodges in marrow niches and occasionally circulates in the blood. Ideally, a therapeutic strategy that targets LSCs must spare self-renewing normal HSCs so as to protect ongoing hematopoiesis. The comparison of LSCs vs. HSCs functionally is crucial to identifying unique properties of the LSC which can be targeted. These will include surface antigen phenotyping (Amadori and Stasi, 2006), comparison of signal transduction pathway activation, response to reactive oxygen species and stress protein responses at baseline and in response to chemotherapeutic agents. Also, understanding differences in interactions with vasculature peripherally and in marrow may allow for differential targeting of LSCs (Doan and Chute, 2012). The ideal target will thus be expressed on a large fraction of LSCs, be stable through treatment types and disease stages, be present on cell-cycle quiescent AML-initiating cells residing within the endosteal niche, and be non-toxic to normal HSCs. Determining the clinical effectiveness of agents which target stem cells and proving that this is clinically relevant is hard to achieve even in AML, but novel agents and appropriate biomarkers may allow application of these strategies for the future (Rasheed et al., 2011). LSCs are heterogeneous, grow in subclones which have some degree of genetic instability, and evolve with time. Many LSC-derived subclones may be undetectable at diagnosis, but after therapy, they may become the dominant clone with relapsing disease (Nguyen et al., 2012). Both rare cancer stem cells and dominant clones will need to be eliminated for successful disease control (Adams and Strasser, 2008). Understanding the interaction between LSCs and microenvironmental components may also elucidate means to target these rare cells (Klyuchnikov and Kroger, 2009). Due to the heterogeneity of the LSC and the similarities between HSCs and LSCs, many challenges remain in effective targeting of these rare cells which are thought to require elimination if AML therapies are to have long-term success (Krause and van Etten, 2007).

REFERENCES

Adams, J. M., and Strasser, A. (2008). Is tumor growth sustained by rare cancer stem cells or dominant clones? *Cancer Res.* 68, 4018–4021.

Altman, J. K., Sassano, A., Kaur, S., Glaser, H., Kroczynska, B., Redig, A. J., Russo, S., Barr, S., and Platanias, L. C. (2011). Dual mTORC2/mTORC1 targeting results in potent suppressive effects on acute myeloid leukemia (AML) progenitors. *Clin. Cancer Res.* 17, 4378–4386.

Amadori, S., and Stasi, R. (2006). Monoclonal antibodies and immunoconjugates in acute myeloid leukemia. *Best Pract. Res. Clin. Haematol.* 19, 715–736.

Baghdadi, T. A., Abonour, R., and Boswell, H. S. (2012). Novel combination treatments targeting chronic myeloid leukemia stem cells. *Clin. Lymphoma Myeloma Leuk.* 12, 94–105.

Baum, C. M., Weisman, I. L., Tsukamoto, A. S., Buckle, A. M., and Peault, B. (1992). Isolation of a candidate human hematopoietic stem-cell population. *Proc. Natl. Acad. Sci. U.S.A.* 89, 2804–2808.

Becker, P. S., Kopecky, K. J., Wilks, A. W., Chien, S., Harlan, J. M., Willman, C. L., Petersdorf, S. H., Stirewalt, D. L., Papayannopoulou, T., and Appelbaum, F. R. (2009). Very late antigen-4 function of myeloblasts with improved survival for patients with acute myeloid leukemia. *Blood* 113, 866–874.

Blair, A., Hogge, D. E., and Sutherland, H. J. (1998). Most acute myeloid leukemia progenitor cells with long-term proliferative ability in vitro and in vivo have the phenotype CD34(+)/CD71(−)/HLA-DR−. *Blood* 92, 4325–4335.

Bonnet, D., and Dick, J. E. (1997). Human acute myeloid leukemia is organized as a hierarchy that originates from a primitive hematopoietic cell. *Nat. Med.* 3, 730–737.

Buccisano, F., Maurillo, L., Del Principe, M. I., Del Peota, G., Sconocchia, G., Lo-Coco, F., Arcese, W., Amadori, S., and Vendiiti, A. (2012). Prognostic and therapeutic implications of minimal residual disease detection in acute myeloid leukemia. *Blood* 119, 332–341.

Castaigne, S., Paulas, C., Terre, C., Farroux, E., Bordessoule, D., Bastie, J. N., Legrand, O., Thomas, X., Turlure, P., Reman, O., de Revel, T., Gastaud, L., de Gunzburg, N., Contentin, N., Henry, E., Marolleau, J. P., Aljijakli, A., Rousselot, P., Fenaux, P., Preudhomme, C., Chevret, S., and Dombret, H. (2012). Effect of gemtuzumab ozogamicin on survival of adult patients with de novo acute myeloid leukaemia (ALFA-0701): a randomized, open-label, phase 3 study. *Lancet* 379, 1508–1516.

Colmone, A., Amorim, M., Pontier, A. L., Wang, S., Jablonski, E., and Sipkins, D. A. (2008). Leukemic cells create bone marrow niches that disrupt the behavior of normal hematopoietic progenitor cells. *Science* 322, 1861–1865.

Doan, P. L., and Chute, J. P. (2012). Vascular niche: home for normal and malignant hematopoietic stem cells. *Leukemia* 26, 54–62.

Fiegl, M., Samudio, I., Clise-Dwyer, K., Burks, J. K., Mnjoyan, Z., and Andreeff, M. (2009). CXCR4 expression and biologic activity in acute myeloid leukemia are dependent on oxygen partial pressure. *Blood* 113, 1504–1512.

Folkman, J. (2001). Angiogenesis-dependent disease. *Semin. Oncol.* 28, 536–542.

Frelin, C., Imbert, V., Griessinger, E., Peyron, A. C., Rochet, N., Philip, P., Dagevile, C., Sirvent, A., Hummelsberger, M., Bernard, E., Dreano, M., Sirvent, N., and Peyron, J. F. (2005). Targeting NF-κB activation via pharmacologic inhibition of IKK2-induced apoptosis of human acute myeloid leukemia cells. *Blood* 105, 804–811.

Gerber, J. M., Smith, B. D., Nywang, B., Zhang, H., Vala, M. S., Morsberger, L., Galkin, S., Collector, M. I., Perkins, B., Levis, M. J., Griffin, C. A., Sharkis, S. J., Borowitz, M. J., Karp, J. E., and Jones, R. J. (2012). A clinically relevant population of leukemic CD34+CD38− cells in acute myeloid leukemia. *Blood* 119, 3571–3577.

Goarden, N., Marchi, E., Atzberger, A., Quek, L., Schuh, A., Soneji, S., Wolf, P., Mead, A., Alford, K. A., Rout, R., Dhaudhury, S., Gilkes, A., Knapper, S., Beldjord, K., Begum, S., Rose, S., Geddes, N., Griffiths, M., Standen, G., Sternberg, A., Cavenagh, J., Hunter, H., Bowen, D., Killick, S., Robinson, L., Price, A., MacIntyre, E., Virgo, P., Burnett, A., Craddock, C., Enver, T., Jacobsen, S. E., Porcher, C., and Vyas, P. (2011). Coexistence of LMPP-like and GMP-like leukemia stem cells in acute myeloid leukemia. *Cancer Cell* 19, 138–152.

Guzman, M. L., and Jordan, C. T. (2004). Considerations for targeting malignant stem cells in leukemia. *Cancer Control* 11, 97–104.

Hamann, P. R., Hinman, L. M., Hollander, I., Beyer, C. F., Lindh, D., Holcomb, R., Hallett, W., Tsou, H. R., Upeslacis, J., Shochat, D., Mountain, A., Flowers, D. A., and Bernstein, I. (2002). Gemtuzumab ozogamicin, a potent and selective anti-CD33 antibody–calicheamicin conjugate for treatment of acute myeloid leukemia. *Bioconjug. Chem.* 13, 47–58.

Hermann, H., Kneidinger, M., Cerny-Reiterer, S., Rulicke, T., Willmann, M., Gleixner, K. V., Blatt, K., Hormann, G., Peter, B., Samorapoompichit, P., Picki, W., Bharate, G. Y., Mayerhofer, M., Sperr, W. R., Maeda, H., and Valent, P. (2012a). The Hsp32 inhibitors SMA-ZnPP and PEG-ZnPP exert major growth-inhibitory effects on CD34+CD38− and CD34−CD38− AML progenitor cells. *Curr. Cancer Drug Targets* 12, 51–63.

Hermann, H., Cerny-Reiterer, S., Gleixner, K. V., Blatt, K., Herndhofer, S., Rabitsch, W., Jager, E., Mitterbauer-Hohendanner, G., Struebel, B., Selzer, E., Schwarzinger, I., Sperr, W. R., and Valent, P. (2012b). CD34(+)CD38(−) stem cells in chronic myeloid leukemia express Siglec-3 (CD33) and are responsive to the CD33-targeting drug gemtuzumab/ozogamicin. *Haematologica* 97, 219–226.

Hofmann, I., Stover, E. H., Cullen, D. E., Mao, J., Morgan, K. J., Lee, B. H., Kharas, M. G., Miller, P. G., Cornejo, M. G., Okabe, R., Armstrong, S. A., Ghilardi, N., Gould, S., de Saugage, F. J., McMahon, A. P., and Gilliland, D. G. (2009). Hedgehog signaling is dispensable for adult murine hematopoietic stem cell function and hematopoiesis. *Cell Stem Cell* 5, 559–567.

Hole, P. S., Darley, R. I., and Tonks, A. (2011). Do reactive oxygen species play a role in myeloid leukemias? *Blood* 117, 5816–5826.

Hosen, N., Park, C. Y., Tatsumi, N., Oji, Y., Sugiyama, H., Gramatzki, M., Krensky, A. M., and Weissman, I. L. (2007). CD96 is a leukemic stem cell-specific marker in human acute myeloid leukemia. *Proc. Natl. Acad. Sci. U.S.A.* 104, 11008–11013.

Ishikawa, F., Yasukawa, M., Lyons, B., Yoshida, S., Miyamoto, T., Yoshimoto, G., Watanabe, T., Akashi, K., Shultz, L. D., and Harada, M. (2005). Development of functional human blood and immune systems in NOD/SCID/IL2 receptor {gamma} chain (null) mice. *Blood* 106, 1565–1573.

Ishikawa, F., Yoshida, S., Saito, Y., Hijikata, A., Kitamura, H., Tanaka, S., Nakamura, R., Tanaka, T., Tomiyama, H., Saito, N., Fukata, M., Miyamoto, T., Lyons, B., Ohshima, K., Uchida, N., Taniguchi, S., Ohara, O., Akashi, K., Harada, M., and Shultz, L. D. (2004). Chemotherapy-resistant human AML stem cells home to and engraft within the bone-marrow endosteal region. *Nat. Biotechnol.* 25, 1315–1321.

Jaiswal, S., Jamieson, C. H., Pang, W. W., Park, C. Y., Chao, M. P., Majeti, R., Traver, D., van Rooijen, N., and Weisman, I. L. (2009). CD47 is upregulated on circulating hematopoietic stem cells and leukemia cells to avoid phagocytosis. *Cell* 138, 271–285

Jawad, M., Seedhouse, C., Mony, U., Grundy, M., Russell, N. H., and Pallis, M. (2010). Analysis of factors that affect in vitro chemosensitivity of leukaemic stem and progenitor cells to gemtuzumab ozogamicin (Mylotarg) in acute myeloid leukaemia. *Leukemia* 24, 74–80.

Jin, L., Hope, K. J., Zhia, Q., Smadja-Joffe, F., and Dick, J. E. (2006). Targeting of CD44 eradicates human acute myeloid leukemic stem cells. *Nat. Med.* 12, 1167–1174

Jin, L., Lee, E. M., Ramshaw, H. S., Busfield, S. J., Peoppl, A. G., Wilkinson, L., Guthridge, M. A., Thomas, D., Barry, E. F., Boyd, A., Geraing, D. P., Vairo, G., Lopez, A. F., Dick, J. E., and Lock, R. B. (2009). Monoclonal antibody-mediated targeting of CD123, IL-3 receptor alpha chain, eliminates human acute myeloid leukemic stem cells. *Stem Cell* 5, 31–42.

Jordan, C. T., Guzman, M. L., and Noble, M. (2006). Cancer stem cells. *N. Engl. J. Med.* 355, 1253–1261.

Jordan, C. T., Pchruch, D., Szilvassy, S. J., Guzman, M. L., Howard, D. S., Pettigrew, A. L., Meyerrose, T., Rossi, R., Grimes, B., Rizzieri, D. A., Luger, S. M., and Phillips, G. L. (2000). The interleukin-3 receptor alpha chain is a unique marker for human acute myelogenous leukemia stem cells. *Leukemia* 14, 1777–1784.

Kelly, P. N., Dakic, A., Adams, J. M., Nutt, S. L., and Strasser, A. (2007). Tumor growth need not be driven by rare cancer stem cells. *Science* 317, 337.

Konopleva, M. Y., and Jordan, C. T. (2011). Leukemia stem cells and microenvironment: biology and therapeutic targeting. *J. Clin. Oncol.* 28, 591–599.

Klyuchnikov, E., and Kroger, N. (2009). Sensitizing leukemic cells by targeting microenvironment. *Leuk. Lymphoma* 50, 319–320.

Krause, D. S., Lazarides, K., von Andrian, U. H., and van Etten, R. A. (2006). Requirement of CD44 in homing and engraftment of BCR-ABL-expressing leukemic cells. *Nat. Med.* 12, 1175–1180.

Krause, D. S., and van Etten, R. A. (2007). Right on target: eradicating leukemic stem cells. *Trends Mol. Med.* 13, 470–481

Kuo, S. R., Alfano, R. W., Frankel, A. E., and Liu, J. S. (2009). Antibody internalization after cell surface antigen binding is critical for immunotoxin development. *Bioconjug. Chem.* 20, 1975–1982.

Lapidot, T., Sirard, C., Vormoor, J., Murdoch, B., Hoang, T., Caceres-Cortes, J., Minden, M., Paterson, B., Caligiuir, M. A., and Dick, J. E. (1994). A cell initiating human acute myeloid leukemia after transplantation into SCID mice. *Nature* 367, 645–648.

Lee, J. Y., Nakada, D., Yilmaz, O. H., Tothova, Z., Joseph, N. M., Lim, M. S., Gilliland, D. G., and Morrison, S. J. (2010). mTOR activation induces tumor suppressors that inhibit leukemogenesis and deplete hematopoietic stem cells after Pten deletion. *Cell Stem Cell* 7, 593–605.

Majeti, R. (2011). Monoclonal antibody therapy directed against human acute myeloid leukemia stem cells. *Oncogene* 30, 1009–1019.

Majeti, R., Chao, M. P., Alizadeh, A. A., Pang, W. W., Jaiswal, S., Gibbs, K. D. Jr., van Rooijen, N., and Weissman, I. L. (2009). CD47 is an adverse prognostic factor and therapeutic antibody target on human acute myeloid leukemia stem cells. *Cell* 138, 286–299.

Mather, J. P. (2012). Concise review: cancer stem cells: in vitro models. *Cancer Stem Cells* 30, 95–99.

Matsunaga, T., Takemoto, N., Sato, T., Takimoto, R., Tanaka, I., Fujimi, A., Akiyaam, T., Kuroda, H., Kawan, Y., Kobune, M., Kato, J., Hirayama, Y., Sakamiaki, S., Kohda, K., Miyeake, K., and Niitsu, Y. (2003). Interaction between leukemic-cell VLA-4 and stromal fibronectin is a decisive factor for minimal residual disease of acute myelogenous leukemia. *Nat. Med.* 9, 1158–1165.

McDermott, S. P., Eppert, K., Notta, F., Isaac, M., Datti, A., Al-Awar, R., Wrana, J., Minden, M. D., and Dick, J. E. (2012). A small molecule screening strategy with validation on human leukemia stem cells uncovers the therapeutic efficacy of kinetin riboside. *Blood* 119, 1200–1207.

McDonald, G. B. (2002). Management of hepatic sinusoidal obstruction syndrome following treatment with gemtuzumab ozogamicin (Mylotarg). *Clin. Lymphoma* 2(Suppl. 1), S35-S39.

Mikkola, H. K., Radu, C. G., and Witte, O. N. (2010). Targeting leukemia stem cells. *Nat. Biotechnol.* 38, 237–238.

Misaghian, N., Ligresti, G., Steelman, L. S., Bertrand, F. E., Basecke, J., Libra, M., Nicoletti, F., Stivala, F., Miella, M., Tafun, A., Cervello, M., Martelli, A. M., and McCubrey, J. A. (2009). Targeting the leukemic stem cell: the Holy Grail of leukemia therapy. *Leukemia* 23, 25–42.

Mitchell, M. J., Chen, C. S., Ponmudi, V., Hughes, A. D., and King, M. W. (2012). E-selectin liposomal and nanotube-targeted delivery of doxorubicin to circulating tumor cells. *J. Control. Release* 160, 609–617.

Muranyi, A. L., Dedhar, S., and Hogge, D. E. (2010). Targeting integrin linked kinase and FMS-like tyrosine kinase-3 is cytotoxic to acute myeloid leukemia stem cells but spares normal progenitors. *Leuk. Res.* 34, 1358–1365.

Narasipura, S. D., Wojciechowski, J. C., Charles, N., Liesveld, J. L., and King, M. R. (2008). P-selectin coated microtube for enrichment of CD34+ hematopoietic stem and progenitor cells from human bone marrow. *Clin. Chem.* 54, 77–85.

Neelakantan, S., Nasim, S., Guzman, M. L., Jordan, C. T., and Crooks, P. A. (2009). Aminoparthenolides as novel anti-leukemic agents: discovery of the NF-κB inhibitor, DMAPT (LC-1). *Bioorg. Med. Chem. Lett.* 19, 4346–4349.

Nguyen, L. V., Vanner, R., Dirks, P., and Eaves, C. J. (2012). Cancer stem cells: an evolving concept. *Nat. Rev. Cancer* 12, 133–143.

Pabst, T., Vellenga, E., van Putten, W., Schouten, H. C., Graux, C., Vekemans, M. C., Biemond, B., Sonneveld, P., Passweg, J., Verdonck, L., Legdeur, M. C., Theobald, M., Jacky, E., Bargetzi, M., Maertens, J., Ossenkoppele, G. J., Löwenberg, B.; for the Dutch-Belgian Hemato-Oncology Cooperative Group (HOVON); the German AML Study Group (AMLSG); the Swiss Collaborative Group for Clinical Cancer Research (SAKK). (2012). Favorable effect of priming with granulocyte colony-stimulating factor in remission induction of acute myeloid leukemia restricted to dose escalation of cytarabine. *Blood* 119, 5367–5373.

Pearce, D. J., Taussig, D., Zhara, K., Smith, L. L., Ridler, C. M., Preudhomme, C., Young, B. D., Rohatiner, A. Z., Lister, T. A., and Bonnet, D. (2006). AML engraftment in the NOD/SCID assay reflects the outcome of AML: implications for our understanding of the heterogeneity of AML. *Blood* 107, 1166–1173.

Peng, C., Chen, Y., Li, D., and Li, S. (2010). Role of PTEN in leukemia stem cells. *Oncotarget* 1, 156–160.

Petit, I., Karajannis, M. A., Vincent, L., Young, L., Butler, J., Hooper, A. T., Shido, K., Steller, H., Chaplin, D. J., Feldman, E., and Rafii, S. (2008). The microtubule-targeting agent CA4P regresses leukemic xenografts by disrupting interaction with vascular cells and mitochondrial-dependent cell death. *Blood* 111, 1951–1961.

Pollard, J. A., Alonzo, T. A., Loken, M., Berbineg, R. B., Ho, P. A., Bernstein, I. D., Raimondi, S. C., Hirsch, B., Franklin, J., Walter, R. B., Gamis, A., and Meshinchi, S. (2012). Correlation of CD33 expression level with disease characteristics and response to gemtuzumab ozogamicin containing chemotherapy in childhood AML. *Blood* 119, 3705–3711.

Quere', R., Andradottir, S., Brun, A. C., Zubarev, R. A., Karlsson, G., Olsson, K., Magnusson, M., Cammenga, J., and Karlsson, S. (2011). High levels of the adhesion molecule CD44 on leukemic cells generate acute myeloid leukemia relapse after withdrawal of the initial transforming event. *Leukemia* 25, 515–526.

Ran, D., Schubert, M., Taubert, I., Eckstein, V., Bellos, F., Jauch, A., Chen, H., Bruckner, T., Saffrich, R., Wuchter, P., and Ho, A. D. (2012). Heterogeneity of leukemia stem cell candidates at diagnosis of acute myeloid leukemia and their clinical significance. *Exp. Hematol.* 40, 155–165.

Rana, K., Liesveld, J. L., and King, M. R. (2009). Delivery of apoptotic signal to rolling cancer cells: a novel biomimetic technique using immobilized TRAIL and E-selectin. *Biotechnol. Bioeng.* 102, 1692–1702.

Rasheed, Z. A., Kowalski, J., Smith, B. D., and Matsui, W. (2011). Concise review: emerging concepts in clinical targeting of cancer stem cells. *Stem Cells* 29, 883–887.

Risueno, R. M., Campbell, C. J., Dingwell, S., Levadoux-Martin, M., Leber, B., Xenocostas, A., and Bhatia, M. (2011). Identification of T-lymphocytic leukemia-initiating stem cells residing in a small subset of patients with acute myeloid leukemic disease. *Blood* 117, 7112–7120.

Rombouts, E. J., Pavic, B., Lowenberg, B., and Ploemacher, R. E. (2004). Relation between CXCR-4 expression, Flt3 mutations, and unfavorable prognosis of adult acute myeloid leukemia. *Blood* 104, 550–557.

Saito, Y., Kitamura, H., Hijikata, A., Tomizawa-Murasawa, M., Tanaka, S., Takagi, S., Uchida, N., Suzuki, N., Sone, A., Najima, Y., Ozawa, H., Wake, A., Taniguchi, S., Shultz, L. D., Ohara, O., and Ishikawa, F. (2010). Identification of therapeutic targets for quiescent, chemotherapy-resistant human leukemia stem cells. *Sci. Transl. Med.* 2, 2–22.

Sarry, J. E. Murphy, K., Perry, R., Sanchez, P. V., Secreto, A., Keefer, C., Swide, C. R., Strzelecki, A. C., Cavellier, C., Recher, C., Mansat-De Mas, V., Delabesse, E., Danet-Desnoyers, G., and Carroll, M. (2011). Human acute myelogenous leukemia stem cells are rare and heterogeneous when assayed in NOD/SCID/IL2Rγc-deficient mice. *J. Clin. Invest.* 121, 384–395.

Satoh, C., and Ogata, K. (2006). Hypothesis: myeloid-restricted hematopoietic stem cells with self-renewal capacity may be the transformation site in acute myeloid leukemia. *Leuk. Res.* 30, 491–495.

Schliemann, C., Bieker, R., Thoennissen, N., Gerss, J., Liersch, R., Kessler, T., Buchner, T., Berdel, W. E., and Mesters, R. M. (2007). Circulating angiopoietin-2 is a strong prognostic factor in acute myeloid leukemia. *Leukemia* 21, 1901–1906.

Sergeeva, A., Alatrash, G., He, H., Ruissard, K., Lu, S., Wygant, J., McIntyre, B. W., Ma, Q., Li, D., St. John, L., Clise-Dwyer, K., and Molldrem, J. J. (2011). An anti-PR1/HLA-A2 T-cell receptor-like antibody mediates complement-dependent cytotoxicity against acute myeloid leukemia progenitor cells. *Blood* 227, 4262–4272.

Sipkins, D. A., Wei, X., Wu, J. W., Runnels, J. M., Cote, D., Means, T. K., Luster A. D., Scadden, D. R., and Lin, C. P. (2005). In vivo imaging of specialized bone marrow endothelial microdomains for tumour engraftment. *Nature* 435, 969–973.

Stein, C., Kellner, C., Kugler, M., Reiff, N., Mentz, K., Schwenkert, M., Stockmeyer, B., Mackensen, A., and Fey, G. H. (2009). Novel conjugates of single-chain Fv antibody fragments specific for stem cell antigen CD123 mediate potent death of acute myeloid cells. *Br. J. Haematol.* 14, 879–889.

Su, W., Meng, F., Huang, L., Zheng, M., Liu, W., and Sun, H. (2012). Sonic hedgehog maintains survival and growth of chronic myeloid leukemia progenitor cells through beta-catenin signaling. *Exp. Hematol.* 40, 418–427.

Sutherland, H., Blair, A., Vercauteren, S., and Zapf, R. (2001). Detection and clinical significance of human acute myeloid leukaemia progenitors capable of long-term proliferation in vitro. *Br. J. Haematol.* 114, 296–306.

Taussig, D. C., Miraki-Moud, F., Anjos-Afonso, F., Pearce, D. J., Allen, K., Ridler, C., Lillington, D., Oakervee, H., Cavenagh, J., Agrawal, S. G., Listger, T. A., Gribben, J. G., and Bonnet, D. (2008). Anti-CD38 antibody-mediated clearance of human repopulating cells masks the heterogeneity of leukemia-initiating cells. *Blood* 122, 568–575.

Taussig, D. C., Vargaftig, J., Miraki-Moud, F., Griessinger, E., Sharrock, K., Luke, T., Lillington, D., Oakervee, H., Cavenagh, J., Agrawal, S. G., Lister, T. A., Gribben, J. G., and Bonnet, D. (2010). Leukemia initiating cells from some acute myeloid leukemia patients with mutated nucleophosmin reside in the CD34− fraction. *Blood* 115, 1976–1984.

van Rhenen, A., Feller, N., Kelder, A., Westra, A. H., Rombouts, E., Zweegman, S., van der Pol, M. A., Waisfisz, Q., Ossenkoppele, G. J., and Schuuhuis, G. J. (2005). High stem cell frequency in acute myeloid leukemia at diagnosis predicts high minimal residual disease and poor survival. *Clin. Cancer Res.* 11, 6520–6527.

van Rhenen, A., van Dongen, G. A., Kelder, A., Rombouts, E. J., Feller, N., Moshaver, B., Stigter-van Walsum, M., Zweegamn, S., Ossenkoppele, G. J., and Schuurhuis, G. (2007). The novel AML stem cell associated antigen CLL-1 aids in discrimination between normal and leukemic stem cells. *Blood* 110, 2659–2666.

Veiga, J. P., Costa, L. F., Sallan, S. E., Nadler, L. M., and Cardoso, A. A. (2006). Leukemia-stimulated bone marrow endothelium promotes leukemia cell survival. *Exp. Hematol.* 34, 610–621.

Walter, R. B., Appelbaum, F. R., Estey, E. H., and Bernstein, I. D. (2012).

Acute myeloid leukemia stem cells and CD33-targeted immunotherapy. *Blood* 119, 6198–6208.

Wang, Y., Lui, Y., Malek, S. N., Zheng, P., and Liu, Y. (2011). Targeting HIF-1α eliminates cancer stem cells in hematological malignancies. *Stem Cell* 8, 399–411.

Yamazaki, Y., Kunimoto, S., Ikeda, D., and Rakicidin, A. (2007). A hypoxia-selective cytotoxin. *Biol. Pharm. Bull.* 30, 261–265.

Zeng, Z., Shi, Y. X., Samudio, I. J., Wang, R. Y., Ling, X., Forlova, O., Levis, M., Rubin J. B., Negrin, R. R., Estey, E. H., Konoplev, S., Andreeff, M., and Konopleva, M. (2009). Targeting the leukemia microenvironment by CXCR4 inhibition overcomes resistance to kinase inhibitors and chemotherapy in AML. *Blood* 113, 6215–6224.

Zhang, H., Luo, J., Li, Y., Henderson, P. T., Wang, Y., Wachsmann-Hogiu, S., Zhao, W., Lam, K. S., and Pan, C. (2011). Characterization of high-affinity peptides and their feasibility for use in nanotherapeutics targeting leukemia stem cells. *Nanomedicine*. doi: 10.1016/j.nano.2011.12.004 [Epub ahead of print].

Zhao, C., Chen, A., Jamieson, C. H., Fereshteh, M., Abrahamsson, A., Bum, J., Kwon, H. Y., Kim, J., Chue, J. P., Rizzieri, D., Munchhof, M., VanArsdale, T., Beachy, P. A., and Reya, T. (2009). Hedgehog signaling is essential for maintenance of cancer stem cells in myeloid leukaemia. *Nature* 458, 776–779

Zhao, X., Singh, S., Pardoux, C., Zhao, J., His, E. D., Abo, A., and Korver, W. (2010). Targeting C-type lectin-like molecule-1 from antibody-mediated immunotherapy in acute myeloid leukemia. *Haematologica* 95, 71–78.

Ziegler, B. L., Valtieri, M., Porada, G. A., De Maria, R., Muller, R., Massella, B., Gabbianelli, M., Casella, I., Pelosi, E., Bock, T., Zanjani, E. D., and Peschle, C. (1999). KDR receptor: a key marker defining hematopoietic stem cells. *Science* 285, 1553–1558.

Conflict of Interest Statement: The author declares that the research was conducted in the absence of any commercial or financial relationships that could be construed as a potential conflict of interest.

Received: 11 June 2012; paper pending published: 22 June 2012; accepted: 16 July 2012; published online: 02 August 2012.

*Citation: Liesveld J (2012) Targeting myelogenous leukemia stem cells: role of the circulation. Front. Oncol. **2**:86. doi: 10.3389/fonc.2012.00086*

This article was submitted to Frontiers in Cancer Molecular Targets and Therapeutics, a specialty of Frontiers in Oncology.

frontiers in ONCOLOGY

ORIGINAL RESEARCH ARTICLE
published: 15 November 2012
doi: 10.3389/fonc.2012.00161

Modulating the vascular behavior of metastatic breast cancer cells by curcumin treatment

Anna L. Palange[1,2,3], Daniele Di Mascolo[1,2,3], Jaykrishna Singh[1,2], Maria S. De Franceschi[3], Claudio Carallo[3], Agostino Gnasso[3] and Paolo Decuzzi[1,2,3]*

[1] Department of Translational Imaging, The Methodist Hospital Research Institute, Houston, TX, USA
[2] Department of Nanomedicine, The Methodist Hospital Research Institute, Houston, TX, USA
[3] Department of Experimental and Clinical Medicine, University of Magna Graecia, Catanzaro, Italy

Edited by:
Michael R. King, Cornell University, USA

Reviewed by:
Hao Xu, University of Texas Southwestern Medical Center, USA
Jocelyn Marshall, Cornell University, USA

***Correspondence:**
Paolo Decuzzi, Department of Translational Imaging, The Methodist Hospital Research Institute, Houston, TX 77030, USA.
e-mail: pdecuzzi@tmhs.org

The spreading of tumor cells to secondary sites (*tumor metastasis*) is a complex process that involves multiple, sequential steps. Vascular adhesion and extravasation of circulating tumor cells (CTCs) is one, critical step. Curcumin, a natural compound extracted from *Curcuma longa*, is known to have anti-tumoral, anti-proliferative, anti-inflammatory properties and affect the expression of cell adhesion molecules, mostly by targeting the NF-κB transcription factor. Here, upon treatment with curcumin, the vascular behavior of three different estrogen receptor negative (ER^-) breast adenocarcinoma cell lines (SK-BR-3, MDA-MB-231, MDA-MB-468) is analyzed using a microfluidic system. First, the dose response to curcumin is characterized at 24, 48, and 72 h using a XTT assay. For all three cell lines, an IC_{50} larger than 20 μM is observed at 72 h; whereas no significant reduction in cell viability is detected for curcumin concentrations up to 10 μM. Upon 24 h treatment at 10 μM of curcumin, SK-BR3 and MDA-MB-231 cells show a decrease in adhesion propensity of 40% ($p = 0.02$) and 47% ($p = 0.001$), respectively. No significant change is documented for the less metastatic MDA-MB-468 cells. All three treated cell lines show a 20% increase in rolling velocity from 48.3 to 58.7 μm/s in SK-BR-3, from 64.1 to 73.77 μm/s in MDA-MB-231, and from 57.5 to 74.4 μm/s in MDA-MB-468. Collectively, these results suggest that mild curcumin treatments could limit the metastatic potential of these adenocarcinoma cell lines, possibly by altering the expression of adhesion molecules, and the organization and stiffness of the cell cytoskeleton. Future studies will elucidate the biophysical mechanisms regulating this curcumin-induced behavior and further explore the clinical relevance of these findings.

Keywords: circulating tumor cells, vascular adhesion, parallel plate flow chamber, curcumin treatment, metastasis

INTRODUCTION

The spreading of primary tumors to secondary sites (*tumor metastasis*) is responsible for a dramatic decrease in survival rate, with about 90% of the deaths in cancer patients being related to metastasis (Wittekind and Neid, 2005). Although, for a long time, this has been considered as a late stage process in tumor growth, recently it has been realized that metastatic niches can form and progress almost simultaneously with the primary mass (Klein, 2009). Metastasis is a multi-step process where tumor cells have to overcome several barriers before growing at secondary sites: (i) invade the normal tissue surrounding the tumor mass; (ii) enter the bloodstream; (iii) survive in the circulatory system; (iv) leave the blood stream and infiltrate the normal tissue; and (v) proliferate there, evading the immune system surveillance (Morris et al., 1997; Fidler, 2003; Chaffer and Weinberg, 2011). Each of these steps represents an impediment to the distant spreading of the disease that only a few primary tumor cells (one CTC out of a billion of blood cells) can overcome. Yet, metastasis occurs very often in cancer patients (Wong et al., 2001; Chambers et al., 2002).

A critical step in this process is the vascular transport of tumor cells in the hostile hemodynamic environment and the extravasation to secondary sites (Wyckoff et al., 2000). Circulating tumor cells (CTCs), transported by the blood flow, are subjected to *mechanical stress*, generated by high shear forces and collisions with other cells; and *immunological stress*, as these cells can be recognized and attacked by lymphocytes (Al-Mehdi et al., 2000; Chang et al., 2008; Vivier et al., 2008). Extravasation and infiltration are generally associated with pro-metastasis modifications of the CTCs (i.e., epithelial–mesenchymal transition) that originate in the primary mass and continue in the circulation (Iwatsuki et al., 2010; Labelle et al., 2011). The actual mechanism for extravasation depends on the tumor type and metastatic environment and can involve the (i) geometrical trapping of CTCs in narrow blood vessels (diameter <40 μm); (ii) adhesion to endothelial cells, in a leukocyte-like fashion, mediated or not mediated by platelets; and (iii) a combination of these mechanisms (Ribatti et al., 2006; Miles et al., 2008).

In this study, the main focus is on the vascular adhesion of CTCs under flow, as schematically shown in **Figure 1**. This process consists of two sequential steps: (i) CTC rolling over the vascular walls, regulated by the engagement of endothelial E-selectin and P-selectin with tumor cell glycoprotein such as CD44, CEA, CD24, sulfate glycosaminoglycans (CS-GAGs), sialylated glycosphingolipids; (ii) CTC firm arrest, regulated by other

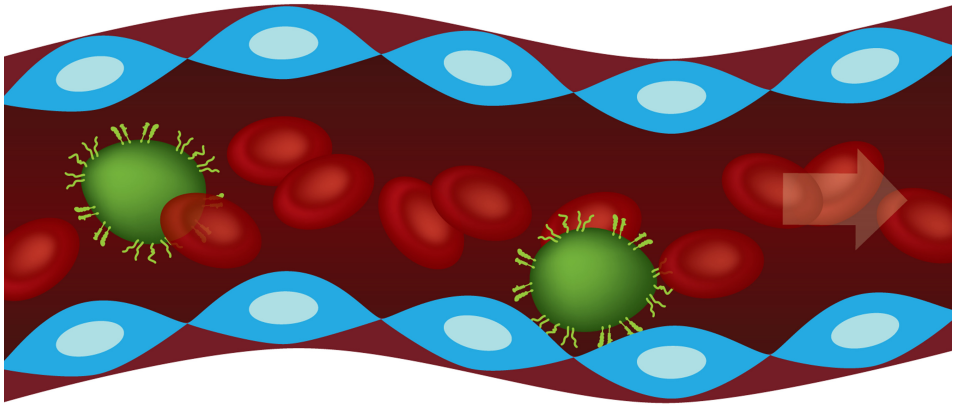

FIGURE 1 | Schematic representation of circulating tumor cells (CTCs in green) transported by the blood flow and tethering the endothelial cells (blue) through ligand molecules.

endothelial receptors (ICAM-1, VCAM-1), and different families of integrin molecules ($\alpha_v\beta_3$, β_2 integrins; Wirtz et al., 2011; Geng et al., 2012). In organs with high occurrence of metastasis, such as the liver, this picture is even more complicated in that the characteristic discontinuous and fenestrated endothelium leaves the underlying extracellular matrix directly accessible to CTCs. Moreover, vascular adhesion is also supported by the reorganization and deformation under flow of the cell cytoskeleton. Although tumor cells do not exhibit a leukocyte-like cortical cytoskeleton which is capable of extensive and rapid deformation, it is possible that CTCs exposed to shear stresses in the circulation could undergo transformations facilitating attachment to the vessel walls (Davies et al., 2005). Indeed, firm arrest is a necessary condition for the subsequent extravasation and colonization of the surrounding tissue.

The development of therapeutic agents against metastatic disease is still in its infancy, due to a lack in understanding the leading pathways and, most importantly, their alterations in secondary tumor cells. Also, most of the efforts have been traditionally oriented to eradicate tumor cells already proliferating at the secondary sites, neglecting the opportunity of blocking or modulating one or multiple steps in the metastatic cascade (Chambers et al., 2000). Novel micro- and nanotechnologies detecting, capturing, and characterizing CTCs are providing new and more accurate information on the biomechanical properties of malignant cells in the circulation. Microfluidic systems used as diagnostic tools are demonstrating the significant correlation between higher CTC counts in blood and lower patient survival (Cristofanilli et al., 2004; King et al., 2009; Han et al., 2010; Hughes and King, 2012). It is then reasonable to speculate that novel therapies, possibly nanoparticle-based, could open new avenues for an effective treatment of metastatic diseases by eradicating, or dramatically lowering, the number of CTCs.

In this work, the effect of curcumin on the rolling and adhesion mechanics under flow of three estrogen receptor (ER^-) breast adenocarcinoma cell lines, namely SK-BR-3, MDA-MB-231, and MDA-MB-468, is analyzed. These cell lines were chosen for their different metastatic potential. Curcumin is a natural multi-target compound with anti-tumoral and anti-inflammatory properties (Kumar et al., 1998; Ray et al., 2003; Kunnumakkara et al., 2008; Binion et al., 2009; Yodkeeree et al., 2010). Their rolling velocity and adhesion propensity are measured experimentally upon treatment with curcumin, using a parallel plate flow chamber system.

MATERIALS AND METHODS

MATERIALS AND CHEMICALS

SK-BR-3, MDA-MB-231, MDA-MB-468 breast adenocarcinoma cells were obtained from the American Type Cell Culture Collection (ATCC) and cultured in the recommended medium. SK-BR-3 were grown at 37°C, under a humidified 5% CO_2 and 95% air at one atmosphere, MDA-MB-231 and MDA-MB-468 were grown at 37°C in a free gas exchange with atmospheric air. Collagen type I from calf skin was obtained from Sigma Aldrich (St. Louis, MO, USA). Curcumin (diferuloylmethane) and dimethyl sulfoxide (DMSO) were obtained from Fisher Scientific. XTT kit was obtained from Trevigen (Gaithersburg, Maryland).

CYTOTOXIC EFFECT OF CURCUMIN AND XTT ASSAYS

Curcumin was first dissolved in DMSO as a 10 mM stock solution and subsequently diluted in cell culture medium. Medium containing the same amount of DMSO was used as control at concentrations not exceeding the 0.1% v/v of the culture medium. Cells were incubated with curcumin at 1, 10, 20, and 40 μM, at three time points namely 24, 48, and 72 h. Cell proliferation was measured with conventional XTT reduction assays. Briefly, SK-BR-3, MDA-MB-231, and MDA-MB-468 cells were inoculated at a density of 5×10^3 cells in 96-well plates for 24 h in 200 μl of recommended medium. The culture supernatant was then removed and medium containing the above mentioned curcumin concentrations was added to cells, subsequently incubated for 24, 48, and 72 h. After that, XTT-dye was mixed with phenol-free medium and added to the samples. The plate was incubated for at least 1 h before reading. The absorbance of XTT-formazan dye was then measured using a microplate reader at 490 nm. Twenty-five repetitions were performed for each time point and concentration.

PARALLEL PLATE FLOW CHAMBER FOR CELL ROLLING AND ADHESION

Before flow adhesion experiments, cells were first incubated with medium containing no FBS for 7 h and then treated with or without curcumin at 10 μM for 24 h. Subsequently, cells were detached from culture dishes by mild trypsinization (0.25% trypsin/EDTA) for 2 min at 37°C and incubated at 37°C for 1 h to allow the regeneration of surface glycoproteins. After that, cells were washed in PBS and resuspended at 10^6 cells/ml in serum-free medium containing 0.1% bovine serum albumin, following standard protocols (McCarty et al., 2000).

The rolling and adhesion behavior of the tumor cells, was studied using a parallel plate flow chamber system (Chen et al., 1997; Brown and Larson, 2001; GlycoTech Corporation; **Figure 2**). The system comprises a commercially available flow chamber, a syringe pump (Harvard Apparatus, MA), an inverted epifluorescent microscope (Nikon Ti-Eclipse) and a desktop computer for data storage and analysis. The main constituents of the flow chamber are a deck, a rubber gasket and a glass slide. The rubber gasket defines the geometry of the flow region (length $l = 20$ mm; width $b = 10$ mm; height $h = 0.254$ mm). The coverslips (slide), closing the bottom of the chamber, were covered with a uniform collagen layer. In particular, autoclaved 35 mm coverslips were covered by a collagen solution obtained diluting collagen type I from calf skin (Sigma Aldrich) in PBS to reach a concentration of about 50 mg/cm^2. After about 5 h at room temperature, the cover slips were rinsed in PBS and left under the bio-hood to dry. To perfuse the solution at a fixed wall shear rate S, flow rate Q is finely controlled through the syringe pump given that $S = 6Q/bh^2$.

After assembling all the components, the system was placed on the stage of an epifluorescent microscope (Nikon Ti-Eclipse). The Andor's Luca EM S camera utilizes a 658 × 496 "interline frame transfer" EMCCD sensor to acquire the region of interest (ROI) and allows for real time monitoring. For each experiment 10^6/ml cells were perfused in 1 ml of serum-free medium, at a wall shear rate of $S = 10$ s^{-1} (mimicking the circulation environment of microvascular tumor vessels). Eight experiments were performed for the SK-BR-3 and MDA-MB-468-treated and untreated cells, and 10 experiments for the MDA-MB-231. All the experiments lasted 12 min each.

Through offline data analysis on the movies derived from each experiment, the number of firmly adhering cells on the substrate and their mean rolling velocity were quantified. Firmly adhering cells were those cells staying within the region of interest (10× objective, ROI = 658 × 496 pixel) till the end of the experiment. This number was normalized by the total number of injected cells and the area of the ROI (∼0.33 × 10^{-6} m^2) deriving the adhesion propensity. The rolling velocity was calculated as the displacement of the centroid of the cells divided by the time interval of their observation (on average about 10 s). The rolling velocity was calculated for 12 cells in three different SK-BR-3 experiments ($n = 36$), and six cells in eight different MDA-MB-231 and MDA-MB-468 experiments ($n = 48$), for both the treated and the control group.

STATISTICAL ANALYSIS

Data are expressed as means ± SD. Statistical significance of differences between means was determined by one-way ANOVA. Probability values of $p < 0.05$ were considered statistically significant.

RESULTS AND DISCUSSION

The cytotoxic effect of curcumin on SK-BR-3, MDA-MB-231, and MDA-MB-468 cells was analyzed using a XTT proliferation assay. Cells were incubated with curcumin at different doses, namely 1, 10, 20, and 40 μM, and for three time points, namely 24, 48,

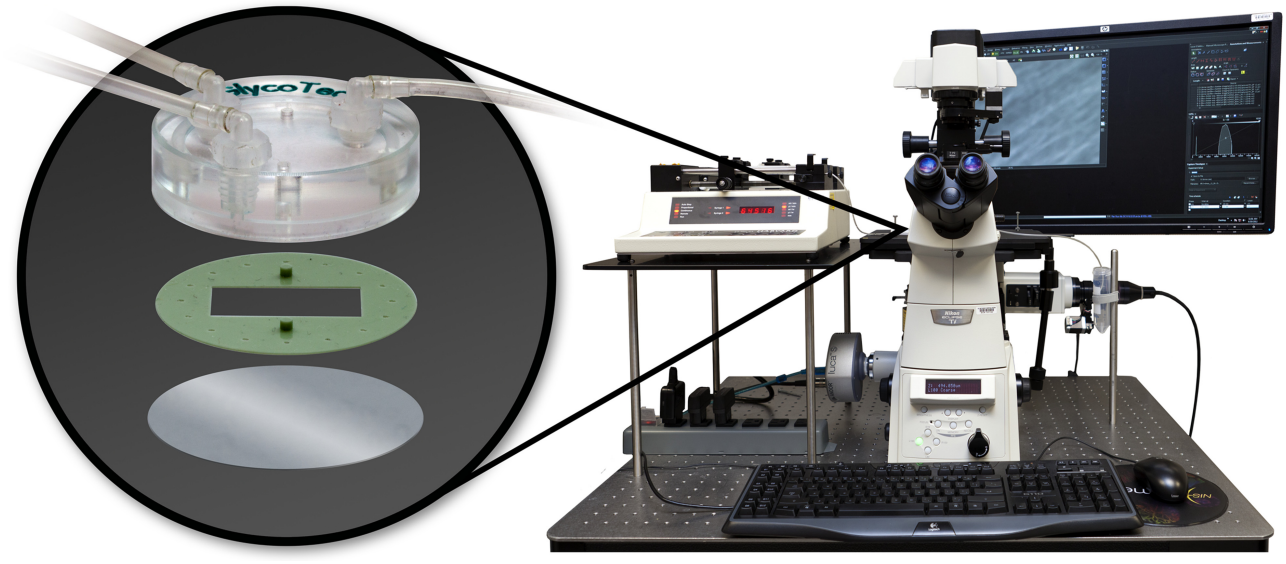

FIGURE 2 | The parallel plate flow chamber system composed of the microfluidic chamber (deck, gasket, and microscope slide represented in the oval at left); the syringe pump, the epifluorescent microscope and a desktop computer.

and 72 h. The cell viability was measured following the protocols described in Section "Materials and Methods" and is reported in the bar charts of **Figure 3**, for 25 repetitions in each cell line. As expected the percentage of viable cells reduces as the concentration and the duration of the treatment increase. Interestingly, for concentrations lower and equal to 10 μM, curcumin has no significant effect on the cell viability. Note that for the control experiments, cell culture medium was added with the same amount of DMSO used in the actual experiments for dissolving curcumin. This volume was about 0.1% of the total medium volume and no sign of toxicity was observed on the cells. For larger concentrations, 20 and 40 μM, the curcumin treatment limits cell proliferation in a dose and time dependent manner. Cell viabilities lower than 50% can only be observed at the highest concentration and longer time points (48 and 72 h). The IC_{50} is reached at ∼20 μM for the SK-BR-3 and MDA-MB-468 at 72 h; and at ∼40 μM for the MDA-MB-231 at 72 h. This is in agreement with most literature on curcumin (Aoki et al., 2007). From this assay, the exposure to 10 μM of curcumin for 24 h was considered a mild treatment inducing no significant, direct effects on cell viability.

The effect of curcumin on the rolling and adhesion behavior of the three breast adenocarcinoma cells lines SK-BR-3, MDA-MB-231, and MDA-MB-468 was analyzed using a parallel plate flow chamber, traditionally employed for the analysis of leucocyte adhesion and rolling (Lawrence et al., 1987). The cells, mildly pretreated with curcumin (24 h at 10 μM) as detailed in Section "Materials and Methods," were infused in the apparatus depicted in **Figure 2** and their rolling velocity and firm adhesion was quantified via post processing of the images taken with an epifluorescent microscope. The bar charts of **Figure 4** present the results of the flow chamber assay. **Figure 4A** shows the adhesion propensity of the curcumin-treated cells (Curc-treated) and untreated cells (Ctr), as the ratio between the absolute number of adhering cells (n_{adh}), the total number of injected cells ($n_{inj} = 10^6$), and the area of the region of interest ($A = 0.33 \times 10^{-6}$ m^2). SK-BR-3, MDA-MB-231, and MDA-MB-468-treated cells present an adhesion propensity of 90.7 ± 29.2, 58.58 ± 19.70, and 132.97 ± 31.34#/m^2, respectively. This means that for a vessel of 50 μm in diameter with a 500 μm length (vascular area ∼1 mm^2), about 300 SK-BR-3, 180 MDA-MB-231, and 400 MDA-MB-468 cells would firmly adhere under the same biophysical conditions and assuming that 10^6 CTCs enter the specific vessel. On the other hand, the untreated cells exhibit a larger adhesion propensity of 151.1 ± 60.84, 109.69 ± 38.19, and 155.42 ± 20.74#/m^2, for the SK-BR-3, MDA-MB-231, and MDA-MB-468, respectively. The difference between the two populations (Curc-treated and Ctr) is significant for the SK-BR-3 and even more for the highly metastatic MDA-MB-231 cells. More specifically, the curcumin-treated SK-BR-3 cells show a 40% decrease ($p = 0.02$) in adhesion and the curcumin-treated MDA-MD-231 a 47% decrease ($p = 0.001$) as compared to the control group. Conversely, the difference in adhesion propensity between curcumin-treated MDA-MB-468 cells and the control group is not statistically significant ($p = 0.099$).

Rolling velocity is reported in **Figure 4B**. This physical quantity was estimated as the ratio between the displacement of the cell centroid over the corresponding observation time. Despite the large standard deviation, this analysis shows that there is a significant difference between the two groups (Curc-treated and Ctr) in all three cell lines: SK-BR-3 and MDA-MB-231-treated tumor cells roll ∼1.2 times faster than the control cells ($p = 0.01$, $p = 0.009$, respectively), MDA-MB-468-treated tumor cells rolls ∼1.3 times faster than the control cells ($p = 0.00005$). In particular, the rolling velocities are 58.66 ± 20.29 and 48.33 ± 11.3 μm/s for SK-BR-3-treated and untreated cells, 73.77 ± 21.21 and 64.1 ± 12.89 for MDA-MB-231-treated and untreated cells, 74.38 ± 24.88 and 57.49 ± 11.96 for MDA-MB-468-treated and untreated cells, respectively. Indeed, the higher rolling velocity correlates well with the lower adhesion propensity observed above.

These preliminary results collectively would suggest that mild treatments with curcumin could impair cell adhesion and increase cell rolling under flow over normal, untreated cells. Indeed, this could reduce the metastatic potential of CTCs. Understanding the mechanisms regulating the observed alteration in the behavior of SK-BR-3, MDA-MB-231, and MDA-MB-468 cells is out of the scope of this preliminary study. However, it has already been reported that curcumin treatments alter the organization of microfilaments and increase the overall quantity of F-actin. This would affect cell motility and deformability, which are crucial elements in supporting tumor cell circulation and survival in the blood stream. Moreover, recently it has been shown that CTCs reattach in distant tissues by a mechanism that is tubulin-dependent and suppressed by polymerized actin (Holy, 2004; Matrone et al., 2010). In addition, curcumin is known to decrease the expression and

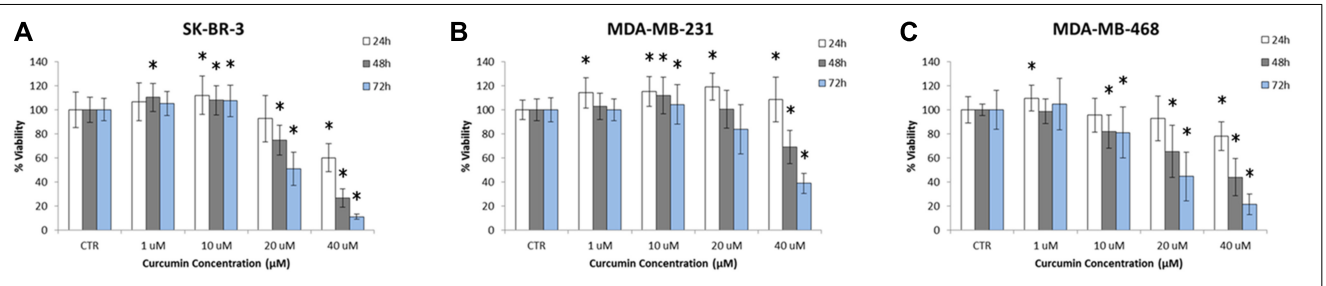

FIGURE 3 | Proliferation of (A) SK-BR-3, (B) MDA-MB-231, (C) MDA-MB-468 cells exposed to different concentrations of curcumin (1, 10, 20, and 40 μM) at three time points (24, 48, and 72 h). Note that cell proliferation is not affected at curcumin concentrations below 10 μM up to 72 h ($n = 25$). The asterisk symbol "*" denotes significant difference ($p < 0.05$) as compared to control (Ctr).

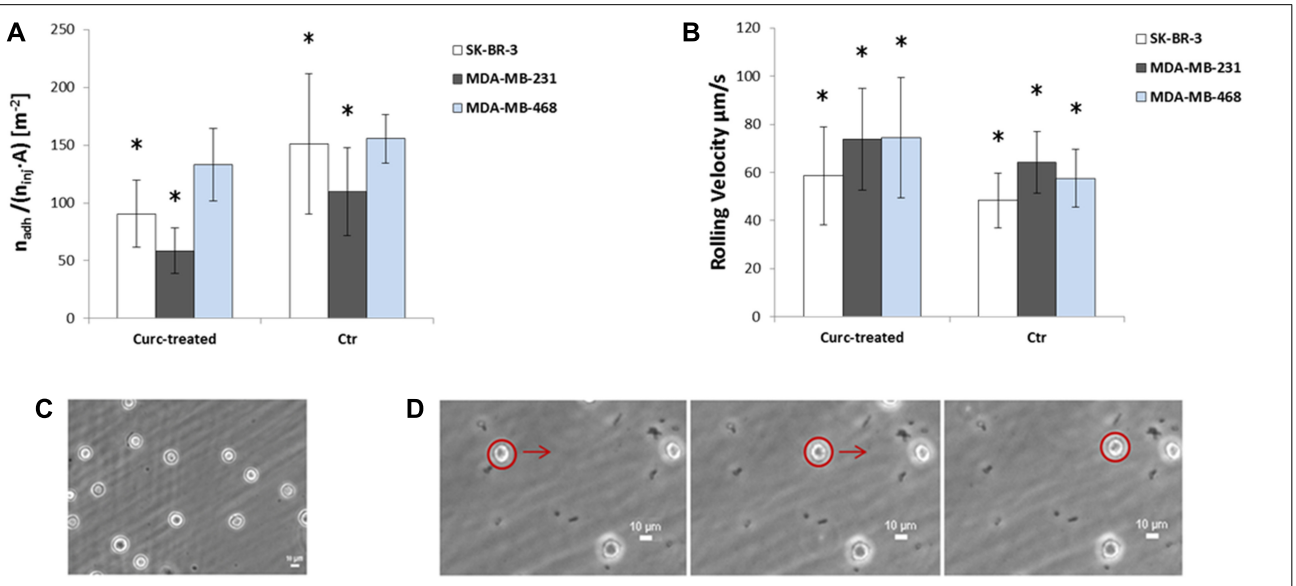

FIGURE 4 | (A) Adhesion and **(B)** rolling behavior of SK-BR-3 (white), MDA-MB-231(gray), MDA-MB-468 (blue) cells treated with curcumin (Curc-treated) at 10 μM for 24 h, and not treated cells (Ctr). The number of firmly adhering cells (n_{adh}) is normalized by the total number of injected cells ($n_{inj} = 10^6$) and the area of the region of interest ($A = 0.33 \times 10^{-6}$ m^2). Data are plotted as mean ± SD. The asterisk symbol "*" denotes significant difference ($p < 0.05$) as compared to control (Ctr). **(C)** Image of firmly adhering SK-BR3 cells on the substrate at the end of the experiment. **(D)** Captured frames showing the displacement of a rolling cell on the substrate.

modulate the activity of membrane adhesion molecules by acting on the transcription factor NF-κB. For instance, the curcumin inhibition of NF-κB completely blocked TNF-α induced expression of adhesion molecules (ICAM-1, VCAM-1, and E-selectin) on HUVECs and human intestinal microvascular endothelial cells attenuating leucocytes adhesion (Kumar et al., 1998; Ray et al., 2003; Binion et al., 2009). Therefore, in the present case, it is reasonable to speculate that curcumin effects could depend, at least in part, on a reduced expression or more likely, on the modulation of integrins receptor activity (mostly $\alpha_1\beta_1$ and $\alpha_2\beta_1$) thus limiting the adhesion propensity under flow (Park et al., 2006; Ivascu and Kubbies, 2007). Here, it is important to note that integrins, expressed on cellular membrane, can specifically bind to the collagen type I, deposited on the flow chamber glass slide. Also, in organs with high metastatic occurrence, such as the liver, the discontinuous, fenestrated endothelium allows the CTCs to directly interact and bind to ECM components. For this reason, collagen type I, has been also used in flow chamber experiments to assess the adhesive behavior of cells and CTCs (Haier et al., 1999; Wendel et al., 2012).

Finally, curcumin, a natural compound extracted from *Curcuma longa*, has been demonstrated to have a wide spectrum of biological and pharmacological activities. In particular, it exhibits antiviral, antibacterial, antioxidant, anti-inflammatory, anti-proliferative, and anti-angiogenic properties (Aggarwal et al., 2003; Holt et al., 2005). Animal and human studies have suggested its potential use in the treatment of inflammation and cancer, mostly because of its potent effect on the NF-κB pathway (Kawamori et al., 1999; Aggarwal, 2004). However, the major drawback in its clinical use is the very low bioavailability and biodistribution, mostly due to its poor absorption from the gut, rapid metabolism and elimination (Shoba et al., 1998; Anand et al., 2007). The formulation of curcumin into nanoparticles could avoid the drawbacks listed above and enhance its curative properties.

CONCLUSION

The ER negative breast metastatic cells, SK-BR-3, MDA-MB-231, and MDA-MB-468, cells were treated with curcumin, at three different time points. For sufficiently large curcumin doses (≥20 μM), significant cell death is induced at 72 h. Conversely, a mild treatment with curcumin (≤10 μM at 24 h), did not show any significant change in cell viability but did affect the vascular behavior of the cells. This was demonstrated by assessing the cell adhesion and rolling velocity in a parallel plate flow chamber system. The SK-BR-3 cells showed a 40% decrease ($p = 0.02$) in cell adhesion propensity and 20% increase ($p = 0.001$) in rolling velocity. The MDA-MB-231-treated cells showed almost a 50% decrease ($p = 0.001$) in cell adhesion propensity and about 15% increase ($p = 0.009$) in rolling velocity. The MDA-MB-468-treated cells did not show any statistically significant decrease in adhesion propensity, but did roll 1.3 times faster than the control group ($p = 0.00005$).

Collectively, these results suggest that mild curcumin treatments of CTCs could lower or even prevent the occurrence of metastasis, by reducing CTCs adhesion at secondary vascular sites. Future works will have to elucidate the mechanisms regulating the observed alteration in tumor cell behavior and the specific pathways involved in each cell line studied, by characterizing the expression and activity of cell membrane receptors, the organization of the cell cytoskeleton and its deformability. However, the proper delivery of sufficient doses of curcumin

to CTCs could provide a new strategy to prevent the metastatic spread.

ACKNOWLEDGMENTS

This work was partially supported by the Cancer Prevention Research Institute of Texas through the grant CPRIT RP110262; the National Institutes of Health (NIH, USA) through the grants U54CA143837 and U54CA151668. Anna L. Palange and Daniele Di Mascolo acknowledge the Doctoral School of The University of Magna Graecia (Italy) for travel support. Daniele Di Mascolo also acknowledges the support of the EU Commission, the European Social Fund and the department 11 "Culture - Education - University - Research - Technological Innovation – Higher Education" of Calabria Region (POR Calabria FSE 2007/2013). The authors wish to thank Mr. Matthew Landry at TMHRI for his help with the artwork.

REFERENCES

Aggarwal, B. B. (2004). Nuclear factor-κB: the enemy within. *Cancer Cell* 6, 203–208.

Aggarwal, B. B., Kumar, A., and Bharti, A. C. (2003). Anticancer potential of curcumin: preclinical and clinical studies. *Anticancer Res.* 23, 363–398.

Al-Mehdi, A. B., Tozawa, K., Fisher, A. B., Shientag, L., Lee, A., and Muschel, R. J. (2000). Intravascular origin of metastasis from the proliferation of endothelium-attached tumor cells: a new model for metastasis. *Nat Med.* 6, 100–102.

Anand, P., Kunnumakkara, A. B., Newman, R. A., and Aggarwal, B. B. (2007). Bioavailability of curcumin: problems and promises. *Mol. Pharm.* 4, 807–818.

Aoki, H., Takada, Y., Kondo, S., Sawaya, R., Aggarwal, B. B., and Kondo, Y. (2007). Evidence that curcumin suppresses the growth of malignant gliomas *in vitro* and *in vivo* through induction of autophagy: role of Akt and extracellular signal-regulated kinase signaling pathways. *Mol. Pharmacol.* 72, 29–39.

Binion, D. G., Heidemann, J., Li, M. S., Nelson, V. M., Otterson, M. F., and Rafiee, P. (2009). Vascular cell adhesion molecule-1 expression in human intestinal microvascular endothelial cells is regulated by PI 3-kinase/Akt/MAPK/NF-kappaB: inhibitory role of curcumin. *Am. J. Physiol. Gastrointest. Liver Physiol.* 297, G259–G268.

Brown, D. C., and Larson, R. S. (2001). Improvements to parallel plate flow chambers to reduce reagent and cellular requirements. *BMC Immunol.* 2, 9. doi: 10.1186/1471-2172-2-9

Chaffer, C. L., and Weinberg, R. A. (2011). A perspective on cancer cell metastasis. *Science*331, 1559–1564.

Chambers, A. F., Groom, A. C., and MacDonald, I. C. (2002). Dissemination and growth of cancer cells in metastatic sites. *Nat. Rev. Cancer* 2, 563–572.

Chambers, A. F., MacDonald, I. C., Schmidt, E. E., Morris, V. L., and Groom, A. C. (2000). Clinical targets for anti-metastasis therapy. *Adv. Cancer Res.* 79, 91–121.

Chang, S. F., Chang, C. A., Lee, D. Y., Lee, P. L., Yeh, Y. M., Yeh, C. R., et al. (2008). Tumor cell cycle arrest induced by shear stress: roles of integrins and Smad. *Proc. Natl. Acad. Sci. U.S. A.* 105, 3927–3932.

Chen, S., Alon, R., Fuhlbrigge, R. C., and Springer, T. A. (1997). Rolling and transient tethering of leukocytes on antibodies reveal specializations of selectins. *Proc. Natl. Acad. Sci. U.S.A.* 94, 3172–3177.

Cristofanilli, M., Budd, G. T., Ellis, M. J., Stopeck, A., Matera, J., Miller, M. C., et al. (2004). Circulating tumor cells, disease progression, and survival in metastatic breast cancer. *N. Engl. J. Med.* 351, 781–791.

Davies, P. F., Spaan, J. A., and Krams, R. (2005). Shear stress biology of the endothelium. *Ann. Biomed. Eng.* 33, 1714–1718.

Fidler, I. J. (2003). The pathogenesis of cancer metastasis: the "seed and soil" hypothesis revisited. *Nat. Rev. Cancer* 3, 453–458.

Geng, Y., Marshall, J. R., and King, M. R. (2012). Glycomechanics of the metastatic cascade: tumor cell–endothelial cell interactions in the circulation. *Ann. Biomed. Eng.* 40, 790–805.

Haier, J., Marwan, Y. N., and Nicolson, G. L. (1999). β1-integrin-mediated dynamic adhesion of colon carcinoma cells to extracellular matrix under laminar flow. *Clin. Exp. Metastasis* 17, 377–387.

Han, W., Allio, B. A., Foster, D. G., and King, M. R. (2010). Nanoparticle coatings for enhanced capture of flowing cells in microtubes. *ACS Nano* 4, 174–180.

Holt, P. R., Katz, S., and Kirshoff, R. (2005). Curcumin therapy in inflammatory bowel disease: a pilot study. *Dig. Dis. Sci* 50, 2191–2193.

Holy, J. (2004). Curcumin inhibits cell motility and alters microfilament organization and function in prostate cancer cells. *Cell Motil. Cytoskeleton* 58, 253–268.

Hughes, A. D., and King, M. R. (2012). Nanobiotechnology for the capture and manipulation of circulating tumor cells. *Wiley Interdiscip. Rev. Nanomed. Nanobiotechnol.* 4, 291–309.

Ivascu, A., and Kubbies, M. (2007). Diversity of cell-mediated adhesions in breast cancer spheroids. *Int. J. Oncol.* 31, 1403–1413.

Iwatsuki, M., Mimori, K., Yokobori, T., Ishi, H., Beppu, T., Nakamori, S., et al. (2010). Epithelial–mesenchymal transition in cancer development and its clinical significance. *Cancer Sci.* 101, 293–299.

Kawamori, T., Lubet, R., Steele, V. E., Kelloff, G. J., Kaskey, R. B., Rao, C. V., et al. (1999). Chemopreventive effect of curcumin, a naturally occurring anti-inflammatory agent, during the promotion/progression stages of colon cancer. *Cancer Res.* 59, 597–601.

King, M. R., Western, L. T., Rana, K., and Liesveld, J. L. (2009). Biomolecular surfaces for the capture and reprogramming of circulating tumor cells. *J. Bionic Eng.* 6, 311–317.

Klein, C. A. (2009). Parallel progression of primary tumor and metastasis. *Nat. Rev. Cancer* 9, 302–312.

Kumar, A., Dhawan, S., Hardegen, N. J., and Aggarwal, B. B. (1998). Curcumin (Diferuloylmethane) inhibition of tumor necrosis factor (TNF)-mediated adhesion of monocytes to endothelial cells by suppression of cell surface expression of adhesion molecules and of nuclear factor-kappaB activation. *Biochem. Pharmacol.* 55, 775–783.

Kunnumakkara, A. B., Anand, P., and Aggarwal, B. B. (2008). Curcumin inhibits proliferation, invasion, angiogenesis and metastasis of different cancers through interaction with multiple cell signaling proteins. *Cancer Lett.* 269, 199–225.

Labelle, M., Begum, S., and Hynes, R. O. (2011). Direct signaling between platelets and cancer cells induces an epithelial-mesenchymal-like transition and promotes metastasis. *Cancer Cell* 120, 576–590.

Lawrence, M. B., McIntire, L. V., and Eskin, S. G. (1987). Effect of flow on polymorphonuclear leukocyte/endothelial cell adhesion. *Blood* 70, 1284–1290.

Matrone, M. A., Whipple, R. A., and Balzer, E. M. and Martin, S. S. (2010). Microtentacles tip the balance of cytoskeletal forces in circulating tumor cells. *Cancer Res.* 70, 7737–7741.

McCarty, O. J. T., Mousa, S. A., Bray, P. F., and Konstantopoulos, K. (2000). Immobilized platelets support human colon carcinoma cell tethering, rolling, and firm adhesion under dynamic flow conditions. *Blood* 96, 1789–1797.

Miles, F. L., Pruitt, F. L., Van Golen, K. L., and Cooper, C. R. (2008). Stepping out of the flow: capillary extravasation in cancer metastasis. *Clin. Exp. Metastasis* 25, 305–324.

Morris, V. L., Schmidt, E. E., Mac Donald, I. C., Groom, A. C., and Chambers, A. F. (1997). Sequential steps in hematogenous metastasis of cancer cells studied by *in vivo* videomicroscopy. *Invasion Metastasis* 17, 281–296.

Park, C. C., Zhang, H., Pallavicini, M., Gray, J. W., Baehner, W., Park, C. J., et al. (2006). β1 integrin inhibitory antibody induces apoptosis of breast cancer cells, inhibits growth, and distinguishes malignant from normal phenotype in three dimensional cultures and *in vivo*. *Cancer Res.* 66, 1526–1535.

Ray, S., Chattopadhyay, N., Mitra, A., Siddiqi, M., and Chatterjee, A. (2003). Curcumin exhibits antimetastatic properties by modulating integrin receptors, collagenase activity, and expression of Nm23 and E-cadherin. *J. Environ. Pathol. Toxicol. Oncol.* 22, 49–58.

Ribatti, D., Mangialardi, G., and Vacca, A. (2006). Stephen Paget and the "seed and soil" theory of metastatic dissemination. *Clin. Exp. Med.* 6, 145–149.

Shoba, G., Joy, D., Joseph, T., Majeed, M., Rajendran, R., and Srinivas, P. S. (1998). Influence of piperine on the pharmacokinetics of curcumin in animals and human volunteers. *Planta Med.* 64, 353–356.

Vivier, E., Tomasello, E., Baratin, M., Walzer, T., and Ugolini, S. (2008). Functions of natural killer cells. *Nat Immunol.* 9, 503–510.

Wendel, C., Hemping-Bovenkerk, A., Krasnyanska, J., Torge Mees, S.,

Kochetkova, M., Stoeppeler, S., et al. (2012). CXCR4/CXCL12 participate in extravasation of metastasizing breast cancer cells within the liver in a rat model. *PLoS ONE* 7, e30046. doi: 10.1371/journal.pone.0030046

Wirtz, D., Konstantopoulos, K., and Searson, P. C. (2011). The physics of cancer: the role of physical interactions and mechanical forces in metastasis. *Nat. Rev. Cancer* 11, 512–522.

Wittekind, C., and Neid, M. (2005). Cancer invasion and metastasis. *Oncology* 69(Suppl. 1), 14–16.

Wong, C. W., Lee, A., Shientag, L., Yu, J., Dong, Y., Kao, G., et al. (2001). Apoptosis: an early event in metastatic inefficiency. *Cancer Res.* 61, 333–338.

Wyckoff, J. B., Jones, J. G., Condeelis, J. S., and Segall, J. E. (2000). A critical step in metastasis: *in vivo* analysis of intravasation at the primary tumor. *Cancer Res.* 60, 2504–2511.

Yodkeeree, S., Ampasavate, C., Sung, B., Aggarwal, B. B., and Limtrakul, P. (2010). Demethoxycurcumin suppresses migration and invasion of MDA-MB-231 human breast cancer cell line. *Eur. J. Pharmacol.* 627, 8–15.

Conflict of Interest Statement: The authors declare that the research was conducted in the absence of any commercial or financial relationships that could be construed as a potential conflict of interest.

Received: 03 July 2012; accepted: 23 October 2012; published online: 15 November 2012.

*Citation: Palange AL, Di Mascolo D, Singh J, De Franceschi MS, Carallo C, Gnasso A and Decuzzi P (2012) Modulating the vascular behavior of metastatic breast cancer cells by curcumin treatment. Front. Oncol. **2**:161. doi: 10.3389/fonc.2012.00161*

This article was submitted to Frontiers in Cancer Molecular Targets and Therapeutics, a specialty of Frontiers in Oncology.

frontiers in ONCOLOGY

ORIGINAL RESEARCH ARTICLE
published: 27 July 2012
doi: 10.3389/fonc.2012.00076

Three to tango: MUC1 as a ligand for both E-selectin and ICAM-1 in the breast cancer metastatic cascade

Yue Geng†, Kimberly Yeh†, Tait Takatani and Michael R. King*

Department of Biomedical Engineering, Cornell University, Ithaca, NY, USA

Edited by:
James L. Gulley, National Cancer Institute, USA

Reviewed by:
Min Hee Kang, School of Medicine Texas Tech University Health Sciences Center, USA
Jacalyn Rosenblatt, Harvard Medical School, USA

***Correspondence:**
Michael R. King, Department of Biomedical Engineering, Cornell University, 205 Weill Hall, NY 14853, USA.
e-mail: mike.king@cornell.edu

†Yue Geng and Kimberly Yeh have contributed equally to this work.

Cancer cell tethering and rolling on the vascular wall is facilitated by various selectin: glycoprotein interactions which lead to eventual extravasation and metastases. The aberrantly underglycosylated mucin MUC1 has been shown to both abundantly express selectin binding moieties (sialyl Lewis x and a) and to consistently expose its core epitope. Flow cytometry was used to determine MUC1 expression on ZR-75-1 and MCF7 cells, while immunofluorescence microscopy was used to confirm the aberrant form of MUC1 and MUC1:ICAM-1 interactions. Each cell line was then perfused through combined E-selectin and ICAM-1 coated microtubes, as a model of the microvascular endothelium. ZR-75-1 and MCF7 were found to express abundant and low levels of underglycosylated MUC1, respectively. The rolling/adhesion profiles showed that ZR-75-1 cells, when compared to MCF7 cells, interact with E-selectin more efficiently resulting in sufficiently slow rolling velocities to form MUC1:ICAM-1 interactions thereby facilitating firm adhesion. The purpose and novelty of this work is the demonstration of the synergistic adhesion capabilities of MUC1 in the metastatic adhesion cascade, where the observed differential adhesion is consistent with the relative metastatic potential of the ZR-75-1 (highly metastatic) and MCF7 (weakly metastatic) cell lines.

Keywords: adhesion, breast cancer, circulation, E-selectin, ICAM-1, MUC1

INTRODUCTION

The mucin family of glycoproteins is traditionally associated with the protection of the epithelial layer and provides lubrication of luminal epithelial surfaces. More recently, certain mucins have been identified as markers for metastatic cancers. Of particular importance, the mucin MUC1 is overexpressed in numerous cancers including breast, ovarian, lung, pancreatic, prostate, gastric, and colorectal (Zotter et al., 1987; Girling et al., 1989; Ajioka et al., 1996; Burdick et al., 1997; Retz et al., 1998), where high expression generally correlates with increased mortality rates (MacLean et al., 1997; Guddo et al., 1998; Kocer et al., 2004; Duncan et al., 2007; Tewes et al., 2009). It is then reasonable to hypothesize that cancer's adaptation and alteration of MUC1 may play a vital role in metastatic progression.

Cancer metastasis through the bloodstream is initiated by the invasion of tumor cells from the primary site into the blood vessel (Moss and Anderson, 2000). These circulating tumor cells (CTCs) can then adhere to the endothelial lining, which leads to extravasation and the formation of secondary tumor sites. For CTC adhesion, cells may first establish transient interactions with the activated endothelium which facilitates cell tethering and rolling events (Tremblay et al., 2008; St Hill, 2011; Wirtz et al., 2011). These types of interactions are produced via selectins, a family of adhesion molecules expressed by the endothelium, and carbohydrate moieties, such as sialyl Lewis x (sLe^x) or sialyl Lewis a (sLe^a), present on the selectin ligands expressed by CTCs (Borsig et al., 2002; Varki and Varki, 2007). Once the cell has sufficiently reduced its rolling velocity, firm adhesion can be acquired through the interaction between the intracellular cell adhesion molecule 1 (ICAM-1) on the endothelium and integrins on CTCs. This series of events is commonly referred to as the metastatic adhesion cascade (Orr et al., 2000).

MUC1 is not only overexpressed in many cancer types but is also aberrantly underglycosylated. The core structure of the extracellular domain of MUC1 mainly consists of 25–150 repeat units of 20 identical amino acid sequences rich in serines and threonines resulting in a length 5–10 times that of most membrane proteins. Normally, these amino acids would be richly O-glycosylated however aberrant MUC1 has been shown to express shortened oligosaccharides such as sLe^x and sLe^a, and binds efficiently to E-selectin (Lloyd et al., 1996). Interestingly, high levels of MUC1 carrying $sLe^{x/a}$ correlate to poor prognosis in patients with lung adenocarcinoma (Inata et al., 2007). Aberrant MUC1 also has the propensity to expose its core epitope due to underglycosylation where it has become the target of various probes to determine MUC1 expression (Moore et al., 2004). Furthermore, ICAM-1 has been shown to recognize and bind to the core epitope of MUC1 (Hayashi et al., 2001). Therefore, CTCs may utilize aberrant MUC1 to facilitate tethering and rolling due to the increased length of MUC1 relative to other selectin ligands, and firmly adhere to the endothelium via ICAM-1 interactions (Regimbald et al., 1996).

In this study, we investigate the role of MUC1 in breast cancer cell adhesion under flow with two cell lines: ZR-75-1 which is known to have a high metastatic potential, and MCF7 which is weakly metastatic. The differential adhesion of these two cell lines

to the endothelium are studied *in vitro* via micro-renathane tubes coated with varying ratios of E-selectin and ICAM-1 which represent a model of metastasis-prone microvasculature (Finzel et al., 2004). We hypothesize that the underglycosylated form of MUC1 may serve as a ligand for both E-selectin and ICAM-1, which would allow for efficient interaction between CTCs in transit and the inflamed endothelium.

MATERIALS AND METHODS

REAGENTS

Recombinant E-selectin-IgG_1 chimera and recombinant ICAM-1-IgG_1 chimera were purchased from R&D systems (Minneapolis, MN, USA). Blotting grade blocker non-fat dry milk was obtained from Bio-Rad Laboratories (Hercules, CA, USA) and Protein-G was purchased from EMD Biosciences (San Diego, CA, USA). FITC mouse anti-human CD227 (clone HMPV), FITC mouse IgG1 k isotype control, purified mouse anti-human CD15s (clone CSLEX), APC rat anti-mouse IgM, and FITC goat anti-mouse IgG/IgM were all purchased from BD Biosciences (San Jose, CA, USA). FITC mouse anti-human CD44v4 was obtained from AbD Serote (Germany). FITC and APC anti-human IgG antibodies were purchased from Invitrogen (Carmarillo, CA, USA). Ca^{2+} and Mg^{2+} free DPBS (Invitrogen, Camarillo, CA, USA), calcium carbonate (Sigma Chemical Co., St. Louis, MO, USA), low endotoxin (1 ng/mg), and essentially globulin-free Bovine Serum Albumin (Sigma Chemical Co., St. Louis, MO, USA) were used to prepare flow buffer for cell adhesion assays.

BREAST CANCER CELL CULTURE

Breast cancer cell lines ZR-75-1 and MCF7 were purchased from ATCC and maintained in 10% Fetal Bovine Serum (FBS; Cellgro), 1% penicillin-streptomycin (Invitrogen), and RPMI 1640 medium (ZR-75-1) or eagle's minimal essential medium with 0.01 mg/mL bovine insulin (MCF7) at 37°C with 5% CO_2 in a humidified incubator.

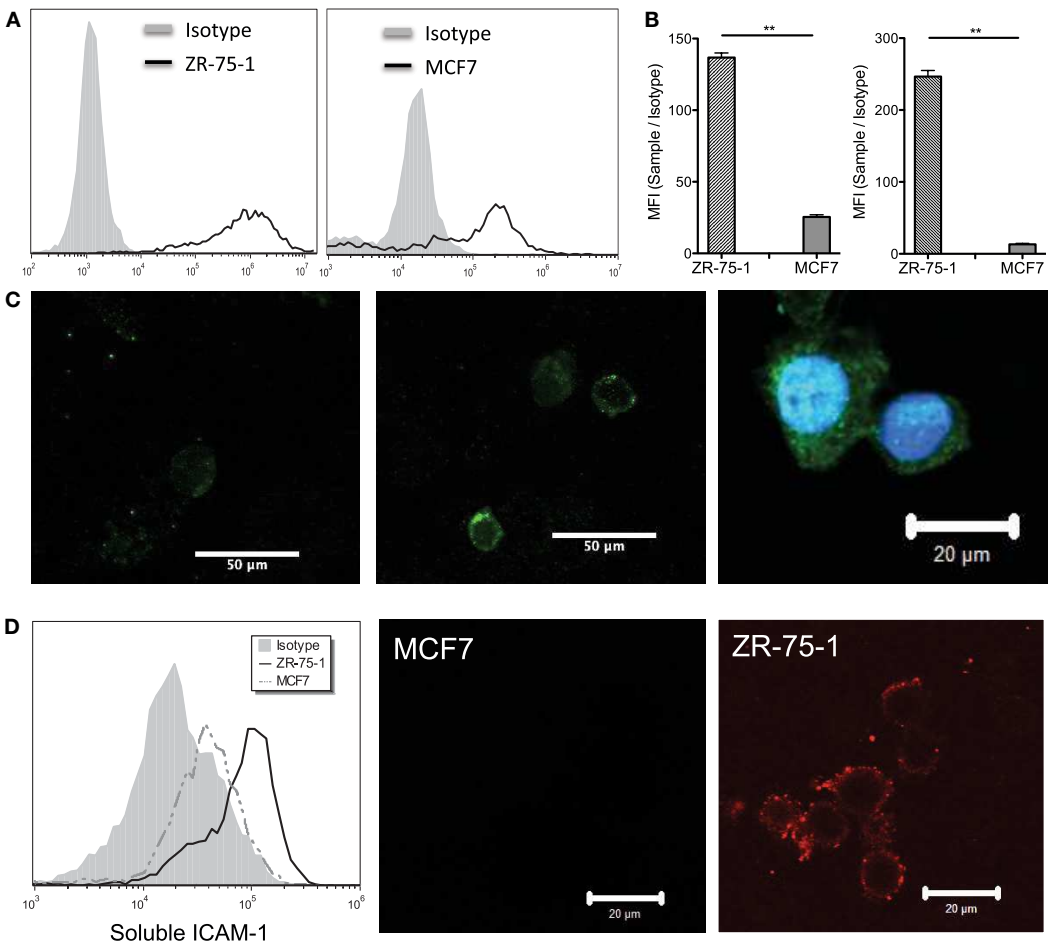

FIGURE 1 | (A) Flow cytometry histogram plots of ZR-75-1 and MCF7 labeled with anti-MUC1 mAb clone HMPV, respectively. **(B)** Quantification of the MFI ratio of sample/isotype for both cell types with anti-MUC1 mAb clone SM3 and HMPV, respectively. Student's *t*-test was used for statistical analysis and results from both labeling experiments were found to be significantly different for ZR-75-1 and MCF7 cells ($p \leq 0.01$). **(C)** Left and middle: confocal microscopy images of MCF7 and ZR-75-1 labeled with anti-MUC1 mAb (clone SM3), respectively. Right: strong signal of SM3 anti-MUC1 mAb in the cytoplasmic region of select ZR-75-1 cells. **(D)** Left: flow cytometry histogram of fluorescently tagged ICAM-1 labeling on ZR-75-1 and MCF7 cells. Middle and right: confocal microscopy images of MCF7 and ZR-75-1 cells labeled with fluorescently tagged ICAM-1.

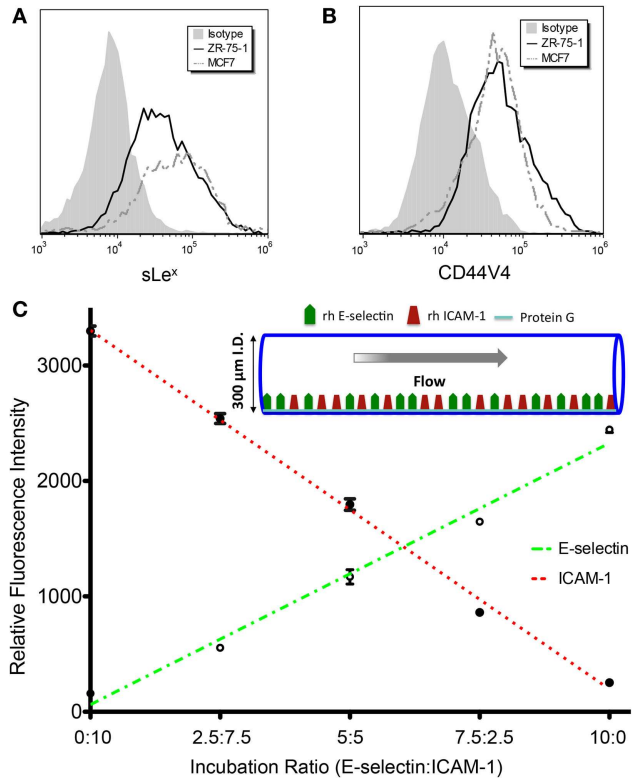

FIGURE 2 | (A,B) Flow cytometry histogram overlays of ZR-75-1 and MCF7 cells labeled with anti-sLe^x (clone CSLEX) mAb and anti-CD44V4 mAb, respectively. **(C)** E-selectin and ICAM-1 fluorescence intensities as concentration ratios vary during surface preparation. The r^2 values for E-selectin and ICAM-1 fluorescence intensity trend lines were found to be 0.986 and 0.995, respectively.

FLOW CYTOMETRY

Cells were removed from tissue culture flasks prior to antibody incubation using an enzyme-free cell dissociation buffer solution. After washing with 1× DPBS, the cells were resuspended in 1% BSA in DPBS to a final concentration of approximately 250,000 cells in each sample. Antibodies against MUC1 or appropriate isotype controls were added to the cell suspensions and incubated over ice for 45 min. Specifically, mouse anti-human MUC1 mAb clone HMPV (reacts with the core peptide of MUC1) and mouse anti-human MUC1 mAb clone SM3 (recognizes the underglycosylated form of MUC1) were used in this study. Following incubation, cells were washed twice with 500 μL of 1% BSA to remove any unbound antibody. Flow cytometry samples were analyzed using a BD Accuri C6 flow cytometer (Ann Arbor, MI, USA).

SOLUBLE ICAM-1 BINDING ASSAY

Recombinant human ICAM-1-IgG$_1$ chimeric protein (R&D) was fluorescently tagged with Alexa 647 anti-human IgG antibody and incubated with ZR-75-1 and MCF7 cells in 1× DPBS with 2% BSA for 30 min at room temperature. Unbound proteins were washed off with 1× DPBS twice prior to flow cytometry and confocal microscopy imaging.

PREPARATION OF COMBINED PROTEIN SURFACES

Micro-renathane tubings (microtubes) with an inner diameter of 300 μm (Braintree Scientific Inc., Braintree, MA, USA) were cut to lengths of 50 cm. Recombinant human E-selectin-IgG$_1$ and ICAM-1-IgG$_1$ chimeric proteins were each dissolved in 1× PBS and mixed in various ratios (E-sel/ICAM-1: 10/0, 7.5/2.5, 5/5, 2.5/7.5, 0/10) to a final protein concentration of 10 μg/mL. The microtube surface was first rinsed with 1× DPBS and then incubated with 10 μg/mL of protein-G solution for 1 h, followed by a 2 h incubation with the premixed E-selectin and ICAM-1 protein solution, then blocked with 5% milk protein in PBS for 1 h. To evaluate the correlation between incubation concentrations and surface coverage, FITC conjugated E-selectin and APC conjugated ICAM-1 were mixed in the ratios described above. Fluorescence images were taken and analyzed using Image J.[1]

CELL ADHESION ASSAY

After surface functionalization as described above, microtubes were secured to the stage of an Olympus IX81 motorized inverted microscope (Olympus America, Melville, NY, USA). A CCD camera (model no: KP-M1AN, Hitachi, Tokyo, Japan) and a DVD recorder (model no: DVD-1000MD, Sony Electronics) were used to record experiments for offline analysis. ZR-75-1 and MCF7 breast cancer cells suspended in flow buffer were perfused through protein coated microtubes using a syringe pump (KDS 230, IITC Life Science, Woodland Hills, CA, USA) at a wall shear stress of 1.0 dyne/cm^2.

CONFOCAL IMMUNOFLUORESCENCE MICROSCOPY

ZR-75-1 and MCF7 cells were removed from tissue culture flasks, washed with 1× DPBS, resuspended with 2% BSA in 1× DPBS, loaded to a pre-assembled cytospin cuvette, and spun at 750 rpm for 3 min in a Shandon Cytospin 3 centrifuge (Harlow Scientific, Arlington, MA, USA). Cytospin slides were then dried and fixed with 4% paraformaldehyde (Electron Microscopy Sciences, Hatfield, PA, USA) prior to antibody labeling. Indirect surface staining for MUC1 was performed using mouse anti-human MUC1 mAb (clone SM3) and Alexa 647 rat anti-mouse mAb as a secondary antibody. For some cytospin slides, nuclear staining with DAPI was performed for 10 min at room temperature prior to imaging. Samples from the soluble ICAM-1 binding assay were deposited on cytospin slides for imaging. A Zeiss 710 laser scanning confocal microscope at the Cornell University microscopy and imaging core facility was used to collect images using a 40× objective.

DATA ACQUISITION AND ANALYSIS

"Rolling" cells were defined as those observed to translate in the direction of flow with an average velocity less than 50% of the calculated hydrodynamic free stream velocity. The rolling velocity was calculated by measuring the distance a rolling cell traveled over a 30 s interval. Videos of rolling cells were taken at three randomly selected locations along the microtube. "Tethering" cells were defined as cells that were observed to roll intermittently with fluctuating velocity. The quantity of cells rolling, adherent and

[1] http://rsbweb.nih.gov/ij/

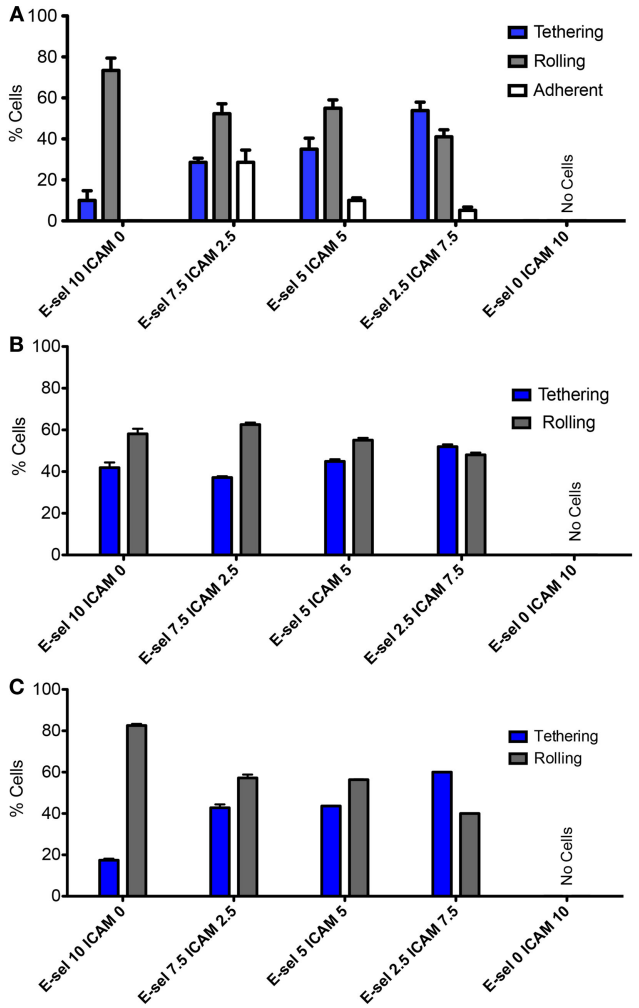

FIGURE 3 | Adhesion phenotypes on combined protein surface under physiological flow of (A) ZR-75-1, (B) MCF7, and (C) SM3 blocked ZR-75-1 cells. Two-way ANOVA was used for statistical analysis and results from all conditions were found to be significantly different ($p \leq 0.001$).

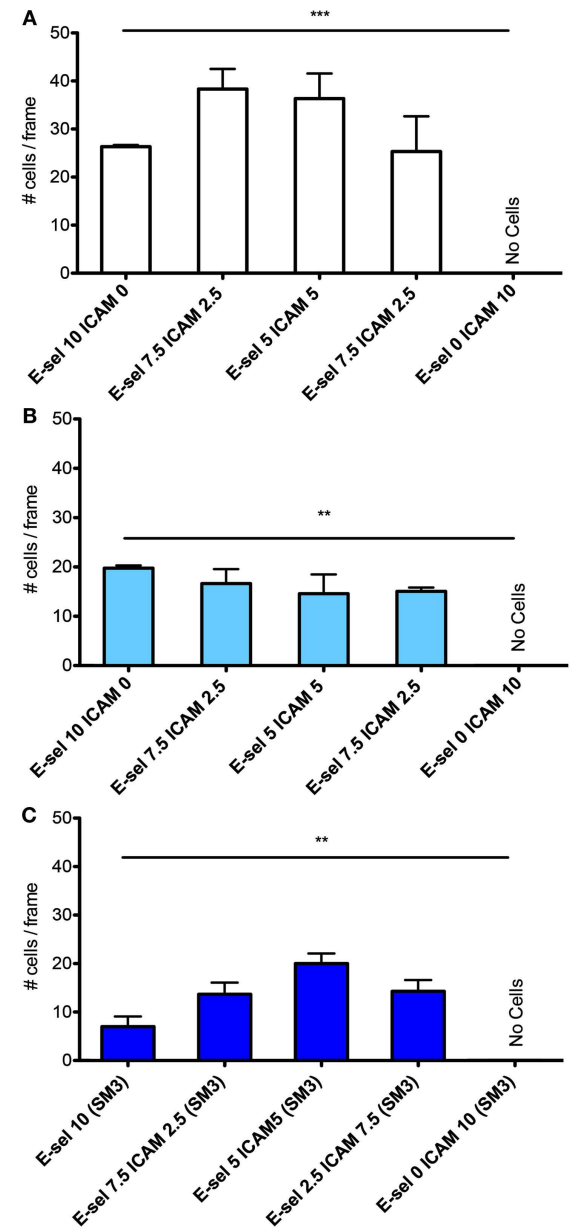

FIGURE 4 | Quantification of average number of cells captured on the surfaces with varying ratios of E-selectin and ICAM-1 for (A) ZR-75-1, (B) MCF7, and (C) SM3 blocked ZR-75-1 cells. One-way ANOVA was used for statistical analysis. For all three experiments, results from all conditions were found to be significantly different with *p*-values of 0.0008, 0.0093, and 0.0016 for ZR-75-1, MCF7, and SM3 blocked ZR-75-1, respectively. $^{**}p \leq 0.01$; $^{***}p \leq 0.001$.

tethering was determined by recording images at 30 randomly selected locations along the microtube. All errors are reported as standard error of the mean, and statistical analyses were performed using Prism (GraphPad Software, San Diego, CA, USA).

MOLECULAR DYNAMICS

The crystal structure of SM3 bound to the MUC1 core fragment (1SM3; Dokurno et al., 1998) was obtained from the Protein Data Bank for use as starting coordinates. The MUC1 fragment was equally extended beyond the SM3:MUC1 interaction to include all amino acids of one complete tandem repeat unit (PATSGPAPRTDPASTVGHAP) and the furthest threonine/serine from SM3 was O-glycosylated with the sLe^x carbohydrate group. Using the YASARA[2] package of molecular dynamics (MD) programs, the complex was solvated in a water cube with an initial length of 100 Å to allow for free protein rotation and neutralized to 0.9% NaCl with physiologically neutral pH (7.4). The YAMBER3 self-parameterizing force field (Krieger et al., 2004) was implemented with periodic boundary conditions, the particle mesh Ewald method for electrostatic interactions (Essmann et al., 1995) and a recommended 7.86 Å force cutoff for long-range interactions. Temperature and pressure were held constant

[2]http://yasara.org

at 300 K and 1 atm, respectively, while the water box was allowed to adjust slightly to constrain the water density to 0.997 g/L. Conformational stresses were then removed via short steepest descent minimizations and simulated annealing was run until sufficient convergences were reached. A free dynamics simulation was then run for 10 ns to obtain the final equilibrated structure.

RESULTS

DIFFERENTIAL MUC1 EXPRESSION ON ZR-75-1 AND MCF7 CELLS AND THEIR ABILITY TO BIND TO ICAM-1 UNDER STATIC CONDITIONS

MUC1 core peptide expression was measured for both ZR-75-1 and MCF7 cells via flow cytometry using MUC1 mAb clone HMPV and found to be significantly higher on ZR-75-1 cells (**Figure 1A**). MUC1 mAb clone SM3 was also used to detect the underglycosylated form of MUC1, which has been identified as a tumor associated form of MUC1 (Mommers et al., 1999). Although no significant shift was observed, mean fluorescence intensity (MFI) of sample/isotype for ZR-75-1 cells was observed to be five times higher than MCF7 cells (**Figure 1B**). Furthermore, confocal microscopy images with MUC1 antibody (SM3) labeling showed brighter signals on ZR-75-1 cells (**Figure 1C**). Strong homogenous cytoplasmic staining of MUC1 (SM3) was observed on some ZR-75-1 cells (**Figure 1C** right) but not on MCF7 cells. To assay MUC1:ICAM-1 binding under static conditions, human recombinant ICAM-1 was conjugated with a fluorescently tagged secondary antibody and incubated with both cell types. Flow cytometry and confocal microscopy results both showed significantly stronger binding of ICAM-1 to ZR-75-1 cells compared to MCF7 cells (**Figure 1D**).

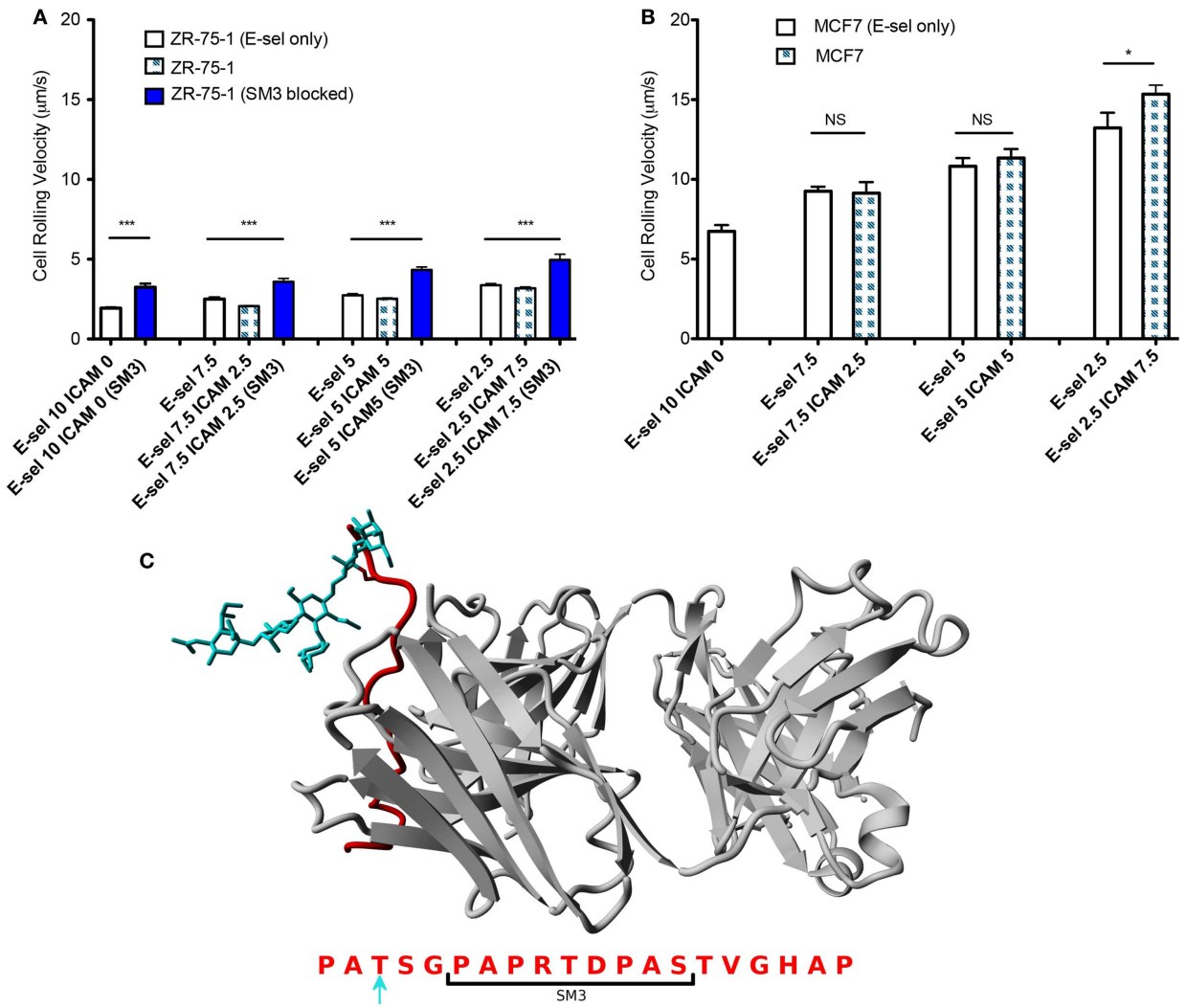

FIGURE 5 | (A,B) Rolling velocities of ZR-75-1 (untreated and blocked) and MCF7 cells on combined and E-selectin surfaces with varying incubation concentrations under flow, respectively. **(C)** Equilibrated structure of SM3 (gray) bound to the core epitope of one repeat unit of MUC1 (red) singly O-glycosylated with sLe^x (blue) on a threonine residue. Below is the amino acid sequence of a MUC1 repeat unit where the bracket indicates the interaction site of SM3 and the blue arrow indicates the chosen O-glycosylated amino acid. Student's *t*-test and ANOVA were used for statistical analysis. $*p \leq 0.05$; $***p \leq 0.001$; NS, non-significant.

E-SELECTIN LIGAND AND BINDING MOIETY EXPRESSION ON ZR-75-1 AND MCF7 CELLS

The MFI ratios of sample over isotype control for the E-selectin binding moiety sLe^x expression on ZR-75-1 and MCF7 were found to be 8.43 and 8.56, respectively, via flow cytometry (**Figure 2A**). CD44 variant 4 (CD44v4), among the multiple variants of common E-selectin ligand CD44, has been identified as a major E-selectin ligand for breast cancer cells (Zen et al., 2008). CD44v4 expression was measured on ZR-75-1 and MCF7 cells via flow cytometry and no significant difference was observed (**Figure 2B**).

E-SELECTIN AND ICAM-1 COMBINED SURFACE

The initial layer of protein-G orients the adhesion molecules to maximally interact with cell surfaces as the cells are perfused through the tubes. As the E-selectin:ICAM-1 concentration ratios were increased, the fluorescence intensity of bound E-selectin in the microtube was found to linearly increase while ICAM-1 fluorescence linearly decreased (**Figure 2C**), verifying the desired protein concentrations on the microtube surfaces.

MUC1 IS INVOLVED IN THE CANCER ADHESION CASCADE IN ASSOCIATION WITH E-SELECTIN AND ITS LIGANDS

Figures 3A,B divide the cells that interact with the surface into three categories: tethering, rolling, and adherent. ZR-75-1 cells were found to roll quite consistently when E-selectin was present at any concentration on the surface where there was a slight decrease in the percent of rolling cells as the E-selectin concentration decreases (**Figure 3A**). Conversely, the percent of ZR-75-1 tethering cells increased as the E-selectin:ICAM-1 ratio decreased. Interestingly, adherent ZR-75-1 cells were observed only when both E-selectin and ICAM-1 exist on the surface and 7.5:2.5 was found to be the optimal ratio of E-selectin:ICAM-1 that yields the greatest number of adherent cells. However, as the E-selectin:ICAM-1 ratio decreased so did the percent of adherent cells. On the other hand, MCF7 rolling and tethering showed little sensitivity to varying the E-selectin:ICAM-1 ratios where MCF7 tethering cells only slightly increased as the ratio decreased, as shown in **Figure 3B**. Most notably, no adherent MCF7 cells were observed on the surface for any concentration ratio. For both ZR-75-1 and MCF7 cells, when only ICAM-1 coats the surface no cells interacted adhesively under flow. Anti-MUC1 mAb (clone SM3) was found to block the adhesive interactions of ZR-75-1 cells with the surface, leaving only the tethering and rolling populations (**Figure 3C**).

The cell flux for each cell type (**Figures 4A–C**) shows little sensitivity to the combined surface concentration ratios. However, overall the ZR-75-1 cell flux is much greater than both MCF7 and SM3 blocked ZR-75-1 cell fluxes, roughly by a factor of 2. Comparing ZR-75-1 to MCF7 and SM3 blocked ZR-75-1 cells, the cell fluxes inversely correlate with the cell rolling velocities, as shown in **Figures 5A,B**, where the ZR-75-1 cell rolling velocities were found to be slower than MCF7 cell rolling velocities. For example, for surfaces coated with only E-selectin, MCF7 cells rolled at $6.74 \pm 0.40\ \mu m/s$ whereas ZR-75-1 cells rolled at $1.93 \pm 0.06\ \mu m/s$. SM3 blockade was found to cause an increase in rolling velocity to approximately $4\ \mu m/s$, significantly faster than untreated cells. A structure of SM3 bound to the underglycosylated core epitope of MUC1 is depicted in **Figure 5C**, where SM3 not only blocks

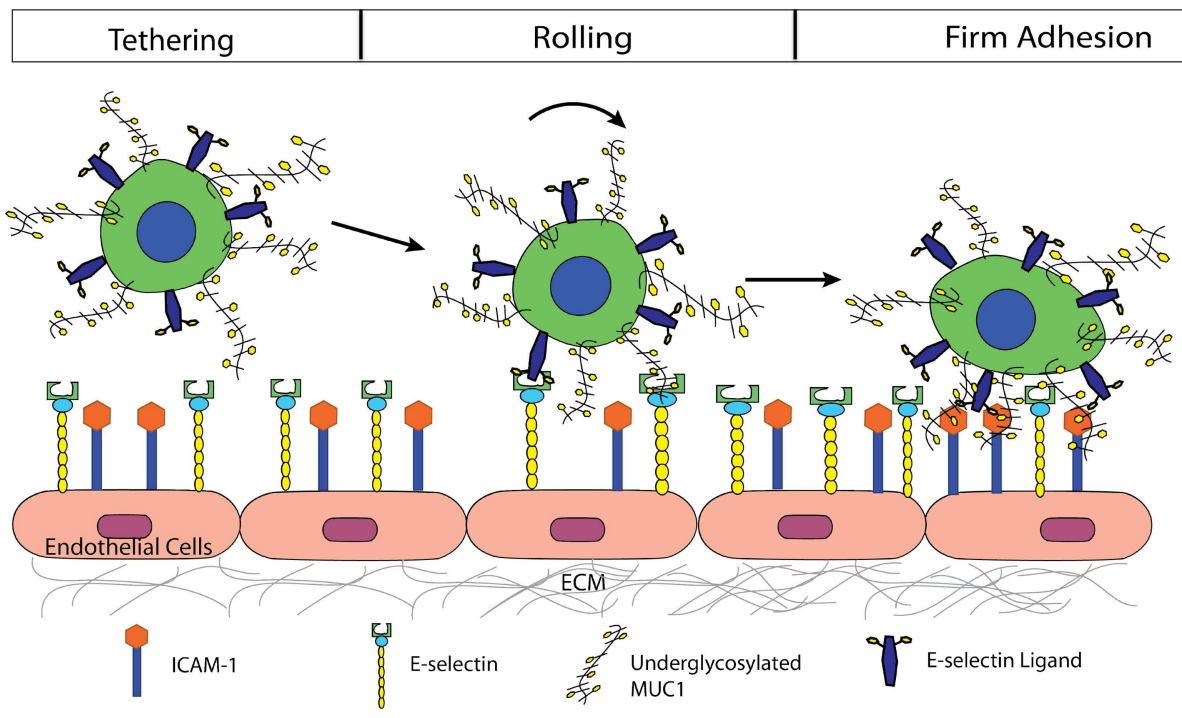

FIGURE 6 | Proposed mechanism by which MUC1 can act as a ligand for E-selectin, initiating tethering, and rolling events of CTCs on the endothelium, and subsequently serve as an ICAM-1 ligand, mediating firm adhesion of CTCs.

ICAM-1 interactions, but is sufficiently bulky compared to sLe^x to inhibit some amount of E-selectin interactions as well. Unlike cell flux, both ZR-75-1 (untreated and blocked) and MCF7 cell rolling velocities were sensitive to the E-selectin concentration where cell rolling velocities increased as the E-selectin concentration decreased (**Figures 5A,B**). Furthermore, the MCF7 cell rolling velocity at the lowest E-selectin concentration was double that of the cell rolling velocity at the highest E-selectin concentration which shows a greater sensitivity to E-selectin compared to ZR-75-1 cells.

DISCUSSION

The detection and enumeration of CTCs holds great potential in breast, colorectal, and prostate cancer prognosis, yet the basic biophysics of how these CTCs interact with the endothelium is not fully understood. Similar to leukocyte recruitment to the endothelium, CTC tethering and rolling on the blood vessel wall under hydrodynamic shear stress are also mediated by the selectin family of adhesion molecules (Geng et al., 2012). After stable rolling on the endothelium, leukocytes can firmly adhere to the inflamed endothelium via leukocyte beta-2 integrin (Mac-1, LFA-1): ICAM-1 binding (Diamond et al., 1990; Ding et al., 1999; King, 2006). Similarly for epithelial-type CTCs, tumor associated MUC1 may play the role of beta-2 integrins on leukocytes by binding ICAM-1 to enable firm adhesion and initiate subsequent events in the metastatic cascade (Rahn et al., 2005).

Tumor associated MUC1 on breast cancer cells was first identified as a novel adhesion ligand for endothelial ICAM-1 by Regimbald et al. (1996) via static adhesion assays between MCF7 cells and stimulated HUVEC cells as well as immobilized recombinant ICAM-1. MCF7 cells do not express common ICAM-1 ligands, such as LFA-1, Mac-1, or CD43. However under static conditions, MUC1 was found to interact with ICAM-1, which could mediate firm adhesion of CTCs to the inflamed endothelium. In contrast, we characterized the adhesive role of tumor associated MUC1 under hydrodynamic shear stress by perfusing both ZR-75-1 (which overexpresses MUC1) and MCF7 cells through functionalized microtubes, more representative of the blood vessel microenvironment. Furthermore, the inflamed endothelium was simulated by immobilizing both E-selectin and ICAM-1 with varying ratios on the microtube surface, creating a more physiologically relevant and controllable environment to study the adhesion events of circulating ZR-75-1 and MCF7 cells under flow.

ZR-75-1 cells show a much greater expression of underglycosylated MUC1 compared to MCF7 cells, which significantly affects their adhesion behavior when perfused through the combined surface microtubes. Interestingly, although ZR-75-1 and MCF7 cells have similar expression levels of sLe^x, one of the E-selectin binding moieties, ZR-75-1 cells roll on the combined protein surface at a significantly slower rolling velocity, indicating that ZR-75-1 cells establish stronger interactions with E-selectin. Recall that underglycosylated forms of MUC1 also contain shortened oligosaccharides where sLe^x is one of the most common carbohydrates of aberrant MUC1 (Burdick et al., 1997). Therefore MUC1, when appropriately decorated with sLe^x in its underglycosylated form, is expected to extend further from the cell surface compared to other selectin ligands due to its size and is perhaps more able to interact with E-selectin to efficiently mediate tethering and rolling events. The greater rolling velocities of ZR-75-1 cells blocked with SM3 also suggests MUC1 is an important E-selectin ligand because SM3 could inhibit some amount of E-selectin:MUC1 interactions due to the size of SM3 compared to sLe^x (**Figure 5C**). As a result of the slower rolling velocity and greater MUC1 expression, only ZR-75-1 cells firmly adhered to the combined surface, where firm adhesion is facilitated by MUC1:ICAM-1 interactions. In our study, the observation of firmly adhered cells to the combined surface under shear stress is consistent with the metastatic potential of the ZR-75-1 cell line (highly metastatic) and the MCF7 cell line (weakly metastatic).

In conclusion, we propose a mechanism by which MUC1 can act as a ligand for E-selectin, initiating tethering and rolling events of CTCs on the endothelium, and subsequently serve as an ICAM-1 ligand, mediating firm adhesion of CTCs (**Figure 6**). The synergistic effect of MUC1:E-selectin and MUC1:ICAM-1 may play an important role in breast cancer metastasis through the bloodstream where underglycosylated MUC1 can significantly slow the rolling velocity of CTCs thereby allowing for more frequent occurrence of firm adhesion events and subsequent extravasation. In summary, our results provide new insights into the roles of MUC1 in the metastatic adhesion cascade and suggests future examination into clinical aspects where the underglycosylated form of MUC1 can be targeted since aberrantly underglycosylated MUC1 expression is highly correlated to poor prognosis in breast and colon cancer patients.

ACKNOWLEDGMENTS

This work was funded by NIH Grant U54CA143876 to Michael R. King, and NSF Graduate Fellowship to Yue Geng.

REFERENCES

Ajioka, Y., Allison, L. J., and Jass, J. R. (1996). Significance of MUC1 and MUC2 mucin expression in colorectal cancer. *J. Clin. Pathol.* 49, 560–564.

Borsig, L., Wong, R., Hynes, R. O., Varki, N. M., and Varki, A. (2002). Synergistic effects of L- and P-selectin in facilitating tumor metastasis can involve non-mucin ligands and implicate leukocytes as enhancers of metastasis. *Proc. Natl. Acad. Sci. U.S.A.* 99, 2193–2198.

Burdick, M. D., Harris, A., Reid, C. J., Iwamura, T., and Hollingsworth, M. A. (1997). Oligosaccharides expressed an MUC1 produced by pancreatic and colon tumor cell lines. *J. Biol. Chem.* 272, 24198–24202.

Diamond, M. S., Staunton, D. E., Defougerolles, A. R., Stacker, S. A., Garciaaguilar, J., Hibbs, M. L., and Springer, T. A. (1990). ICAM-1 (CD54) – a counter-receptor for MAC-1 (CD11B CD18). *J. Cell Biol.* 111, 3129–3139.

Ding, Z. M., Babensee, J. E., Simon, S. I., Lu, H. F., Perrard, J. L., Bullard, D. C., Dai, X. Y., Bromley, S. K., Dustin, M. L., Entman, M. L., Smith, C. W., and Ballantyne, C. M. (1999). Relative contribution of LFA-1 and Mac-1 to neutrophil adhesion and migration. *J. Immunol.* 163, 5029–5038.

Dokurno, P., Bates, P. A., Band, H. A., Stewart, L. M. D., Lally, J. M., Burchell, J. M., Taylor-Papadimitriou, J., Snary, D., Sternberg, M. J., and Freemont, P. S. (1998). Crystal structure at 1.95 angstrom resolution of the breast tumour-specific antibody SM3 complexed with its peptide epitope reveals novel hypervariable loop recognition. *J. Mol. Biol.* 284, 713–728.

Duncan, T. J., Watson, N. F. S., Al-Attar, A. H., Scholefield, J. H., and Durrant, L. G. (2007). The role of MUC1 and MUC3 in the biology and prognosis of colorectal cancer. *World J. Surg. Oncol.* 5, 31.

Essmann, U., Perera, L., Berkowitz, M. L., Darden, T., Lee, H., and Pedersen, L. G. (1995). A smooth particle mesh Ewald method. *J. Chem. Phys.* 103, 8577–8593.

Finzel, A., Reininger, A., Bode, P., and Wurzinger, L. (2004). ICAM-1 supports adhesion of human small-cell lung carcinoma to endothelial cells. *Clin. Exp. Metastasis* 21, 185–189.

Geng, Y., Marshall, J. R., and King, M. R. (2012). Glycomechanics of the metastatic cascade: tumor cell-endothelial cell interactions in the circulation. *Ann. Biomed. Eng.* 40, 790–805.

Girling, A., Bartkova, J., Burchell, J., Gendler, S., Gillett, C., and Taylor-Papadimitriou, J. (1989). A core protein epitope of the polymorphic epithelial mucin detected by the monoclonal-antibody SM-3 is selectively exposed in a range of primary carcinomas. *Int. J. Cancer* 43, 1072–1076.

Guddo, F., Giatromanolaki, A., Koukourakis, M. I., Reina, C., Vignola, A. M., Chlouverakis, G., Hilkens, J., Gatter, K. C., Harris, A. L., and Bonsignore, G. (1998). MUC1 (episialin) expression in non-small cell lung cancer is independent of EGFR and c-erbB-2 expression and correlates with poor survival in node positive patients. *J. Clin. Pathol.* 51, 667–671.

Hayashi, T., Takahashi, T., Motoya, S., Ishida, T., Itoh, F., Adachi, M., Hinoda, Y., and Imai, K. (2001). MUC1 mucin core protein binds to the domain 1 of ICAM-1. *Digestion* 63 (Suppl. 1), 87–92.

Inata, J., Hattori, N., Yokoyama, A., Ohshimo, S., Doi, M., Ishikawa, N., Hamada, H., and Kohno, N. (2007). Circulating KL-6/MUC1 mucin carrying sialyl Lewis(a) oligosaccharide is an independent prognostic factor in patients with lung adenocarcinoma. *Int. J. Cancer* 120, 2643–2649.

King, M. R. (2006). *Principles of Cellular Engineering: Understanding the Biomolecular Interface.* Burlington: Academic Press.

Kocer, B., Soran, A., Kiyak, G., Erdogan, S., Eroglu, A., Bozkurt, B., Solak, C., and Cengiz, O. (2004). Prognostic significance of mucin expression in gastric carcinoma. *Dig. Dis. Sci.* 49, 954–964.

Krieger, E., Darden, T., Nabuurs, S. B., Finkelstein, A., and Vriend, G. (2004). Making optimal use of empirical energy functions: force-field parameterization in crystal space. *Proteins* 57, 678–683.

Lloyd, K. O., Burchell, J., Kudryashov, V., Yin, B. W. T., and Taylor-Papadimitriou, J. (1996). Comparison of O-linked carbohydrate chains in MUC-1 mucin from normal breast epithelial cell lines and breast carcinoma cell lines – demonstration of simpler and fewer glycan chains in tumor cells. *J. Biol. Chem.* 271, 33325–33334.

MacLean, G. D., Reddish, M. A., and Longenecker, B. M. (1997). Prognostic significance of preimmunotherapy serum CA27.29 (MUC-1) mucin level after active specific immunotherapy of metastatic adenocarcinoma patients. *J. Immunother.* 20, 70–78.

Mommers, E. C., Leonhart, A. M., von Mensdorff-Pouilly, S., Schol, D. J., Hilgers, J., Meijer, C. J., Baak, J. P., and van Diest, P. J. (1999). Aberrant expression of muc1 mucin in ductal hyperplasia and ductal carcinoma in situ of the breast. *Int. J. Cancer* 84, 466–469.

Moore, A., Medarova, Z., Potthast, A., and Dai, G. (2004). In vivo targeting of underglycosylated MUC-1 tumor antigen using a multimodal imaging probe. *Cancer Res.* 64, 1821–1827.

Moss, M. A., and Anderson, K. W. (2000). Adhesion of cancer cells to endothelial monolayers: a study of initial attachment versus firm adhesion. *J. Adhes.* 74, 19–40.

Orr, F. W., Wang, H. H., Lafrenie, R. M., Scherbarth, S., and Nance, D. M. (2000). Interactions between cancer cells and the endothelium in metastasis. *J. Pathol.* 190, 310–329.

Rahn, J., Chow, J., Horne, G., Mah, B., Emerman, J., Hoffman, P., and Hugh, J. C. (2005). MUC1 mediates transendothelial migration in vitro by ligating endothelial cell ICAM-1. *Clin. Exp. Metastasis* 22, 475–483.

Regimbald, L. H., Pilarski, L. M., Longenecker, B. M., Reddish, M. A., Zimmermann, G., and Hugh, J. C. (1996). The breast mucin MUC1 as a novel adhesion ligand for endothelial intercellular adhesion molecule 1 in breast cancer. *Cancer Res.* 56, 4244–4249.

Retz, M., Lehmann, J., Roder, C., Plotz, B., Harder, J., Eggers, J., Pauluschke, J., Kalthoffm, H., and Stöckle, M. (1998). Differential mucin MUC7 gene expression in invasive bladder carcinoma in contrast to uniform MUC1 and MUC2 gene expression in both normal urothelium and bladder carcinoma. *Cancer Res.* 58, 5662–5666.

St Hill, C. A. (2011). Interactions between endothelial selectins and cancer cells regulate metastasis. *Front. Biosci.* 16, 3233–3251.

Tewes, M., Aktas, B., Welt, A., Mueller, S., Hauch, S., Kimmig, R., and Kasimir-Bauer, S. (2009). Molecular profiling and predictive value of circulating tumor cells in patients with metastatic breast cancer: an option for monitoring response to breast cancer related therapies. *Breast Cancer Res. Treat.* 115, 581–590.

Tremblay, P. L., Huot, J., and Auger, F. A. (2008). Mechanisms by which E-selectin regulates diapedesis of colon cancer cells under flow conditions. *Cancer Res.* 68, 5167–5176.

Varki, N. M., and Varki, A. (2007). Diversity in cell surface sialic acid presentations: implications for biology and disease. *Lab. Invest.* 87, 851–857.

Wirtz, D., Konstantopoulos, K., and Searson, P. C. (2011). The physics of cancer: the role of physical interactions and mechanical forces in metastasis. *Nat. Rev. Cancer* 11, 512–522.

Zen, K., Liu, D.-Q., Guo, Y.-L., Wang, C., Shan, J., Fang, M., Zhang, C. Y., and Liu, Y. (2008). CD44v4 is a major E-selectin ligand that mediates breast cancer cell transendothelial migration. *PLoS ONE* 3, e1826 doi:10.1371/journal.pone.0001826

Zotter, S., Lossnitzer, A., Hageman, P. C., Delemarre, J. F. M., Hilkens, J., and Hilgers, J. (1987). Immunohistochemical localization of the epithelial marker mam-6 in invasive malignancies and highly dysplastic adenomas of the large-intestine. *Lab. Invest.* 57, 193–199.

Conflict of Interest Statement: The authors declare that the research was conducted in the absence of any commercial or financial relationships that could be construed as a potential conflict of interest.

Received: 18 May 2012; accepted: 03 July 2012; published online: 27 July 2012.
Citation: Geng Y, Yeh K, Takatani T and King MR (2012) Three to tango: MUC1 as a ligand for both E-selectin and ICAM-1 in the breast cancer metastatic cascade. Front. Oncol. ***2****:76. doi: 10.3389/fonc.2012.00076*
This article was submitted to Frontiers in Cancer Molecular Targets and Therapeutics, a specialty of Frontiers in Oncology.

frontiers in ONCOLOGY

HYPOTHESIS AND THEORY ARTICLE
published: 20 August 2012
doi: 10.3389/fonc.2012.00103

Expression of E-selectin ligands on circulating tumor cells: cross-regulation with cancer stem cell regulatory pathways?

Monica M. Burdick[1,2]*, Karissa A. Henson[2], Luis F. Delgadillo[1], Young Eun Choi[3], Douglas J. Goetz[1,2], David F. J. Tees[2,3] and Fabian Benencia[2,4]

[1] Department of Chemical and Biomolecular Engineering, Russ College of Engineering and Technology, Ohio University, Athens, OH, USA
[2] Biomedical Engineering Program, Russ College of Engineering and Technology, Ohio University, Athens, OH, USA
[3] Department of Physics and Astronomy, College of Arts and Sciences, Ohio University, Athens, OH, USA
[4] Department of Biomedical Sciences, Heritage College of Osteopathic Medicine, Ohio University, Athens, OH, USA

Edited by:
Michael R. King, Cornell University, USA

Reviewed by:
Yue Geng, Cornell University, USA
Gail M. Seigel, University at Buffalo, USA

***Correspondence:**
Monica M. Burdick, Department of Chemical and Biomolecular Engineering, Russ College of Engineering and Technology, Ohio University, Stocker Center 171, Athens, OH 45701, USA.
e-mail: burdick@ohio.edu

Although significant progress has been made in the fight against cancer, successful treatment strategies have yet to be developed to combat those tumors that have metastasized to distant organs. Poor characterization of the molecular mechanisms of cancer spread is a major impediment to designing predictive diagnostics and effective clinical interventions against late stage disease. In hematogenous metastasis, it is widely suspected that circulating tumor cells (CTCs) express specific adhesion molecules that actively initiate contact with the vascular endothelium lining the vessel walls of the target organ. This "tethering" is mediated by ligands expressed by CTCs that bind to E-selectin expressed by endothelial cells. However, it is currently unknown whether expression of functional E-selectin ligands on CTCs is related to cancer stem cell regulatory or maintenance pathways, particularly epithelial-to-mesenchymal transition and the reverse, mesenchymal-to-epithelial transition. In this hypothesis and theory article, we explore the potential roles of these mechanisms on the dynamic regulation of selectin ligands mediating CTC trafficking during metastasis.

Keywords: circulating tumor cells, cancer stem cells, epithelial-to-mesenchymal transition, selectins, selectin ligands, cell adhesion

INTRODUCTION

Distant metastasis is the culmination of an elaborate cascade of events in which cancer cells break away from the primary tumor, intravasate through blood vessel walls into the circulatory system, travel throughout the body, and finally extravasate through the vessels of a distant organ to establish a secondary colony. While resident in the blood vasculature, circulating tumor cells (CTCs) must survive biochemical and biophysical assaults inducing necrosis or apoptosis, plus avoid elimination by immune cells, in order to metastasize. Regardless of their ultimate fate, the clinical interpretation of CTCs arising from solid tumors has been the subject of much debate, with definitive answers yet to emerge as to if, when, and for which cancers these cells offer significant diagnostic, prognostic, or therapeutic value. Despite lack of consensus on their clinical utility, CTCs can still provide a meaningful portrait of a cancer patient's health, or rather disease, status. CellSearch, a test marketed by Johnson & Johnson's Veridex division, is FDA-approved to capture and enumerate CTCs in metastatic breast, colon, and prostate cancer patients for prognostic purposes (Dawood et al., 2008; Mostert et al., 2009; Riethdorf and Pantel, 2010). More recently, the development of next-generation fluidics-based CTC isolation devices by the Haber and Toner groups, the CTC-chip and herringbone (HB)-chip (Nagrath et al., 2007; Stott et al., 2010; Yu et al., 2011), has generated increased attention to CTCs and the use of "liquid biopsies" or "blood biopsies" to enumerate and capture CTCs for further study. As with any portrait, further examination reveals nuances not observed at first glance. For instance, post-capture investigation using RT-PCR in the AdnaTest (AdnaGen) may reveal upregulated pathways related to cancer stem cells (CSCs), metastatic aggressiveness, or responsiveness to treatment (i.e., trastuzumab for HER-2 overexpressing breast cancers) that are impossible to observe through a simple CTC count (Fehm et al., 2007; Dawood et al., 2008; Riethdorf and Pantel, 2008, 2010; Mostert et al., 2009). Though the scientific and medical communities may achieve significant new insights from these blood biopsies, the information itself is static. Cancer is dynamic. How medical professionals interpret a particular patient's case, as well as predict future outcomes of an ever-changing disease, will depend partially on information gleaned from CTC assessments at single moments in time.

In general, CTCs possessing enhanced survival capabilities will generate metastatic colonies in distant organs, as well as reseed the original primary tumor with more aggressive cells (Kim et al., 2009). Uncovering the molecular mediators by which CTCs initiate adhesion with endothelial cells lining the blood vessel walls of the target site may therefore prove useful in predicting and thwarting metastasis. In particular, stimulated vascular endothelium expressing E-selectin can capture CTCs expressing E-selectin ligands, thereby initiating adhesion and subsequent CTC invasion. However, this statement is a simplification of a tangle of issues underlying functional selectin ligand expression on cancer

cells. To be qualified as a true selectin ligand, Varki (1997) proposed that the purported ligand must be expressed "in the right place at the right time" among other criteria. So do all CTCs express selectin ligands, or even the "right" selectin ligands? How and when do these selectin ligands arise? Are they modulated by pathways associated with epithelial-to-mesenchymal transition (EMT) or other mechanisms of CSC generation and maintenance, or are they independent of these pathways? In this article, we explore the complex networks through which selectin ligands on CTCs may be regulated and propose working theories based on ongoing studies with breast cancer in our laboratories. New findings from these investigations, coupled with additional discoveries from other labs, will address significant shortcomings in our understanding of the molecular networks promoting cancer metastasis.

CTCs AND CELL ADHESION MEDIATED BY E-SELECTIN AND ITS LIGANDS

It has been proposed that the early steps by which CTCs cells leave the bloodstream to invade secondary sites mimic the physiologic trafficking of leukocytes to sites of inflammation and hematopoietic stem cells to bone marrow. Because numerous excellent review articles on cell trafficking have been published through the years (Springer, 1994; Sackstein, 2005; Barthel et al., 2007; Konstantopoulos and Thomas, 2009; Zarbock et al., 2011; Bendas and Borsig, 2012; Chase et al., 2012; Geng et al., 2012), only a general overview is presented here (**Figure 1**). Circulating cells are first captured or "tethered" from bulk blood flow onto vascular endothelial cells, which is immediately followed by rolling on the endothelium. Tethering and rolling are typically mediated by interactions between ligands expressed on the surface of the circulating cells that recognize E-selectin, an endothelial adhesion molecule upregulated in response to inflammatory stimuli as well as constitutively expressed by bone and dermal endothelial cells (Springer, 1994; Sackstein, 2004). Subsequently, rolling cells firmly adhere and migrate through the vessel wall into the underlying tissue in response to specific cytokines and chemokines.

Therefore, this multi-step model indicates that CTCs must initially tether on endothelial cells, presumably through E-selectin ligand recognition of E-selectin, in order to trigger the series of events necessary for metastatic growth. These adhesive interactions occur under hydrodynamic shear stresses generated by blood flow (post-capillary venule and bone marrow endothelial venule wall shear stress ranges from 0.5 to 4.0 dyn/cm^2; Jones et al., 1991; Mazo et al., 1998), enabled by the hallmark catch-slip bonds and rapid bond formation/breakage kinetics of selectins and their ligands (Dembo et al., 1988; Marshall et al., 2003; Zhu and McEver, 2005; Evans and Calderwood, 2007; Ham et al., 2007; McEver and Zhu, 2007). E-selectin has been established as a mediator of colon and prostate cancer adhesion and distant metastasis (Khatib et al., 2002; Barthel et al., 2007, 2009), and there is clinical and *in vitro* evidence for the role of E-selectin in promoting metastasis of several other cancers, including breast, pancreatic, and head and neck cancers (Wenzel et al., 1995; Eshel et al., 2000; Barthel et al., 2007; Geng et al., 2012). The other two members of the selectin family, P-selectin expressed by activated platelets and activated endothelium and L-selectin expressed by most leukocytes, also have been proposed to participate in cancer metastasis (Laubli and Borsig, 2010; St Hill, 2012).

Notably, the expression levels of the minimal selectin-binding epitopes sialyl Lewis X (sLe^X,NeuAcα(2,3)Galβ(1,4)[Fucα(1,3)] GlcNAc) and its stereoisomer sialyl Lewis A (sLe^A, NeuAcα(2,3) Galβ(1,3)[Fucα(1,4)]GlcNAc) on certain glycoproteins and glycolipids increase progressively from normal tissue to early stage cancer to metastatic disease, consistent with aberrant glycosylation rendering altered cell adhesion molecules relative to normal tissue in most cancers, including breast, bladder, and colon cancers (Izumi et al., 1995; Klopocki et al., 1996; Renkonen et al., 1997; Skorstengaard et al., 1999; Kajiwara et al., 2005). Transfer of sialic acid (NeuAc) onto a terminal galactose (Gal) residue occurs through the action of α(2,3) sialyltransferases. The enzymes directing α(1,3) fucosylation for sLe^X production are multiple-fucosyltransferases (FTs) III, IV, V, VI, and VII while FTIII and FTV are also α(1,4) FTs involved in the production of sLe^A (Edbrooke et al., 1997; de Vries et al., 2001; Dupuy et al., 2004).

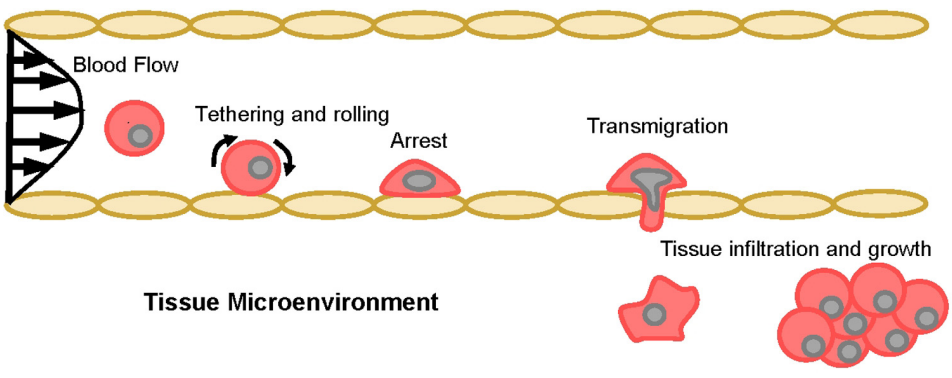

FIGURE 1 | The multi-step model of cell adhesion and migration in blood vessels. Schematic representation of the cascade of events involved in cellular transit from the vasculature into the underlying tissue space. Tethering recruits circulating cells from the bulk flow stream, then rolling slows lateral translocation across the endothelium and facilitates firm arrest. If the correct cytokine and/or chemokine gradients are present, adherent cells will transmigrate through the endothelium and infiltrate the tissue microenvironment.

Clearly, these enzymes must be (dys)regulated in cancer cells through the transition from primary tumor to advanced stage cancer to result in the observed upregulation of $sLe^{X/A}$ and thus selectin ligands (Renkonen et al., 1997; Matsuura et al., 1998). Although the tumor stroma and hypoxic conditions are known to influence tumor cell glycosylation (Stern et al., 2001, 2002; Kannagi, 2004), the exact biochemical (or biophysical) regulators of cancer glycosylation are unknown. Nevertheless, the presence of sialofucosylated moieties such as $sLe^{X/A}$ is significant in that upregulated expression of functional selectin ligands may indicate their role in promoting CTC adhesion during metastasis (Burdick et al., 2001; Kannagi et al., 2004; Barthel et al., 2007). Thus, it is necessary to identify the core proteins or lipids presenting sialofucosylated glycans to better characterize roles for specific selectin ligands.

To date, several major tumor cell surface glycoprotein selectin ligands that may fulfill the criteria of "real" selectin ligands have been identified, most prominently the specialized CD44 glycoform HCELL as an E-/L-/P-selectin ligand on colon cancer cells (Hanley et al., 2005, 2006; Burdick et al., 2006), and an E-selectin ligand on prostate and breast cancer cells (Barthel et al., 2009; manuscript in preparation). Carcinoembryonic antigen (CEA, CD66) and podocalyxin-type protein-1 (PCLP-1) have also been named E-selectin ligands expressed on colon and prostate cancer cells (Barthel et al., 2009; Thomas et al., 2009). On breast cancer cells, CD24 acts as a P-selectin ligand but not an E-selectin ligand (Aigner et al., 1998), and Mac-2bp acts as an E-selectin ligand (Shirure et al., 2012). Additional mucinous proteins, such as MUC-1, CD43, and PSGL-1, have also been proposed as selectin ligands on a variety of cancer cells (Barthel et al., 2007; Geng et al., 2012). Contributory roles have also been identified for colon, prostate, breast, and head and neck cancer sialofucosylated glycolipids in adhesion to endothelial E-selectin (Burdick et al., 2003; Dimitroff et al., 2004; Barthel et al., 2007; Shirure et al., 2011; Geng et al., 2012). Though the understanding of selectins and their ligands is growing, it is imperative to consider their functionalities in the wider context of biochemical and biophysical factors encountered by CTCs in transit.

CTC TRANSIT THROUGH CAPILLARIES

The ability of cancer cells to enter small vessels such as capillaries (as well as to roll in larger vessels such as post-capillary venules described above) depends critically on the mechanical deformability of the cells. Capillaries range from 2 to 8 μm in diameter (Doerschuk et al., 1993) and cancer cells, which tend to be large and stiff, may not be able to deform enough to enter at least some portions of the capillary bed (Liotta, 1987; Weiss et al., 1988; Chambers et al., 1992; Lafrenie et al., 1993). Organs with small vessels that are susceptible to metastasis include the lung microcirculation (which is particularly important because it is the first capillary bed that a metastasizing cancer cell entering the venous circulation will encounter after passing through the first two chambers of the heart), bone marrow and liver sinusoids, and the kidney microcirculation. The mechanical properties of cancer cells surely play a role in transit: if certain CTCs are stiff and resistant to deformation, then the possibility of sequestration at the entrance of small vessels should be large. Conversely, if CTCs are less stiff (more deformable), then their potential to pass through the microcirculation and metastasize could be enhanced. Furthermore, it is possible that deformation is not a by-stander process for the cell; deformation itself may induce changes affecting molecular and mechanical phenotype, perhaps in a manner that promotes CTC survival and metastasis.

Protocols to quantify cellular mechanical properties have existed for nearly 30 years, and parameters for models of cell mechanics have been measured using many experimental techniques: micropipette aspiration (**Figure 2**), magnetic twisting rheometry, cell stretching with optical tweezers or mechanical stretching devices, nanoscale indentation with probes or AFM tips, particle tracking microrheology, etc. (Mason and Weitz, 1995; Shroff et al., 1995; Choquet et al., 1997; Mason et al., 1997; Thoumine and Ott, 1997; Bausch et al., 1999; Yap and Kamm, 2005; Sirghi et al., 2006). As a result of these efforts, much is known about the deformability of red and white blood cells (which are known to undergo massive deformations in the normal course of circulation) and a sampling of other cell types. On the basis of these collective works (Mason and Weitz, 1995; Shroff et al., 1995; Choquet et al., 1997; Mason et al., 1997; Thoumine and Ott, 1997; Bausch et al., 1999; Yap and Kamm, 2005; Sirghi et al., 2006), it was found that the major distinction in cell rheological properties is whether the cell behaves like a liquid drop with a cortical tension (as white blood cells clearly do) or as a viscoelastic solid (most other cell types). Devices to identify cell subsets based on differences in cellular mechanical properties are in early development stages (Oakey et al., 2010; Sraj et al., 2010), and these methodologies are being considered for identifying and isolating normal healthy mesenchymal stem cells (MSCs) for use as therapeutics and in regenerative medicine (Porada et al., 2006; Parekkadan and Milwid, 2010). These cells lack unique cell surface molecules through which they can be easily isolated from their sources (e.g., bone marrow, umbilical cord; Porada et al., 2006; Pountos et al., 2007) but have distinct mechanical properties compared to their

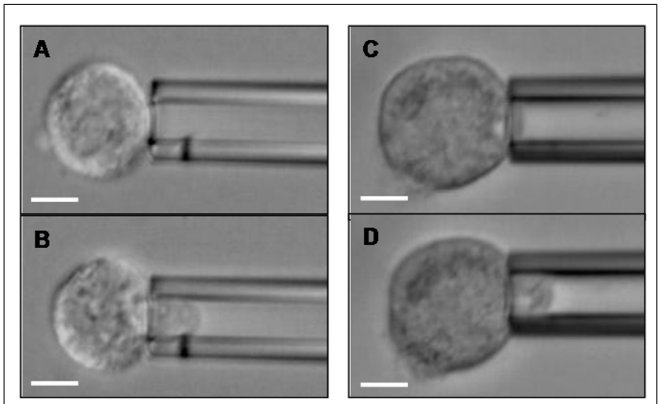

FIGURE 2 | Breast cancer cells can be aspirated into a glass micropipette. A $CD44^+/CD24^-$ Hs578T breast cancer cell **(A)** before and **(B)** after partial aspiration into a micropipette of 8.4 μm diameter. A $CD44^+/CD24^+$ BT-20 breast cancer cell **(C)** before and **(D)** after partial aspiration into a 9.0 μm diameter micropipette. Scale bar is 10 μm in all Figures.

differentiated daughter cells. These differences are currently being explored as specific identifying MSC characteristics (Darling et al., 2008; Tan et al., 2008; Yu et al., 2010). Similarly, benign versus tumorigenic cancer cells have been explored for differing traits (Kim et al., 2008; Hou et al., 2010). However, much more work needs to be performed to understand CTC metastatic potential attributable to inherent or alterable molecular and mechanical properties. It is tantalizing to speculate a role for biophysical modulation of CTC properties, including effects on selectin ligand expression or function.

CSCs, EMT, AND MESENCHYMAL-TO-EPITHELIAL TRANSITION

The discovery and identification of leukemic stem cells (LSCs) effectively ushered in a new era of cancer research (Lapidot et al., 1994; Bonnet and Dick, 1997). LSCs share the properties of self-renewal and pluripotency with their normal hematopoietic stem cell brethren, but are also leukemogenic. LSCs are particularly dangerous in that they can survive chemotherapy (Costello et al., 2000; Graham et al., 2002; Holtz et al., 2002), leading to relapse with LSCs even more aggressive than their previous incarnation (Oravecz-Wilson et al., 2009). Shortly after LSC identification, a groundbreaking report by Al-Hajj et al. (2003) found that breast cancers similarly harbor deadly CSCs, which exhibited a much greater propensity for tumor formation than cells of a different phenotype. These breast CSCs were putatively characterized by the expression levels of glycoprotein markers on the surface of the cell: high expression of CD44, little to no expression of CD24, high expression of epithelial-specific antigen (ESA), and lack of lineage markers (lin), or $CD44^+/CD24^{-/low}/ESA^+/lin^-$ (Al-Hajj et al., 2003). These CSCs were able to form heterogeneous tumors from a relatively small number of cells. Specifically, only 200 $CD44^+/CD24^{-/low}/ESA^+/lin^-$ breast cancer cells, isolated from patient primary tumors, could regenerate and expand to form secondary tumors that also contained CSCs, in as little as 12 weeks in mice (Al-Hajj et al., 2003). In contrast, as many as 20,000 cells of alternate phenotypes from the same tumor origin as the $CD44^+/CD24^{-/low}/ESA^+/lin^-$ cells were unable to form new tumors. Thus, the breast CSCs were capable of self-renewal and differentiation, two general properties possessed by normal stem cells, and the ability to generate new tumors (Al-Hajj et al., 2003; Ponti et al., 2005; Fillmore and Kuperwasser, 2008). Since this initial breast cancer study, CSCs have reportedly been found in nearly all solid cancers, with a specific molecular phenotype for each type of cancer. However, the cancer research community continues to debate the true nature of CSCs (Campbell and Polyak, 2007; Gupta et al., 2009; Badve and Nakshatri, 2012; Liu et al., 2012; Magee et al., 2012), including whether CSCs are tumor-initiating or metastasis-initiating cells (Kelly et al., 2007; Adams and Strasser, 2008; Fillmore and Kuperwasser, 2008). The reasons for the extended scientific discussion are many and are outlined in a comprehensive review from the Morrison lab (Magee et al., 2012).

Perhaps some of the confusion and seemingly contradictory findings surrounding CSCs will be allayed by the growing evidence demonstrating that CSCs are not a single population of cells identified by one specific molecular signature. Rather, while all CSCs possess general stem cell properties, CSCs are actually comprised of heterogeneous subpopulations with multiple molecular and functional phenotypes that are generated through different pathways (Liu et al., 2012; Magee et al., 2012). It is becoming abundantly clear for breast cancer that such heterogeneity exists in its CSCs. Breast CSCs that are $CD44^+/CD24^-$ (the simplified breast CSC phenotype) are the result of cytokine-induced EMT (Mani et al., 2008; Morel et al., 2008; Blick et al., 2010; Liu et al., 2012), a process by which cells lose epithelial characteristics (E-cadherin expression, cell–cell contacts, polarity) and become more mesenchymal (N-cadherin expression, mesenchymal morphology, enhanced migration abilities; Onder et al., 2008; Zeisberg and Neilson, 2009). Many of the properties EMT confers are normally helpful to development (Kalluri and Weinberg, 2009), but EMT can also contribute to cancer progression in adult tissue (Mani et al., 2008; Onder et al., 2008). Often, cancer cells at the invasive front of a primary tumor have a mesenchymal phenotype (Kalluri and Weinberg, 2009). Interestingly, in breast cancer patients with metastases, CTCs have been found to express markers of EMT in addition to stem cell traits (Aktas et al., 2009; Bonnomet et al., 2010; Kallergi et al., 2011). It is important to note that EMT is reversible, such that cells can undergo mesenchymal-to-epithelial transition (MET). The Wicha group reported that CSCs can exist in an MET state (Liu et al., 2012) as well as an EMT state previously found by the Weinberg group (Mani et al., 2008; Liu et al., 2012). MET CSCs actively self-renew and express aldehyde dehydrogenase (ALDH, a marker independently identified as a CSC indicator in several types of cancer (Ginestier et al., 2007; Clay et al., 2010; Silva et al., 2011; Kryczek et al., 2012), epithelial cell adhesion molecule (EpCAM, the same molecule that forms the basis for the capture of CTCs by CellSearch and the CTC-and HB-chips), and CD49f (α_6 integrin subunit) in contrast to quiescent yet invasive $CD44^+/CD24^-/EpCAM^-/CD49f^+$ EMT CSCs (Liu et al., 2012). Given the interconversions between CSC states, which are regulated by microRNAs (miRNAs), it is not surprising that there exists a subpopulation of $CD44^+/CD24^-$ and $ALDH^+$ cells (Liu et al., 2012). However, studies linking CSCs with properties facilitating CTC lodgment at sites of metastasis (i.e., selectin ligands and cell mechanical properties) are lacking.

PUTTING IT ALL TOGETHER: HYPOTHESIZED BREAST CANCER MODELS LINKING REGULATION OF CSCs, CTCs, AND E-SELECTIN LIGANDS

Arguably, CSCs and CTCs from breast cancer are the most well-studied among all cancers, thereby easing efforts aimed at uncovering crosstalk between CSC regulatory pathways, CTC characteristics, and expression of functional selectin ligands. Such investigations may aid in diagnosing breast cancer at an early stage, when it is largely considered curable, or assist in identifying new therapeutic targets or treatment modalities for those women diagnosed at the metastatic stage, for whom the 5-year survival rate is ∼20% (DeSantis et al., 2011). Most commonly, breast cancer metastases are found in the lungs and bone marrow (Moore, 2001; Minn et al., 2005; Balic et al., 2006; Riethdorf and Pantel, 2010), exhibiting a tropism not explainable by circulation pattern alone (Minn et al., 2005; Talmadge and Fidler,

2010). Recently, it has been reported that disseminated breast cancer cells in human bone marrow are largely $CD44^+/CD24^-$ (Abraham et al., 2005; Balic et al., 2006), corresponding to EMT CSCs. These $CD44^+/CD24^-$ are also resistant to radiotherapy and chemotherapy (Diehn and Clarke, 2006; Phillips et al., 2006; Reim et al., 2009). It is therefore necessary to understand the reasons for $CD44^+/CD24^-$ breast cancer cells in bone: whether CTCs are $CD44^+/CD24^-$ CSCs that preferentially migrate and establish metastases, or if non-$CD44^+/CD24^-$ CTCs are induced to the $CD44^+/CD24^-$ phenotype in the bone marrow.

As mentioned previously, E-selectin is constitutively expressed on bone marrow endothelium (Keelan et al., 1994; Schweitzer et al., 1996), and breast cancer cells have been shown to express E-selectin ligands on their surface (Tozeren et al., 1995; Narita et al., 1996; Zen et al., 2008; Julien et al., 2011; Shirure et al., 2011, 2012). Previous studies have also demonstrated the E-selectin-dependence of binding interactions between commercially available breast cancer cell lines and human umbilical vein endothelial cells (HUVECs; Giavazzi et al., 1993; Narita et al., 1996; Julien et al., 2011; Shirure et al., 2011, 2012). As the expression levels of the minimal selectin-binding epitopes sLe^X and sLe^A increase progressively from normal tissue to early stage breast cancer to metastatic disease (Renkonen et al., 1997), it may be hypothesized that CTCs retain expression of selectin ligands that were generated in the primary site, then upregulate such ligands during transit to the metastatic site. Altogether, these findings imply that E-selectin and its ligands are likely to comprise important elements of breast cancer metastasis *in vivo*. Since breast cancer cells at the invasive front of a primary tumor tend to be mesenchymal (Kalluri and Weinberg, 2009) and breast CTCs have been found to express markers of EMT in addition to stem cell traits (Aktas et al., 2009; Bonnomet et al., 2010), it would seem a logical extension of the hypothesis that E-selectin ligands are upregulated with EMT and the corresponding $CD44^+/CD24^-$ CSC phenotype. However, our studies with human breast cancer cell lines revealed surprising results: non-$CD44^+/CD24^-$ cells expressed much greater E-selectin ligand activity than $CD44^+/CD24^-$ cells (**Figure 3** and **Table 1**; Shirure et al., 2011, 2012; manuscript in preparation). These findings imply that lower expression of E-selectin ligands correlates with $CD44^+/CD24^-$ breast CSCs arising from EMT. Notably, the bone marrow microenvironment is enriched in TGF-β, a cytokine that is well-known to induce EMT (Brown et al., 2004; Lee et al., 2008; Mani et al., 2008; Lenferink et al., 2010), and production of TGF-β by microenvironment stromal cells may be responsible for $CD44^+/CD24^-$ breast cancer cells in bone (Abraham et al., 2005; Balic et al., 2006). Thus, it may be speculated that soluble TGF-β decreases the expression of E-selectin ligands either before or during CTC engagement with bone marrow endothelium (**Figure 4**), thus throwing into doubt the relevance of E-selectin ligands on breast CTCs in establishing bone metastases. Studies in which EMT is induced in breast cancer cells need to be performed, with coordinated monitoring of glycosylation machinery, core E-selectin ligand protein and lipid expression, E-selectin ligand activity under flow conditions, and EMT and CSC markers, in order to verify or refute mechanistic links between functional E-selectin ligand expression and transition/maintenance of $CD44^+/CD24^-$ CSCs. Ultimately, it may be found that downregulation of E-selectin ligands is not dependent on EMT *per se*, since E-selectin ligand activity fails to decrease consistently from the least mesenchymal luminal to the

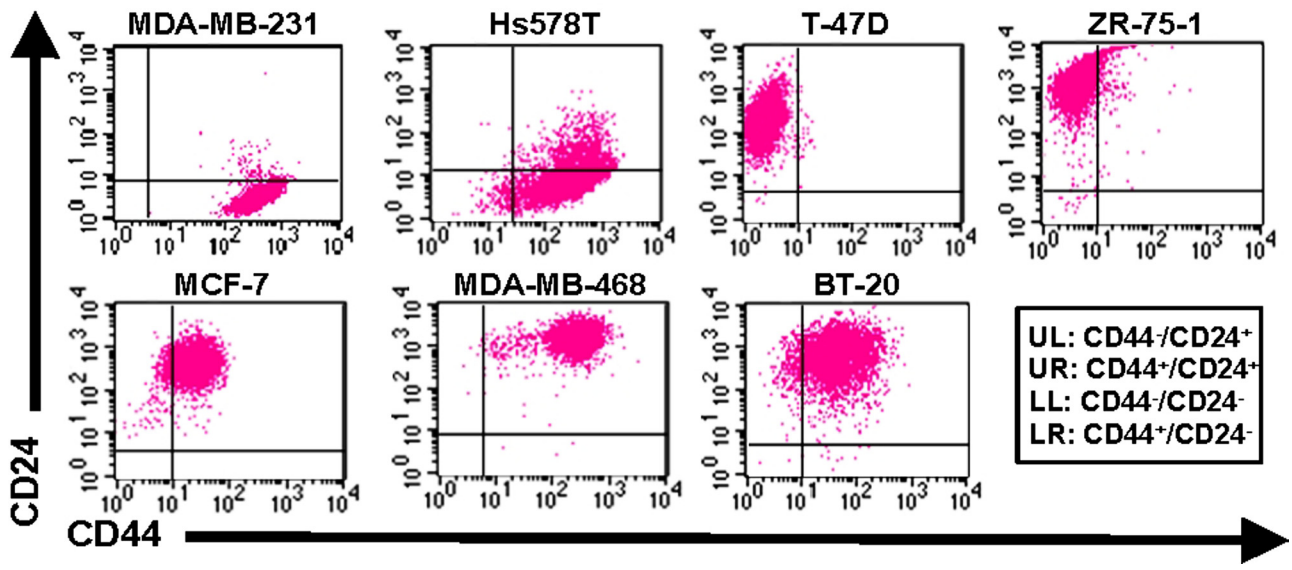

FIGURE 3 | Expression of CD44 and CD24 on breast cancer cell lines. Flow cytometric analysis of cell surface expression on human breast cancer cells from the American Type Culture Collection (ATCC). Cells were simultaneously stained with CD44-FITC and CD24-PE mAbs and analyzed on a BD FACSort cytometer/sorter. Quadrants were set using appropriate FITC or PE-labeled isotype controls. The upper left quadrant represents $CD44^-/CD24^+$ cells, upper right quadrant represents $CD24^+/CD24^+$, the lower right quadrant represents $CD44^+/CD24^-$ cells (i.e., phenotype of purported breast cancer stem cells), and lower left quadrant represents $CD44^-/CD24^-$. Data are representative of $n = 6$ independent experiments.

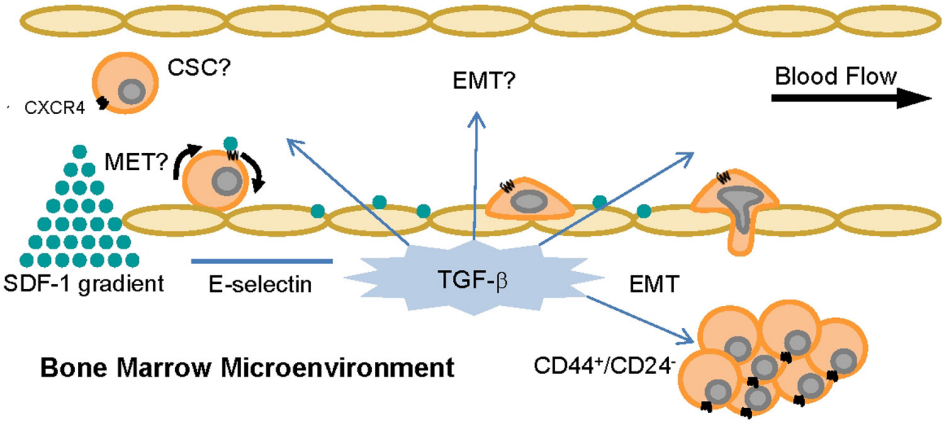

FIGURE 4 | TGF-β and SDF-1 can alter CTC phenotype and behavior in the bone. The cytokine TGF-β and the chemokine SDF-1 are constitutively expressed in the bone microenvironment and control pathways related to cell adhesion and homing, EMT, MET, cell cycle, and tumorigenicity. It is currently unknown if inducible EMT or MET affects cancer cell expression of functional E-selectin ligands and thus CTC capacity to metastasize.

somewhat mesenchymal basal A to the most mesenchymal basal B cells (**Table 1**). Instead, persistent suppression of E-selectin ligands in $CD44^+/CD24^-$ CSCs may be controlled by EMT pathways.

Alternatively, the MET state of CSCs (indicated by ALDH expression but not necessarily $CD44^+/CD24^-$ cells; Liu et al., 2012) may regulate E-selectin ligand expression or function. Interestingly, a recent study of all cell lines in **Table 1** except Hs578T revealed that BT-20 and MDA-MB-468 cells, both $CD44^+/CD24^+$ cell lines of the basal A type with relatively high E-selectin ligand activity (**Figure 3** and **Table 1**), possessed the highest percentage of cells with ALDH activity (Deng et al., 2010). CSCs in the MET state may thus maintain or potentially upregulate E-selectin ligands, in contrast to CSCs in EMT. This notion merits further investigation, in that CTCs from breast cancer patients can simultaneously express mesenchymal and stem cell markers in addition to epithelial markers, and not just EMT markers (Aktas et al., 2009; Bonnomet et al., 2010; Armstrong et al., 2011; Kallergi et al., 2011). Moreover, the bone resident chemokine stromal derived factor-1 (SDF-1, **Figure 4**), known to mediate HSC homing and breast cancer migration through ligation of CXCR4, has been shown to regulate miRNAs in breast cancer cells and stromal cells that control breast cancer cell tumorigenicity and quiescence (Lim et al., 2011; Rhodes et al., 2011a,b). It may only be a matter of time until it is shown that SDF-1 also regulates miRNAs associated with EMT-MET phenotypes of CSCs. Thus, bone microenvironment expression of E-selectin, TGF-β, and SDF-1 may beckon a certain type of CTC to establish a metastatic colony: a circulating CSC already equipped to infiltrate the bone parenchyma, or else another cell, CSC or otherwise, that will undergo EMT or MET as needed to attach to endothelium, invade, and grow.

Epithelial-to-mesenchymal transition and MET are, by their very names, dynamic transitional regulators of cellular phenotypes and behaviors. Thus far, we have proposed that these pathways modulate E-selectin ligands on breast CTCs and CSCs. However, it is valid to explore the potential roles of E-selectin and its ligands as regulators of EMT and MET. The proper E-selectin ligands expressed at the right time in the right place (e.g., HCELL, Mac-2bp, and/or glycolipids; Burdick et al., 2006; Shirure et al., 2011, 2012; manuscript in preparation) on a breast CTC in the vasculature at the metastatic site) could facilitate EMT- or MET-generated/maintained CSCs in response to microenvironmental cues. E-selectin-primed cells may then effectively establish metastatic colonies. If a CTC encounters a small capillary rather than a larger venule, another possibility arises. Assuming the CTC can sufficiently deform to enter the capillary, which can be tested

Table 1 | Expression of CD44, CD24, and E-selectin ligands on human breast cancer cell lines.

Cell line	CD44/CD24 status	Subtype	E-selectin ligand activity
MDA-MB-231	+/low	Basal B	+
Hs578T	+/low	Basal B	+
ZR-75-1	low/+	Luminal	+++
T-47D	low/+	Luminal	++
MCF-7	+/+	Luminal	+++
MDA-MB-468	+/+	Basal A	+++
BT-20	+/+	Basal A	++++

Column 1: Human breast cancer cell lines from ATCC. Column 2: Flow cytometric analysis of cell surface expression on breast cancer cells. Key: − is <2% positive (i.e., same intensity as isotype control antibody), low is 2–10% positive, moderate is 10–80% positive, + is >80% positive. Column 3: Breast cancer cell subtype as reported by Neve et al. (2006). Column 4: E-selectin ligand activity was assessed in the parallel plate flow chamber (Shirure et al., 2011, 2012; and manuscript in preparation). Key: +, upper limit of E-selectin-dependent tethering (i.e., recruitment from fluid flow) to IL-1β-stimulated HUVECs typically observed at wall shear stress of 0.5 dyn/cm^2, beyond which no tethering was observed; ++, upper limit of tethering observed at wall shear stress of 0.8 dyn/cm^2; +++, upper limit of tethering observed at wall shear stress of 1.0 dyn/cm^2; ++++, upper limit of tethering observed at wall shear stress of 2.0 dyn/cm^2. Data are representative of n > 5 independent experiments.

in vitro in a micropipette assay (**Figure 2**), transit through the capillary with or without E-selectin ligand/E-selectin engagement could also effectively modulate CTC and CSC phenotype. For now, these complex, highly speculative models remain in the theoretical realm, but as separate discoveries are made about CTCs, CSCs, cancer cell mechanical properties, and selectin ligands, comprehensive investigations linking these subjects will become less daunting and perhaps even routine.

Thus, several intriguing theories proposing crosstalk among biochemical and biophysical factors and selectin ligands on CTCs remain to be tested, and are the subject of ongoing collaborative studies in our laboratories. It is anticipated that the results of these investigations will contribute to the fundamental understanding of the cross-regulation of functional selectin ligands with transformative molecular pathways in breast cancer progression, as well as other cancers for which selectins and their ligands are suspected promoters of metastasis.

BEYOND THE HYPOTHESIZED MODEL

Although this article has been focused on presenting the potential relationships between CSCs, CTCs, and E-selectin ligands in hematogenous distant metastasis, the pathways mediating metastasis in total are far more extensive. Restricting the discussion to the selectins, CTCs may engage P-selectin expressed on blood vascular endothelial cells (Ludwig et al., 2004; Laubli and Borsig, 2010; St Hill, 2012), which is arguably less understood than endothelial E-selectin-mediated pathways. CTCs in the bloodstream may also form multicellular aggregates with platelets and/or leukocytes (Borsig et al., 2002), and the presence of these other cells can alter the manner in which CTCs interact with the vascular endothelium (Kim et al., 1999; Burdick and Konstantopoulos, 2004; Liang and Dong, 2008; Gong et al., 2012). The initial formation of heterotypic aggregates presumably occurs through engagement of P-selectin on platelets or L-selectin on leukocytes with their respective ligands on CTCs (Mannori et al., 1995; Jadhav et al., 2001; McCarty et al., 2002), such as the aforementioned HCELL (Hanley et al., 2005, 2006; Burdick et al., 2006; Barthel et al., 2009), sulfated glycosaminoglycans or proteoglycans (Ma and Geng, 2002; Monzavi-Karbassi et al., 2007; Cooney et al., 2011), or sulfatides (Needham and Schnaar, 1993; Simonis et al., 2010). Perhaps multicellular aggregation induces CSC phenotype(s). This theory warrants further investigation, given the discovery in HB-chips of CTC aggregates indicating prior CTC–leukocyte engagement (Stott et al., 2010), and a recent publication revealing that platelet–cancer cell contact can induce EMT in breast and colon cancer cells (Labelle et al., 2011). Alternatively, completely novel mechanisms of CTC–CSC regulation may be encountered in lymph node metastasis, considering the vastly different biochemical and biophysical environment of the lymphatic system compared to the blood vasculature (Lund and Swartz, 2010; Swartz and Lund, 2012). Thus, other compelling models of CTC–CSC regulation may be proposed and tested, which could lead to new ways to inhibit cancer metastasis.

CONCLUSION

A full understanding of how a cancer cell progresses from primary tumor cell to CTC to disseminated tumor cell remains elusive. Although EMT, MET, and stem cell pathways are clearly relevant, their effects relative to selectin ligands (and vice versa) on CTCs remain to be determined. On their directed journey to establish new metastatic colonies, CTCs are subject to the influences of a bevy of biochemical and biophysical stressors that may change their phenotype at specific times and at specific locations. CTCs captured from the blood of cancer patients by CellSearch, CTC-or HB-chips, AdnaTest, and other devices reflect only a single temporal data point from which inferences about disease status, treatment strategies, and survival predictions are extrapolated. While this information from blood biopsies is extraordinarily important, some caution is warranted. Molecular markers and phenotypes serving as the basis of capture in these assays have limitations, and information derived from these assays may have further shortcomings in light of CTC dynamism. Therefore, novel CTC capture techniques and therapeutic strategies currently in development must respect the changing epithelial, mesenchymal, CSC-associated, etc., markers and functional phenotypes (e.g., expression of selectin ligands) to be truly meaningful for patients. Ultimately, collective efforts to elucidate the molecular descriptors of CTCs, including selectin ligands and their regulators such as CSC generation/maintenance pathways, will greatly improve the clinical utility of CTCs as diagnostics, prognostics, therapeutic indicators, or therapeutic targets.

ACKNOWLEDGMENTS

This work was supported by CBET-1106118 (to Monica M. Burdick, Fabian Benencia, David F. J. Tees), CBET-1039869 (to Douglas J. Goetz, Monica M. Burdick, Fabian Benencia, David F. J. Tees), and BES-0547165 (to David F. J. Tees) from the National Science Foundation, 1R15CA161830-01 from the National Institutes of Health (to Monica M. Burdick), and a seed grant from the Ohio Cancer Research Associates (to Monica M. Burdick). For helpful discussions and assistance with manuscript preparation, we wish to thank our graduate students Mr. Grady Carlson, Ms. Tiantian Liu, Mr. Eric Martin, Ms. Ameneh Mohammadalipour, Mr. John O'Brien, Mr. Venktesh Shirure, and Ms. Chengkai Xiong, as well as our undergraduate students Ms. Emily Blaha, Mr. Aaron Burdette, Mr. Chaz Cuckler, Ms. Jacquelyn Hawes, and Mr. Nate Reynolds.

REFERENCES

Abraham, B. K., Fritz, P., McClellan, M., Hauptvogel, P., Athelogou, M., and Brauch, H. (2005). Prevalence of CD44+/CD24−/low cells in breast cancer may not be associated with clinical outcome but may favor distant metastasis. *Clin. Cancer Res.* 11, 1154–1159.

Adams, J. M., and Strasser, A. (2008). Is tumor growth sustained by rare cancer stem cells or dominant clones? *Cancer Res.* 68, 4018–4021.

Aigner, S., Ramos, C. L., Hafezi-Moghadam, A., Lawrence, M. B., Friederichs, J., Altevogt, P., and Ley, K. (1998). CD24 mediates rolling of breast carcinoma cells on P-selectin. *FASEB J.* 12, 1241–1251.

Aktas, B., Tewes, M., Fehm, T., Hauch, S., Kimmig, R., and Kasimir-Bauer, S. (2009). Stem cell and epithelial-mesenchymal transition markers are frequently overexpressed in circulating tumor cells of metastatic breast cancer patients. *Breast Cancer Res.* 11, R46.

Al-Hajj, M., Wicha, M. S., Benito-Hernandez, A., Morrison, S. J., and Clarke, M. F. (2003). Prospective identification of tumorigenic breast

cancer cells. *Proc. Natl. Acad. Sci. U S A* 100, 3983–3988.

Armstrong, A. J., Marengo, M. S., Oltean, S., Kemeny, G., Bitting, R. L., Turnbull, J. D., Herold, C. I., Marcom, P. K., George, D. J., and Garcia-Blanco, M. A. (2011). Circulating tumor cells from patients with advanced prostate and breast cancer display both epithelial and mesenchymal markers. *Mol. Cancer Res.* 9, 997–1007.

Badve, S., and Nakshatri, H. (2012). Breast-cancer stem cells-beyond semantics. *Lancet Oncol.* 13, e43–e48.

Balic, M., Lin, H., Young, L., Hawes, D., Giuliano, A., McNamara, G., Datar, R. H., and Cote, R. J. (2006). Most early disseminated cancer cells detected in bone marrow of breast cancer patients have a putative breast cancer stem cell phenotype. *Clin. Cancer Res.* 12, 5615–5621.

Barthel, S. R., Gavino, J. D., Descheny, L., and Dimitroff, C. J. (2007). Targeting selectins and selectin ligands in inflammation and cancer. *Expert Opin. Ther. Targets* 11, 1473–1491.

Barthel, S. R., Wiese, G. K., Cho, J., Opperman, M. J., Hays, D. L., Siddiqui, J., Pienta, K. J., Furie, B., and Dimitroff, C. J. (2009). Alpha 1,3 fucosyltransferases are master regulators of prostate cancer cell trafficking. *Proc. Natl. Acad. Sci. U.S.A.* 106, 19491–19496.

Bausch, A. R., Möller, W., and Sackmann, E. (1999). Measurement of local viscoelasticity and forces in living cells by magnetic tweezers. *Biophys. J.* 76, 573–579.

Bendas, G., and Borsig, L. (2012). Cancer cell adhesion and metastasis: selectins, integrins, and the inhibitory potential of heparins. *Intl. J. Cell Biol.* 2012, 676731.

Blick, T., Hugo, H., Widodo, E., Waltham, M., Pinto, C., Mani, S. A., Weinberg, R. A., Neve, R. M., Lenburg, M. E., and Thompson, E. W. (2010). Epithelial mesenchymal transition traits in human breast cancer cell lines parallel the CD44(hi/)CD24 (lo/−) stem cell phenotype in human breast cancer. *J. Mammary Gland Biol. Neoplasia* 15, 235–252.

Bonnet, D., and Dick, J. E. (1997). Human acute myeloid leukemia is organized as a hierarchy that originates from a primitive hematopoietic cell. *Nat. Med.* 3, 730–737.

Bonnomet, A., Brysse, A., Tachsidis, A., Waltham, M., Thompson, E. W., Polette, M., and Gilles, C. (2010). Epithelial-to-mesenchymal transitions and circulating tumor cells. *J. Mammary Gland Biol. Neoplasia* 15, 261–273.

Borsig, L., Wong, R., Hynes, R. O., Varki, N. M., and Varki, A. (2002). Synergistic effects of L- and P-selectin in facilitating tumor metastasis can involve non-mucin ligands and implicate leukocytes as enhancers of metastasis. *Proc. Natl. Acad. Sci. U.S.A.* 99, 2193–2198.

Brown, K. A., Aakre, M. E., Gorska, A. E., Price, J. O., Eltom, S. E., Pietenpol, J. A., and Moses, H. L. (2004). Induction by transforming growth factor-beta1 of epithelial to mesenchymal transition is a rare event in vitro. *Breast Cancer Res.* 6, R215–R231.

Burdick, M. M., Chu, J. T., Godar, S., and Sackstein, R. (2006). HCELL is the major E- and L-selectin ligand expressed on LS174T colon carcinoma cells. *J. Biol. Chem.* 281, 13899–13905.

Burdick, M. M., and Konstantopoulos, K. (2004). Platelet-induced enhancement of LS174T colon carcinoma and THP-1 monocytoid cell adhesion to vascular endothelium under flow. *Am. J. Physiol. Cell Physiol.* 287, C539–C547.

Burdick, M. M., McCaffery, J. M., Kim, Y. S., Bochner, B. S., and Konstantopoulos, K. (2003). Colon carcinoma cell glycolipids, integrins, and other glycoproteins mediate adhesion to HUVECs under flow. *Am. J. Physiol. Cell Physiol.* 284, C977–C987.

Burdick, M. M., McCarty, O. J., Jadhav, S., and Konstantopoulos, K. (2001). Cell-cell interactions in inflammation and cancer metastasis. *IEEE Eng. Med. Biol. Mag.* 20, 86–91.

Campbell, L. L., and Polyak, K. (2007). Breast tumor heterogeneity: cancer stem cells or clonal evolution? *Cell Cycle* 6, 2332–2338.

Chambers, A. F., Schmidt, E. E., MacDonald, I. C., Morris, V. L., and Groom, A. C. (1992). Early steps in hematogenous metastasis of B16F1 melanoma cells in chick embryos studied by high-resolution intravital videomicroscopy. *J. Natl. Cancer Inst.* 84, 797–803.

Chase, S. D., Magnani, J. L., and Simon, S. I. (2012). E-selectin ligands as mechanosensitive receptors on neutrophils in health and disease. *Ann. Biomed. Eng.* 40, 849–859.

Choquet, D., Felsenfeld, D. P., and Scheetz, M. P. (1997). Extracellular matrix rigidity causes strengthening of integrin-cytoskeleton linkages. *Cell* 88, 39–48.

Clay, M. R., Tabor, M., Owen, J. H., Carey, T. E., Bradford, C. R., Wolf, G. T., Wicha, M. S., and Prince, M. E. (2010). Single-marker identification of head and neck squamous cell carcinoma cancer stem cells with aldehyde dehydrogenase. *Head Neck* 32, 1195–1201.

Cooney, C. A., Jousheghany, F., Yao-Borengasser, A., Phanavanh, B., Gomes, T., Kieber-Emmons, A. M., Siegel, E. R., Suva, L. J., Ferrone, S., Kieber-Emmons, T., and Monzavi-Karbassi, B. (2011). Chondroitin sulfates play a major role in breast cancer metastasis: a role for CSPG4 and CHST11 gene expression in forming surface P-selectin ligands in aggressive breast cancer cells. *Breast Cancer Res.* 13, R58.

Costello, R. T., Mallet, F., Gaugler, B., Sainty, D., Arnoulet, C., Gastaut, J. A., and Olive, D. (2000). Human acute myeloid leukemia CD34+/CD38− progenitor cells have decreased sensitivity to chemotherapy and Fas-induced apoptosis, reduced immunogenicity, and impaired dendritic cell transformation capacities. *Cancer Res.* 60, 4403–4411.

Darling, E. M., Topel, M., Zauscher, S., Vail, T. P., and Guilak, F. (2008). Viscoelastic properties of human mesenchymally-derived stem cells and primary osteoblasts, chondrocytes, and adipocytes. *J. Biomech.* 41, 454–464.

Dawood, S., Broglio, K., Valero, V., Reuben, J., Handy, B., Islam, R., Jackson, S., Hortobagyi, G. N., Fritsche, H., and Cristofanilli, M. (2008). Circulating tumor cells in metastatic breast cancer: From prognostic stratification to modification of the staging system? *Cancer* 113, 2422–2430.

de Vries, T., Knegtel, R. M., Holmes, E. H., and Macher, B. A. (2001). Fucosyltransferases: Structure/function studies. *Glycobiology* 11, 119R–128R.

Dembo, M., Torney, D. C., Saxman, K., and Hammer, D. (1988). The reaction-limited kinetics of membrane-to-surface adhesion and detachment. *Proc. R. Soc. Lond. B Biol. Sci.* 234, 55–83.

Deng, S., Yang, X., Lassus, H., Liang, S., Kaur, S., Ye, Q., Li, C., Wang, L. P., Roby, K. F., Orsulic, S., Connolly, D. C., Zhang, Y., Montone, K., Butzow, R., Coukos, G., and Zhang, L. (2010). Distinct expression levels and patterns of stem cell marker, aldehyde dehydrogenase isoform 1 (ALDH1), in human epithelial cancers. *PLoS ONE* 5, e10277. doi: 10.1371/journal.pone.0010277

DeSantis, C., Siegel, R., Bandi, P., and Jemal, A. (2011). Breast cancer statistics, 2011. *CA Cancer J. Clin.* 61, 409–418.

Diehn, M., and Clarke, M. F. (2006). Cancer stem cells and radiotherapy: new insights into tumor radioresistance. *J. Natl. Cancer Inst.* 98, 1755–1757.

Dimitroff, C. J., Lechpammer, M., Long-Woodward, D., and Kutok, J. L. (2004). Rolling of human bone-metastatic prostate tumor cells on human bone marrow endothelium under shear flow is mediated by E-selectin. *Cancer Res.* 64, 5261–5269.

Doerschuk, C. M., Beyers, N., Coxson, H. O., Wiggs, B., and Hogg, J. C. (1993). Comparison of neutrophil and capillary diameters and their relation to neutrophil sequestration in the lung. *J. Appl. Physiol.* 74, 3040–3045.

Dupuy, F., Germot, A., Julien, R., and Maftah, A. (2004). Structure/function study of Lewis alpha3- and alpha3/4-fucosyltransferases: The alpha1,4 fucosylation requires an aromatic residue in the acceptor-binding domain. *Glycobiology* 14, 347–356.

Edbrooke, M. R., Britten, C. J., Kelly, V. A., Martin, S. L., Smithers, N., Winder, A. J., Witham, S. J., and Bird, M. I. (1997). The alpha(1-3)-fucosyltransferases come of age. *Biochem. Soc. Trans.* 25, 880–886.

Eshel, R., Zanin, A., Sagi-Assif, O., Meshel, T., Smorodinsky, N. I., Dwir, O., Alon, R., Brakenhoff, R., van Dongen, G., and Witz, I. P. (2000). The GPI-linked Ly-6 antigen E48 regulates expression levels of the FX enzyme and of E-selectin ligands on head and neck squamous carcinoma cells. *J. Biol. Chem.* 275, 12833–12840.

Evans, E. A., and Calderwood, D. A. (2007). Forces and bond dynamics in cell adhesion. *Science* 316, 1148–1153.

Fehm, T., Becker, S., Duerr-Stoerzer, S., Sotlar, K., Mueller, V., Wallwiener, D., Lane, N., Solomayer, E., and Uhr, J. (2007). Determination of HER2 status using both serum HER2 levels and circulating tumor cells in patients with recurrent breast cancer whose primary tumor was HER2 negative or of unknown HER2 status. *Breast Cancer Res.* 9, R74.

Fillmore, C. M., and Kuperwasser, C. (2008). Human breast cancer cell lines contain stem-like cells that self-renew, give rise to phenotypically diverse progeny and survive chemotherapy. *Breast Cancer Res.* 10, R25.

Geng, Y., Marshall, J. R., and King, M. R. (2012). Glycomechanics of the metastatic cascade: Tumor cell-endothelial cell interactions in the

circulation. *Ann. Biomed. Eng.* 40, 790–805.

Giavazzi, R., Foppolo, M., Dossi, R., and Remuzzi, A. (1993). Rolling and adhesion of human tumor cells on vascular endothelium under physiological flow conditions. *J. Clin. Invest.* 92, 3038–3044.

Ginestier, C., Hur, M. H., Charafe-Jauffret, E., Monville, F., Dutcher, J., Brown, M., Jacquemier, J., Viens, P., Kleer, C. G., Liu, S., Schott, A., Hayes, D., Birnbaum, D., Wicha, M. S., and Dontu, G. (2007). ALDH1 is a marker of normal and malignant human mammary stem cells and a predictor of poor clinical outcome. *Cell Stem Cell* 1, 555–567.

Gong, L., Mi, H. J., Zhu, H., Zhou, X., and Yang, H. (2012). P-selectin-mediated platelet activation promotes adhesion of non-small cell lung carcinoma cells on vascular endothelial cells under flow. *Mol. Med. Rep.* 5, 935–942.

Graham, S. M., Jorgensen, H. G., Allan, E., Pearson, C., Alcorn, M. J., Richmond, L., and Holyoake, T. L. (2002). Primitive, quiescent, Philadelphia-positive stem cells from patients with chronic myeloid leukemia are insensitive to STI571 in vitro. *Blood* 99, 319–325.

Gupta, P. B., Chaffer, C. L., and Weinberg, R. A. (2009). Cancer stem cells: mirage or reality? *Nat. Med.* 15, 1010–1012.

Ham, A. S., Goetz, D. J., Klibanov, A. L., and Lawrence, M. B. (2007). Microparticle adhesive dynamics and rolling mediated by selectin-specific antibodies under flow. *Biotechnol. Bioeng.* 96, 596–607.

Hanley, W. D., Burdick, M. M., Konstantopoulos, K., and Sackstein, R. (2005). CD44 on LS174T colon carcinoma cells possesses E-selectin ligand activity. *Cancer Res.* 65, 5812–5817.

Hanley, W. D., Napier, S. L., Burdick, M. M., Schnaar, R. L., Sackstein, R., and Konstantopoulos, K. (2006). Variant isoforms of CD44 are P- and L-selectin ligands on colon carcinoma cells. *FASEB J.* 20, 337–339.

Holtz, M. S., Slovak, M. L., Zhang, F., Sawyers, C. L., Forman, S. J., and Bhatia, R. (2002). Imatinib mesylate (STI571) inhibits growth of primitive malignant progenitors in chronic myelogenous leukemia through reversal of abnormally increased proliferation. *Blood* 99, 3792–3800.

Hou, H. W., Bhagat, A. A., Chong, A. G., Mao, P., Tan, K. S., Han, J., and Lim, C. T. (2010). Deformability based cell margination – a simple microfluidic design for malaria-infected erythrocyte separation. *Lab Chip* 10, 2605–2613.

Izumi, Y., Taniuchi, Y., Tsuji, T., Smith, C. W., Nakamori, S., Fidler, I. J., and Irimura, T. (1995). Characterization of human colon carcinoma variant cells selected for sialyl Le^x carbohydrate antigen: liver colonization and adhesion to vascular endothelial cells. *Exp. Cell Res.* 216, 215–221.

Jadhav, S., Bochner, B. S., and Konstantopoulos, K. (2001). Hydrodynamic shear regulates the kinetics and receptor specificity of polymorphonuclear leukocyte-colon carcinoma cell adhesive interactions. *J. Immunol.* 167, 5986–5993.

Jones, R. J., Ambinder, R. F., Piantadosi, S., and Santos, G. W. (1991). Evidence of a graft-versus-lymphoma effect associated with allogeneic bone marrow transplantation. *Blood* 77, 649–653.

Julien, S., Ivetic, A., Grigoriadis, A., QiZe, D., Burford, B., Sproviero, D., Picco, G., Gillett, C., Papp, S. L., Schaffer, L., Tutt, A., Taylor-Papadimitriou, J., Pinder, S. E., and Burchell, J. M. (2011). Selectin ligand sialyl-Lewis x antigen drives metastasis of hormone-dependent breast cancers. *Cancer Res.* 71, 7683–7693.

Kajiwara, H., Yasuda, M., Kumaki, N., Shibayama, T., and Osamura, Y. (2005). Expression of carbohydrate antigens (SSEA-1, sialyl-Lewis X, DU-PAN-2 and CA19-9) and E-selectin in urothelial carcinoma of the renal pelvis, ureter, and urinary bladder. *Tokai J. Exp. Clin. Med.* 30, 177–182.

Kallergi, G., Papadaki, M. A., Politaki, E., Mavroudis, D., Georgoulias, V., and Agelaki, S. (2011). Epithelial to mesenchymal transition markers expressed in circulating tumour cells of early and metastatic breast cancer patients. *Breast Cancer Res.* 13, R59.

Kalluri, R., and Weinberg, R. A. (2009). The basics of epithelial-mesenchymal transition. *J. Clin. Invest.* 119, 1420–1428.

Kannagi, R. (2004). Molecular mechanism for cancer-associated induction of sialyl Lewis X and sialyl Lewis A expression-The Warburg effect revisited. *Glycoconj. J.* 20, 353–364.

Kannagi, R., Izawa, M., Koike, T., Miyazaki, K., and Kimura, N. (2004). Carbohydrate-mediated cell adhesion in cancer metastasis and angiogenesis. *Cancer Sci.* 95, 377–384.

Keelan, E. T., Licence, S. T., Peters, A. M., Binns, R. M., and Haskard, D. O. (1994). Characterization of E-selectin expression in vivo with use of a radiolabeled monoclonal antibody. *Am. J. Physiol.* 266, H278–H290.

Kelly, P. N., Dakic, A., Adams, J. M., Nutt, S. L., and Strasser, A. (2007). Tumor growth need not be driven by rare cancer stem cells. *Science* 317, 337.

Khatib, A. M., Fallavollita, L., Wancewicz, E. V., Monia, B. P., and Brodt, P. (2002). Inhibition of hepatic endothelial E-selectin expression by C-raf antisense oligonucleotides blocks colorectal carcinoma liver metastasis. *Cancer Res.* 62, 5393–5398.

Kim, M. Y., Oskarsson, T., Acharyya, S., Nguyen, D. X., Zhang, X. H., Norton, L., and Massague, J. (2009). Tumor self-seeding by circulating cancer cells. *Cell* 139, 1315–1326.

Kim, Y. C., Park, S. J., and Park, J. K. (2008). Biomechanical analysis of cancerous and normal cells based on bulge generation in a microfluidic device. *Analyst* 133, 1432–1439.

Kim, Y. J., Borsig, L., Han, H. L., Varki, N. M., and Varki, A. (1999). Distinct selectin ligands on colon carcinoma mucins can mediate pathological interactions among platelets, leukocytes, and endothelium. *Am. J. Pathol.* 155, 461–472.

Klopocki, A. G., Krop-Watorek, A., Dus, D., and Ugorski, M. (1996). Adhesion of human uroepithelial cells to E-selectin: possible involvement of sialosyl $Lewis^A$-ganglioside. *Int. J. Cancer* 68, 239–244.

Konstantopoulos, K., and Thomas, S. N. (2009). Cancer cells in transit: the vascular interactions of tumor cells. *Annu. Rev. Biomed. Eng.* 11, 177–202.

Kryczek, I., Liu, S., Roh, M., Vatan, L., Szeliga, W., Wei, S., Banerjee, M., Mao, Y., Kotarski, J., Wicha, M. S., Liu, R., and Zou, W. (2012). Expression of aldehyde dehydrogenase and CD133 defines ovarian cancer stem cells. *Int. J. Cancer* 130, 29–39.

Labelle, M., Begum, S., and Hynes, R. O. (2011). Direct signaling between platelets and cancer cells induces an epithelial-mesenchymal-like transition and promotes metastasis. *Cancer cell* 20, 576–590.

Lafrenie, R. M., Buchanan, M. R., and Orr, F. W. (1993). Adhesion molecules and their role in cancer metastasis. *Cell Biophys.* 23, 3–89.

Lapidot, T., Sirard, C., Vormoor, J., Murdoch, B., Hoang, T., Caceres-Cortes, J., Minden, M., Paterson, B., Caligiuri, M. A., and Dick, J. E. (1994). A cell initiating human acute myeloid leukaemia after transplantation into SCID mice. *Nature* 367, 645–648.

Laubli, H., and Borsig, L. (2010). Selectins promote tumor metastasis. *Semin. Cancer Biol.* 20, 169–177.

Lee, Y. H., Albig, A. R., Regner, M., Schiemann, B. J., and Schiemann, W. P. (2008). Fibulin-5 initiates epithelial-mesenchymal transition (EMT) and enhances EMT induced by TGF-beta in mammary epithelial cells via a MMP-dependent mechanism. *Carcinogenesis* 29, 2243–2251.

Lenferink, A. E., Cantin, C., Nantel, A., Wang, E., Durocher, Y., Banville, M., Paul-Roc, B., Marcil, A., Wilson, M. R., and O'Connor-McCourt, M. D. (2010). Transcriptome profiling of a TGF-beta-induced epithelial-to-mesenchymal transition reveals extracellular clusterin as a target for therapeutic antibodies. *Oncogene* 29, 831–844.

Liang, S., and Dong, C. (2008). Integrin VLA-4 enhances sialyl-Lewisx/a-negative melanoma adhesion to and extravasation through the endothelium under low flow conditions. *Am. J. Physiol. Cell Physiol.* 295, C701–C707.

Lim, P. K., Bliss, S. A., Patel, S. A., Taborga, M., Dave, M. A., Gregory, L. A., Greco, S. J., Bryan, M., Patel, P. S., and Rameshwar, P. (2011). Gap junction-mediated import of microRNA from bone marrow stromal cells can elicit cell cycle quiescence in breast cancer cells. *Cancer Res.* 71, 1550–1560.

Liotta, L. A. (1987). Biochemical mechanisms of tumor invasion and metastases. *Clin. Physiol. Biochem.* 5, 190–199.

Liu, S., Clouthier, S. G., and Wicha, M. S. (2012). Role of microRNAs in the regulation of breast cancer stem cells. *J. Mammary Gland Biol. Neoplasia* 17, 15–21.

Ludwig, R. J., Boehme, B., Podda, M., Henschler, R., Jager, E., Tandi, C., Boehncke, W. H., Zollner, T. M., Kaufmann, R., and Gille, J. (2004). Endothelial P-selectin as a target of heparin action in experimental melanoma lung metastasis. *Cancer Res.* 64, 2743–2750.

Lund, A. W., and Swartz, M. A. (2010). Role of lymphatic vessels in tumor immunity: passive conduits or active participants? *J. Mammary Gland Biol. Neoplasia* 15, 341–352.

Ma, Y. Q., and Geng, J. G. (2002). Obligatory requirement of sulfation for P-selectin binding to human salivary gland carcinoma Acc-M cells and breast carcinoma ZR-75-30 cells. *J. Immunol.* 168, 1690–1696.

Magee, J. A., Piskounova, E., and Morrison, S. J. (2012). Cancer stem cells:

impact, heterogeneity, and uncertainty. *Cancer cell* 21, 283–296.

Mani, S. A., Guo, W., Liao, M. J., Eaton, E. N., Ayyanan, A., Zhou, A. Y., Brooks, M., Reinhard, F., Zhang, C. C., Shipitsin, M., Campbell, L. L., Polyak, K., Brisken, C., Yang, J., and Weinberg, R. A. (2008). The epithelial-mesenchymal transition generates cells with properties of stem cells. *Cell* 133, 704–715.

Mannori, G., Crottet, P., Cecconi, O., Hanasaki, K., Aruffo, A., Nelson, R. M., Varki, A., and Bevilacqua, M. P. (1995). Differential colon cancer cell adhesion to E-, P-, and L-selectin: role of mucin-type glycoproteins. *Cancer Res.* 55, 4425–4431.

Marshall, B. T., Long, M., Piper, J. W., Yago, T., McEver, R. P., and Zhu, C. (2003). Direct observation of catch bonds involving cell-adhesion molecules. *Nature* 423, 190–193.

Mason, T. G., Ganesan, K., van Zanten, J. H., Wirtz, D., and Kuo, S. C. (1997). Particle tracking microrheology of complex fluids. *Phys. Rev. Lett.* 79, 3282–3285.

Mason, T. G., and Weitz, D. A. (1995). Optical measurements of frequency-dependent linear viscoelastic moduli of complex fluids. *Phys. Rev. Lett.* 74, 1250–1253.

Matsuura, N., Narita, T., Hiraiwa, N., Hiraiwa, M., Murai, H., Iwase, T., Funahashi, H., Imai, T., Takagi, H., and Kannagi, R. (1998). Gene expression of fucosyl- and sialyltransferases which synthesize sialyl Lewis^x, the carbohydrate ligands for E-selectin, in human breast cancer. *Int. J. Oncol.* 12, 1157–1164.

Mazo, I. B., Gutierrez-Ramos, J. C., Frenette, P. S., Hynes, R. O., Wagner, D. D., and von Andrian, U. H. (1998). Hematopoietic progenitor cell rolling in bone marrow microvessels: Parallel contributions by endothelial selectins and vascular cell adhesion molecule 1. *J. Exp. Med.* 188, 465–474.

McCarty, O. J., Jadhav, S., Burdick, M. M., Bell, W. R., and Konstantopoulos, K. (2002). Fluid shear regulates the kinetics and molecular mechanisms of activation-dependent platelet binding to colon carcinoma cells. *Biophys. J.* 83, 836–848.

McEver, R. P., and Zhu, C. (2007). A catch to integrin activation. *Nat. Immunol.* 8, 1035–1037.

Minn, A. J., Kang, Y., Serganova, I., Gupta, G. P., Giri, D. D., Doubrovin, M., Ponomarev, V., Gerald, W. L., Blasberg, R., and Massague, J. (2005). Distinct organ-specific metastatic potential of individual breast cancer cells and primary tumors. *J. Clin. Invest.* 115, 44–55.

Monzavi-Karbassi, B., Stanley, J. S., Hennings, L., Jousheghany, F., Artaud, C., Shaaf, S., and Kieber-Emmons, T. (2007). Chondroitin sulfate glycosaminoglycans as major P-selectin ligands on metastatic breast cancer cell lines. *Int. J. Cancer* 120, 1179–1191.

Moore, M. A. (2001). The role of chemoattraction in cancer metastases. *Bioessays* 23, 674–676.

Morel, A. P., Lievre, M., Thomas, C., Hinkal, G., Ansieau, S., and Puisieux, A. (2008). Generation of breast cancer stem cells through epithelial-mesenchymal transition. *PLoS ONE* 3, e2888. doi: 10.1371/journal.pone.0002888

Mostert, B., Sleijfer, S., Foekens, J. A., and Gratama, J. W. (2009). Circulating tumor cells (CTCs): detection methods and their clinical relevance in breast cancer. *Cancer Treat. Rev.* 35, 463–474.

Nagrath, S., Sequist, L. V., Maheswaran, S., Bell, D. W., Irimia, D., Ulkus, L., Smith, M. R., Kwak, E. L., Digumarthy, S., Muzikansky, A., Ryan, P., Balis, U. J., Tompkins, R. G., Haber, D. A., and Toner, M. (2007). Isolation of rare circulating tumour cells in cancer patients by microchip technology. *Nature* 450, 1235–1239.

Narita, T., Kawasaki-Kimura, N., Matsuura, N., Funahashi, H., and Kannagi, R. (1996). Adhesion of human breast cancer cells to vascular endothelium mediated by sialyl Lewis^x/E-selectin. *Breast Cancer* 3, 19–23.

Needham, L. K., and Schnaar, R. L. (1993). The HNK-1 reactive sulfoglucuronyl glycolipids are ligands for L-selectin and P-selectin but not E-selectin. *Proc. Natl. Acad. Sci. U.S.A.* 90, 1359–1363.

Neve, R. M., Chin, K., Fridlyand, J., Yeh, J., Baehner, F. L., Fevr, T., Clark, L., Bayani, N., Coppe, J. P., Tong, F., Speed, T., Spellman, P. T., DeVries, S., Lapuk, A., Wang, N. J., Kuo, W. L., Stilwell, J. L., Pinkel, D., Albertson, D. G., Waldman, F. M., McCormick, F., Dickson, R. B., Johnson, M. D., Lippman, M., Ethier, S., Gazdar, A., and Gray, J. W. (2006). A collection of breast cancer cell lines for the study of functionally distinct cancer subtypes. *Cancer Cell* 10, 515–527.

Oakey, J., Applegate, R. W., Jr., Arellano, E., Di Carlo, D., Graves, S. W., and Toner, M. (2010). Particle focusing in staged inertial microfluidic devices for flow cytometry. *Anal. Chem.* 82, 3862–3867.

Onder, T. T., Gupta, P. B., Mani, S. A., Yang, J., Lander, E. S., and Weinberg, R. A. (2008). Loss of E-cadherin promotes metastasis via multiple downstream transcriptional pathways. *Cancer Res.* 68, 3645–3654.

Oravecz-Wilson, K. I., Philips, S. T., Yilmaz, O. H., Ames, H. M., Li, L., Crawford, B. D., Gauvin, A. M., Lucas, P. C., Sitwala, K., Downing, J. R., Morrison, S. J., and Ross, T. S. (2009). Persistence of leukemia-initiating cells in a conditional knockin model of an imatinib-responsive myeloproliferative disorder. *Cancer cell* 16, 137–148.

Parekkadan, B., and Milwid, J. M. (2010). Mesenchymal stem cells as therapeutics. *Annu. Rev. Biomed. Eng.* 12, 87–117.

Phillips, T. M., McBride, W. H., and Pajonk, F. (2006). The response of CD24(−/low)/CD44+ breast cancer-initiating cells to radiation. *J. Natl. Cancer Inst.* 98, 1777–1785.

Ponti, D., Costa, A., Zaffaroni, N., Pratesi, G., Petrangolini, G., Coradini, D., Pilotti, S., Pierotti, M. A., and Daidone, M. G. (2005). Isolation and in vitro propagation of tumorigenic breast cancer cells with stem/progenitor cell properties. *Cancer Res.* 65, 5506–5511.

Porada, C. D., Zanjani, E. D., and Almeida-Porad, G. (2006). Adult mesenchymal stem cells: a pluripotent population with multiple applications. *Curr. Stem Cell Res. Ther.* 1, 365–369.

Pountos, I., Corscadden, D., Emery, P., and Giannoudis, P. V. (2007). Mesenchymal stem cell tissue engineering: techniques for isolation, expansion and application. *Injury* 38(Suppl. 4), S23–S33.

Reim, F., Dombrowski, Y., Ritter, C., Buttmann, M., Hausler, S., Ossadnik, M., Krockenberger, M., Beier, D., Beier, C. P., Dietl, J., Becker, J. C., Honig, A., and Wischhusen, J. (2009). Immunoselection of breast and ovarian cancer cells with trastuzumab and natural killer cells: selective escape of CD44^{high}/CD24^{low}/HER2^{low} breast cancer stem cells. *Cancer Res.* 69, 8058–8066.

Renkonen, J., Paavonen, T., and Renkonen, R. (1997). Endothelial and epithelial expression of sialyl Lewis(x) and sialyl Lewis(a) in lesions of breast carcinoma. *Int. J. Cancer* 74, 296–300.

Rhodes, L. V., Bratton, M. R., Zhu, Y., Tilghman, S. L., Muir, S. E., Salvo, V. A., Tate, C. R., Elliott, S., Nephew, K. P., Collins-Burow, B. M., and Burow, M. E. (2011a). Effects of SDF-1-CXCR4 signaling on microRNA expression and tumorigenesis in estrogen receptor-alpha (ER-alpha)-positive breast cancer cells. *Exp. Cell Res.* 317, 2573–2581.

Rhodes, L. V., Short, S. P., Neel, N. F., Salvo, V. A., Zhu, Y., Elliott, S., Wei, Y., Yu, D., Sun, M., Muir, S. E., Fonseca, J. P., Bratton, M. R., Segar, C., Tilghman, S. L., Sobolik-Delmaire, T., Horton, L. W., Zaja-Milatovic, S., Collins-Burow, B. M., Wadsworth, S., Beckman, B. S., Wood, C. E., Fuqua, S. A., Nephew, K. P., Dent, P., Worthylake, R. A., Curiel, T. J., Hung, M. C., Richmond, A., and Burow, M. E. (2011b). Cytokine receptor CXCR4 mediates estrogen-independent tumorigenesis, metastasis, and resistance to endocrine therapy in human breast cancer. *Cancer Res.* 71, 603–613.

Riethdorf, S., and Pantel, K. (2008). Disseminated tumor cells in bone marrow and circulating tumor cells in blood of breast cancer patients: current state of detection and characterization. *Pathobiology* 75, 140–148.

Riethdorf, S., and Pantel, K. (2010). Advancing personalized cancer therapy by detection and characterization of circulating carcinoma cells. *Ann. N. Y. Acad. Sci.* 1210, 66–77.

Sackstein, R. (2004). The bone marrow is akin to skin: HCELL and the biology of hematopoietic stem cell homing. *J. Invest. Dermatol.* 122, 1061–1069.

Sackstein, R. (2005). The lymphocyte homing receptors: gatekeepers of the multistep paradigm. *Curr. Opin. Hematol.* 12, 444–450.

Schweitzer, K. M., Drager, A. M., van der Valk, P., Thijsen, S. F., Zevenbergen, A., Theijsmeijer, A. P., van der Schoot, C. E., and Langenhuijsen, M. M. (1996). Constitutive expression of E-selectin and vascular cell adhesion molecule-1 on endothelial cells of hematopoietic tissues. *Am. J. Pathol.* 148, 165–175.

Shirure, V. S., Henson, K. A., Schnaar, R. L., Nimrichter, L., and Burdick, M. M. (2011). Gangliosides expressed on breast cancer cells are E-selectin ligands. *Biochem. Biophys. Res. Commun.* 18, 423–429.

Shirure, V. S., Reynolds, N. M., and Burdick, M. M. (2012). Mac-2 binding protein is a novel E-selectin ligand expressed by breast cancer cells. *PLoS ONE.* doi: 10.1371/journal.pone.0044529

Shroff, S. G., Saner, D. R., and Lal, R. (1995). Dynamic micromechanical properties of cultured rat atrial

myocytes measured by atomic force microscopy. *Am. J. Physiol.* 269, C286–C292.

Silva, I. A., Bai, S., McLean, K., Yang, K., Griffith, K., Thomas, D., Ginestier, C., Johnston, C., Kueck, A., Reynolds, R. K., Wicha, M. S., and Buckanovich, R. J. (2011). Aldehyde dehydrogenase in combination with CD133 defines angiogenic ovarian cancer stem cells that portend poor patient survival. *Cancer Res.* 71, 3991–4001.

Simonis, D., Schlesinger, M., Seelandt, C., Borsig, L., and Bendas, G. (2010). Analysis of SM4 sulfatide as a P-selectin ligand using model membranes. *Biophys. Chem.* 150, 98–104.

Sirghi, L., Kylian, O., Gilliland, D., Ceccone, G., and Rossi, F. (2006). Cleaning and hydrophilization of atomic force microscopy silicon probes. *J. Phys. Chem. B* 110, 25975–25981.

Skorstengaard, K., Vestergaard, E. M., Langkilde, N. C., Christensen, L. L., Wolf, H., and Orntoft, T. F. (1999). Lewis antigen mediated adhesion of freshly removed human bladder tumors to E-selectin. *J. Urol.* 161, 1316–1323.

Springer, T. A. (1994). Traffic signals for lymphocyte recirculation and leukocyte emigration: the multistep paradigm. *Cell* 76, 301–314.

Sraj, I., Eggleton, C. D., Jimenez, R., Hoover, E., Squier, J., Chichester, J., and Marr, D. W. (2010). Cell deformation cytometry using diode-bar optical stretchers. *J. Biomed. Optics* 15, 047010.

St Hill, C. A. (2012). Interactions between endothelial selectins and cancer cells regulate metastasis. *Front. Biosci.* 17, 3233–3251.

Stern, R., Shuster, S., Neudecker, B. A., and Formby, B. (2002). Lactate stimulates fibroblast expression of hyaluronan and CD44: the Warburg effect revisited. *Exp. Cell Res.* 276, 24–31.

Stern, R., Shuster, S., Wiley, T. S., and Formby, B. (2001). Hyaluronidase can modulate expression of CD44. *Exp. Cell. Res.* 266, 167–176.

Stott, S. L., Hsu, C. H., Tsukrov, D. I., Yu, M., Miyamoto, D. T., Waltman, B. A., Rothenberg, S. M., Shah, A. M., Smas, M. E., Korir, G. K., Floyd, F. P., Jr., Gilman, A. J., Lord, J. B., Winokur, D., Springer, S., Irimia, D., Nagrath, S., Sequist, L. V., Lee, R. J., Isselbacher, K. J., Maheswaran, S., Haber, D. A., and Toner, M. (2010). Isolation of circulating tumor cells using a microvortex-generating herringbone-chip. *Proc. Natl. Acad. Sci. U.S.A.* 107, 18392–18397.

Swartz, M. A., and Lund, A. W. (2012). Lymphatic and interstitial flow in the tumour microenvironment: linking mechanobiology with immunity. *Nat. Rev. Cancer* 12, 210–219.

Talmadge, J. E., and Fidler, I. J. (2010). AACR centennial series: The biology of cancer metastasis: historical perspective. *Cancer Res.* 70, 5649–5669.

Tan, S. C., Pan, W. X., Ma, G., Cai, N., Leong, K. W., and Liao, K. (2008). Viscoelastic behaviour of human mesenchymal stem cells. *BMC Cell Biol.* 9, 40. doi: 10.1186/1471-2121-9-40

Thomas, S. N., Schnaar, R. L., and Konstantopoulos, K. (2009). Podocalyxin-like protein is an E-/L-selectin ligand on colon carcinoma cells: Comparative biochemical properties of selectin ligands in host and tumor cells. *Am. J. Physiol. Cell Physiol.* 296, C505–C513.

Thoumine, O., and Ott, A. (1997). Comparison of the mechanical properties of normal and transformed fibroblasts. *Biorheology* 34, 309–326.

Tozeren, A., Kleinman, H. K., Grant, D. S., Morales, D., Mercurio, A. M., and Byers, S. W. (1995). E-selectin-mediated dynamic interactions of breast- and colon-cancer cells with endothelial-cell monolayers. *Int. J. Cancer* 60, 426–431.

Varki, A. (1997). Selectin ligands: will the real ones please stand up? *J. Clin. Invest.* 99, 158–162.

Weiss, L., Orr, F. W., and Honn, K. V. (1988). Interactions of cancer cells with the microvasculature during metastasis. *FASEB J.* 2, 12–21.

Wenzel, C. T., Scher, R. L., and Richtsmeier, W. J. (1995). Adhesion of head and neck squamous cell carcinoma to endothelial cells. The missing links. *Arch. Otolaryngol. Head Neck Surg.* 121, 1279–1286.

Yap, B., and Kamm, R. D. (2005). Mechanical deformation of neutrophils into narrow channels induces pseudopod projection and changes in biomechanical properties. *J. Appl. Phys.* 98, 1930–1939.

Yu, H., Tay, C. Y., Leong, W. S., Tan, S. C., Liao, K., and Tan, L. P. (2010). Mechanical behavior of human mesenchymal stem cells during adipogenic and osteogenic differentiation. *Biochem. Biophys. Res. Commun.* 393, 150–155.

Yu, M., Stott, S., Toner, M., Maheswaran, S., and Haber, D. A. (2011). Circulating tumor cells: Approaches to isolation and characterization. *J. Cell. Biol.* 192, 373–382.

Zarbock, A., Ley, K., McEver, R. P., and Hidalgo, A. (2011). Leukocyte ligands for endothelial selectins: specialized glycoconjugates that mediate rolling and signaling under flow. *Blood* 118, 6743–6751.

Zeisberg, M., and Neilson, E. G. (2009). Biomarkers for epithelial-mesenchymal transitions. *J. Clin. Invest.* 119, 1429–1437.

Zen, K., Liu, D. Q., Guo, Y. L., Wang, C., Shan, J., Fang, M., Zhang, C. Y., and Liu, Y. (2008). CD44v4 is a major E-selectin ligand that mediates breast cancer cell transendothelial migration. *PLoS ONE* 3, e1826. doi: 10.1371/journal.pone.0001826

Zhu, C., and McEver, R. P. (2005). Catch bonds: physical models and biological functions. *Mol. Cell. Biomech.* 2, 91–104.

Conflict of Interest Statement: The authors declare that the research was conducted in the absence of any commercial or financial relationships that could be construed as a potential conflict of interest.

Received: 07 June 2012; paper pending published: 19 June 2012; accepted: 02 August 2012; published online: 20 August 2012.

Citation: Burdick MM, Henson KA, Delgadillo LF, Choi YE, Goetz DJ, Tees DFJ and Benencia F (2012) Expression of E-selectin ligands on circulating tumor cells: cross-regulation with cancer stem cell regulatory pathways? Front. Oncol. ***2****:103. doi: 10.3389/fonc.2012.00103*

This article was submitted to Frontiers in Cancer Molecular Targets and Therapeutics, a specialty of Frontiers in Oncology.

frontiers in ONCOLOGY

ORIGINAL RESEARCH ARTICLE
published: 18 September 2012
doi: 10.3389/fonc.2012.00111

Investigating dynamical deformations of tumor cells in circulation: predictions from a theoretical model

Katarzyna A. Rejniak*[1,2]

[1] *Integrated Mathematical Oncology, H. Lee Moffitt Cancer Center and Research Institute, Tampa, FL, USA*
[2] *Department of Oncologic Sciences, College of Medicine, University of South Florida, Tampa, FL, USA*

Edited by:
Michael R. King, Cornell University, USA

Reviewed by:
Paul Kenneth Newton, University of Southern California, USA
David Gee, Rochester Institute of Technology, USA

****Correspondence:***
Katarzyna A. Rejniak, Integrated Mathematical Oncology, H. Lee Moffitt Cancer Center and Research Institute, 12902 Magnolia Drive, SRB-4 24000G, Tampa, FL 33612, USA.
e-mail: kasia.rejniak@moffitt.org

It is inevitable for tumor cells to deal with various mechanical forces in order to move from primary to metastatic sites. In particular, the circulating tumor cells that have detached from the primary tumor and entered into the bloodstream need to survive in a completely new microenvironment. They must withstand hemodynamic forces and overcome the effects of fluid shear before they can leave the vascular system (extravasate) to establish new metastatic foci. One of the hypotheses of the tumor cell extravasation process is based on the so called "adhesion cascade" that was formulated and observed in the context of leukocytes circulating in the vascular system. During this process, the cell needs to switch between various locomotion strategies, from floating with the blood stream, to rolling on the endothelial wall, to tumor cell arrest and crawling, and finally tumor cell transmigration through the endothelial layer. The goal of this project is to use computational mechanical modeling to investigate the fundamental biophysical parameters of tumor cells in circulation. As a first step to build a robust *in silico* model, we consider a single cell exposed to the blood flow. We examine parameters related to structure of the actin network, cell nucleus and adhesion links between the tumor and endothelial cells that allow for successful transition between different transport modes of the adhesion cascade.

Keywords: circulating tumor cells, metastatic cascade, cell deformation, computational modeling, immersed boundary method

INTRODUCTION

The metastatic cascade is a multistep process in which cancer cells from the primary side (of the solid tumor) are relocated to the distant organs in which they grow to form new colonies. This process, called a metastatic cascade, consists of several steps during which cancer cells must first invade the stroma surrounding the primary tumor, intravasate, i.e., enter into the blood or lymphatic system, survive in the circulation, extravasate into the secondary site, invade the local matrix, and grow in the target organ (Chambers et al., 2002; Nguyen et al., 2009; Psaila and Lyden, 2009; Mina and Sledge, 2011).

The tumor cells in circulation (called the circulating tumor cells, CTCs) are exposed to various microenvironmental factors that are novel for the cells arising from the solid tumor mass. In order to survive, the cells must withstand hemodynamic forces and overcome the effects of fluid shear (Wirtz et al., 2011). In order to metastasize, the cells must leave the circulation system, and one of the extravasation hypotheses is the so called "adhesion cascade" that was formulated and observed in the context of circulating leukocytes (reviewed in Nourshargh et al., 2010). During this process, the tumor cell needs to switch between various locomotion strategies, from floating with the blood stream, to rolling on the endothelial wall (EW), to tumor cell arrest and crawling, and finally tumor cell transmigration through the endothelial layer (Nourshargh et al., 2010; Wirtz et al., 2011).

The recent advent of technical devices capturing the CTCs from patient's peripheral blood (Hsieh et al., 2006; Alunni-Fabbroni and Sandri, 2010; Farace et al., 2011; Kirby et al., 2012), allows the cancer biology community to gain enormous knowledge about the biology of CTCs and their correlations with clinical outcomes (Hou et al., 2010; Oakman et al., 2010; Swaby and Cristofanillli, 2011; Wendel et al., 2012). However, many aspects of CTC transport and extravasation processes are still unknown. In particular, the biophysical properties of CTCs that enable the completion of the adhesive cascade have not been investigated in detail, and many questions are still unanswered. How big are the CTCs? How deformable are they? Are the CTC's biophysical properties similar or distinct from the properties of the primary tumor cells and other cells in the circulation? Do these physical properties change over time? This provides a challenge from both biomechanical and therapeutical perspectives.

The goal of this project is to use mathematical modeling to investigate how cell deformability affects its translocation within the vascular duct under the blood flow, and how the physical properties of the cells change (globally or locally) when the cells switch their locomotion strategies. This will allow us to identify combinations of parameters that can be manipulated experimentally in order to disrupt some steps of the adhesive cascade.

MATERIALS AND METHODS

We use the *IBCell* mathematical framework (the Immersed Boundary model of a Cell; Rejniak, 2007a) to model a two-dimensional (2D) deformable tumor cell traveling through a microvessel. The cell is exposed to both hemodynamic forces exerted by the blood

plasma flow, and adhesive–repulsive forces between the tumor cell attaching to or migrating along the EW of the microvessel (**Figure 1**).

CTC STRUCTURE

The CTC structure is simplified to include two key elements defining cell shape and stiffness: the cell actin cortex and cell nuclear envelope. Both of these intracellular structures are modeled as dense networks of linear Hookean springs indicated by blue links C and gray links N in **Figure 1**, and mathematically defined by Eq. 5. The spring stiffness can be modified either globally (i.e., for each spring forming the nuclear envelope) or locally (i.e., for an individual actin filament in the cortex). This allows us to test their relative role in preserving the overall cell shape under the blood flow as well as in cell attachment and migration capabilities. The whole cell is interpenetrated by the viscous incompressible cytoplasm, but other intracellular elements (such as organelles, microtubules, intermediate filaments) are omitted for simplicity and to reduce computational costs. However, they can be incorporated in this model in a form of additional collections and/or networks of springs.

EW STRUCTURE

Similarly, the EW is modeled as a mesh of short and relatively stiff linear springs (shown as red links E in **Figure 1** and Eq. 5) that form a uniform rigid wall. For simplicity, no individual endothelial cells are included in the model, but in principle, they can be modeled in a similar fashion as CTCs.

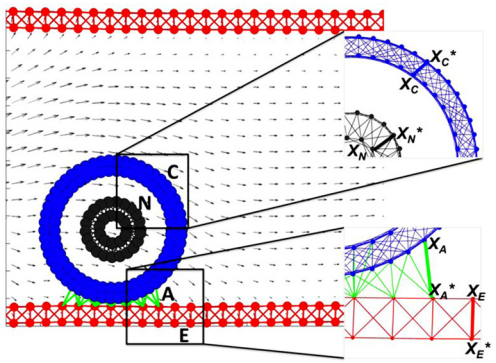

$$Eq1: \quad \rho\left(\frac{\partial \mathbf{u}(\mathbf{x},t)}{\partial t} + (\mathbf{u}(\mathbf{x},t)\cdot\nabla)\mathbf{u}(\mathbf{x},t)\right) = -\nabla p(\mathbf{x},t) + \mu\Delta\mathbf{u}(\mathbf{x},t) + \mathbf{f}^*(\mathbf{x},t),$$

$$Eq2: \quad \rho\nabla\cdot\mathbf{u}(\mathbf{x},t) = 0,$$

$$Eq3: \quad \mathbf{f}(\mathbf{x},t) = \int_{\Gamma_t\cup\Gamma_e} \mathbf{F}(l,t)\,\delta(\mathbf{x}-\mathbf{X}(l,t))\,dl,$$

$$Eq4: \quad \frac{\partial \mathbf{X}(l,t)}{\partial t} = \mathbf{u}(\mathbf{x},t) = \int_\Omega \mathbf{u}(\mathbf{x},t)\,\delta(\mathbf{x}-\mathbf{X}(l,t))\,d\mathbf{x},$$

$$Eq5: \quad \mathbf{F}(l,t) = \mathcal{S}\,\frac{\|\mathbf{X}(l,t)-\mathbf{X}^*(l,t)\|-\mathcal{L}}{\|\mathbf{X}(l,t)-\mathbf{X}^*(l,t)\|}\,(\mathbf{X}(l,t)-\mathbf{X}^*(l,t)), \quad \text{if} \quad \|\mathbf{X}(l,t)-\mathbf{X}^*(l,t)\| \le \mathcal{L}_{max}.$$

FIGURE 1 | Model schematics and equations. A schematic representation of the 2D model of the tumor cell in circulation. The blood vessel (red walls, E) is interpenetrated by a laminar flow (gray arrows representing blood velocity field) that interacts with a circulating tumor cell (CTC). The cell nucleus (gray, N) is surrounded by the cell cortex (blue, C) that both define cell shape and stiffness. The cell near the endothelial wall (EW) develops CTC–EW adhesive connections (green links, A). Insets show the magnification of a meshwork defining the nucleus and the cortex (top), and the network defining the EW and CTC–EW adhesive springs (bottom). Representative springs of the cortex, nucleus, endothelium, and adhesive CTC–EW links (X_C–X_C*, X_N–X_N*, X_A–X_A*, X_E–X_E*) are indicated by thick lines. Equations 1–5 define the mathematical frameworks of the Immersed Boundary method.

CTC–EW INTERACTIONS

The CTCs interact with EWs upon contact via the membrane receptors located on both the tumor cell and the endothelium. The proximity between CTC and EW results in the emergence of adhesive links that are modeled as short linear Hookean springs (indicated by green links A in **Figure 1** and Eq. 5). These adhesive links can be dynamically assembled and disassembled based on the distance between CTC's and EW's receptors, as well as adhesive spring stiffness. Since the main goal is to investigate cell deformability, we assume that receptor–ligand binding is always effective when the CTC–EW distance is small.

BLOOD PLASMA FLOW

We do not include the red blood cells or any other non-tumor cells and take into account only the fluid phase of the blood, i.e., the plasma. We model the blood plasma as a viscous incompressible Newtonian fluid governed by the Navier–Stokes equations (**Figure 1**, Eqs 1 and 2). We assume that the velocity of the plasma inside the microvessel has a parabolic profile with zero velocity at the microvessel walls. Thus, in the presence of no other obstacles inside the microvessel, the fluid flow is laminar. However, in the presence of the deformable tumor cells inside the duct, as well as adhesive interactions between the flowing cells and the endothelium, the plasma flow profile may be distorted. For simplicity, we neglect any changes that the plasma flow may have on the endothelium. However, we are aware that the blood flow can, for example, alter the expression of certain membrane receptors in the endothelial cells that in turn may modify the CTC–EW interactions.

IMMERSED BOUNDARY METHOD

Interactions between the CTCs, EWs, and the plasma flow are solved using the classical fluid–structure interaction approach, i.e., the immersed boundary method (Peskin, 2002 and Eqs 1–5 in **Figure 1**). In this system, Eq. 1 is the Navier–Stokes equation of a viscous incompressible fluid defined on the Cartesian grid $\boldsymbol{x} = (x_1, x_2)$, where p is the fluid pressure, μ is the fluid viscosity, ρ is the fluid density, $\boldsymbol{u}$ is the fluid velocity, and $\boldsymbol{f}$ is the external force density. Equation 2 is the law of mass balance. Interactions between the fluid and the material points $\mathbf{X}(l,t)$ on the tumor cell and the EW boundaries (l is an index along either the boundaries of the tumor cells Γ_t or the boundaries of the EWs Γ_e), are defined in Eqs 3 and 4. Here, the force density $\mathbf{F}(l,t)$ acting on the cell and wall boundaries is applied to the fluid using the 2D Dirac delta function δ, while all material boundary points $\mathbf{X}(l,t)$ are carried along with the fluid. The boundary forces $\mathbf{F}(l,t)$ arise from elastic properties of the tumor cell membranes, from rigid properties of the EWs and from CTC–EW adhesion, and are all represented by the short linear Hookean springs in Eq. 5, where S is the spring stiffness, L is the spring resting length, and $\mathbf{X}^*(l,t)$ is the adjacent, opposite, or neighboring point for the elastic, rigid, or adhesive forces, respectively (the pairs of connected boundary points in the endothelium,

the EW–CTC adhesion, the CTC nucleus, and cortex are indicated in **Figure 1** by wide red, green, gray, or blue segments, respectively). These equations are solved using the finite difference methods with a discrete approximation of the Dirac delta function and are described in detail in Rejniak (2007a) and Rejniak and Dillon (2007).

RESULTS

Individual tumor cells in circulation are exposed to the hemodynamic forces and fluid shear that the cells need to withstand in order to keep their physical integrity. The goal of this investigation is to determine the biomechanical properties of the CTCs (either persistent or dynamically changing during the course of CTC voyage through the vascular system) that allow the cells to survive in the blood stream and attach to the EW. First, we examine how the relative stiffness of the CTC cortex versus the stiffness of the CTC nuclear envelope controls CTC deformation under the blood flow (see CTC Survival in the Blood Flow). Next, we test how CTC cytoskeletal properties need to be modified in order to attach and roll on the EW (see CTC Rolling on the Endothelium). Finally, we examine how CTC cytoskeleton reorganization and cell membrane receptor redistribution enable CTC anchorage and migration on the endothelium (see CTC Anchorage to the EW). Since, we are concerned here with the fundamental biophysical parameters of a single deformable tumor cell only, the current model does not include other kinds of cells (such as red blood cells, leukocytes, platelets) that the CTC can collide with, or the formation and dynamics of multicellular emboli. These could be easily added to the model and will be considered in further research.

CTC SURVIVAL IN THE BLOOD FLOW

We consider a single tumor cell under the blood plasma flow in a small 30-micron-wide and 75-micron-long vessel. The fluid flow is assumed to have a parabolic profile with a maximal velocity of 0.6 mm/s in the center of the microvessel and 0 on the vessel walls. Initially, the cell is circular with a diameter of 10 microns, a 4-micron-wide nucleus, and a 2-micron-wide cortex band. We independently simulated two cases that varied only by initial cell location within the vessel, i.e., whether the cell was placed near the EW or at the middle of the microvessel. The latter cell was exposed to symmetrical hemodynamic forces, whereas the former cell was exposed to non-uniform blood shear stress with increasing blood velocity afar from the EW. We used computer simulations to trace how each cell is carried with the blood flow through the straight segment of the microvessel. Only two model parameters were varied: the stiffness constant of individual fibers forming the cell cortex and the stiffness constant of the cell nuclear envelope. The baseline value in each case was assumed to be 50 dyn/cm and was varied separately over the sixfold range. The final cell shapes after reaching 2/3 of the vessel length was recorded for comparison and overexposed on the same picture. A table showing final cell configurations for the whole range of stiffness constants is shown in **Figure 2**. Except for the case of a very stiff cortex (column 6 in **Figure 2**), when all cells retain their initial circular shapes, the cells located near the EW underwent significant deformations due to the non-uniform blood flow shear stress. However, when the stiffness of the cell cortex is fixed, the increasing stiffness of the cell nuclear envelope results in diminished deformation of the whole cell. This is the most visible in **Figure 2**, column 4, where the difference in the shape of the near-wall cell in the bottom row versus the top row changes from elliptical to circular. A very flexible cortex results in cell elongation that in extreme cases (**Figure 2**, column 1) may resemble cytoplasmic fragmentation (clasmatosis). Thus, actin cortex stiffness is crucial for cell survival during its passive transport by the blood flow, and a combination of soft cortex and soft nuclear envelope may lead to cell damage by the blood stream.

CTC ROLLING ON THE ENDOTHELIUM

Based on simulations from the previous section (**Figure 2**), we consider only these combinations of parameters for which the CTCs were able to survive under the blood flow, i.e., the stiffness values for both the cortex and the nucleus from the top-right quarter in **Figure 2**. The goal was to investigate which of these CTCs were able to attach to and roll on the endothelium wall. Four time snapshots from each simulation are shown in **Figures 3A–D**. Only in the case of a very stiff cortex (sixfold of the baseline, **Figures 3B,D**) the cell was able to roll over the endothelium wall (a fixed part of the cell cortex is stained to show its translocation along the cell perimeter). However, there is a difference in the speed of cell rolling, and a less stiff nucleus contributes to faster cell movement (**Figure 3B**). When both the cell cortex and the nucleus are softer, the cell deforms and is carried with the blood plasma flow (**Figure 3A**). In case of a stiff nucleus and a softer cortex, the cell was initially deformed and attached to the endothelium, but finally, its adhesive connections were broken, and the cell moved apart from the endothelium (**Figure 3C**). These simulations indicate that the transition in the CTC transport phase from floating with the blood flow to attaching and rolling on the EW requires stiffening of the whole CTC cortex. The uniformly flexible cell cytoskeleton prevents the tumor cell from its stable anchoring to the endothelium. In contrast, since the flexible cell becomes more easily elongated due to the blood shear stress, it is more likely that it will be shredded out of the surface in contact and returned to the blood stream. Increased CTC–EW adhesions have been tested but did not improve cell adhesion and rolling abilities (results not shown).

CTC ANCHORAGE TO THE EW

Simulations from the previous section (**Figure 3C**) showed that the cell with a relatively stiff nucleus and softer cortex was able to attach to the endothelium and migrate a short distance until it was detached by the flow. We tested the case in which the CTC–EW attachment resulted in further softening of the cell cortex around cell focal adhesions, but was unchanged elsewhere. Four snapshots taken over a 10t period (2.5 times longer than shown in **Figure 3C**) were overexposed on the same picture in **Figures 4A,B**. Dynamical changes in the cell cortex allow the cell to migrate successfully on the endothelium when simultaneously exposed to the blood plasma flow. Here, the cortex fibers were softened around the cell focal adhesions with the EW, and they became stiffer immediately after the focal adhesions were broken.

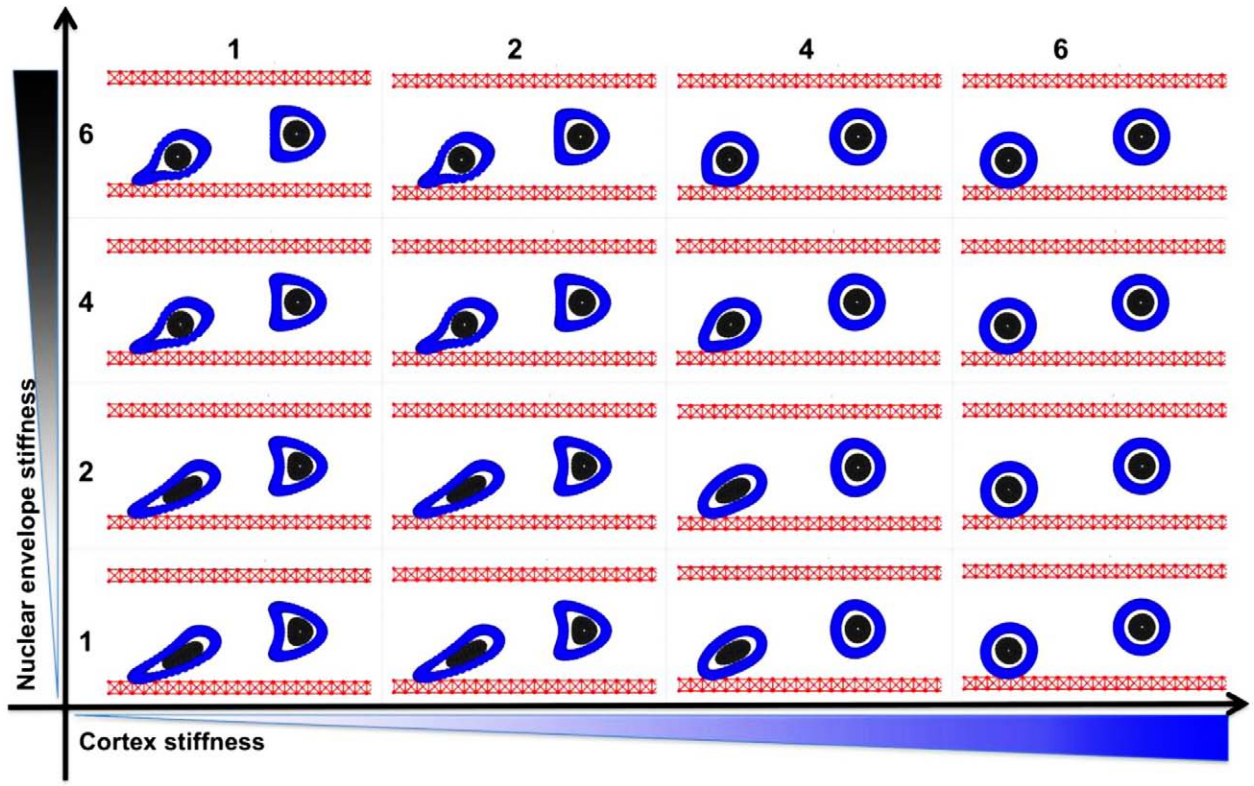

FIGURE 2 | Circulating tumor cell stiffness relationship. Circulating tumor cell deformation under steady blood flow in relation to the cell cortex versus cell nuclear envelope stiffness. Final configurations of two separately simulated cells that vary only by their location within the vessel (red) are overexposed on one picture. The cell cortex stiffness (blue) and cell nuclear envelope stiffness (gray) were varied by sixfold each.

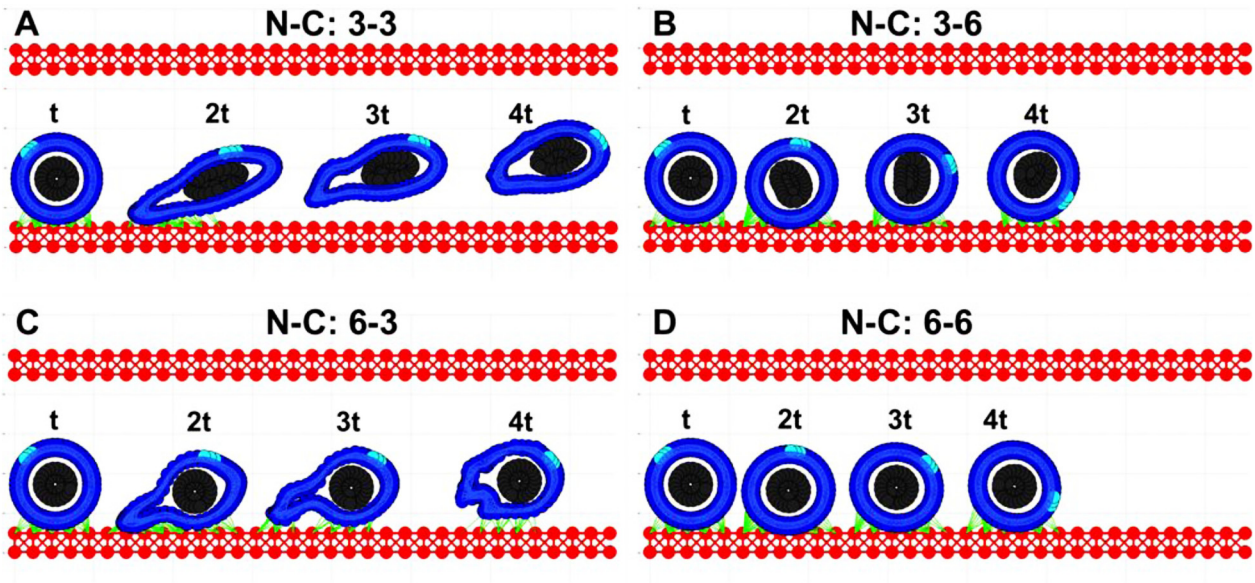

FIGURE 3 | Circulating tumor cell rolling on the endothelium. Each of the four cases **(A–D)** is characterized by a different cortex C and nucleus N stiffness value, however the strength of all adhesive bonds is fixed. The values are reported similarly as in **Figure 2**. **(A)** both the cortex and nucleus stiffness are 3-fold higher than the baseline; **(B)** the nucleus stiffness is 3-fold and cortex stiffness is 6-fold higher than the baseline; **(C)** nucleus 6-fold and cortex 3-fold; **(D)** both the nucleus and cortex stiffness is 6-fold higher than the baseline. For each case, four time snapshots (taken at time t, 2t, 3t, and 4t) are overexposed on the same picture for comparison of cell deformation and translocation in each case. A fixed small part of the cell cortex is stained for illustration of the rolling effect.

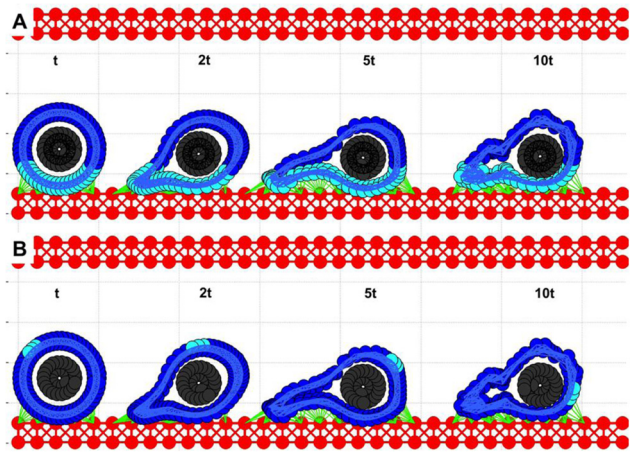

FIGURE 4 | Circulating tumor cell migrating on the endothelium. Four time snapshots (taken at time t, 2t, 5t, and 10t) are overexposed on the same picture for comparison of cell deformation and translocation. **(A)** The cell cortex is stained differently depending on its local stiffness: soft (cyan) close to cell focal adhesion with EW, and stiff (blue) far from EW contacts. **(B)** A fixed small part of the cell cortex is stained for illustration of the rolling effect.

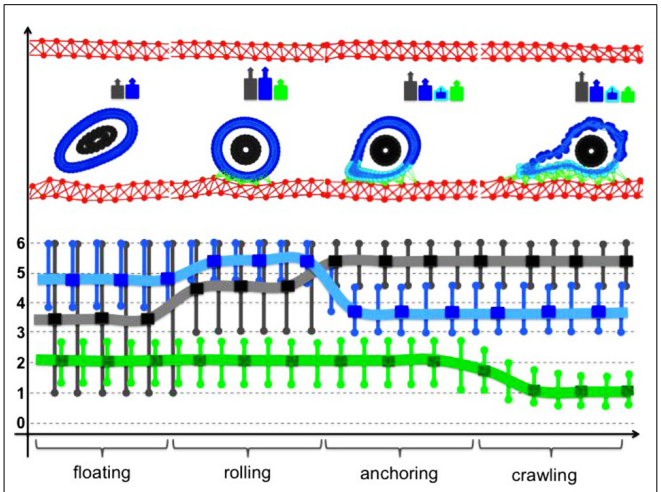

FIGURE 5 | Dynamical changes in the cell cytoskeleton during CTC intravenous transport. Each of the steps of the adhesive cascade requires different cytoskeletal properties of the CTC actin cortex stiffness (blue), cortex stiffness near the adhesion sites (cyan), stiffness of the CTC nuclear envelope (gray), and strength of the CTC–EW adhesion bonds (green). A typical cell configuration for each of the steps of the adhesive cascade is shown in the top row together with a color-coded cell stiffness signature. Lines represent the best continuous fit of the computational data.

All other cortex fibers remained stiff. The softer and stiffer parts of the cell cortex are stained differently in **Figure 4A**. The corresponding images in **Figure 4B** show translocation of a small fixed part of the cell cortex around the cell circumference. These simulations showed that transition from cell rolling, which requires a quite stiff cytoskeleton, to cell anchoring and crawling, in which the contact area between the CTCs and the EWs needs to increase gradually, demands alterations in the cell cortex stiffness. This local softening of the cell cytoskeleton along the contact area with the EW may be potentially modulated by signals from the endothelial cells in contact.

DYNAMICAL CHANGES IN THE CTC CYTOSKELETON DURING ITS INTRAVENOUS TRANSPORT

Simulations of the *IBCell* model revealed that in order for the CTC to progress from floating to rolling, to anchoring, and finally to crawling, the stiffness of its cytoskeleton needs to be modified differently in different cell compartments in a very dynamical way (**Figure 5**). Cell rolling requires quite a stiff actin cortex that can be pushed by the blood flow without extensive deformation. It also demands dynamical assembly–disassembly of CTC–EW adhesion bonds between the cell front and its back. Upon transition to anchoring, the CTC cytoskeleton must become more flexible along the contact surface. Too weak a cytoskeleton leads to cell elongation and its drift with the blood flow; too stiff a cytoskeleton will result in persistent cell rolling. Cell crawling requires weaker adhesive bonds and simultaneous changes in the CTC cytoskeletal stiffness: softening in the cell compartment in contact with the EWs, and stiffening in the cell compartment opposite to the contact surface. These complementary and dynamic changes in the CTC cytoskeletal properties enable the cell to complete the whole adhesive cascade.

DISCUSSION

Recent experimental studies (Fuhrmann et al., 2011; Swaminathan et al., 2011; Ketene et al., 2012) showed that normal, dysplastic, and metastatic cells (derived either from patient tumors or from cancer cell lines) exhibit a different degree of mechanical stiffness and cell deformability. The overarching conclusion is that even in the earliest stages of cancer development, the mechanical properties of the cells are altered. As cancer cells get progressively more invasive and metastatic, they display softer mechanical characteristics that result in larger cell deformations and more pronounced shape changes. There is also evidence of changes in the structural components of the nuclear envelope in various kinds of cancer cells (reviewed in Chow et al., 2012) that may result in altered mechanical properties of the cells. Numerous *in vivo* studies (Yamauchi et al., 2005; Stoletov et al., 2007, 2010) showed that metastatic tumor cells are quite deformable, and both the cell cytoplasm and cell nucleus can undergo strong compression and shape deformation in small capillaries. In particular, the length of cell nucleus can increase 1.6-fold, and the cell major axis 3.9-fold in comparison to the same cell kind in larger microvessels (Yamauchi et al., 2005). Moreover, the cells arrested at the capillary bifurcation points can stretch and extend their bodies in both directions (Figure 3, Yamauchi et al., 2005; Figure 2, Stoletov et al., 2010). A change in nuclear morphology is used as a criterion in the current pathological assessment of tumor grade and progression. Nuclear deformations are also observed during tumor cell migration, especially in confined microenvironments, which have been linked to altered rigidity of the cell nuclear envelope and changes in its fiber (laminins, actins, spectrins, titins) composition (Rowat et al., 2008; Friedl et al., 2011; Chow et al., 2012).

However, the precise mechanisms and extent of such deformations in the CTCs in the blood flow are not known. Despite the continuously increasing library of biomechanical assays and sophisticated bioengineering techniques for assessing various properties of cancer cells and their cytoskeleton (reviewed in Suresh, 2007), such precise measurements are difficult to carry in the fluid microenvironment. Most of the currently used methods for capturing CTCs require cell attachment or anchorage to the substrate. This may result in changes in the cytoskeletal properties of the cell in a way that subsequent measurements will not reflect cell properties in circulation. We propose here to use computational simulations to determine cell shape deformations that may be compared to morphologies of CTCs from *in vivo* or *in vitro* studies. This will provide a qualitative not quantitative comparison; nevertheless it may point to possible alterations in cell cytoskeleton stiffness.

The computational *IBCell* framework employed in this paper, has been previously established as a model of a deformable eukaryotic cell (Rejniak, 2007a), and it was used to investigate the formation of abnormal invaginations of the trophoblast tissue in the human placenta (Rejniak et al., 2004), the development of normal and aberrant morphologies of mammary epithelial acini (Rejniak and Anderson, 2008a,b; Rejniak et al., 2010), as well as various emerging patterns of invasive tumor colonies (Rejniak, 2005; Anderson et al., 2009). Here, we used it to model various forms of transport of an individual CTC through the microvessel and CTC–EW interactions. We considered a single cell with a deformable cortex and nucleus and tested parameters related to the actin network and cell nuclear envelope stiffness that allow for successful completion of the adhesion cascade steps. We did not address the kinetics of the receptor–ligand pair, since this mechanism has been extensively simulated by others, but mostly under the assumption that the cells were non-deformable solid spheres. Our goal was to investigate the complementary case. We assumed that cell-endothelium adhesion is effective, but that the cells are deformable. Thus, this model differs significantly from previously published models of cells in circulation. The individual deformable but nucleus-free red blood cells were modeled in (Pozrikidis, 2003, 2005) showing results similar to the soft nucleus cases consider in this paper. The large colonies of interacting red blood cells and platelets under the blood flow were modeled in (Zhang et al., 2009; Crowl and Fogelson, 2011; Zhao et al., 2012), where platelet's passive translocation within the cellular suspension of red blood cells was investigated. Adhesion and rolling of leukocytes on EWs was modeled in (King and Hammer, 2001; Migliorini et al., 2002; Eniola et al., 2003; Sun et al., 2003; Jadhav et al., 2005; Bose et al., 2010), where various mechanisms of receptor–ligand bond formation and hydrodynamic interactions between individual cells under the blood flow were investigated. However, these models have not addressed all the various modes of intercapillary cell translocation using one comprehensive modeling framework, as has been presented in this paper. Our work shows that the CTC cytoskeleton needs to be dynamically modified in a controlled way to enable the cell to pass through different modes of translocation (i.e., from floating to rolling, to anchoring, to crawling). In particular, the physical properties of the fibers forming the cell actin cortex need to be altered in response to both blood shear stress and adhesive contacts with the endothelium. In the case of cell rolling, we found out that the soft cells were not able to roll in contrast to the stiff cells (such as solid spheres). However, the cell cortex needed to be softened in order for the cell to anchor and crawl on the EW, a case that has not been modeled previously in this context. Such dynamical alterations in cell mechanical properties might be modulated by intercellular signaling and might be a subject of further experimental studies.

The model described in this paper is 2D, however, this computational framework can be easily extended to 3D (Peskin, 2002; Griffith et al., 2007; Rejniak, 2007b). In the 3D version, the cell cortex and nucleus can be discretized using a dense set of boundary points connected with short linear springs in the form of cross-linked fibers (**Figure 6**). Similar discretization can be used for the boundary of the vessel that together with stiff connecting springs will form a rigid wall (**Figure 6**). The CTC–EW adhesion links can be modeled using short springs like in the 2D case. The immersed boundary equations in both cases have a similar form (**Figures 1 and 6**). One advantage of the 3D model is the

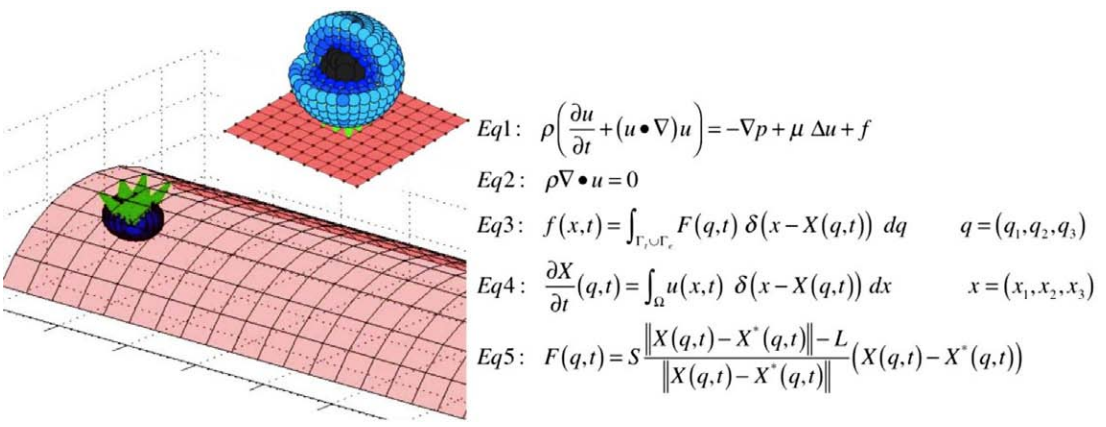

$$Eq1: \quad \rho\left(\frac{\partial u}{\partial t}+(u\bullet\nabla)u\right)=-\nabla p+\mu\,\Delta u+f$$

$$Eq2: \quad \rho\nabla\bullet u=0$$

$$Eq3: \quad f(x,t)=\int_{\Gamma_i\cup\Gamma_e}F(q,t)\,\delta\big(x-X(q,t)\big)\,dq \qquad q=(q_1,q_2,q_3)$$

$$Eq4: \quad \frac{\partial X}{\partial t}(q,t)=\int_{\Omega}u(x,t)\,\delta\big(x-X(q,t)\big)\,dx \qquad x=(x_1,x_2,x_3)$$

$$Eq5: \quad F(q,t)=S\frac{\big\|X(q,t)-X^*(q,t)\big\|-L}{\big\|X(q,t)-X^*(q,t)\big\|}\big(X(q,t)-X^*(q,t)\big)$$

FIGURE 6 | Three-dimensional model schematics and equations. A schematic representation of the structure of the 3D cell (left, top), the microvessel with a single attached cell (left, bottom), and model equations in three dimensions (right).

possibility of investigating blood vessels of different curvatures and sizes. A disadvantage is in the required computational power. The 3D model needs to be run with a very small time step to ensure the fluid dynamics code stability and convergence, and thus it will take much longer to complete full 3D computations. However, we do not expect that the 2D and 3D models will differ in their qualitative predictions.

Other extensions of the current model can include a comparison of cell deformations under blood flow of different velocities, and in vessels of different size, including small capillaries. We will also test cells of different nucleus-to-cytoplasm ratios, since it has been shown that CTC can vary significantly among each other (Marrinucci et al., 2010). Recent studies indicate that CTCs can form aggregates in the blood system that may also contain other circulating cells, such as leukocytes, macrophages, and platelets (Cho et al., 2012). We will investigate the dynamics of such emboli in the circulation, and whether the presence of other cells can increase the chance of CTC attachment to the EWs. Further experimental studies, out of the scope of our computational group, will be required to determine whether the cell physical properties observed using this computational approach can be manipulated experimentally to disrupt some steps of the adhesive cascade, and may be potentially used to develop the next generation of therapeutic interventions.

ACKNOWLEDGMENTS

We gratefully acknowledge the Physical Sciences-Oncology Program at the National Institute of Health for its support via the Moffitt-PSOC Center grant U54-CA-143970 Moffitt Pilot Project, and the PSOC Trans-Network Project.

REFERENCES

Alunni-Fabbroni, M., and Sandri, M. T. (2010). Circulating tumour cells in clinical practice: methods of detection and possible characterization. *Methods* 50, 289–297.

Anderson, A. R. A., Rejniak, K. A., Gerlee, P., and Quaranta, V. (2009). Microenvironment driven invasion: a multiscale multimodel investigation. *J. Math. Biol.* 58, 579–624.

Bose, S., Das, S. K., Karp, J. M., and Karnik, R. (2010). A semianalytical model to study the effect of cortical tension on cell rolling. *Biophys. J.* 99, 3870–3879.

Chambers, A. F., Groon, A. C., and MacDonald, I. C. (2002). Dissemination and growth of cancer cells in metastatic sites. *Nat. Rev. Cancer* 2, 563–572.

Cho, E. H., Wendel, M., Luttgen, M., Yoshioka, C., Marrinucci, D., Lazar, D., Schram, E., Nieva, J., Bazhenova, L., Morgan, A., Ko, A. H., Korn, W. M., Kolatkar, A., Bethel, K., and Kuhn, P. (2012). Characterization of circulating tumor cell aggregates identified in patients with epithelial tumors. *Phys. Biol.* 9, 016001.

Chow, K.-H., Factor, R. E., and Ullman, K. S. (2012). The nuclear envelope environment and its cancer connections. *Nat. Rev. Cancer* 12, 196–209.

Crowl, L., and Fogelson, A. L. (2011). Analysis of mechanisms for platelet near-wall excess under arterial blood flow conditions. *J. Fluid Mech.* 676, 348–375.

Eniola, O., Willcox, P. J., and Hammer, D. A. (2003). Interplay between rolling and firm adhesion elucidated with a cell-free system engineered with two distinct receptor–ligand pairs. *Biophys. J.* 85, 2720–2731.

Farace, F., Massard, C., Vimond, N., Drusch, F., Jacques, N., Billiot, F., Laplanche, A., Chauchereau, A., Lacroix, L., Planchard, D., Le Moulec, S., Andre, F., Fizazi, K., Soria, J. C., and Vielh, P. (2011). A direct comparison of cellSearch and ISET for circulating tumour-cell detection in patients with metastatic carcinomas. *Br. J. Cancer* 105, 847–853.

Friedl, P., Wolf, K., and Lammerding, J. (2011). Nuclear mechanics during cell migration. *Curr. Opin. Cell Biol.* 23, 55–64.

Fuhrmann, A., Staunton, J. R., Nandakumar, V., Banyai, N., Davies, P. C. W., and Ros, R. (2011). AFM stiffness nanotomography of normal, metaplastic and dysplastic human esophageal cells. *Phys. Biol.* 8, 015007.

Griffith, B. E., Hornung, R. D., McQueen, D. M., and Peskin, C. S. (2007). An adaptive, formally second order accurate version of the immersed boundary method. *J. Comput. Phys.* 223, 10–49.

Hou, J. M., Krebs, M., Ward, T., Morris, K., Sloane, R., Blackhall, F., and Dive, C. (2010). Circulating tumor cells, enumeration and beyond. *Cancers* 2, 1236–1250.

Hsieh, H. B., Marrinucci, D., Bethel, K., Curry, D. N., Humphrey, M., Krivacic, R. T., Kroener, J., Kroener, L., Ladanyi, A., Lazarus, N., Kuhn, P., Bruce, R. H., and Nieva, J. (2006). High speed detection of circulating tumor cells. *Biosens. Bioelectron.* 21, 1893–1899.

Jadhav, S., Eggleton, C. D., and Konstantopoulos, K. (2005). A 3-D computational model predicts that cell deformation affects selectin-mediated leukocyte rolling. *Biophys. J.* 88, 96–104.

Ketene, A. N., Schmelz, E. M., Roberts, P. C., and Agah, M. (2012). The effects of cancer progression on the viscoelasticity of ovarian cell cytoskeleton structures. *Nanomedicine* 8, 93–102.

King, M. R., and Hammer, D. A. (2001). Multiparticle adhesive dynamics: hydrodynamic recruitment of rolling leukocytes. *Proc. Natl. Acad. Sci. U.S.A.* 26, 14919–14924.

Kirby, B. J., Jodari, M., Loftus, M. S., Gakhar, G., Pratt, E. D., Chanel-Vos, C., Gleghorn, J. P., Santana, S. M., Liu, H., Smith, J. P., Navarro, V. N., Tagawa, S. T., Bander, N. H., Nanus, D. M., and Giannakakou, P. (2012). Functional characterization of circulating tumor cells with a prostate-cancer-specific microfluidic device. *PLoS ONE* 7, e35976. doi: 10.1371/journal.pone.0035976

Marrinucci, D., Bethel, K., Lazar, D., Fisher, J., Huynh, E., Clark, P., Bruce, R., Nieve, J., and Kuhn, P. (2010). Cytomorphology of circulating colorectal tumor cells: a small case series. *J. Oncol.* 2010, 1–7.

Migliorini, C., Qian, Y. C., Chen, H., Brown, E. B., Jain, R. K., and Munn, L. L. (2002). Red blood cells augment leukocyte rolling in a virtual blood vessel. *Biophys. J.* 83, 1834–1841.

Mina, L. A., and Sledge, G. W. Jr. (2011). Rethinking the metastatic cascade as a therapeutic target. *Nat. Rev. Clin. Oncol.* 8, 325–332.

Nguyen, D. X., Bos, P. D., and Massague, J. (2009). Metastasis: from dissemination to organ-specific colonization. *Nat. Rev. Cancer* 9, 274–284.

Nourshargh, S., Hordijk, P. L., and Sixt, M. (2010). Breaching multiple barriers: leukocyte motility through venular walls and interstitium. *Nat. Rev. Mol. Cell Biol.* 11, 366–378.

Oakman, C., Pestrin, M., Bessi, S., Galardi, F., and Di Leo, A. (2010). Significance of micrometastases: circulating tumor cells and disseminated tumor cells in early breast cancer. *Cancers* 2, 1221–1235.

Peskin, C. S. (2002). The immersed boundary method. *Acta Numer.* 11, 479–517.

Pozrikidis, C. (2003). *Modeling and Simulation of Capsules and Biological Cells. Mathematical Biology and Medicine Series.* Boca Raton: Chapman & Hall/CRC.

Pozrikidis, C. (2005). Numerical simulation of cell motion in tube flow. *Ann. Biomed. Eng.* 33 165–178.

Psaila, B., and Lyden, D. (2009). The metastatic niche: adapting the foreign soil. *Nat. Rev. Cancer* 8, 285–293.

Rejniak, K. A. (2005). A single-cell approach in modelling the dynamics of tumour microregions. *Math. Biosci. Eng.* 2, 643–655.

Rejniak, K. A. (2007a). An immersed boundary framework for modelling the growth of individual cells: an application to the early tumour development. *J. Theor. Biol.* 247, 186–204.

Rejniak, K. A. (2007b). Modelling the development of complex tissues using individual viscoelastic cells," in *Single-Cell-Based Models in Biology and Medicine*, eds A. Anderson, M. Chaplain, and K. A. Rejniak (Basel: Birkhäuser Verlag), 301–324.

Rejniak, K. A., and Anderson, A. R. A. (2008a). A computational study of the development of epithelial acini. I. Sufficient conditions for the formation of a hollow structure. *Bull. Math. Biol.* 70, 677–712.

Rejniak, K. A., and Anderson, A. R. A. (2008b). A computational study of the development of epithelial acini. II. Necessary conditions for structure and lumen stability. *Bull. Math. Biol.* 70, 1450–1479.

Rejniak, K. A., and Dillon, R. H. (2007). A single cell based model of the ductal tumor microarchitecture. *Comput. Math. Methods Med.* 8, 51–69.

Rejniak, K. A., Kliman, H. J., and Fauci, L. (2004). A computational model of the mechanics of growth of the villous trophoblast bilayer. *Bull. Math. Biol.* 66, 199–232.

Rejniak, K. A., Wang, S. E., Bryce, N. S., Chang, H., Parvin, B., Jourquin, J., Estrada, L., Gray, J. W., Arteaga, C. L., Weaver, A. M., Quaranta, V., and Anderson, A. R. A. (2010). Linking changes in epithelial morphogenesis to cancer mutations using computational modeling. *PLoS Comput. Biol.* 6, e1000900. doi: 10.1371/journal.pcbi.1000900

Rowat, A. C., Lammerding, J., Herrmann, H., and Aebi, U. (2008). Towards an integrated understanding of the structure and mechanics of the cell nucleus. *Bioessays* 30, 226–236.

Stoletov, K., Kato, H., Zardouzian, E., Kelber, J., Yang, J., Shattil, S., and Klemke, R. (2010). Visualizing extravasation dynamics of metastatic tumor cells. *J. Cell Biol.* 123, 2332–2341.

Stoletov, K., Montel, V., Lester, R. D., Gonias, S. L., and Klemke, R. (2007). High-resolution imaging of the dynamic tumor cell–vascular interface in transparent zebrafish. *Proc. Natl. Acad. Sci. U.S.A.* 104, 17406–17411.

Sun, C., Migliorini, C., and Munn, L. L. (2003). Red blood cells initiate leukocyte rolling in postcapillary expansions: a lattice Boltzmann analysis. *Biophys. J.* 85, 208–222.

Suresh, S. (2007). Biomechanics and biophysics of cancer cell. *Acta Biomater.* 3, 413–438.

Swaby, R. F., and Cristofanillli, M. (2011). Circulating tumor cells in breast cancer: a tool whose time has come of age. *BMC Med.* 9, 43, doi: 10.1186/1741-7015-9-43

Swaminathan, V., Mythreye, K., O'Brien, E. T., Berchuck, A., Blobe, G. C., and Superfine, R. (2011). Mechanical stiffness grades metastatic potential in patient tumor cells and in cancer cell lines. *Cancer Res.* 71, 5075–5080.

Wendel, M., Bazhenova, L., Boshuizen, R., Kolatkar, A., Honnatti, M., Cho, E. H., Marrinucci, D., Sandhu, A., Perricone, A., Thistlethwaite, P., Bethel, K., Nieva, J., van den Heuvel, M., and Kuhn, P. (2012). Fluid biopsy for circulating tumor cell identification in patients with early- and late-stage non-small cell lung cancer: a glimpse into lung cancer biology. *Phys. Biol.* 9, 016005.

Wirtz, D., Konstantopoulos, K., and Searson, P. C. (2011). The physics of cancer: the role of physical interactions and mechanical forces in metastasis. *Nat. Rev. Cancer* 11, 512–522.

Yamauchi, K., Yang, M., Jiang, P., Yamamoto, N., Xu, M., Amoh, Y., Tsuji, K., Bouvet, M., Tsuchiya, H., Tomita, K., Moossa, A. R., and Hoffman, R. M. (2005). Real-time in vivo dual-color imaging of intracapillary cancer cell and nucleus deformation and migration. *Cancer Res.* 65, 4246–4252.

Zhang, J., Johnson, P. C., and Popel, A. S. (2009). Effects of erythrocyte deformability and aggregation on the cell free layer and apparent viscosity of microscopic blood flows. *Microvasc. Res.* 77, 265–272.

Zhao, H., Shaqfeh, E. S. G., and Narsimhan, V. (2012). Shear-induced particle migration and margination in a cellular suspension. *Phys. Fluids* 24, 011902.

Conflict of Interest Statement: The author declares that the research was conducted in the absence of any commercial or financial relationships that could be construed as a potential conflict of interest.

Received: 04 June 2012; paper pending published: 20 June 2012; accepted: 15 August 2012; published online: 18 September 2012.

Citation: Rejniak KA (2012) Investigating dynamical deformations of tumor cells in circulation: predictions from a theoretical model. Front. Oncol. ***2****:111. doi: 10.3389/fonc.2012.00111*

This article was submitted to Frontiers in Cancer Molecular Targets and Therapeutics, a specialty of Frontiers in Oncology.

frontiers in ONCOLOGY

MINI REVIEW ARTICLE
published: 10 September 2012
doi: 10.3389/fonc.2012.00115

Do circulating tumor cells play a role in coagulation and thrombosis?

Garth W. Tormoen[1]*, Kristina M. Haley[2], Ross L. Levine[3] and Owen J. T. McCarty[1,4]

[1] Department of Biomedical Engineering, School of Medicine, Oregon Health & Science University, Portland, OR, USA
[2] Division of Pediatric Hematology/Oncology, Department of Pediatrics, Oregon Health & Science University, Portland, OR, USA
[3] Human Oncology and Pathogenesis Program, Memorial Sloan–Kettering Cancer Center, New York, NY, USA
[4] Department of Cell & Developmental Biology, School of Medicine, Oregon Health & Science University, Portland, OR, USA

Edited by:
Michael R. King, Cornell University, USA

Reviewed by:
Soldano Ferrone, University of Pittsburgh Cancer Institute, USA
Massimiliano Agostini, Medical Research Council, UK
Tara L. Beattie, University of Calgary, Canada

***Correspondence:**
Garth W. Tormoen, Department of Biomedical Engineering, School of Medicine, Oregon Health & Science University, 3303 South West Bond Avenue, Portland, OR 97239, USA.
e-mail: tormoeng@ohsu.edu

Cancer induces a hypercoagulable state, and patients with cancer who suffer a thrombotic event have a worse prognosis than those who do not. Recurrent pathologic thrombi in patients with cancer are clinically managed with anticoagulant medications; however, anticoagulant prophylaxis is not routinely prescribed owing to a complex variety of patient and diagnosis related factors. Early identification of patients at risk for cancer-associated thrombosis would allow for personalization of anticoagulant prophylaxis and likely reduce morbidity and mortality for many cancers. The environment in which a thrombosis develops in a patient with cancer is complex and unique from patients without cancer, which creates therapeutic challenges but may also provide targets for the development of clinical assays in this context. Circulating tumor cells (CTCs) may play a role in the association between cancer and thrombosis. Cancer metastasis, the leading cause of cancer-related deaths, is facilitated by the hematogenous spread of CTCs, and CTCs accompany metastatic disease across all major types of carcinomas. The role of CTCs in the pathogenesis of thrombosis has not been studied due to the previous difficulty in identifying these rare cells, but the interaction between these circulating cells and the coagulation system is an area of study that demands attention. The development of CTC detection platforms presents a new tool by which to characterize the role for CTCs in cancer-related hypercoagulability. In addition, this area of study presents a new avenue for assessing the risk of cancer-associated thrombosis and represents a potential tool for predicting which patients may benefit from anticoagulant prophylaxis. In this review, we will discuss the evidence in support of CTC induced hypercoagulability, and highlight areas where CTC-detection platforms may provide prognostic insight into the risk of developing thrombosis for patients with cancer.

Keywords: circulating tumor cells, thrombosis, tissue factor, metastasis, blood

INTRODUCTION

Cancer is a hypercoagulable state, and the association of venous thrombosis with cancer has been observed for centuries (Trousseau, 1865). Thrombosis is a significant contributor to morbidity and mortality in cancer patients. Patients with cancer who suffer a thrombosis as a part of their disease endure worse outcomes (Sorensen et al., 2000). Despite the well established link between cancer and venous thrombosis, anticoagulation is not routine care for these patients (Akl et al., 2011a,b). This is due in part to the increased bleeding risk associated with anticoagulation in a population where only a fraction of patients develop symptomatic thrombosis, and the risks of anticoagulation therapy in patients treated with systemic chemotherapy and with disease and/or therapy related thrombocytopenia. No clinical marker has been developed which is capable of predicting in which patients the benefit of anticoagulation outweighs the increased risk of bleeding.

The underlying cause of thrombosis in cancer is multifactorial, including but not limited to, personal and family history of thrombosis, pre-treatment fibrinogen and platelet levels, immobility and fatigue, the increased use of indwelling catheters, and the administration of certain chemotherapeutics and other anti-cancer therapies which increase thrombotic risk (Dimopoulos and Eleutherakis-Papaiakovou, 2004; Elice et al., 2009). However, thrombosis can also herald the diagnosis of cancer, preceding any cancer-related symptoms or treatments. This, in itself, underlines the role for cancer in disrupting the normal physiological balance of the hemostatic system. The incidence of thrombosis in cancer is strongly tied to cancer subtype and origin, suggesting that cancer cells directly contribute to the hypercoagulable state associated with cancer (i.e., adenocarcinoma vs. carcinoma or colon vs. breast; Baron et al., 1998; Sorensen et al., 1998; Rickles and Levine, 2001; Blom et al., 2004). A multifactorial model to estimate risk of thrombosis in patients receiving chemotherapy has been validated which includes the cancer site, factors such as platelet and leukocyte count, and hemoglobin level or the use of erythropoiesis-stimulating agents, and body mass index to stratify patients by risk to develop thrombosis. However, the majority of patients predicted to have the highest risk of developing thrombosis in this model do not subsequently suffer from thrombosis

(Khorana et al., 2008). Therefore, efforts to identify patients with cancer who will develop venous thrombosis need to achieve better specificity by including additional factors, such as circulating tumor cell (CTC) count, which may have a role in developing cancer-related thrombosis.

CTC–BLOOD PROTEIN INTERACTIONS

Tissue factor (TF) is the physiological initiator of coagulation and is essential for hemostasis. TF is a transmembrane glycoprotein and requires phospholipids in order to be procoagulant (Nemerson, 1968). TF-expressing cells are not typically exposed to the blood. Only upon injury, when the architecture of the blood vessel is disrupted, does the blood gain exposure to extravascular TF-expressing cells. Therefore, in hemostasis, the activation of coagulation is essentially localized to sites of hemorrhage.

In the context of metastatic cancer, CTCs intravasate into the vasculature in order to reach distant locations and establish metastatic foci. CTCs accompany metastatic disease across all major types of carcinomas (Allard et al., 2004). Tumors have been shown to express TF *in vivo*, and TF expression has been shown to correlate with metastatic potential (Zacharski et al., 1983, 1986; Lee et al., 2011; Liu et al., 2011; Ma et al., 2011; Tian et al., 2011; Xu et al., 2011; Gil-Bernabe et al., 2012). Therefore, the process of hematogenous metastasis may present TF-expressing tumor cells to blood in the absence of a blood vessel injury. Whether metastasizing cancer cells are involved in the development of thrombosis has not been established. *In vitro*, cancer cells added to blood or plasma promote coagulation in a TF- and phosphatidylserine (PS)-dependent manner, and the coagulation kinetics are strongly dependent upon the number of cancer cells tested (Berny-Lang et al., 2011; Tormoen et al., 2011; Yates et al., 2011; Welsh et al., 2012). However, extrapolation of *in vitro* coagulation assays to *in vivo* phenomenon is not straightforward. Cancer cell lines may not reproduce CTC procoagulant phenotypes, and extrapolation of *in vitro* coagulation kinetics to physiological scenarios is complicated by dynamic physiological environments seen *in vivo*. Along these lines, blood flow is a strong determinant of procoagulant activity (Gemmell et al., 1988), yet a metastasizing cancer cell has dynamic temporal and spatial relationships with the blood which are unique from TF-bearing cells exposed at the site of a blood vessel injury. For instance, an intravasating or extravasating tumor cell is stationary relative to the blood flow, and thereby would experience rapid changes in coagulation kinetics due to the blood flow-mediated transport of coagulation factors to the stationary cell. In contrast, CTCs in the bloodstream experience very little relative blood flow, as these cells are transported by viscous forces within the flowing blood. The resulting coagulation kinetics for CTCs is therefore reliant upon diffusion of coagulation factors to/from the cell surface; thus the coagulation kinetics for CTCs is diffusion-limited.

The extent to which spatial and temporal relationships affect procoagulant activity of CTCs is a topic of recent investigation. In this issue, Lee et al. (2011) model the generation and coalescence of thrombin by procoagulant CTCs within the circulation and predict local thrombin concentration gradients surrounding the CTCs to have complex relationships with cell counts and distributions within the vasculature. This work suggests that procoagulant CTC counts strongly determine local thrombin concentrations, which would likely be prognostic for risk of developing thrombosis.

Cell-mediated coagulation requires the binding of coagulation factors from solution, followed by the assembly of enzyme complexes on the cell surface. This assembly is facilitated by the exposure of PS. The exposure of PS and subsequent assembly of enzyme complexes on the cell surface may be rate-limiting for the cell's procoagulant activity. *In vitro*, the procoagulant activity of several cancer cell lines has been shown to correlate with the extent of PS exposure, more so than the relative expression of TF, supporting the notion that facilitation of enzyme complex assembly is the rate determining mechanism for cancer cell-mediated coagulation (Barrowcliffe et al., 2002; Pickering et al., 2004). Further, space limitations of the PS-regions can severely reduce coagulation kinetics, indicating a role for quantification of procoagulant surface area to assess the procoagulant activity of a cell (Haynes et al., 2012). This limitation suggests that the procoagulant phenotype of CTCs may be dependent upon the physical parameters (size and surface area) of CTCs. In this issue, Phillips et al. (2012a,b) demonstrate methods to utilize light microscopy to quantify the physical parameters of volume, mass, surface area, and density of CTCs, providing a novel technique to assess CTC heterogeneity in cancer-associated hypercoagulability.

Characterizing the role for procoagulant CTCs to initiate coagulation requires a method to functionally probe the ability of CTC to mediate coagulation. Surface expression of TF could be determined through immunofluorescent labeling methods, but these approaches do not capture the activity of TF. The ability of TF to initiate coagulation is dependent upon the cell membrane environment, specifically the exposure of PS, as well as an "active" or "decrypted" form of TF in order to facilitate coagulation. In this issue, Tormoen et al. (2012) describe an approach utilizing fluorescently labeled coagulation factors to characterize the procoagulant nature of CTCs. This approach has potential to functionally characterize the ability of CTCs to bind coagulation factors, which is crucial for their ability to facilitate coagulation. This functional labeling lends itself to current CTC detection platforms (Krivacic et al., 2004; Hsieh et al., 2006), providing a novel method with which CTC platforms can provide novel insight into cancer-related thrombosis.

CTC–PLATELET INTERACTIONS

It has been shown that platelets, the primary mediators of hemostasis, play a key a role in mediating hematogenous metastasis (Gasic et al., 1968, 1973). *In vitro*, tumor cells bind platelets under shear stress (McCarty et al., 2000, 2002) and cause platelet aggregation, and this ability correlates with metastatic potential *in vivo* (Karpatkin et al., 1988; Amirkhosravi et al., 2003; Palumbo et al., 2005; Erpenbeck et al., 2010). The mechanisms by which platelet interactions confer metastatic potential upon CTCs are complex. Platelets can deter NK cell destruction of CTCs in the blood (Karpatkin et al., 1988; Im et al., 2004; Kopp et al., 2009). Releasates from activated platelets include growth factors such as platelet-derived growth factor, vascular endothelial growth factor, and transforming growth factor beta, and may support tumor growth and may promote the establishment of metastatic tumor

sites (Kepner and Lipton, 1981; Assoian et al., 1983; Mohle et al., 1997; Nierodzik and Karpatkin, 2006). Recently, a murine model of superficial venous thrombophlebitis, a specific clinical presentation of thrombosis that can be associated with mucinous tumors, was shown to depend upon platelet activation (Shao et al., 2011). However, the role for platelet–CTC interactions for venous thrombosis has not been established in different cancer-related contexts.

LEUKEMIA CELL–BLOOD PROTEIN INTERACTIONS

While the extreme rarity of CTCs in human solid tumors has prevented their characterization, leukemias, which are composed of circulating cancer cells, or "liquid tumors," supply vast numbers of cancer cells to the bloodstream, making their isolation straightforward. Thrombosis is commonly seen with specific leukemia subtypes, and surface expression of TF has been identified on some leukemic cells associated with coagulopathy (De Stefano et al., 2005; Falanga et al., 2008; Liu et al., 2008; Falanga and Marchetti, 2009; Ku et al., 2009; Musil and Krc, 2010). However, converse to solid tumors and certain leukemia subtypes, hemorrhage is more common in most acute leukemias as compared to thrombosis (Barbui et al., 1998; Barbui and Falanga, 2001; Falanga and Barbui, 2001; Falanga and Rickles, 2003). Suggested mechanisms by which leukemias induce hemorrhage include bone marrow crowding and suppression of platelet production leading to thrombocytopenia. Acute myelogenous leukemia French-American-British subtype M3 or acute promyelocytic leukemia (APL), is known to surface-express TF as well as Annexin II (Menell et al., 1999), and is associated with the highest risk of thrombosis and bleeding amongst all leukemia subtypes. TF activity has been demonstrated from APL cells *in vitro*, suggesting that these cells are procoagulant. However, rather than developing focal thromboses, patients with APL present with a diffuse coagulopathy that consumes the coagulation factors within the blood leaving the patient unable to maintain hemostasis, resulting in a hemorrhagic phenotype. The surface expression of Annexin II has been shown to correlate with incidence of hemorrhage, and an Annexin II-mediated binding of tissue type plasminogen activator has been demonstrated *in vitro* (Menell et al., 1999). Therefore, in certain conditions, leukemia cells may initiate and propagate coagulation, while simultaneously facilitating anticoagulation, with the net coagulant effect resulting in consumption of coagulation factors until the patient is severely deficient and deposed toward clinically severe hemorrhage.

SUMMARY

Metastasizing CTCs must survive the blood circulation, and the role that blood protein and blood cell interactions with CTCs plays in the progression of metastatic disease in human cancers remains ill-defined. The association between cancer and thrombosis suggests that the circulation is not inert toward CTCs, however the characterization of human CTC and blood interactions has been hampered by the technical difficulty in isolating and analyzing these rare cells. The emergence of clinical CTC detection platforms in recent years has opened the possibility to characterize the role that CTCs play in metastatic disease. One of the challenges facing researchers in this field is how to functionally characterize CTCs within the technical constraints that current CTC detection platforms require. This special edition of Frontiers in Oncology describes several methods with which CTCs are biophysically characterized using light microscopy techniques (see Phillips et al., 2012a,b). The development of CTC detection platforms to probe procoagulant properties of these cells presents new opportunities for investigators to understand the relationship between CTCs and blood proteins and/or blood cells. This theme is explored in Tormoen et al. (2012). Finally, understanding the complex environment that CTCs within the blood circulation traverse, and the effects that this environment has on the procoagulant phenotype of CTCs is addressed in Lee et al. (2012). The therapeutic targeting of CTCs may provide new insight into metastatic disease, including methods to interrogate the procoagulant nature of CTCs and understand how these relationships impact cancer progression and cancer-related morbidities and the response to antithrombotic therapies.

ACKNOWLEDGMENTS

This research was supported in part by the OHSU Knight Cancer Institute (Owen J. T. McCarty), the American Heart Association (12PRE11930019 to Garth W. Tormoen), and the NIH (R01HL101972 and U54CA143906 to Owen J. T. McCarty, U54CA143798 to Ross L. Levine, T32-CA106195 to Garth W. Tormoen). Kristina M. Haley is a Medical Research Foundation Early Career Investigator. Garth W. Tormoen is an Achievement Rewards for College Scientists scholar.

REFERENCES

Akl, E. A., Labedi, N., Barba, M., Terrenato, I., Sperati, F., Muti, P., and Schünemann, H. (2011a). Anticoagulation for the long-term treatment of venous thromboembolism in patients with cancer. *Cochrane Database Syst. Rev.* 6, CD006650.

Akl, E. A., Vasireddi, S. R., Gunukula, S., Yosuico, V. E., Barba, M., Terrenato, I., Sperati, F., and Schünemann, H. (2011b). Oral anticoagulation in patients with cancer who have no therapeutic or prophylactic indication for anticoagulation. *Cochrane Database Syst. Rev.* 12, CD006466.

Allard, W. J., Matera, J., Repollet, M., Connelly, M. C., Rao, C., Tibbe, A. G., Uhr, J. W., and Terstappen, L. W. (2004). Tumor cells circulate in the peripheral blood of all major carcinomas but not in healthy subjects or patients with nonmalignant diseases. *Clin. Cancer Res.* 10, 6897–6904.

Amirkhosravi, A., Mousa, S. A., Amaya, M., Blaydes, S., Desai, H., Meyer, T., and Francis, J. L. (2003). Inhibition of tumor cell-induced platelet aggregation and lung metastasis by the oral GpIIb/IIIa antagonist XV454. *Thromb. Haemost.* 90, 549–554.

Assoian, R. K., Komoriya, A., Meyers, C. A., Miller, D. M., and Sporn, M. B. (1983). Transforming growth factor-beta in human platelets. Identification of a major storage site, purification, and characterization. *J. Biol. Chem.* 258, 7155–7160.

Barbui, T., and Falanga, A. (2001). Disseminated intravascular coagulation in acute leukemia. *Semin. Thromb. Hemost.* 27, 593–604.

Barbui, T., Finazzi, G., and Falanga, A. (1998). The impact of all-*trans*-retinoic acid on the coagulopathy of acute promyelocytic leukemia. *Blood* 91, 3093–3102.

Baron, J. A., Gridley, G., Weiderpass, E., Nyrén, O., and Linet, M. (1998). Venous thromboembolism and cancer. *Lancet* 351, 1077–1080.

Barrowcliffe, T. W., Fabregas, P., Jardi, M., Cancelas, J., Rabaneda, M., and Felez, J. (2002). Procoagulant activity of T lymphoblastoid cells due to exposure of negatively charged phospholipid. *Thromb. Haemost.* 87, 442–449.

Berny-Lang, M. A., Aslan, J. E., Tormoen, G. W., Patel, I. A., Bock, P. E., Gruber, A., and McCarty, O. J. (2011). Promotion of experimental thrombus formation by the procoagulant activity of breast cancer cells. *Phys. Biol.* 8, 015014.

Blom, J. W., Osanto, S., and Rosendaal, F. R. (2004). The risk of a venous thrombotic event in lung cancer patients: higher risk for adenocarcinoma than squamous cell carcinoma. *J. Thromb. Haemost.* 2, 1760–1765.

De Stefano, V., Sora, F., Rossi, E., Chiusolo, P., Laurenti, L., Fianchi, L., Zini, G., Pagano, L., Sica, S., and Leone, G. (2005). The risk of thrombosis in patients with acute leukemia: occurrence of thrombosis at diagnosis and during treatment. *J. Thromb. Haemost.* 3, 1985–1992.

Dimopoulos, M. A., and Eleutherakis-Papaiakovou, V. (2004). Adverse effects of thalidomide administration in patients with neoplastic diseases. *Am. J. Med.* 117, 508–515.

Elice, F., Rodeghiero, F., Falanga, A., and Rickles, F. R. (2009). Thrombosis associated with angiogenesis inhibitors. *Best Pract. Res. Clin. Haematol.* 22, 115–128.

Erpenbeck, L., Nieswandt, B., Schön, M., Pozgajova, M., and Schön, M. P. (2010). Inhibition of platelet GPIb alpha and promotion of melanoma metastasis. *J. Invest. Dermatol.* 130, 576–586.

Falanga, A., and Barbui, T. (2001). Coagulopathy of acute promyelocytic leukemia. *Acta Haematol.* 106, 43–51.

Falanga, A., Barbui, T., and Rickles, F. R. (2008). Hypercoagulability and tissue factor gene upregulation in hematologic malignancies. *Semin. Thromb. Hemost.* 34, 204–210.

Falanga, A., and Marchetti, M. (2009). Venous thromboembolism in the hematologic malignancies. *J. Clin. Oncol.* 27, 4848–4857.

Falanga, A., and Rickles, F. R. (2003). Pathogenesis and management of the bleeding diathesis in acute promyelocytic leukaemia. *Best Pract. Res. Clin. Haematol.* 16, 463–482.

Gasic, G. J., Gasic, T. B., Galanti, N., Johnson, T., and Murphy, S. (1973). Platelet–tumor-cell interactions in mice. The role of platelets in the spread of malignant disease. *Int. J. Cancer* 11, 704–718.

Gasic, G. J., Gasic, T. B., and Stewart, C. C. (1968). Antimetastatic effects associated with platelet reduction. *Proc. Natl. Acad. Sci. U.S.A.* 61, 46–52.

Gemmell, C. H., Turitto, V. T., and Nemerson, Y. (1988). Flow as a regulator of the activation of factor X by tissue factor. *Blood* 72, 1404–1406.

Gil-Bernabe, A. M., Ferjancic, S., Tlalka, M., Zhao, L., Allen, P. D., Im, J. H., Watson, K., Hill, S. A., Amirkhosravi, A., Francis, J. L., Pollard, J. W., Ruf, W., and Muschel, R. J. (2012). Recruitment of monocytes/macrophages by tissue factor-mediated coagulation is essential for metastatic cell survival and premetastatic niche establishment in mice. *Blood* 119, 3164–3175.

Haynes, L. M., Dubief, Y. C., and Mann, K. G. (2012). Membrane binding events in the initiation and propagation phases of tissue factor-initiated zymogen activation under flow. *J. Biol. Chem.* 287, 5225–5234.

Hsieh, H. B., Marrinucci, D., Bethel, K., Curry, D. N., Humphrey, M., Krivacic, R. T., Kroener, J., Kroener, L., Ladanyi, A., Lazarus, N., Kuhn, P., Bruce, R. H., and Nieva, J. (2006). High speed detection of circulating tumor cells. *Biosens. Bioelectron.* 21, 1893–1899.

Im, J. H., Fu, W., Wang, H., Bhatia, S. K., Hammer, D. A., Kowalska, M. A., and Muschel, R. J. (2004). Coagulation facilitates tumor cell spreading in the pulmonary vasculature during early metastatic colony formation. *Cancer Res.* 64, 8613–8619.

Karpatkin, S., Pearlstein, E., Ambrogio, C., and Coller, B. S. (1988). Role of adhesive proteins in platelet tumor interaction in vitro and metastasis formation in vivo. *J. Clin. Invest.* 81, 1012–1019.

Kepner, N., and Lipton, A. (1981). A mitogenic factor for transformed fibroblasts from human platelets. *Cancer Res.* 41, 430–432.

Khorana, A. A., Kuderer, N. M., Culakova, E., Lyman, G. H., and Francis, C. W. (2008). Development and validation of a predictive model for chemotherapy-associated thrombosis. *Blood* 111, 4902–4907.

Kopp, H. G., Placke, T., and Salih, H. R. (2009). Platelet-derived transforming growth factor-beta down-regulates NKG2D thereby inhibiting natural killer cell antitumor reactivity. *Cancer Res.* 69, 7775–7783.

Krivacic, R. T., Ladanyi, A., Curry, D. N., Hsieh, H. B., Kuhn, P., Bergsrud, D. E., Kepros, J. F., Barbera, T., Ho, M. Y., Chen, L. B., Lerner, R. A., and Bruce, R. H. (2004). A rare-cell detector for cancer. *Proc. Natl. Acad. Sci. U.S.A.* 101, 10501–10504.

Ku, G. H., White, R. H., Chew, H. K., Harvey, D. J., Zhou, H., and Wun, T. (2009). Venous thromboembolism in patients with acute leukemia: incidence, risk factors, and effect on survival. *Blood* 113, 3911–3917.

Lee, A., Tormoen, G. W., Kanso, E., McCarty, O. J., and Newton, P. K. (2012). Modeling and simulation of procoagulant circulating tumor cells in flow. *Front. Oncol.* 2:108. doi: 10.3389/fonc.2012.00108

Lee, B. J., Kim, J. H., Woo, S. H., Kim, J. H., Kim, D. H., and Yu, Y. S. (2011). Tissue factor is involved in retinoblastoma cell proliferation via both the Akt and extracellular signal-regulated kinase pathways. *Oncol. Rep.* 26, 665–670.

Liu, Y., Chao, X., Gu, W., Hua, X., and Xu, N. (2008). Acute thrombosis in superior mesenteric artery as first symptom in a AML patient. *Int. J. Gen. Med.* 1, 7–9.

Liu, Y., Jiang, P., Capkova, K., Xue, D., Ye, L., Sinha, S. C., Mackman, N., Janda, K. D., and Liu, C. (2011). Tissue factor-activated coagulation cascade in the tumor microenvironment is critical for tumor progression and an effective target for therapy. *Cancer Res.* 71, 6492–6502.

Ma, Z., Zhang, T., Wang, R., Cheng, Z., Xu, H., Li, W., Wang, Y., and Wang, X. (2011). Tissue factor-factor VIIa complex induces epithelial ovarian cancer cell invasion and metastasis through a monocytes-dependent mechanism. *Int. J. Gynecol. Cancer* 21, 616–624.

McCarty, O. J., Jadhav, S., Burdick, M. M., Bell, W. R., and Konstantopoulos, K. (2002). Fluid shear regulates the kinetics and molecular mechanisms of activation-dependent platelet binding to colon carcinoma cells. *Biophys. J.* 83, 836–848.

McCarty, O. J., Mousa, S. A., Bray, P. F., and Konstantopoulos, K. (2000). Immobilized platelets support human colon carcinoma cell tethering, rolling, and firm adhesion under dynamic flow conditions. *Blood* 96, 1789–1797.

Menell, J. S., Cesarman, G. M., Jacovina, A. T., McLaughlin, M. A., Lev, E. A., and Hajjar, K. A. (1999). Annexin II and bleeding in acute promyelocytic leukemia. *N. Engl. J. Med.* 340, 994–1004.

Mohle, R., Green, D., Moore, M. A., Nachman, R. L., and Rafii, S. (1997). Constitutive production and thrombin-induced release of vascular endothelial growth factor by human megakaryocytes and platelets. *Proc. Natl. Acad. Sci. U.S.A.* 94, 663–668.

Musil, D., and Krc, I. (2010). Migrating venous thrombosis in acute leukemia. *Blood Coagul. Fibrinolysis* 21, 365–367.

Nemerson, Y. (1968). The phospholipid requirement of tissue factor in blood coagulation. *J. Clin. Invest.* 47, 72–80.

Nierodzik, M. L., and Karpatkin, S. (2006). Thrombin induces tumor growth, metastasis, and angiogenesis: evidence for a thrombin-regulated dormant tumor phenotype. *Cancer Cell* 10, 355–362.

Palumbo, J. S., Talmage, K. E., Massari, J. V., La Jeunesse, C. M., Flick, M. J., Kombrinck, K. W., Jirousková, M., and Degen, J. L. (2005). Platelets and fibrin(ogen) increase metastatic potential by impeding natural killer cell-mediated elimination of tumor cells. *Blood* 105, 178–185.

Phillips, K. G., Kolatkar, A., Rees, K. J., Rigg, R., Marrinucci, D., Luttgen, M., Bethel, K., Kuhn, P., and McCarty, O. J. (2012a). Quantification of cellular volume and sub-cellular density fluctuations: comparison of normal peripheral blood cells and circulating tumor cells identified in a breast cancer patient. *Front. Oncol.* 2:96. doi: 10.3389/fonc.2012.00096

Phillips, K. G., Velasco, C. R., Li, J., Kolatkar, A., Luttgen, M., Bethel, K., Duggan, B., Kuhn, P., and McCarty, O. J. (2012b). Optical quantification of cellular mass, volume, and density of circulating tumor cells identified in an ovarian cancer patient. *Front. Oncol.* 2:72. doi: 10.3389/fonc.2012.00072

Pickering, W., Gray, E., Goodall, A. H., Ran, S., Thorpe, P. E., and Barrowcliffe, T. W. (2004). Characterization of the cell-surface procoagulant activity of T-lymphoblastoid cell lines. *J. Thromb. Haemost.* 2, 459–467.

Rickles, F. R., and Levine, M. N. (2001). Epidemiology of thrombosis in cancer. *Acta Haematol.* 106, 6–12.

Shao, B., Wahrenbrock, M. G., Yao, L., David, T., Coughlin, S. R., Xia, L., Varki, A., and McEver, R. P. (2011). Carcinoma mucins trigger reciprocal activation of platelets and neutrophils in a murine model of Trousseau syndrome. *Blood* 118, 4015–4023.

Sorensen, H. T., Mellemkjaer, L., Olsen, J. H., and Baron, J. A. (2000). Prognosis of cancers associated with venous thromboembolism. *N. Engl. J. Med.* 343, 1846–1850.

Sorensen, H. T., Mellemkjaer, L., Steffensen, F. H., Olsen, J. H., and Nielsen, G. L. (1998). The risk of a diagnosis of cancer after primary deep venous thrombosis or pulmonary embolism. *N. Engl. J. Med.* 338, 1169–1173.

Tian, M., Wan, Y., Tang, J., Li, H., Yu, G., Zhu, J., Ji, S., Guo, H., Zhang, N., Li, W., Gai, J., Wang, L., Dai, L., Liu, D., Lei, L., and Zhu, S. (2011). Depletion of tissue factor suppresses hepatic metastasis and tumor growth

in colorectal cancer via the downregulation of MMPs and the induction of autophagy and apoptosis. *Cancer Biol. Ther.* 12, 896–907.

Tormoen, G. W., Cianchetti, F., Bock, P., and McCarty, O. J. (2012). Development of coagulation factor probes for the identification of procoagulant circulating tumor cells. *Front. Oncol.* 2:110. doi: 10.3389/fonc.2012.00110

Tormoen, G. W., Rugonyi, S., Gruber, A., and McCarty, O. J. (2011). The role of carrier number on the procoagulant activity of tissue factor in blood and plasma. *Phys. Biol.* 8, 066005.

Trousseau, A. (1865). "Phlegmasia alba dolens," in *Clinique Medicale de l'Hotel-Dieu de Paris*, ed. A. Trousseau (Paris: The New Sydenham Society), 654–712.

Welsh, J., Smith, J. D., Yates, K. R., Greenman, J., Maraveyas, A., and Madden, L. A. (2012). Tissue factor expression determines tumour cell coagulation kinetics. *Int. J. Lab. Hematol.* 34, 396–402.

Xu, C., Gui, Q., Chen, W., Wu, L., Sun, W., Zhang, N., Xu, Q., Wang, J., and Fu, X. (2011). Small interference RNA targeting tissue factor inhibits human lung adenocarcinoma growth in vitro and in vivo. *J. Exp. Clin. Cancer Res.* 30, 63.

Yates, K. R., Welsh, J., Echrish, H. H., Greenman, J., Maraveyas, A., and Madden, L. A. (2011). Pancreatic cancer cell and microparticle procoagulant surface characterization: involvement of membrane-expressed tissue factor, phosphatidylserine and phosphatidylethanolamine. *Blood Coagul. Fibrinolysis* 22, 680–687.

Zacharski, L. R., Memoli, V. A., and Rousseau, S. M. (1986). Coagulation-cancer interaction in situ in renal cell carcinoma. *Blood* 68, 394–399.

Zacharski, L. R., Schned, A. R., and Sorenson, G. D. (1983). Occurrence of fibrin and tissue factor antigen in human small cell carcinoma of the lung. *Cancer Res.* 43, 3963–3968.

Conflict of Interest Statement: The authors declare that the research was conducted in the absence of any commercial or financial relationships that could be construed as a potential conflict of interest.

Received: 01 June 2012; accepted: 23 August 2012; published online: 10 September 2012.

*Citation: Tormoen GW, Haley KM, Levine RL and McCarty OJT (2012) Do circulating tumor cells play a role in coagulation and thrombosis? Front. Oncol. **2**:115. doi: 10.3389/fonc.2012.00115*

This article was submitted to Frontiers in Cancer Molecular Targets and Therapeutics, a specialty of Frontiers in Oncology.

frontiers in ONCOLOGY

ORIGINAL RESEARCH ARTICLE
published: 14 September 2012
doi: 10.3389/fonc.2012.00108

Modeling and simulation of procoagulant circulating tumor cells in flow

Angela M. Lee[1], Garth W. Tormoen[2], Eva Kanso[1], Owen J. T. McCarty[2,3] and Paul K. Newton[1]*

[1] Department of Aerospace and Mechanical Engineering, Viterbi School of Engineering, University of Southern California, Los Angeles, CA, USA
[2] Department of Biomedical Engineering, School of Medicine, Oregon Health and Science University, Portland, OR, USA
[3] Department of Cell and Developmental Biology, School of Medicine, Oregon Health and Science University, Portland, OR, USA

Edited by:
Michael R. King, Cornell University, USA

Reviewed by:
Amina A. Qutub, Rice University, USA
Katarzyna Anna Rejniak, H. Lee Moffitt Cancer Center & Research Institute, USA

***Correspondence:**
Paul K. Newton, Department of Aerospace and Mechanical Engineering, Viterbi School of Engineering, University of Southern California, Rapp Engineering Bldg, University Park Campus, Los Angeles, CA 90089-1191, USA.
e-mail: newton@usc.edu

We describe a mathematical/computational model for thrombin concentration gradients generated by procoagulant circulating tumor cells (CTCs) in flow. We examine how CTCs enhance blood coagulation as they diffuse tissue factor-dependent coagulation enzymes in a flow environment with vessel walls. Concentration fields of various enzymes, such as prothrombin and thrombin, diffuse, to, and from CTCs, respectively, as they propagate through the bloodstream. The diffusion-dependent generation of these enzymes sets up complex time-dependent concentration fields. The CTCs are modeled as diffusing point particles in an incompressible fluid, and we exploit exact analytical solutions based on three-dimensional Green's functions for unbounded domains with one wall for high resolution numerical simulations. Time-dependent gradient trackers are used to highlight that concentration fields build-up (i) near boundaries (vessel walls), (ii) in regions surrounding the diffusing particles, and (iii) in complex time-dependent regions of the flow where fields associated with different particles overlap. Two flow conditions are modeled: no flow, and unidirectional constant flow. Our results indicate that the CTC-generated thrombin diffuses to and persists at the blood vessel wall, and that the spatial distribution of CTCs in flow determines local thrombin concentration. The magnitude of the diffusion gradient and local thrombin concentration is dependent upon bulk solution concentrations of coagulation factors within normal reported concentration ranges. Therefore, our model highlights the potential to determine patient-specific risks for CTC-induced hypercoagulability as a function of CTC number and individual patient concentration of coagulation factors.

Keywords: procoagulant circulating tumor cells, circulating tumor cells, chemical gradient tracking, tissue factor and coagulation, prothrombin and thrombin fields, circulating tumor cell induced hypercoagulation

INTRODUCTION

Metastatic cancer accounts for the majority of deaths caused by cancer. Metastasis is believed to result from tumor cells from a primary site, migrating toward and intravasating into a blood vessel, navigating the blood circulation to arrive at a distant site whereby it arrests from the blood flow, extravasates, and establishes a metastatic tumor site. The process of metastasis thereby exposes a tumor cell to a variety of new environments, and poses significant physical challenges the tumor cell must overcome if it is to successfully metastasize.

The interactions between circulating tumor cells (CTCs) and blood coagulation proteins have not been fully characterized. Activation of the blood's coagulation system has been associated with cancer, particularly metastatic cancer, for centuries (Gay and Felding-Habermann, 2011). The exact mechanism(s) underlying the activation of blood coagulation in cancer remain ill-defined (Khorana et al., 2007; Gay and Felding-Habermann, 2011). Tumor cell expression of tissue factor (TF) has been associated with advancing stages of cancer progression, and has been shown to correlate with metastatic potential *in vivo* (Mueller et al., 1992; Mueller and Ruf, 1998; Amirkhosravi et al., 2002). TF is a transmembrane glycoprotein that is normally expressed by cells outside of the blood vasculature. The exposure of blood to TF, as occurs in the event of a blood vessel injury, is a physiological initiator of coagulation (Gomez and McVey, 2006; Okorie et al., 2008). TF serves as the cell membrane receptor for and enzyme cofactor of coagulation factor VIIa (FVIIa). In complex, TF-FVIIa activate the extrinsic pathway of coagulation leading to the formation of thrombin which can then convert fibrinogen to fibrin in order to form a plug that stops bleeding at the injury site in order to maintain blood flow and volume.

In the context of a metastasizing tumor cell, a TF-expressing CTC may expose blood within an uninjured blood vessel to TF (Versteeg et al., 2004; Khorana et al., 2007; Berny-Lang et al., 2011; Otero et al., 2011; Tormoen et al., 2011). Levels of intravascular TF correlate with cancer progression and to some extent with the formation of pathological clots or thrombi in the veins of patients with cancer. Thrombosis, the formation of pathological thrombi, accounts for the second leading cause of death for patients with cancer and constitutes a significant source of morbidity in these patients (Versteeg et al., 2004). Anticoagulant measures taken after a thrombotic event are effective at reducing the formation of subsequent thrombi, but no current laboratory assay is capable of predicting which patients are at risk to develop thrombosis. The

incidence of thrombosis is known to correlate with cancer type and tissue of origin, suggesting that the cancerous cells themselves have a role in the formation of pathological thrombi (Blom et al., 2005). *In vitro*, cancer cells are capable of independently initiating coagulation and clotting blood plasma. Similarly, functionally blocking TF on cancer cells prevents the cell's ability to clot blood plasma. Therefore, mounting evidence suggests that cancer cell expressed TF is a likely culprit for the initiation of blood coagulation associated with cancer (Berny-Lang et al., 2011; Marchetti et al., 2011, 2012; Saito et al., 2011; Yates et al., 2011; Welsh et al., 2012).

The ability of TF to activate blood coagulation is dependent upon the presence of phospholipids, suggesting that only cell surface-expressed TF or cell membrane-derived TF bearing microvesicles are capable of activating coagulation (Nemerson, 1968). This also indicates that the activation of coagulation by TF is essentially a surface phenomenon, requiring coagulation factors to transport from the blood to the surface-expressed TF in order to participate in coagulation. *In vitro*, the trafficking of soluble coagulation factors from bulk to a TF-expressing phospholipid surface is rate-limiting with respect to enzyme activation (Gemmell et al., 1988; McGee et al., 1992; Hall et al., 1998). Further, TF activity is augmented in the presence of blood flow where convective transport supplants diffusive transport as the dominant mode of transport for coagulation factors to TF. Taken together, the ability for a TF-expressing CTC to activate blood coagulation is likely dependent upon its spatio-temporal relationship with the blood. *In vitro*, the coagulation kinetics for cancer cells in suspension is dependent upon the number of cells added to plasma (Berny-Lang et al., 2011; Tormoen et al., 2011; Yates et al., 2011; Welsh et al., 2012). Further work has suggested that TF-expressing cells in suspension show synergistic effects on their ability to initiate and propagate coagulation, with the time to initiate coagulation enzymes, and the rate at which these enzymes are generated correlating with the average separation distance between cells rather than the overall cell count (Tormoen et al., 2011). The effects of spatial separation on coagulation kinetics are consistent in assays that utilize closed systems under well-mixed conditions as well as open systems under laminar flow. However, a CTC would experience different flow regimes if it were circulating on the arterial side versus the venous side or if it were free-flowing or adherent to the cell wall, and the effects that these different conditions have on coagulation kinetics have not been established.

In this manuscript, we model the concentration of thrombin generated by dispersed CTCs under constant laminar flow. Our model is based upon exact solutions used in the atmospheric dispersion community (Stockie, 2011) whereby a source of pollution near the ground (i.e., a smokestack) emits a pollutant which enters the atmosphere and is dispersed and diffused downstream as a "Gaussian plume" or a "Gaussian puff" (Stockie, 2011). We adapt and use the solutions, which are based on a Green's function formulation for the concentration field equations (Kevorkian, 1989), to model the dispersing and diffusing thrombin concentration field entering the blood. Since the concentration field equations are linear, we can superpose as many fields from each of the CTCs as needed. We assume that the transport of coagulation factors is diffusion-limited as viscous forces dominate inertial forces of the cells. Our results, obtained in a simple geometry with a single (vessel) wall, suggest that thrombin generated by a CTC collects at the blood vessel wall and correlates with the number and spatial distribution of CTCs in the blood, supporting a role for the CTC count in predicting risk for developing thrombosis. Modeling and simulation of coagulation processes has been performed (Fogelson and Tania, 2005; Fogelson, 2007; Bodnar and Sequeira, 2008; Chatterjee et al., 2010; Gregg, 2010; Leiderman and Fogelson, 2011), but to our knowledge, our work is the first to model the physiologically relevant scenario of a TF-expressing cell entering into and circulating within the bloodstream and simulate its effects on coagulation processes.

MATERIALS AND METHODS

FLUID DYNAMICS AND CONCENTRATION FIELD EQUATIONS

The computational model is based on the partial differential equations for the diffusing concentration field, coupled with the equations for incompressible fluid flow (Pedley, 1980; Kevorkian, 1989):

$$\frac{\partial \vec{c}^{(i)}}{\partial t} + \vec{u} \cdot \nabla \vec{c}^{(i)} = \alpha_i \Delta \vec{c}^{(i)} + \delta\left(\vec{x} - \vec{x}_i\right) \tag{1}$$

$$\dot{\vec{x}}_i = \vec{u} \tag{2}$$

$$\nabla \cdot \vec{u} = 0 \tag{3}$$

$$\rho\left(\frac{\partial \vec{u}}{\partial t} + \vec{u} \cdot \nabla \vec{u}\right) = -\nabla p + \nu \Delta \vec{u} \tag{4}$$

$$\vec{u}\left(\vec{x}, 0\right) = \vec{f}\left(\vec{x}\right) \tag{5}$$

Here, the concentration field associated with the ith species is denoted $\vec{c}^{(i)}(x, y, z;\ t)$, with diffusion coefficient α_i. The fluid (blood) velocity field is denoted by $\vec{u}(\vec{x},\ t)$, blood pressure denoted p, density ρ, and each of the "i" CTCs ($i = 1, \ldots, n$) are located at $\vec{x}_i(t)$, their time derivatives are denoted by the "dot" superscript. δ in Eq. 1 is the Dirac-delta function which is zero everywhere but where the argument is zero, which in this case are the locations of each of the CTCs. The initial locations of the CTCs are given by the function $f(x)$. The diffusion coefficient in Eq. 4 is denoted by ν. Equation 4 are the Navier–Stokes equations representing the background plasma, which at this level of model approximation we treat as an incompressible Newtonian fluid. The flow takes place in the upper-half space, above a solid wall which models the vessel wall, hence boundary conditions for the concentration field and blood velocity at the wall are:

$$\frac{\partial \vec{c}}{\partial n}\Big|_{\text{wall}} = 0 \tag{6}$$

$$\vec{u}\,|_{\text{wall}} = 0 \tag{7}$$

The first is a no penetration condition for the concentration field, while the second is the viscous no slip boundary condition at the wall.

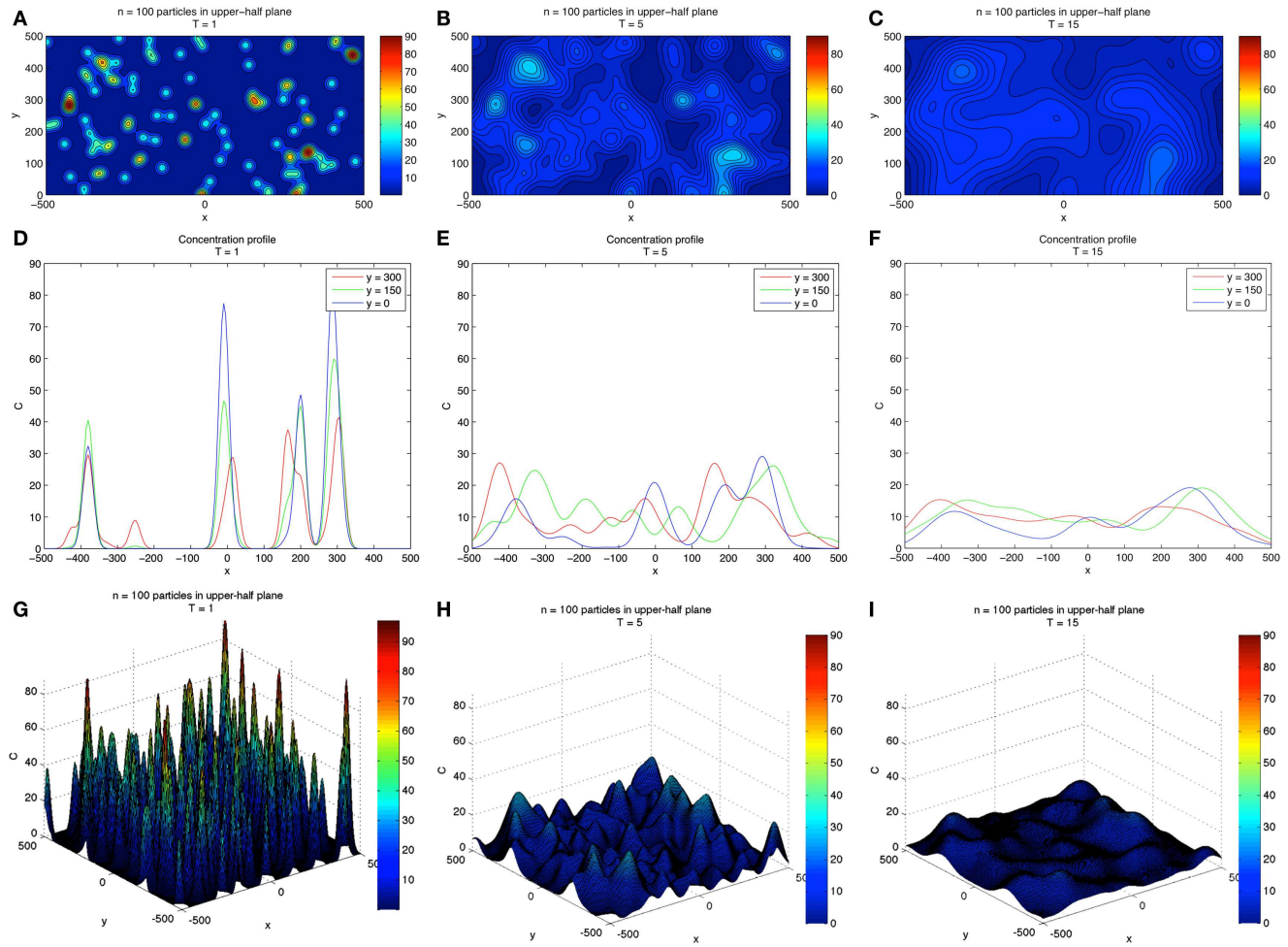

FIGURE 1 | Two-dimensional concentration fields for 100 diffusing CTCs. **(A–C)** Show evolving concentration fields at $T = 1$, 5, 15. **(D–F)** Show concentration profiles at different y-slices: $y = 0$, 150, 300. Vessel wall is located at $y = 0$. **(G–I)** Show 3D surface plot of the concentration fields and gives a sense of how the field diffuses in time. Boundary conditions are discussed in text.

THE GREEN'S FUNCTION APPROACH

In this paper, we focus on the simple geometry associated with the upper-half plane in 2D and upper-half space in 3D, making it possible to use an analytical Green's function formulation to form solutions that satisfy exact boundary conditions. In 2D, with no flow ($u = 0$), we use the standard Green's function associated with the 2D diffusion equation (Kevorkian, 1989):

$$c^{(i)}\left(x, y;\ t\right) = \frac{\Gamma}{\sqrt{4\pi\nu t}} \exp\left(\frac{-(x - x_i)^2 - \left(y - y_i\right)^2}{4\nu t}\right)$$
$$c^{(i)}_{\text{image}}\left(x, y;\ t\right) = \frac{\Gamma}{\sqrt{4\pi\nu t}} \exp\left(\frac{-(x - x_i)^2 - \left(y + y_i\right)^2}{4\nu t}\right) \tag{8}$$

Here, each particle is placed in the upper-half plane ($y > 0$), at positions (x_i, y_i) for $i = 1, \ldots, n$, and image particles are placed at $(x_i, -y_i)$. The no penetration condition Eq. 6 for the concentration field at the wall is enforced exactly, with no other explicit boundary conditions needed.

In 3D, with flow $u =$ constant, the corresponding Green's function is given by Kevorkian (1989), Stockie (2011):

$$c\left(r, x_i, y_i, z_i;\ t\right) = \frac{Q_{\text{T}}}{8(\pi r)^{3/2}} \exp\left(-\frac{(x_i - ut)^2 + y_i^2}{4r}\right) \times \left[\exp\left(-\frac{(z_i - H)^2}{4r}\right) + \exp\left(-\frac{(z_i + H)^2}{4r}\right)\right] \tag{9}$$

Here, $r = \alpha\ x_i/u$, is a new scaled independent variable. The symbol Q_{T} expresses the total amount of TF expressed by the CTC.

Using these solutions as the basic building blocks for flow simulations based on Eqs 1–7, we are able to perform highly resolved concentration-flow simulations described in Section "Results."

CONCENTRATION FIELD GRADIENT TRACKING DIAGNOSTICS

Since the concentration field is fairly complex, we need a diagnostic tool to help with visualization during a simulated run. It

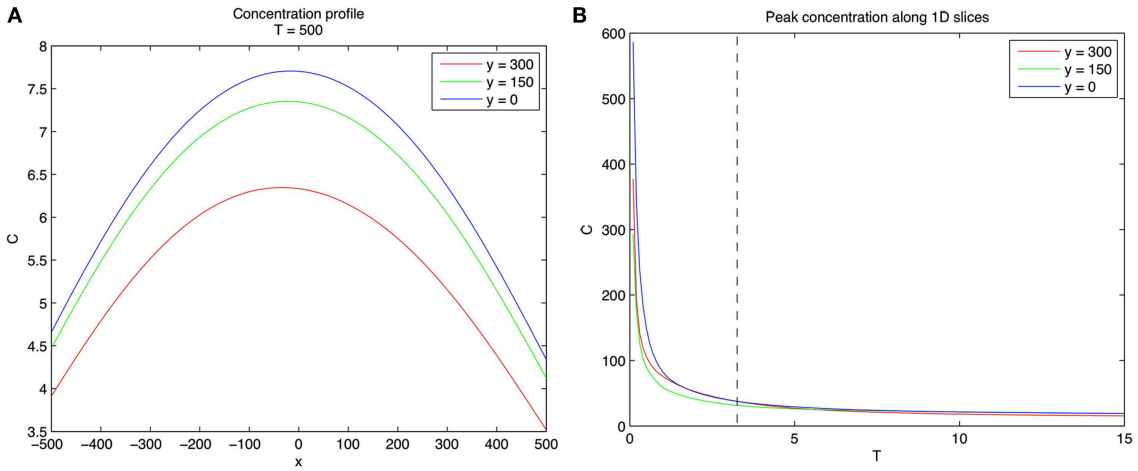

FIGURE 2 | Concentration profiles for 100 diffusing CTCs. (A) Concentration profiles at $y = 0$, 150, 300 for $T = 500$. Note that concentration is highest near wall. **(B)** Concentration profiles as a function of T for $y = 0$, 150, 300. Vertical dashed line separates two distinct regimes. Left of the dashed line ($0 < T < 3$) represents the fast mixing regime of the concentration fields due to the different CTCs, whereas right of the dashed line ($T > 3$) the fields from different CTCs have mixed and are slowly diffusing.

is useful to use what we call "passive gradient trackers," which are diagnostic particles placed in the flow. The gradient trackers do not disturb the flow, but move toward regions of high TF concentration and low TF concentration in time, as the simulation proceeds. A schematic of one of these trackers is shown in the upper left of **Figure 3**. If the tracker is placed at position (x, y, z) at time "t," the concentration field at that point is given by $\vec{c}(x, y, z;\ t)$. The tracker then measures the concentration field at six neighboring points in the field: $\vec{c}(x \pm \varepsilon, y \pm \varepsilon, z \pm \varepsilon,\ t), 0 < \varepsilon << 1$, and measures the differences in concentration at these six points compared to the concentration at $\vec{c}(x, y, z;\ t)$. Thus, it measures the quantities $(\vec{c}(x, y, z;\ t) - \vec{c}(x \pm \varepsilon, y, z;\ t))$, $(\vec{c}(x, y, z;\ t) - \vec{c}(x - \varepsilon, y, z;\ t))$, $(\vec{c}(x, y, z;\ t) - \vec{c}(x, y + \varepsilon, z;\ t))$, $(\vec{c}(x, y, z;\ t) - \vec{c}(x, y - \varepsilon, z;\ t))$, $(\vec{c}(x, y, z;\ t) - \vec{c}(x, y, z + \varepsilon;\ t))$, $(\vec{c}(x, y, z;\ t) - \vec{c}(x, y, z - \varepsilon;\ t))$, and if it is seeking high concentration regions, it moves to the point yielding the largest increase in concentration. If it seeks low concentrations, it moves to the point yielding the largest decrease. Thus, it tracks "gradients" in the concentration field at each time step, and as time evolves, the particles will gather in high/low TF concentration regions giving a useful visual diagnostic tool. For our simulations, we use "red" trackers to follow increases in gradient, and "blue" trackers to follow decreases. We note that there is an inherent timescale associated with the tracking, which is essentially governed by the size of ε. In the limit as this parameter goes to zero, the discrete trackers approximate derivatives in concentrations, hence gradients.

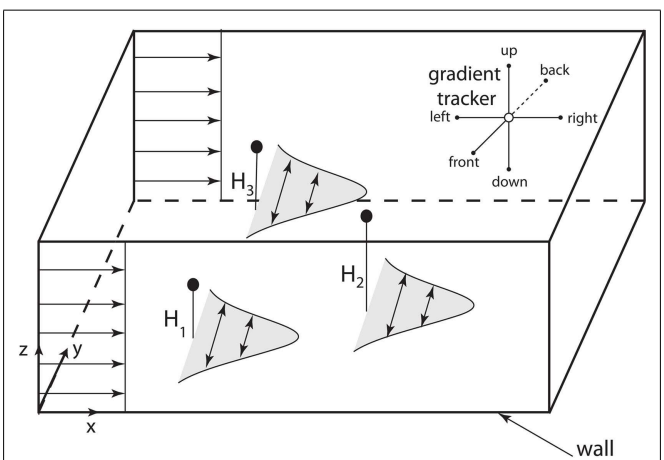

FIGURE 3 | Computational domain for 3D model of diffusing CTCs. Schematic shows 3D computational domain with bottom vessel wall at $z = 0$. CTCs are initially placed at random initial positions and travel downstream with the flow, which is constant. The concentration fields diffuse as "puffs," to model the diffusing TF which initially coats the outer cell surface. Upper right corner of the domain shows the six directions that are "polled" by gradient trackers placed in the flow field.

RESULTS

TWO-DIMENSIONAL CONCENTRATION FIELDS

A two-dimensional simulation of developing concentration gradients for 100 diffusing CTCs with no flow ($u = 0$) is shown in **Figure 1**. **Figures 1A–C** shows the concentration field at times $T = 1$, 5, 15 with $u = 0$ in Eq. 1. The CTCs are randomly placed in the upper-half plane ($y > 0$), with the vessel wall at $y = 0$. On the vessel wall, we use the no penetration condition Eq. 6 for the concentration field. No other explicit boundary conditions are needed when using the Green's functions formulas. **Figures 1D–F** shows the concentration profiles at $y = 0$, 150, 300, while **Figures 1G–I** shows the 3D surface plots of the concentration fields in the (x, y) plane. The CTCs are placed in the region $y > 0$, while their images are placed appropriately at $y < 0$ (see Eq. 8) so that boundary conditions are enforced. The (dimensionless) diffusion coefficient for each particle is taken to be $\alpha_i = 1.5$. We note that here, and in all of the following simulations, equations, and parameters are to be interpreted non-dimensionally since explicit comparisons with *in vivo* experiments are not described

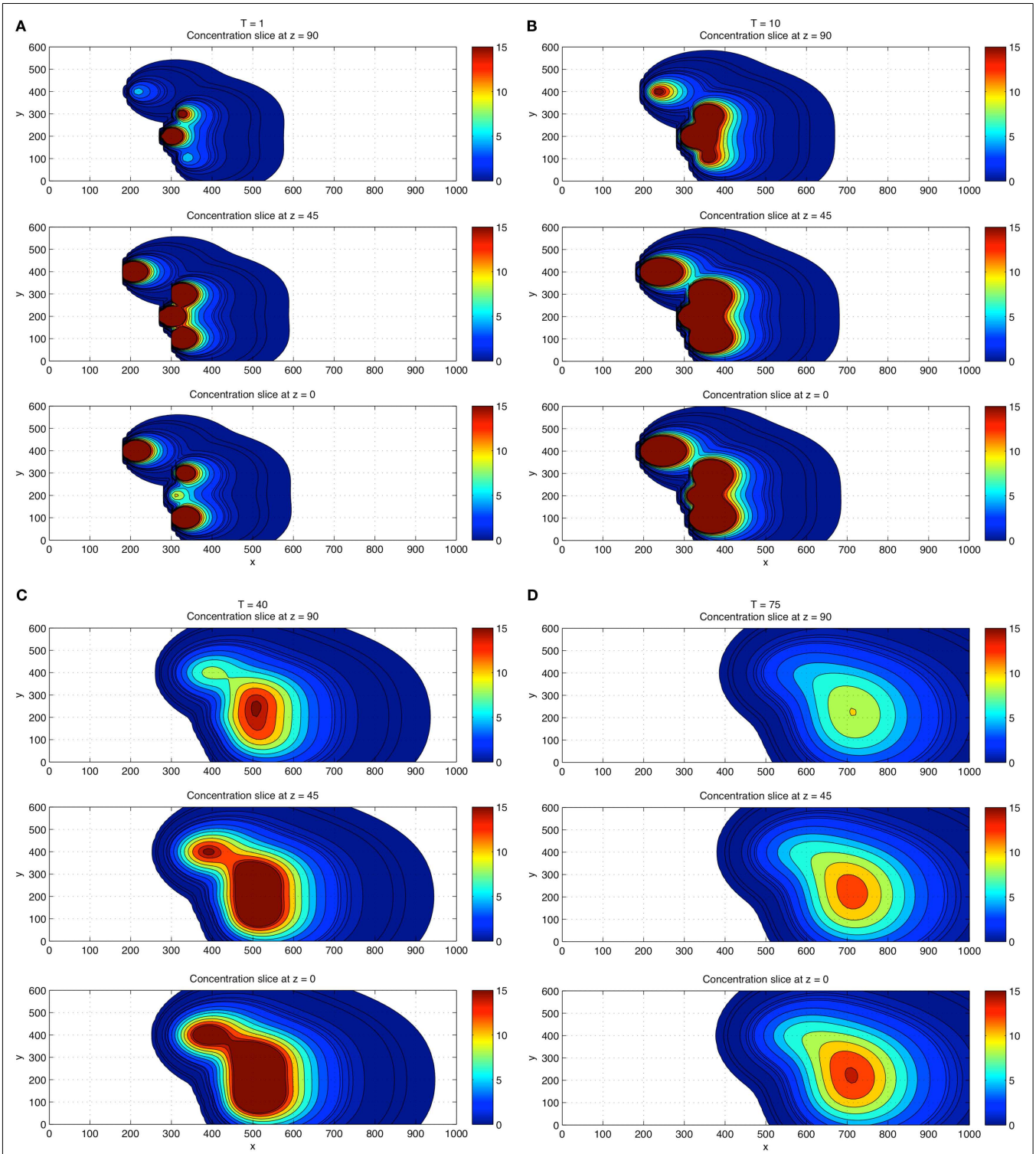

FIGURE 4 | Three-dimensional concentration field simulations using four CTCs. View is top down. Top down view of the x–y plane with four CTCs placed randomly in the flow. Three different z-slices are shown: $z = 0$ (wall), $z = 45$, $z = 90$ at each time $T = 1$ **(A)**, $T = 10$ **(B)**, $T = 40$ **(C)**, and $T = 75$ **(D)**. Coloring shows that fields persist and are strongest near the wall region and in overlap domains from different CTCs.

in this paper. The 2D simulations with no flow clearly show the diffusing fields from each particle merging and smoothing over time, with concentration persisting at the vessel wall because of the no penetration boundary condition. This is seen most clearly in **Figure 2** which shows the concentration profile for $T = 500$ at $y = 0$, 150, 300. **Figure 2A** shows the persistence of the highest

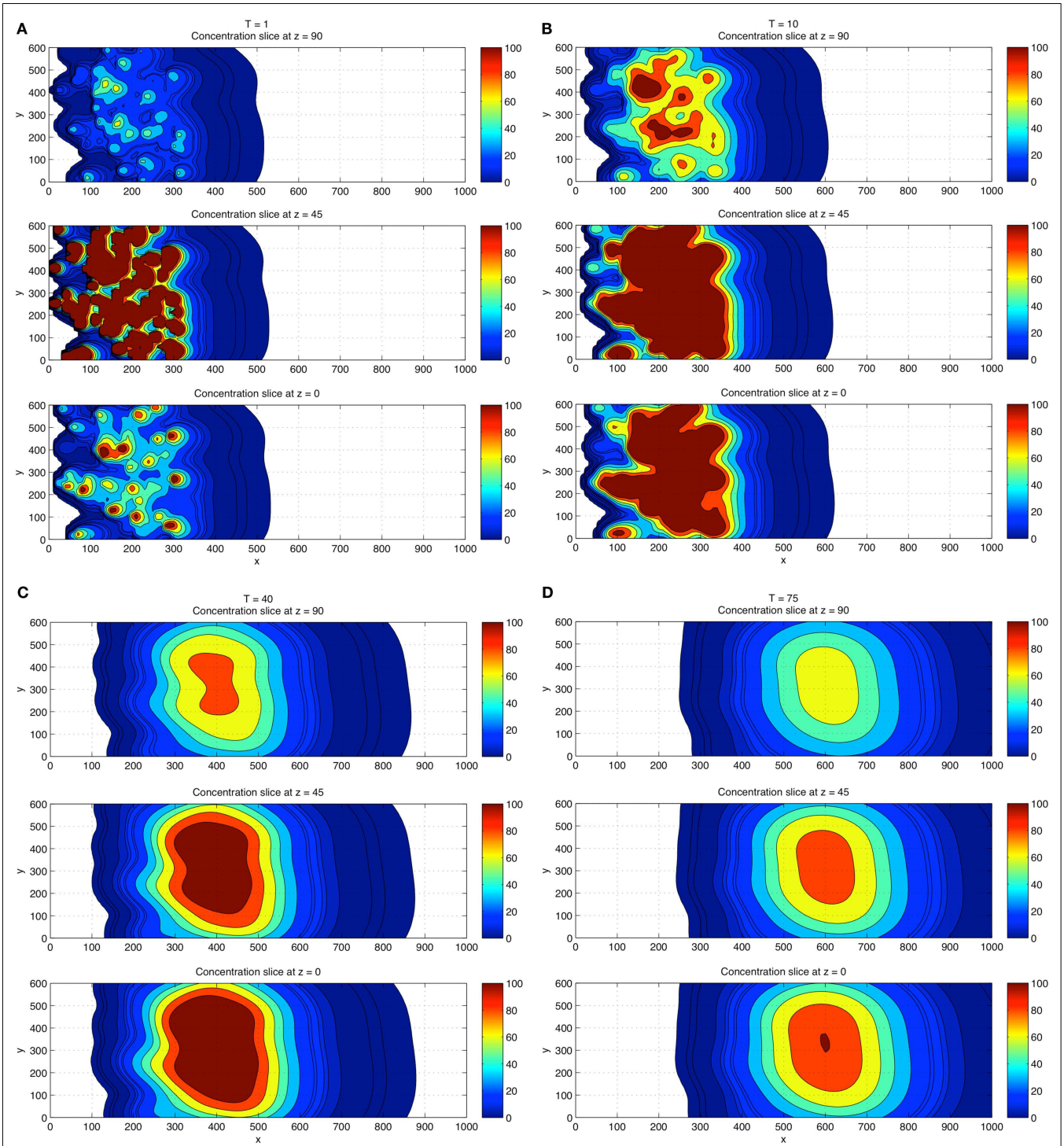

FIGURE 5 | Three-dimensional concentration field simulations using 100 CTCs. View is top down. Top down view of the x–y plane with four CTCs placed randomly in the flow. Three different z-slices are shown: $z = 0$ (wall), $z = 45$, $z = 90$ at each time $T = 1$ **(A)**, $T = 10$ **(B)**, and $T = 40$ **(C)**, and $T = 75$ **(D)**. Coloring shows that fields persist and are strongest near the wall region and in overlap domains from different CTCs. Comparisons of the concentration field levels with those in **Figure 4** indicate that the concentration field varies (roughly) linearly with the number of CTCs in the domain.

concentration at the wall ($y = 0$). **Figure 2B** shows the peak concentration at $y = 0$, 150, 300 as time progresses. The vertical line in this figure separates two distinct temporal regimes: (i) $0 < T < 3$; (ii) $T > 3$. The first early regime represents a "rapid mixing" regime where the concentration fields quickly merge to form a complex combined overlap domain of fields associated with

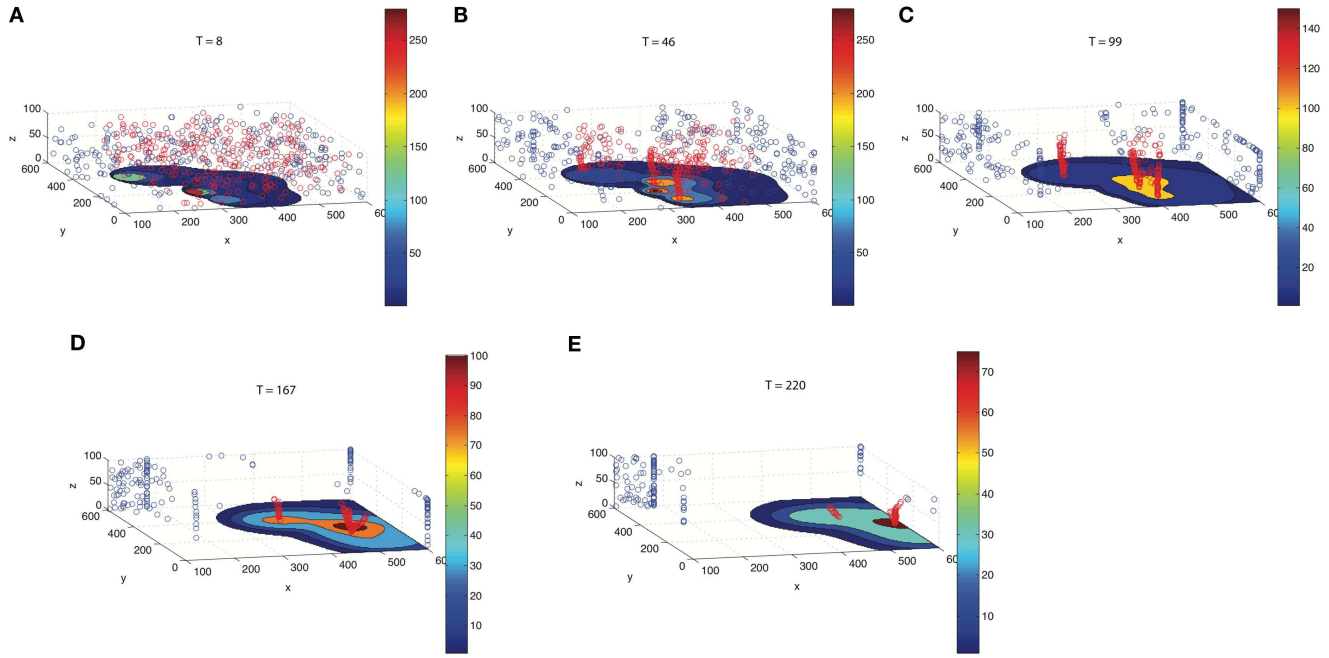

FIGURE 6 | Gradient trackers which move to regions of high concentration (red) and low concentration (blue). As time progresses [**(A)** $T = 8$; **(B)** $T = 46$; **(C)** $T = 99$; **(D)** $T = 167$; **(E)** $T = 220$], red gradient trackers move to regions near the CTCs, then toward regions where the fields from different CTCs overlap, and finally toward the vessel wall where the concentration fields persist. Blue gradient trackers move to regions of low TF concentration.

the different sources merging together. The "long-time" regime ($T > 3$) shows that the peak combined concentration field continues to decay, but rather slowly, with the peak wall concentration ($y = 0$) dominating.

THREE-DIMENSIONAL CONCENTRATION FIELDS

We next performed a high resolution (exact, since we are using the Green's function formulation) simulation of CTCs in three-dimensions with a constant flow velocity profile ($u =$ constant). **Figure 3** shows the general schematic diagram with flow only in the direction of x, with diffusing CTCs initially placed in the domain at random heights $z = H_1, H_2, H_3$. The vessel wall in these simulations is located at $z = 0$. Because the concentration fields are spatially complex and time-dependent, we build in particle gradient tracking capability in our code, also shown schematically in **Figure 3**.

Next, we performed a 3D concentration field simulation (without gradient trackers) using four CTCs, where we show a top down z-projection view of the (x, y) plane for values $z = 0$ (wall), $z = 45$, and $z = 90$, progressively in time $T = 1, 10, 40, 75$ in **Figures 4A–D**. In order to compare with the 2D simulations, we have chosen the same dimensionless diffusion coefficient values $\alpha_i = 1.5$. For these simulations, the initial locations of the particles are $(x, y, z) = (300, 300, 45)$; $(180, 400, 30)$; $(300, 100, 30)$; $(275, 200, 60)$. Careful examination of the coloring of the fields indicates (i) the persistence of the strongest concentration region near the wall, (ii) strong concentrations in overlap domains from different CTCs, and (iii) strong concentrations near each of the CTCs which express TF. These numbers and results are consistent with the experiment described in Tormoen et al. (2011) in which small numbers TF-coated micro-spheres were placed in blood solution and clotting time was carefully measured. Typically, in metastatic patients, measured numbers of CTCs would be in the range of 1–100 CTCs/ml.

For a direct comparison with the 2D results, we show in **Figures 5A–D** the 3D concentration field simulations using 100 CTCs placed randomly (initially). The overall concentration field again persists near the wall, but the overall concentration field level is higher, roughly increasing linearly with the number of CTCs in the flow, also in agreement with results from Tormoen et al. (2011). As the flow progresses in time, flow visualization tools become crucial to help understand the field patterns that develop.

GRADIENT TRACKING RESULTS

To track developing TF concentration gradient patterns, we include gradient tracking capability to our simulation. **Figure 6** illustrates different time points ($T = 8$–220 s) as the flow progresses. The red particles move toward regions of high CTC concentration, whereas the blue move to regions of low CTC concentration. The patterns that develop with the red and blue particles depend on the comparison of relative timescales as determined by the concentration field diffusion rates, α_i, as well as the timescales on which the gradient trackers move. The first three panels in the figure clearly show the red gradient trackers gathering in highly concentrated regions near each of the CTCs, lining up in elongated columnar strands. The timescale in which these trackers locate the diffusing CTCs is *short* compared with the timescales on which the diffusion fields spread.

The last two figures in the panel show the particles then moving toward the vessel wall where concentration fields persist. This movement of the trackers to the vessel walls takes place on a longer timescale, well after the CTCs have been located in the flow.

DISCUSSION

In this paper, we develop novel computational tools to model and characterize the movement of diffusing thrombin fields emitted from CTCs in flow, with the aim of scaling up the techniques to more complex arterial environments and more complex, time-dependent flow assumptions (Pedley, 1980). A main finding from our model is the build-up and persistence of thrombin concentration near vessel walls and in complex time-dependent overlap regions of the flow. The build-up near walls occurs on a relatively long timescale compared to the timescale in which the concentration fields diffuse (regulated by the diffusion constants α_i). We expect this main finding to persist under more complex and realistic flow geometries, as locally, near a vessel wall, the boundary curvature should not play a big role. Furthermore, very near the vessel wall where viscous flow boundary conditions dominate, blood velocity magnitudes are small, so should have minimal effects on disturbing the concentration fields that build-up there, therefore we do not expect the inviscid fluid boundary conditions used in this study to qualitatively alter this main finding. In complex capillary beds where branching of the flow into several different regions is the reality, we do expect the tracking of the diffusive overlap regions of many CTCs to be more computationally challenging, yet the main finding that concentration levels are relatively high in overlap regions should remain valid. Thrombin has several well characterized effects on endothelial cells and platelets which are also located at blood vessel walls under flow. In addition, the proximity of CTCs to each other determined the persistence of thrombin concentrations in the flow, which may help explain the effect of cell count on coagulation kinetics (Tormoen et al., 2011), suggesting that CTC counts may hold significance to understanding the role for CTCs in activating blood coagulation. The gradient tracking capability described here holds strong potential to aid in the understanding of the fate of CTC-generated thrombin in more complex settings that arise within the circulation.

ACKNOWLEDGMENTS

We thank Dr. Peter Kuhn for insightful discussions. This work was supported in part by the National Institute of Health (U54CA143906, R01HL101972, and T32-CA106195) and American Heart Association (12PRE11930019). Angela M. Lee and Garth W. Tormoen are ARCS scholars.

REFERENCES

Amirkhosravi, A., Meyer, T., Chang, J. Y., Amaya, M., Siddiqui, F., Desai, H., and Francis, J. L. (2002). Tissue factor pathway inhibitor reduces experimental lung metastasis of B16 melanoma. *Thromb. Haemost.* 8, 930–936.

Berny-Lang, M. A., Aslan, J. E., Tormoen, G. W., Patel, I. A., Bock, P. E., Gruber, A., and McCarty, O. J. (2011). Promotion of experimental thrombus formation by the procoagulant activity of breast cancer cells. *Phys. Biol.* 8, 015014.

Blom, J. W., Doggen, C. J., Osanto, S., and Rosendaal, F. R. (2005). Malignancies, prothrombotic mutations, and the risk of venous thrombosis. *JAMA* 293, 715–722.

Bodnar, T., and Sequeira, A. (2008). Numerical simulation of the coagulation dynamics of blood. *Comput. Math. Methods Med.* 9, 83–104.

Chatterjee, M. S., Denney, W. S., Jing, H., and Diamond, S. L. (2010). Systems biology of coagulation initiation: kinetics of thrombingeneration in resting and activated human blood. *PLoS Comput. Biol.* 6, e1000950. doi:10.1371/journal.pcbi.1000950

Fogelson, A. L. (2007). "Cell-based models of blood clotting," in *Single Cell-Based Models in Biology and Medicine*, eds A. R. A. Anderson, M. A. J. Chaplain, and K. A. Rejniak (Basel: Birkhauser Verlag), 243–269.

Fogelson, A. L., and Tania, N. (2005). Coagulation under flow: the influence of flow-mediated transport on the initiation and inhibition of coagulation. *Pathophysiol. Haemost. Thromb.* 34, 91–108.

Gay, F. J., and Felding-Habermann, B. (2011). Contribution of platelets to tumor metastasis. *Nat. Rev. Cancer* 11, 123–134.

Gemmell, C. H., Turitto, V. T., and Nemerson, Y. (1988). Flow as a regulator of the activation of factor X by tissue factor. *Blood* 72, 1404–1406.

Gomez, K., and McVey, J. H. (2006). Tissue factor initiated blood coagulation. *Front. Biosci.* 11, 1349–1359.

Gregg, K. L. (2010). *A Mathematical Model of Blood Coagulation and Platelet Deposition Under Flow.* Ph.D. thesis, University of Utah, Salt Lake City.

Hall, C. L., Taubman, M. B., Nemerson, Y., and Turitto, V. T. (1998). Factor Xa generation at the surface of cultured rat vascular smooth muscle cells in an in vitro flow system. *J. Biomech. Eng.* 120, 484–490.

Kevorkian, J. (1989). *Partial Differential Equations: Analytical Solution Techniques.* Pacific Grove, CA: Wadsworth & Brooks/Cole Mathematics Series.

Khorana, A. A., Francis, C. W., Culakova, E., Kuderer, N. M., and Lyman, G. H. (2007). Thromboembolism is a leading cause of death in cancer patients receiving outpatient chemotherapy. *J. Thromb. Haemost.* 5, 632–634.

Leiderman, K., and Fogelson, A. L. (2011). Grow with the flow: a spatial-temporal model of platelet deposition and blood coagulation under flow. *Math. Med. Biol.* 28, 47–84.

Marchetti, M., Diani, E., Ten Cate, H., and Falanga, A. (2012). Characterization of thrombin generation potential of leukemic and solid tumor cells by the calibrated automated thrombography. *Haematologica* 97, 1173–1180.

Marchetti, M., Russo, L., Balducci, D., and Falanga, A. (2011). All trans-retinoic acid modulates the procoagulant activity of human breast cancer cells. *Thromb. Res.* 128, 368–374.

McGee, M. P., Li, L. C., and Xiong, H. (1992). Diffusion control in blood coagulation. Activation of factor X by factors IXa/VIIIa assembled on human monocyte membranes. *J. Biol. Chem.* 267, 24333–24339.

Mueller, B. M., Reisfeld, R. A., Edgington, T. S., and Ruf, W. (1992). Expression of tissue factor by melanoma cells promotes efficient hematogenous metastasis. *Proc. Natl. Acad. Sci. U.S.A.* 89, 11832–11836.

Mueller, B. M., and Ruf, W. (1998). Requirement for binding of catalytically active factor VIIa in tissue factor dependent experimental metastasis. *J. Clin. Invest.* 101, 1372–1378.

Nemerson, Y. (1968). The phospholipid requirement of tissue factor in blood coagulation. *J. Clin. Invest.* 47, 72–80.

Okorie, U. M., Denney, W. S., Chatterjee, M. S., Neeves, K. B., and Diamond, S. L. (2008). Determination of surface tissue factor thresholds that trigger coagulation at venous and arterial shear rates: amplification of 100 fM circulating tissue factor requires flow. *Blood* 111, 3507–3513.

Otero, L. L., Alonso, D. F., Castro, M., Cinat, G., Gabri, M. R., and Gomez, D. E. (2011). Tissue factor as a novel marker for detection of circulating cancer cells. *Biomarkers* 16, 58–64.

Pedley, T. J. (1980). *The Fluid Mechanics of Large Blood Vessels. Cambridge Monographs on Mechanics and Applied Mathematics.* Cambridge: Cambridge University Press.

Saito, Y., Hashimoto, Y., Kuroda, J., Yasunaga, M., Koga, Y., Takahashi, A., and Matsumura, Y. (2011). The inhibition of pancreatic cancer invasion-metastasis cascade in both cellular signal and blood coagulation cascade of tissue factor by its neutralization antibody. *Eur. J. Cancer* 47, 2230–2239.

Stockie, J. M. (2011). The mathematics of atmospheric dispersion modeling. *SIAM Rev. Soc. Ind. Appl. Math.* 53, 349–372.

Tormoen, G. W., Rugonyi, S., Gruber, A., and McCarty, O. J. (2011). The role of carrier number on the procoagulant activity of tissue factor in blood and plasma. *Phys. Biol.* 8, 066005.

Versteeg, H. H., Spek, C. A., Peppelenbosch, M. P., and Richel, D. J. (2004). Tissue factor and cancer metastasis: the role of intracellular and extracellular signaling pathways. *Mol. Med.* 10, 6–11.

Welsh, J., Smith, J. D., Yates, K. R., Greenman, J., Maraveyas, A., and Madden, L. A. (2012). Tissue factor expression determines tumor cell coagulation kinetics. *Int. J. Lab. Hematol*. 34, 396–402.

Yates, K. R., Welsh, J., Echrish, H. H., Greenman, J., Maraveyas, A., and Madden, L. A. (2011). Pancreatic cancer cell and microparticle procoagulant surface characterization: involvement of membrane-expressed tissue factor, phosphatidylserine and phosphatidylethanolamine. *Blood Coagul. Fibrinolysis* 8, 680–687.

Conflict of Interest Statement: The authors declare that the research was conducted in the absence of any commercial or financial relationships that could be construed as a potential conflict of interest.

Received: 01 June 2012; accepted: 14 August 2012; published online: 14 September 2012.

Citation: Lee AM, Tormoen GW, Kanso E, McCarty OJT and Newton PK (2012) Modeling and simulation of procoagulant circulating tumor cells in flow. Front. Oncol. ***2****:108. doi: 10.3389/fonc.2012.00108*

This article was submitted to Frontiers in Cancer Molecular Targets and Therapeutics, a specialty of Frontiers in Oncology.

frontiers in ONCOLOGY

ORIGINAL RESEARCH ARTICLE
published: 06 September 2012
doi: 10.3389/fonc.2012.00110

Development of coagulation factor probes for the identification of procoagulant circulating tumor cells

Garth W. Tormoen[1]*†, Flor A. Cianchetti[1†], Paul E. Bock[2] and Owen J. T. McCarty[1,3,4]

[1] Department of Biomedical Engineering, Oregon Health and Science University, Portland, OR, USA
[2] Department of Pathology, Microbiology and Immunology, Vanderbilt University School of Medicine, Nashville, TN, USA
[3] Department of Cell and Developmental Biology, Oregon Health and Science University, Portland, OR, USA
[4] Division of Hematology and Medical Oncology, Department of Medicine, Oregon Health and Science University, Portland, OR, USA

Edited by:
Michael R. King, Cornell University, USA

Reviewed by:
Jie Ma, Cancer Institute/Hospital, Chinese Academy of Medical Sciences, China
Weiwei Wang, Cornell University, USA

***Correspondence:**
Garth W. Tormoen, Department of Biomedical Engineering, Oregon Health and Science University, 3303 South West Bond Avenue, Portland, OR 97239, USA.
e-mail: tormoeng@ohsu.edu

†Garth W. Tormoen and Flor A. Cianchetti are co-first authors.

Metastatic cancer is associated with a hypercoagulable state, and pathological venous thromboembolic disease is a significant source of morbidity and the second leading cause of death in patients with cancer. Here we aimed to develop a novel labeling strategy to detect and quantify procoagulant circulating tumor cells (CTCs) from patients with metastatic cancer. We hypothesize that the enumeration of procoagulant CTCs may be prognostic for the development of venous thrombosis in patients with cancer. Our approach is based on the observation that cancer cells are capable of initiating and facilitating cell-mediated coagulation *in vitro*, whereby activated coagulation factor complexes assemble upon cancer cell membrane surfaces. Binding of fluorescently labeled, active site-inhibited coagulation factors VIIa, Xa, and IIa to the metastatic breast cancer cell line, MDA-MB-231, non-metastatic colorectal cell line, SW480, or metastatic colorectal cell line, SW620, was characterized in a purified system, in anticoagulated blood and plasma, and in plasma under conditions of coagulation. We conclude that a CTC labeling strategy that utilizes coagulation factor-based fluorescent probes may provide a functional assessment of the procoagulant potential of CTCs, and that this strategy is amenable to current CTC detection platforms.

Keywords: tissue factor, coagulation, circulating tumor cell

INTRODUCTION

Cancer is a hypercoagulable state. Patients with cancer have a 4- to 10-fold increased risk of developing thrombosis, which is a significant source of morbidity and mortality for patients with cancer (Trousseau, 1865; Baron et al., 1998; Sorensen et al., 2000; Rickles and Levine, 2001; Falanga and Marchetti, 2009). Recurrent thrombosis can be clinically managed with anticoagulant therapy; however, the risk of bleeding complications associated with the use of anticoagulants has prevented routine prophylactic anticoagulation for patients with cancer who have not yet developed thrombosis (Akl et al., 2011). Therefore, a method to identify which cancer patients are at imminent risk to develop thrombosis would allow for an objective means by which to administer personalized anticoagulant prophylaxis, reducing the morbidity, and mortality for patients with cancer. There is currently a lack of laboratory assays capable of identifying which patients with cancer are at risk of developing thrombosis.

Blood coagulation is actuated by a system of serine proteases that are contained within the blood in their inactive, zymogen form. In health, activation of coagulation is restricted to sites of blood vessel injury through the localized exposure of tissue factor (TF), a transmembrane protein constitutively expressed by extravascular tissue not normally exposed to the circulating blood. As blood hemorrhages from an injured vessel, it comes into contact with TF-expressing cells outside of the vasculature. TF serves as the membrane receptor and protein cofactor of coagulation factor VIIa (FVIIa). The TF·FVIIa complex initiates the extrinsic blood coagulation pathway by activating factor X (FX) and factor IX (FIX). Activated factor X (FXa) and activated factor IX (FIXa) are initially inhibited by TF pathway inhibitor (TFPI) present in blood at a low concentration (∼2.4 nM) by forming a quaternary FXa·TF·FVIIa·TFPI complex (Baugh et al., 1998; Lu et al., 2004). FIXa forms the tenase complex with its protein cofactor FVIIIa on the surface of phosphatidylserine (PS)-containing cell membranes in the presence of calcium ion, which generates additional FXa. FXa produced on PS-containing cell membranes assembles, in a Ca^{2+}-dependent manner, the prothrombinase complex with its protein cofactor factor Va (FVa). The prothrombinase complex converts prothrombin (FII) into thrombin (FIIa). FIIa cleaves fibrinogen into self-polymerizing, insoluble fibrin to form a plug at the injury site, effectively stemming blood loss. The localization of the procoagulant stimulus to the injury site, as well as anticoagulant effects of the endothelium downstream of the injury, serve to localize blood coagulation to the site of injury. However, pathologically excessive coagulation, or the initiation of coagulation at sites other than blood vessel injury, can result in thrombosis.

Hematogenous spread of metastatic cancer requires tumor cells to intravasate into blood vessels to navigate the bloodstream and establish distant metastases. The existence of tumor cells in the blood of patients with cancer has been known for over a century (Ashworth, 1869), yet only recently has technology allowed the routine cytological detection of these cells, hereafter referred to as circulating tumor cells (CTCs). CTCs have been demonstrated to be prognostic for overall patient survival, yet the impact of CTCs

on cancer associated hypercoagulability has not been established (Cristofanilli et al., 2004; Danila et al., 2007; Cohen et al., 2008; de Bono et al., 2008). *In vitro*, cancer cell lines added to plasma are able to induce coagulation. The ability of cancer cell lines to clot plasma is abrogated by incubating with a TF-blocking antibody, or with Annexin V, which blocks the binding of coagulation factors to the PS-containing cancer cell membrane (Berny-Lang et al., 2011). Further, the clotting kinetics for plasma spiked with cancer cells is strongly dependent upon the number of cells added (Tormoen et al., 2011; Yates et al., 2011; Welsh et al., 2012). Therefore, it appears that cancer cells are wholly capable of cell-mediated coagulation *in vitro*, whereby they can initiate coagulation through surface expression of TF and facilitate the propagation of coagulation by binding and assembling coagulation factor complexes upon their cell membranes.

The ability for CTCs to facilitate coagulation in human disease has not been investigated, primarily due to the previously formidable technical challenge of identifying CTCs in the blood. Technological advancements have allowed the reliable detection of CTCs in patients with cancer through immunofluorescent labeling; specifically, cells that are cytokeratin positive, CD45 negative, and nucleated as apparent with DAPI staining are currently utilized to identify CTCs. On this basis, we sought to develop a functional probe that is amenable to fluorescence microscopic techniques to supplement CTC identification with the ability to characterize the procoagulant nature of CTCs. In this study, we characterized the binding of fluorescently labeled, active site-inhibited coagulation factors VIIa, Xa, and IIa to the metastatic breast cancer cell line, MDA-MB-231, non-metastatic colorectal cell line, SW480, or metastatic colorectal cell line, SW620, in a purified system and in blood plasma. Our approach is modeled after the presumed requirement for procoagulant cells to bind coagulation factors from plasma and subsequently assemble coagulation enzyme complexes on their surface to facilitate cell-mediated coagulation. We focused on coagulation factors in the TF-pathway of coagulation based upon the *in vitro* results demonstrating the TF- and phosphatidylserine (PS)-dependent pathways by which cancer cells mediate coagulation. We hypothesize that the identification and enumeration of procoagulant CTCs will be prognostic for venous thrombosis in patients with cancer.

MATERIALS AND METHODS

All reagents were purchased from Sigma or previously described sources (Berny-Lang et al., 2011). The function-blocking anti-factor XIa antibody 1A6 was obtained as previously described (Tucker et al., 2009). H-Gly-Pro-Arg-Pro-OH (GPRP) was purchased from Calbiochem.

FLUORESCENT PROBES AND REAGENTS

Fluorescein isothiocyante (FITC)-conjugated TF monoclonal antibody was purchased from LifeSpan Biosciences. Human coagulation factors VIIa, Xa, IIa, and fluorescein-conjugated D-Phe-Pro-Arg-chloromethyl ketone (PPACK) were purchased from Haematologic Technologies (Essex Junction, VT, USA).

Coagulation factors were incubated with the fluorophore-conjugated PPACK as previously specified (Bock, 1992; Panizzi et al., 2006). In brief, active site inactivation was verified by comparing PPACK-bound coagulation factor activity toward the chromogenic substrates Spectrozyme FVIIa, Spectrozyme Xa, or Spectrozyme TH (American Diagnostica). Following inactivation, excess PPACK was removed by dialysis using a Slide-A-Lyzer® MINI Dialysis Unit (Thermo Scientific) with 5 mM Hepes and 0.15 M NaCl (pH = 7.40).

CELL CULTURE

The metastatic breast cancer cell line, MDA-MB-231, non-metastatic colorectal cell line, SW480, and metastatic colorectal cell line, SW620, were obtained from American Type Cell Culture. Cells were cultured in Dulbecco's Modified Eagle's Medium (DMEM) containing 10% fetal bovine serum (Gibco) and maintained in a controlled environment at 37°C with 5% CO_2/air atmosphere. Prior to each experiment, cells were detached from the culture flask by immersing in TrypLE Express (Gibco) for 20 min at 37°C, followed by resuspension in complete media, pelleted by subjecting to centrifugation at 210 × *g* for 5 min followed by final resuspension in serum-free DMEM. Resuspended cell concentrations were measured with a hemocytometer.

HUMAN BLOOD AND PLASMA

Blood samples were obtained and managed in accordance with Oregon Health and Science University Review Board approval. Human whole blood was collected from healthy volunteers by venipuncture into 1:9 v/v 3.2% sodium citrate. Platelet poor plasma (PPP) was obtained similarly, except that the collected blood was then subjected to centrifugation step at 2150 × *g* for 10 min, followed by removing the supernatant and mixing with the supernatant from two other donors. The pooled supernatant was then subjected to a second centrifugation step at 2150 × *g* for 10 min. The supernatant (PPP) was then removed, divided into 1 mL aliquots and stored at −80°C prior to use.

ISOLATION OF PERIPHERAL BLOOD CELLS

To isolate human neutrophils, blood was collected 1:9 into 3.8% sodium citrate, followed by a 1:7 dilution into citrate-phosphate-dextrose as previously described (Itakura et al., 2011). In brief, 5 ml of blood suspension was layered over 5 ml of Polymorphprep and subjected to centrifugation at 500 × *g* for 45 min. The neutrophil band was extracted and diluted in Hank's Balanced Salt Suspension (HBSS) to 50 ml, and subjected to centrifugation at 400 × *g* for 10 min. The supernatant was removed and the remaining cell pellet was resuspended in sterile water for 30 s, followed by diluting in 10 mL of 10X PIPES buffer (250 mM piperazine-*N*,*N*′*bis* [2-ethanesulfonic acid], 1.1 mM NaCl, 50 mM KCl, pH = 7.40), then the volume increased to 50 mL with HBSS, and subjected to a final centrifugation step at 400 × *g* for 10 min. Cells were counted with a hemocytometer and diluted to a final concentration of 10^6/mL.

To isolate human platelets, blood was collected as above but then subjected to centrifugation at 200 × *g* for 20 min as previously described (White-Adams et al., 2009). In brief, the supernatant containing plasma and platelets was incubated with 0.10 μg/mL of prostacyclin and subjected to centrifugation at 1000 × *g* for 10 min. The platelet pellet was resuspended in modified Tyrode's buffer (129 mM NaCl, 0.34 mM Na_2HPO_4, 2.9 mM KCl, 12 mM $NaHCO_3$, 20 mM HEPES, 5 mM glucose, 1 mM $MgCl_2$; pH = 7.30).

CLOTTING TIMES

MDA-MB-231, SW480 or SW620 cells were diluted from 3×10^6 to 1.5×10^3 cells/ml in serum-free DMEM. Next, 50 μL of cell suspension or vehicle (DMEM) was mixed with 50 μL of PPP for 180 s at 37°C. Then, 50 μL of 25 mM $CaCl_2$ was added and the time required for the plasma to clot was measured on a KC4 coagulation analyzer (Trinity Biotech, Bray, Co., Wicklow, Ireland). To determine the mechanism of the cancer cell procoagulant activity, 50 μL of 3×10^5 cells/mL were pretreated with a function-blocking anti-TF mAb (50 μg/mL) or the phosphatidylserine function-blocking ligand Annexin V (20 μg/mL) for 5 min at room temperature prior to mixing with plasma. Further, PPP was pretreated with the FXa inhibitor Rivaroxaban (20 μg/mL) for 5 min prior to mixing with cells.

Experiments were performed in duplicate and the average clotting time reported. Clotting time experiments were repeated 3–9 times and plotted as mean ± the standard error of the mean. Statistically significant differences were evaluated using a Student's *T* tests with Bonferroni's correction against untreated cells (⌘ for *p*-value <0.05) or vehicle (* for *p*-value <0.05).

FLOW CYTOMETRY

One-hundred thousand MDA-MB-231 or SW620 cells were suspended in 50 μl of PBS, PPP, or PPP treated with the anti-FXI antibody 1A6 (12.5 μg/mL) and the fibrin polymerization inhibitor Gly-Pro-Arg-Pro-OH (GPRP 10 mM), and 8.3 mM $CaCl_2$ (final concentration). Cell suspensions were incubated with fluorescently labeled coagulation factors FVIIa (50–500 nM), FXa (100–5000 nM) or FIIa (100-10000 nM), or FITC-conjugated anti-TF (10–100 μg/mL) for 30 min at room temperature. Then labeled cells were diluted to 500 μL with PBS and characterized using a FACS Calibur flow cytometer with CellQuest Pro acquisition and analysis software (Becton Dickinson, Franklin Lakes, NJ, USA) as previously described (McCarty et al., 2002).

STATIC ADHESION

Coverslips (#1.5 12 mm; Fischer Scientific) were etched for 30 s in a 70% nitric acid bath, immersed in deionized H_20 ($R = 18.2$ MΩ.cm), rinsed in ethanol, and allowed to air dry. Etched and dried coverslips were then placed in individual wells of a 24-well plate. Five hundred μL of 4% 3-aminopropyltriexothysilane in ethanol was added to the wells and allowed to coat for 2 min. Coverslips were then washed once in ethanol and submerged in H_20 prior to performing the experiments.

Three hundred thousand MDA-MB-231, SW480, or SW620 cells in serum-free DMEM were dispensed onto the etched coverslips and allowed to adhere for 60 min at 37°C. Non-adherent cells were removed by washing with PBS. Recalcified plasma containing the anti-FXIa antibody 1A6 (12.5 μg/mL) and 10 mM GPRP was dispensed over immobilized cells and allowed to incubate for 30 min at room temperature. Cells were washed in PBS, and incubated with fluorescently labeled coagulation factors FVIIa (500 nM), FXa (5 μM), or FIIa (10 μM) or FITC-conjugated anti-TF mAB (50 μg/mL) in PBS for 30 min at room temperature. Labeled cells were washed in PBS, fixed with 3.7% paraformaldehyde, washed in triplicate, and mounted in Fluoromount G (Southern Biotech) and kept at 4°C overnight. Labeled, adherent cells were imaged on a Zeiss Axiovert 200 M at 40× with a Zeiss EC Plan-Neofluar 0.75 NA objective using fluorescence and differential interference contrast (DIC) microscopy. A minimum of three images were recorded from each experimental condition, with representative images shown for each condition.

Binding of coagulation factors to purified populations of peripheral blood cells was performed by dispensing 300 μL of cells onto silanized coverslips and allowing them to adhere for 60 min at 37°C. Cells were then washed and incubated with PBS (vehicle) or PBS containing active site-inhibited, fluorescent coagulation factor probes for 30 min at room temperature. Cells were then washed in PBS, fixed, and mounted as described above.

RESULTS

CLOTTING TIMES

To investigate whether the metastatic breast cancer cell line, MDA-MB-231, non-metastatic colorectal cell line, SW480, or metastatic colorectal cell line, SW620, were sufficient to initiate and propagate blood coagulation, washed cells were suspended in serum-free DMEM and added to recalcified human plasma. The subsequent time required for the plasma to clot (i.e., clotting times) was measured as a function of cell count in a coagulometer (**Figures 1A–C**). All three cancer cell lines hastened the time for plasma to clot as compared to vehicle (DMEM) and the clotting times depended upon the number of cancer cells added to the plasma. To determine the role for cancer cell-expressed TF in initiating clotting, a function-blocking anti-TF mAb (50 μg/mL) was added to the cancer cells prior to mixing with plasma. Our results show that the anti-TF mAb abrogated the ability for SW480 and SW620 cells to clot plasma, and prolonged the clotting times for MDA-MB-231 cells (288.6 s vs. 38.5 s, respectively). We next designed experiments to determine whether cancer cell surface exposed acidic phospholipids were required for clotting. Cancer cells were pretreated with Annexin V (20 μg/mL), which binds to and functionally blocks the ability for PS to bind clotting factors and assemble enzyme complexes on a cell surface. Pretreating SW480 and SW620 cells with Annexin V abrogated the ability of these cells to clot plasma. Pretreatment of MDA-MB-231 cells with Annexin V prolonged clotting times in a concentration-dependent manner (131.2 s at 20 μg/mL vs. 229.1 s at 40 μg/mL). Finally, pretreating the plasma with the FXa inhibitor, Rivaroxaban, prior to mixing with the cancer cells completely abrogated the ability of the three cancer cell lines tested to clot plasma. Taken together, our data demonstrate that MDA-MB-231, SW480, and SW620 cells are procoagulant in a TF, PS, FXa, and cell count dependent manner (**Figures 1D–F**).

FLOW CYTOMETRY OF LABELED CELLS

Labeling of cancer cells in a purified system

We next investigated whether fluorescently labeled, active site-inhibited coagulation factors could be used to label procoagulant cancer cells in a purified system. For this, we utilized the MDA-MB-231 and SW620 cancer cell lines, as they were shown to have the highest and lowest procoagulant activities of the cancer cell lines we tested, respectively, and we aimed to determine if coagulation factor-based probes could label both cell lines as well as contrast the labeling efficacy between cell lines. MDA-MB-231 and SW620 cells

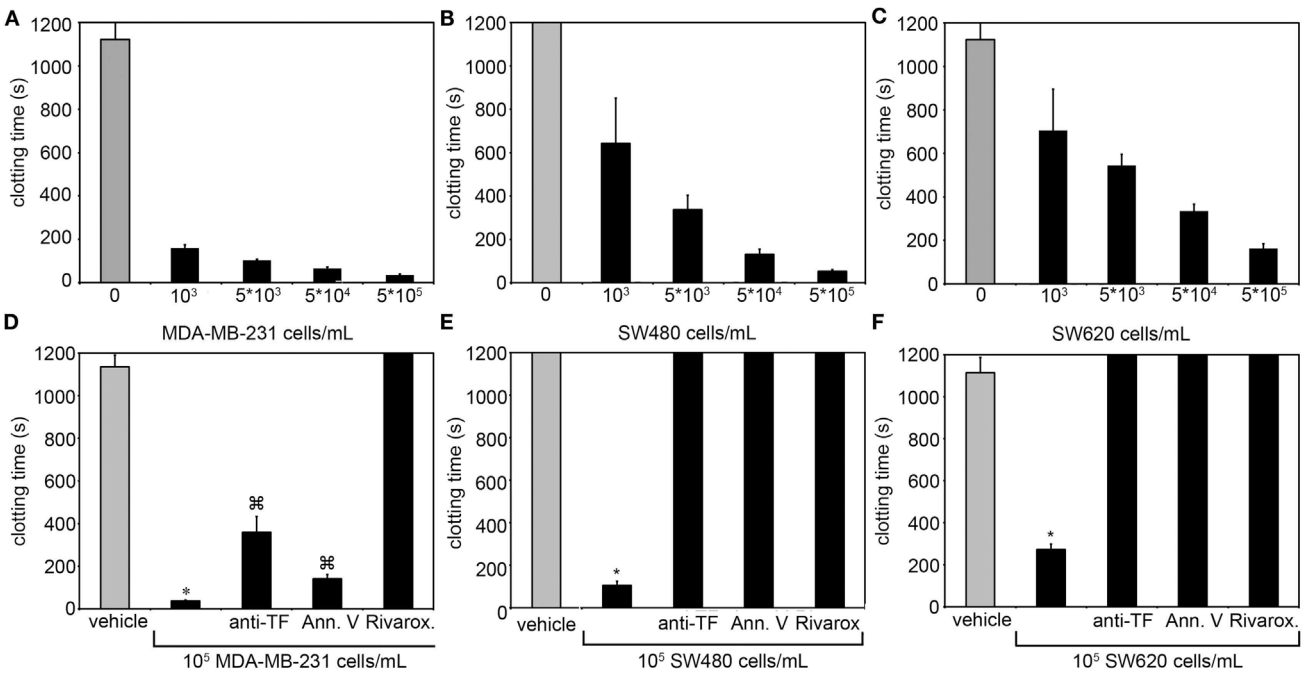

FIGURE 1 | Clotting times for human plasma containing MDA-MB-231, SW480, or SW620 cells. The addition of MDA-MB-231, SW480, and SW620 cells shortened clotting times of plasma in a cell count dependent manner. **(A–C)** The ability for these cells to coagulate plasma was inhibited with a function-blocking antibody to tissue factor (TF) or Annexin V, and completely abrogated with a Factor Xa inhibitor. **(D–F)** Human sodium citrate anticoagulated plasma was pretreated with vehicle or the FXa inhibitor rivaroxaban for 5 min at room temperature. MDA-MB-231, SW480, or SW620 cells were pretreated with vehicle, a neutralizing antibody to TF (anti-TF, 50 μg/mL) or the phosphatidylserine binding protein Annexin V (20 μg/mL) for 5 min at room temperature. Cells and plasma were then mixed together for 3 min on a KC4 coagulation analyzer prior to recalcification to 8.3 mM (final concentration). Clotting time experiments were performed in duplicate for each condition and reported as the average. Each experiment was independently repeated 3–9 times. Data are reported as mean ± SEM. $^{*}P < 0.05$ vs. the absence of cells. $\text{⌘}P < 0.05$ vs. vehicle pretreated cells.

were suspended in serum-free DMEM and incubated with either vehicle or active site-blocked, fluorescently labeled FVIIa (50 nM), FXa (0.5–5 μM), or FIIa (0.5–10 μM) for 30 min at room temperature. Samples were diluted 10-fold in phosphate-buffered saline (PBS) and fluorescence recorded with flow cytometry. **Figure 2** shows the fluorescence intensity histogram for labeled cells vs. vehicle treated controls. The surface expression of TF was verified by staining of the cell lines with a FITC-conjugated anti-TF mAb (data not shown).

Factor VIIa-labeling of MDA-MB-231 cells was clearly evident at 50 nM [mean fluorescence intensity (MFI) = 67 vs. 2.6 for unstained cells] and did not change at 100 nM (MFI = 72; **Figure 2A**). Factor VIIa-labeling of SW620 cells was evident at 50 nM (MFI = 10 vs. 2.86 for unlabeled cells), with further MFI increases observed at 100 and 500 nM (MFI = 16 and 88, respectively; **Figure 2B**). FXa-labeling of MDA-MB-231 and SW620 cells was evident at 500 nM (MFI = 21.05 for MDA-MB-231 and MFI = 33.31 for SW620), with further increases in fluorescence intensity for labeling at 1 and 5 μM (MFI = 49 and 324 for MDA-MB-231, and MFI = 67 and 281 for SW620, respectively). FIIa (thrombin) labeling of MDA-MB-231 cells was not apparent at 100 nM (MFI = 6.17) while SW620 cells (MFI = 9.91) were labeled at 100 nM. MDA-MB-231 cells showed increases in labeling intensity with FIIa-based probes from 500 nM to 10 μM (MFI = 24, 42, 305, and 531 for 500 nM, 1, 5, and 10 μM, respectively). SW620 cells showed increases in labeling intensity from 500 nM to 1 μM (MFI = 37, 90, 282 for 500 nM, 1 and 5 μM, respectively), with no further increase seen at 10 μM (MFI = 258). Labeling of cancer cells in a purified system showed cell and factor-specific characteristics for labeling efficacy. Our data show that a concentration of 50 nM FVIIa-based probe was sufficient to label both the MDA-MB-231 and SW620 cells, while a concentration of 500 nM of the FXa- or FIIa-based probes was required to label both MDA-MB-231 and SW620 cells.

Labeling of cancer cells in human plasma

We next investigated whether fluorescently labeled coagulation factors could be used to label procoagulant cancer cells in plasma. For this, MDA-MB-231and SW620 cells were suspended in sodium citrate anticoagulated PPP containing vehicle or fluorescently labeled FVIIa (50–500 nM), FXa (0.5–5 μM), or FIIa (0.5–10 μM) for 30 min at room temperature. Samples were diluted 10-fold in PBS and fluorescence measured with flow cytometry. **Figure 3** shows the fluorescence intensity histogram for labeled cells vs. vehicle treated controls. The surface expression of TF was verified by staining of the cell lines with a FITC-conjugated anti-TF mAb (data not shown).

Factor VIIa-labeling of MDA-MB-231 cells in plasma was evident at 50 nM (MFI = 13.8 vs. 2.4 for unlabeled cells) and fluorescence labeling increased at probe concentrations of 100 nM

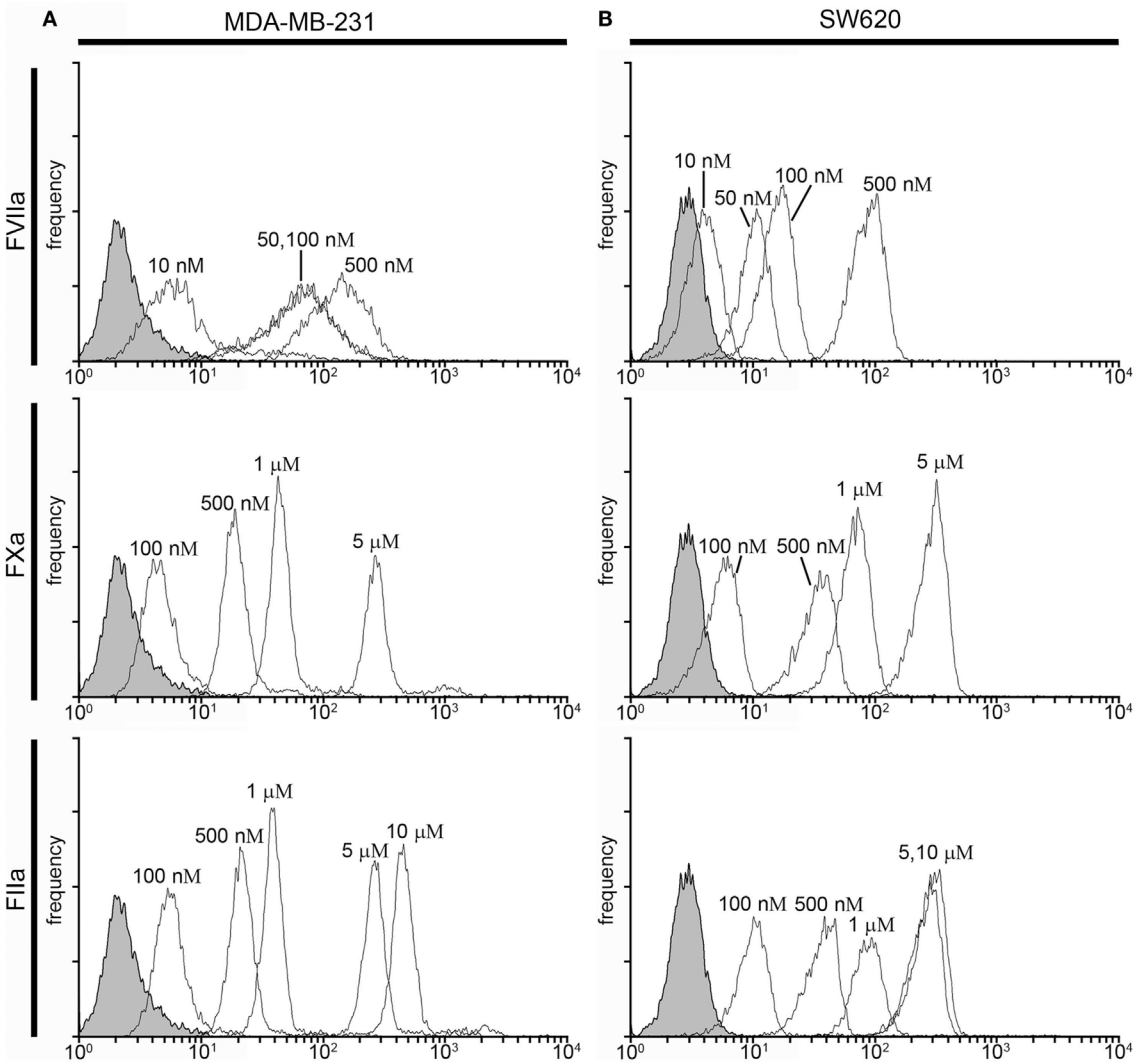

FIGURE 2 | Characterization of fluorescent coagulation factor probe binding to MDA-MB-231 and SW620 cells suspended in DMEM. One-hundred thousand MDA-MB-231 **(A)** or SW620 cells **(B)** were incubated with vehicle or fluorescently modified, active site-inhibited coagulation factors FVIIa (10–500 nM), FXa (100–5000 nM), or FIIa (100–10,000 nM) for 30 min at room temperature. Cells were then diluted 10-fold in sterile-filtered phosphate-buffered saline (PBS, pH = 7.40) and analyzed by flow cytometry. Shaded histograms represent background fluorescence while white histograms represent labeled cells at the fluorescent probe concentrations shown.

(MFI = 18 and 81 for 100 and 500 nM, respectively; **Figure 3A**). FVIIa-based probe labeling of SW620 cells was evident at 50 nM (MFI = 11.7 vs. 2.8 for unlabeled cells) in plasma with a further increases in fluorescence intensity at higher probe concentrations (MFI = 20 and 76 at 100 and 500 nM, respectively; **Figure 3B**). Labeling of MDA-MB-231 cells with the FXa-based probe in plasma was not evident at 100 nM (MFI = 3.9 vs. 2.4 for unlabeled cells), but could be seen at 500 nM (MFI = 11.3), with further increases in fluorescence labeling at higher probe concentrations (MFI = 18.9 and 74.2 for 1 and 5 μM, respectively). Labeling of SW620 cells with the FXa-based probe in plasma was observed at 100 nM (MFI = 8.05 vs. 2.8 for unlabeled cells) and increases in fluorescence intensity were observed at higher probe concentrations (MFI = 22, 35, and 210 at 500 nM, 1 and 5 μM, respectively). FIIa-labeling of MDA-MB-231 cells was observed at 500 nM (MFI = 27 vs. 2.6 for unlabeled cells) with further increases in fluorescence intensity seen with probe concentration (MFI = 47, 321, and 515 for 1, 5, and 10 μM, respectively). In contrast, the FIIa-probe did not label SW620 cells at or below 1 μM FIIa-probe concentration (MFI = 3.8, 4.2, and 6.8 for 100, 500, and 1000 nM, respectively).

Labeling of cancer cells in plasma under conditions of coagulation

In the presence of a procoagulant stimulus, such as a procoagulant cancer cell, coagulation factors in plasma undergo limited proteolysis to become activated. In addition, the presence of Ca^{2+} ions may present Ca-dependent binding sites on cells which are

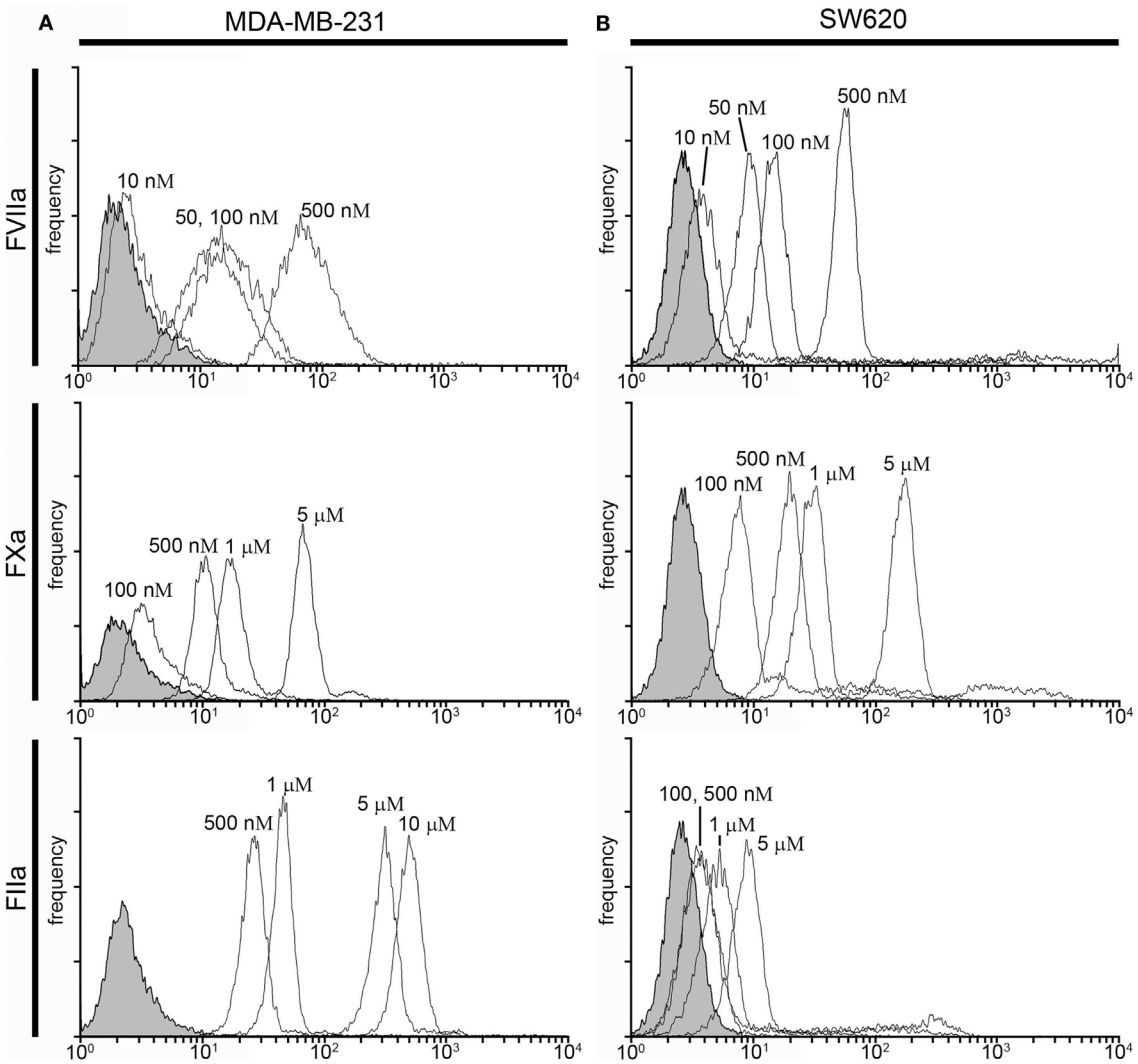

FIGURE 3 | Characterization of fluorescent coagulation factor probe binding to MDA-MB-231 and SW620 cells in human plasma. One-hundred thousand MDA-MB-231 **(A)** or SW620 cells **(B)** were incubated with vehicle or fluorescently modified, active site-inhibited coagulation factors FVIIa (10–500 nM), FXa (100–5000 nM), or FIIa (100–10,000 nM) in 50 μL of PPP for 30 min at room temperature. Cells were then diluted 10-fold in sterile-filtered phosphate-buffered saline (PBS, pH = 7.40) and analyzed by flow cytometry. Shaded histograms represent background fluorescence while white histograms represent labeled cells at the fluorescent probe concentrations shown.

inaccessible in the presence of the anticoagulant, sodium citrate. To determine if coagulation factor-based probes could be used to label procoagulant cancer cells under conditions of coagulation, cancer cells were suspended in PPP pretreated with an anti-FXIa antibody and GPRP and recalcified to 8 mM Ca^{2+} containing vehicle or fluorescently labeled FVIIa (50–500 nM), FXa (0.5–5 μM), or FIIa (0.5–10 μM) for 30 min at room temperature. **Figure 4** shows the fluorescence intensity histogram for labeled cells vs. vehicle treated controls.

FVIIa-labeling of both cell types was evident at 50 nM (MDA-MB-231 MFI = 102 vs. 2.4 for unlabeled cells (**Figure 4A**), SW620 MFI = 11.4 vs. 2.8 for unlabeled cells (**Figure 4B**), and increases in FVIIa-based probe concentrations showed minimal effect on MDA-MB-231 fluorescence intensity (MFI = 122 and 159 for 100 and 500 nM, respectively). SW620 cells exhibited increases in fluorescence intensity with FVIIa-based probe concentrations of 100 and 500 nM (MFI = 23.6 and 112.3, respectively). FXa-labeling of MDA-MB-231 cells was seen at 500 nM (MFI = 15.5 vs. 2.4 for unlabeled cells), and the fluorescence intensity increased with FXa-based probe concentration (MFI = 24 and 90 for 1 and 5 μM, respectively). FXa-based probe labeling of SW620 cells was seen at 500 nM (MFI = 27.3 vs. 2.8 for unlabeled cells) and further increases in fluorescence intensity were seen at FXa-based probe concentrations of 1 and 5 μM, respectively. The FIIa-based probe labeled SW620 cells at but not below 5 μM (MFI = 21 vs. 2.8 for unlabeled cells), while MDA-MB-231 cells were not clearly labeled at 5 μM under conditions of coagulation (MFI = 8.4 vs. 2.4 for unlabeled cells).

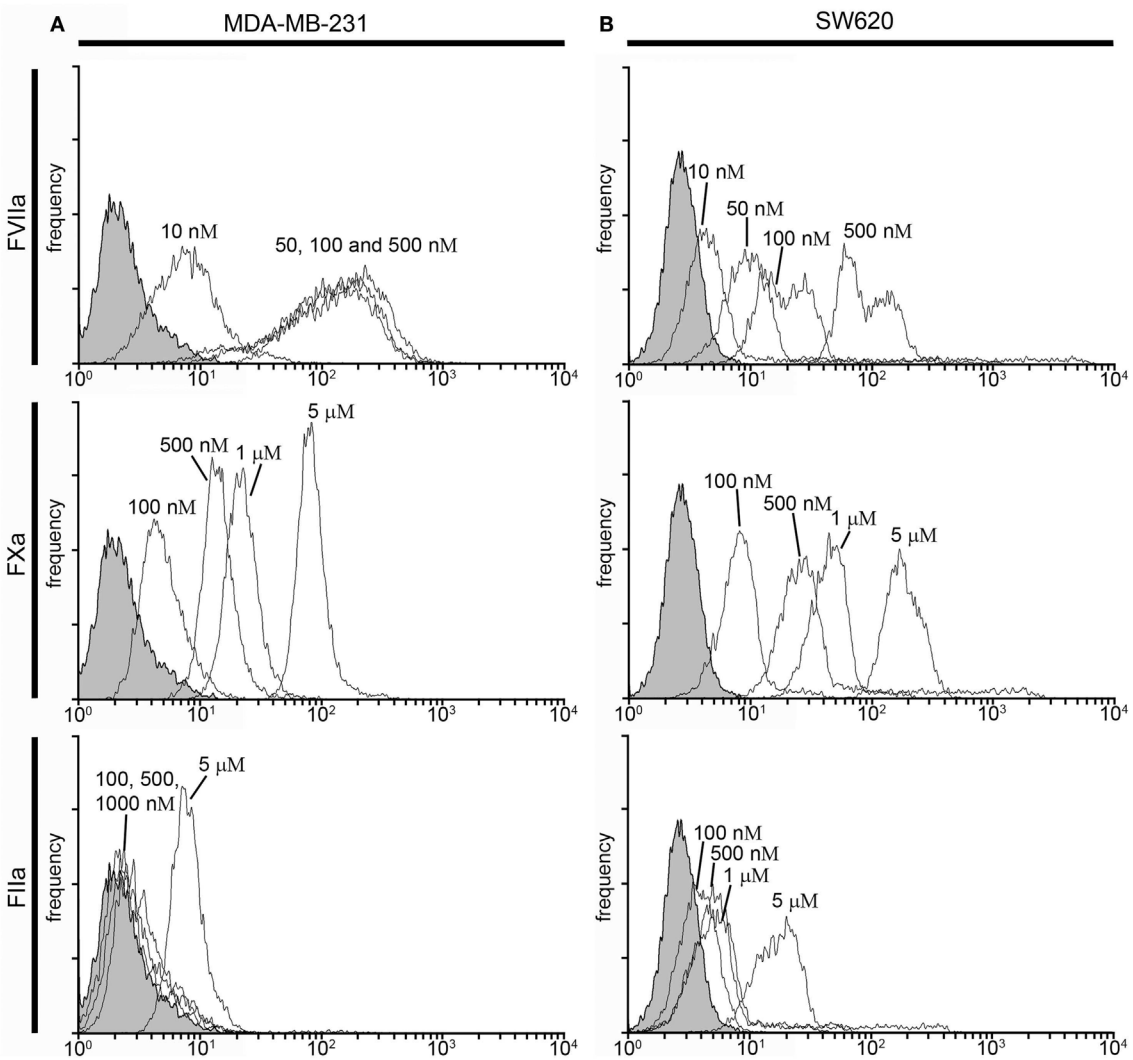

FIGURE 4 | Characterization of fluorescent coagulation factor probe binding to MDA-MB-231 and SW620 cells in human plasma under conditions of coagulation. One-hundred thousand MDA-MB-231 **(A)** or SW620 cells **(B)** were incubated with vehicle or fluorescently modified, active site-inhibited coagulation factors FVIIa (10–500 nM), FXa (100–5000 nM), or FIIa (100–10,000 nM) in 50 μL of recalcified PPP (8 mM, final Ca^{2+} concentration) containing the fibrin polymerization blocker GPRP (10 mM) and the FXIa-blocking antibody 1A6 (12.5 μg/mL) for 30 min at room temperature. Cells were then diluted 10-fold in sterile-filtered phosphate-buffered saline (PBS, pH = 7.40) and analyzed by flow cytometry. Shaded histograms represent background fluorescence while white histograms represent labeled cells at the fluorescent probe concentrations shown.

IMAGING OF IMMOBILIZED CELLS

Labeling of immobilized cancer cells in a purified system

Due to the extreme rarity with which CTCs are present in the blood of patients with cancer, flow cytometry is not routinely utilized to detect CTCs. Rather, various plating or lab-on-chip methods are utilized in combination with fluorescent labels to identify and/or isolate CTCs from a population of cells that consists of both normal blood cell constituents and CTCs (Nagrath et al., 2007; Gleghorn et al., 2010; Marrinucci et al., 2012). We designed a series of experiments to determine whether our labeling strategy was amenable to a cell processing protocol that utilizes cancer cells being plated onto glass slides. We immobilized MDA-MB-231, SW480, and SW620 cells on functionalized glass surfaces and exposed them to fluorescently labeled FVIIa (500 nM), FXa (5 μM), FIIa (10 μM). DIC, fluorescence, and merged images are shown in **Figure 5** for MDA-MB-231, SW480, and SW620 cells. The images showed that the MDA-MB-231 cells were robustly labeled with the FVIIa and FXa probes. The FVIIa and FXa probes weakly labeled the SW480 cells and SW620 cells. The FIIa-probe failed to label any of the three cell lines.

Labeling of immobilized cancer cells following exposure to plasma under conditions of coagulation

Our next set of experiments were designed to determine whether fluorescently labeled coagulation factor probes could label cells that had been exposed to blood plasma under conditions of coagulation. We immobilized MDA-MB-231, SW480, and SW620 cells on functionalized glass surfaces, exposed the immobilized cells

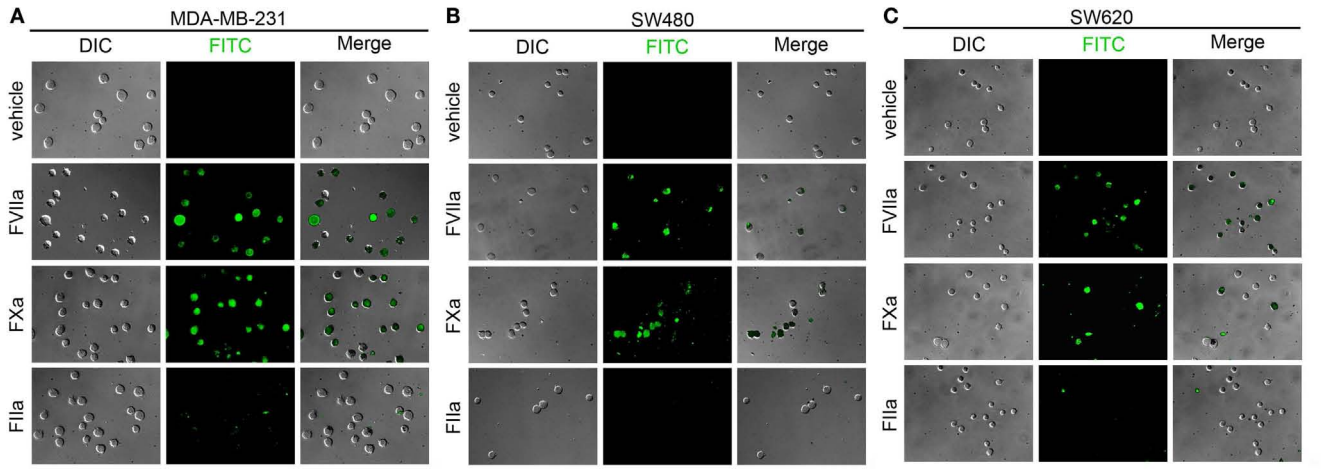

FIGURE 5 | Characterization of fluorescent coagulation factor probe binding to immobilized MDA-MB-231, SW480, and SW620 cells in DMEM. MDA-MB-231 **(A)**, SW480 **(B)**, and SW620 cells **(C)** were immobilized on silanized glass slides prior to incubation with DMEM (vehicle) or DMEM containing fluorescently labeled coagulation factors FVIIa (500 nM), FXa (5 μM), or FIIa (10 μM) for 30 min at room temperature, washed in DMEM and fixed in 3.7% paraformaldehyde. Immobilized cells were imaged using differential interference contrast (DIC) and fluorescence microscopy.

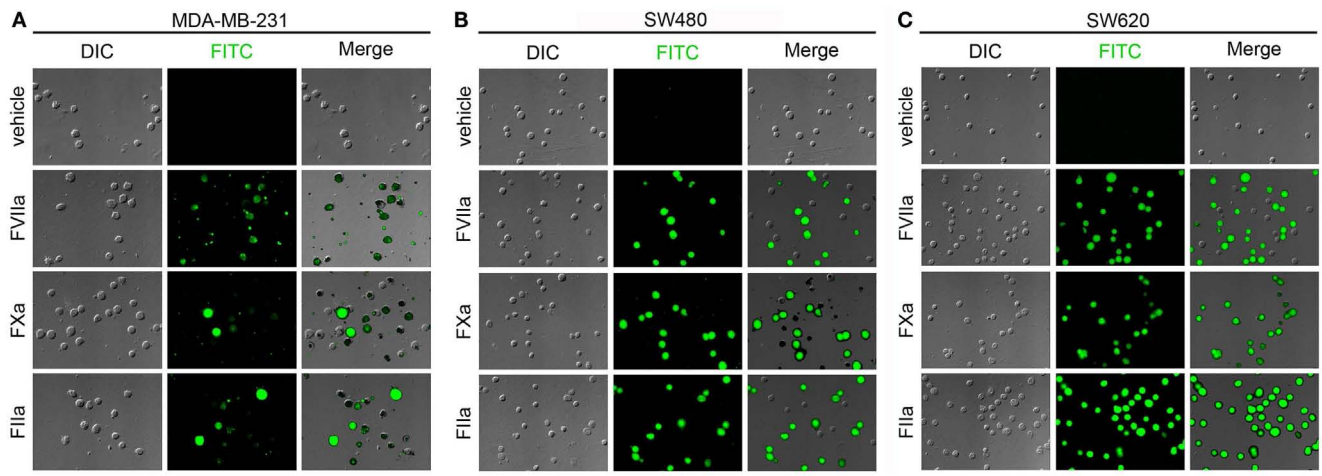

FIGURE 6 | Characterization of fluorescent coagulation factor probe binding to immobilized MDA-MB-231, SW480, and SW620 cells in the presence of coagulation. MDA-MB-231 **(A)**, SW480 **(B)**, and SW620 cells **(C)** were immobilized on silanized glass slides and incubated with recalcified human plasma containing the anti-FXIa antibody, 1A6, and the fibrin polymerization inhibitor, GPRP, for 30 min at room temperature. Cells were then washed and treated with PBS (vehicle) or PBS containing fluorescently labeled coagulation factors FVIIa (500 nM), FXa (5 μM), or FIIa (10 μM) for 30 min at room temperature, washed in PBS, and fixed in 3.7% paraformaldehyde. Immobilized cells were imaged using differential interference contrast (DIC) and fluorescence microscopy.

to recalcified plasma, and then incubated the slides with fluorescently labeled FVIIa (500 nM), FXa (5 μM), or FIIa (10 μM). DIC, fluorescence, and merged images are shown in **Figure 6** for MDA-MB-231, SW480, and SW620 cells. The images showed that all coagulation factor-based probes labeled at least a portion of the adherent cancer cells for all three cancer cell lines. The FVIIa probe labeled all the adherent MDA-MB-231 cells. Heterogeneous FVIIa-labeling was observed for both the SW480 and SW620 cell lines, with some of the adherent cells labeling brightly, while other cells on the same slide were not labeled by the FVIIa probe. The FXa probe showed complete labeling of all three cell lines, but pronounced heterogeneity in labeling was noted as some cells were brightly labeled and others showed dim labeling by the FXa probe. The FIIa-probe showed complete labeling of the MDA-MB-231 and SW620 cell lines and heterogeneous labeling of the SW480 cells.

Labeling of immobilized cancer cells in whole blood

Following our experiments in cell-free labeling buffers, we next determined whether coagulation factor-based probes could be used to label cancer cells in whole blood. Immobilized MDA-MB-231, SW480, and SW620 cells were incubated with anticoagulated

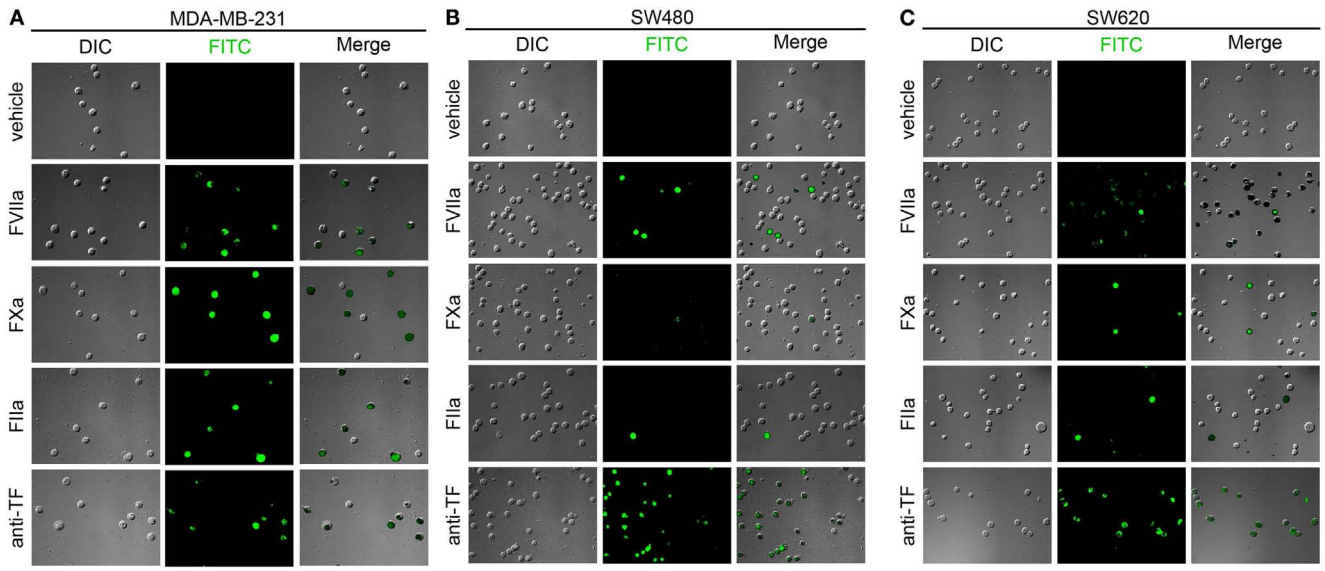

FIGURE 7 | Characterization of fluorescent coagulation factor probe binding to immobilized MDA-MB-231, SW480, and SW620 cells in whole blood. MDA-MB-231 **(A)**, SW480 **(B)**, and SW620 cells **(C)** were immobilized on silanized glass slides and incubated with sodium citrate anticoagulated whole blood (vehicle) containing fluorescently labeled coagulation factors FVIIa (500 nM), FXa (5 μM), FIIa (10 μM), or FITC-conjugated anti-TF mAb (50 μg/mL) for 30 min at room temperature, washed in PBS and fixed in 3.7% paraformaldehyde. Immobilized cells were imaged using differential interference contrast (DIC) and fluorescence microscopy.

whole blood containing either vehicle, or fluorescent, active site-inhibited FVIIa (500 nM), FXa (5 μM), FIIa (10 μM), or FITC-conjugated anti-TF mAb (50 μg/mL) for 30 min at room temperature. DIC, fluorescence, and merged images are shown in **Figure 7**. The FVIIa probe showed heterogeneous labeling of the MDA-MB-231 cells, SW480, and SW620 cells, although the labeling of the SW480 cells was greatly diminished as compared to cells which had been exposed to plasma under conditions of coagulation (**Figure 6**). Heterogeneous labeling of all three cell lines with the FXa and FIIa-probes was observed, with very few SW480 or SW620 cells labeled. All three cell lines were labeled with the anti-TF mAb in whole blood.

Labeling of immobilized platelets and neutrophils

Following the reduced labeling of the MDA-MB-231 cells, SW480, and SW620 cells in whole blood as compared to cell-free labeling solutions, we designed a set of experiments to determine if peripheral blood cells might be binding the probe in solution, and thereby causing diminished labeling of immobilized cancer cells. Neutrophils and platelets were purified from peripheral blood draws and immobilized onto silanized glass slides, and incubated with fluorescent FVIIa (500 nM), FXa (5 μM), and FIIa (10 μM). Coagulation factor-based probes failed to bind immobilized peripheral blood cells in a purified system (**Figure 8**). Our data show that neither the FVIIa (500 nM), FXa (5 μM), FIIa (10 μM) probes labeled purified human platelets (**Figure 8A**) or neutrophils (**Figure 8B**). In a complementary experiment, addition of purified human neutrophils to plasma failed to reduce clotting times (605.3 s vs. 672.7 s for vehicle and 10^5/mL neutrophils, respectively) demonstrating that purified human neutrophils did not exhibit a procoagulant phenotype. Similar fluorescent coagulation factor labeling results were observed in whole blood (data not shown).

DISCUSSION

Metastatic disease accounts for the majority of cancer deaths. VTE events are significant contributors to metastatic disease, with reports indicating 18% of cancer deaths resulting from VTE. For instance, lung adenocarcinoma patients have an estimated 20-fold higher risk for developing VTE than the general population; however, not all patients develop VTE, making the bleeding risks of anticoagulating the entire adenocarcinoma patient population unacceptable. No current technology is available to objectively predict patient risk for VTE in order to personalize anticoagulant prophylaxis therapy. CTC counts have not been evaluated as a potential biomarker for risk to develop cancer associated thrombosis.

In this study, we demonstrate the use of fluorescently modified, active site-inhibited coagulation factors to label procoagulant cancer cells. The metastatic breast cancer cell line, MDA-MB-231, and metastatic colorectal cell line, SW620, were used due to the fact that these cell lines possess the ability to survive circulation in the blood to establish hematogenous metastases in murine models of cancer metastasis (Zhang et al., 1991; Sampson-Johannes et al., 1996). The non-metastatic colorectal cell line, SW480, was derived from the primary tumor from the same individual from which the SW620 was derived. We determined that all three cell lines exhibited a procoagulant phenotype, with the MDA-MB-231 cells resulting in the highest procoagulant activity, while the SW620 cells had the lowest procoagulant activity. The procoagulant activity of the MDA-MB-231, SW480, and SW620 cell lines could be reduced or abrogated by a function-blocking antibody to TF, or

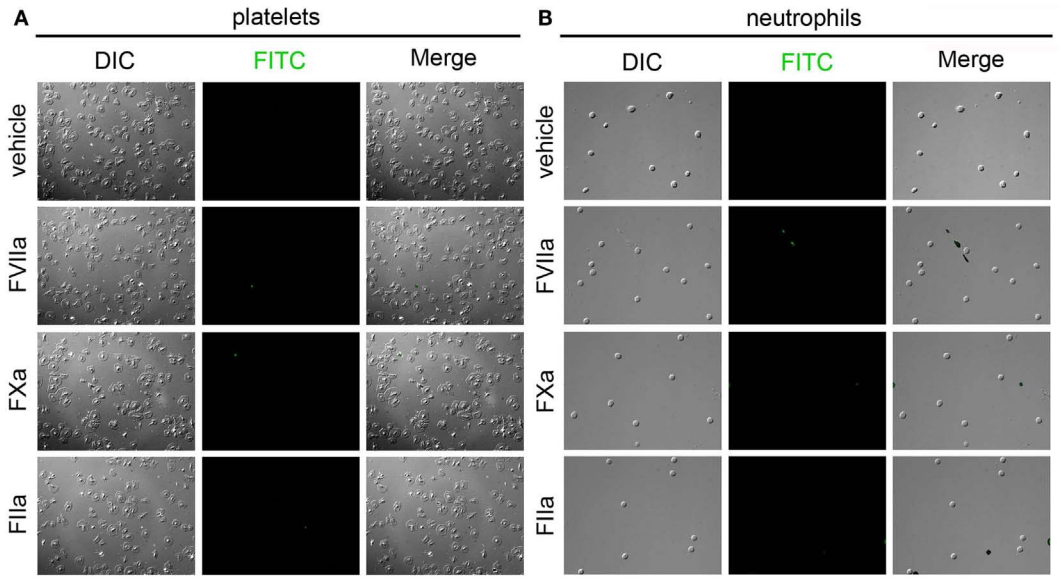

FIGURE 8 | Characterization of fluorescent coagulation factor probe binding to immobilized human neutrophils and platelets. Human platelets **(A)** and neutrophils **(B)** were immobilized on silanized glass slides and incubated with PBS (vehicle) containing fluorescently labeled coagulation factors FVIIa (500 nM), FXa (5 μM), or FIIa (10 μM) for 30 min at room temperature, washed in PBS and fixed in 3.7% paraformaldehyde. Immobilized cells were imaged using differential interference contrast (DIC) and fluorescence microscopy.

by pretreatment with Annexin V. Annexin V blocks the binding of coagulation factors that contain γ-carboxyglutamic acid domains (Gla domains) to PS on the cell membrane. These results support the notion that TF and PS exposure is a general phenomenon seen for cancer cell-mediated coagulation *in vitro*, and support a role for CTC-mediated coagulation as a potential contributor to the hypercoagulability seen for patients with cancer.

Previous studies have shown that cancer cell procoagulant activity correlates better with PS exposure than with overall TF expression levels, supporting a role for cell membrane effects in regulating procoagulant activity as opposed to surface TF expression (Barrowcliffe et al., 2002; Pickering et al., 2004). Therefore, we aim to develop a function-based CTC labeling strategy to determine whether CTCs are procoagulant, and whether CTC enumeration and procoagulant characterization strategies are clinically useful in predicting thrombosis in patients with cancer. We hypothesized that coagulation factors themselves would serve as specific, functional probes with which to identify procoagulant cells. Our approach was based upon the requirement for coagulation factors to for surface-assembled enzyme complexes on the surfaces of procoagulant cells in order to catalyze intermediate steps of the coagulation cascade. We focused on the coagulation factors FVIIa, FXa, and FIIa, as they are key components of the extrinsic (TF) pathway of coagulation.

Our results with flow cytometry show that the cancer cell lines MDA-MB-231, SW480, and SW620 bind coagulation factor probes. Immobilized cells show that cancer cells exhibited heterogeneity in their ability to bind various fluorescently modified active site-inhibited coagulation factors. For instance, we observed heterogeneous labeling of SW480 with the FVIIa probe in a both a purified system and in whole blood. Binding heterogeneity was observed over a range of probe concentrations (data not shown), suggesting the heterogeneity was not due to a scarcity of probe concentration. Further, the K_D for FVIIa to TF is in the pM range, five orders of magnitude below our labeling concentration. A stronger binding of FVIIa could suggest that these cells are more procoagulant than cells that show weak binding, however, currently no method can be used to determine individual cell procoagulant activity. Moreover, protease activated receptor 2 (PAR2) is another known receptor for FVIIa besides TF. MDA-MB-231 and SW620 cells are known to express PAR2, while SW480 cells have been shown to have little PAR2 surface expression (Morris et al., 2006; Zhou et al., 2008). Whether coagulation factor probe binding levels correlate with procoagulant activity or whether PAR2 expression levels affect binding of FVIIa probe is a focus of future studies.

FIIa-based probes brightly labeled immobilized MDA-MB-231, SW480, and SW620 cells in the presence of coagulation. In contrast, FIIa-probes only weakly labeled these cell lines in whole blood and failed to label any cells in DMEM. One prominent difference between FIIa and the other coagulation factor probes is the absence of the Gla domain for FIIa. The Gla domain mediates calcium ion-dependent binding of vitamin K-dependent coagulation factors to PS-containing procoagulant cell membranes. Calcium-dependent binding may account for differences in the FVIIa or FXa probe labeling as compared to FIIa in DMEM, which contains calcium, but fails to account for differences in whole blood in the presence of the calcium-chelator sodium citrate. As FIIa binds fibrinogen and fibrin, it is possible that FIIa labeled cancer cells that are coated in fibrin, a phenomenon that would be expected after exposing a procoagulant cancer cell to plasma under conditions of coagulation. However, using flow cytometry, we observed labeling of cancer cells with a FIIa-based probe in purified systems,

suggesting an alternate mechanism for binding of FIIa to the cancer cell surface. Our future work will be focused on identifying the mechanism(s) of FIIa-cancer cell binding.

In this study, we demonstrated the use of fluorescently modified, active site-inhibited coagulation factors to label procoagulant cancer cells. We demonstrated that coagulation factors based probes bound to cancer cell lines in purified systems and in whole blood, yet failed to bind to peripheral blood cells. Labeling of cancer cells was demonstrated via flow cytometry in purified systems, as well as on an immobilized-cell platform similar to what is currently used in some CTC detection platforms. This work is the first step in the development of a function-based CTC labeling strategy to determine whether CTCs are procoagulant, and whether CTC enumeration and procoagulant characterization strategies are clinically useful in predicting thrombosis in patients with cancer.

ACKNOWLEDGMENTS

We thank Drs. Michelle Berny-Lang, Kelly Bethel, and Peter Kuhn for insightful discussions. We thank Jiaqing Pang for technical assistance in preparing fluorescent probes. This research was supported in part by the OHSU Knight Cancer Institute (Owen J. T. McCarty), the American Heart Association (12PRE11930019 to Garth W. Tormoen), and the NIH (R01HL101972 and U54CA143906 to Owen J. T. McCarty, R01HL101972-S1 to Flor A. Cianchetti, T32-CA106195 to Garth W. Tormoen, and R01HL038779 to Paul E. Bock). Garth W. Tormoen is an Achievement Rewards for College Scientists scholar.

REFERENCES

Akl, E. A., Vasireddi, S. R., Gunukula, S., Yosuico, V. E., Barba, M., Terrenato, I., Sperati, F., and Schunemann, H. (2011). Oral anticoagulation in patients with cancer who have no therapeutic or prophylactic indication for anticoagulation. *Cochrane Database Syst. Rev.* CD006466.

Ashworth, T. R. (1869). A case of cancer in which cells similar to those in the tumours were seen in the blood after death. *Aust. Med. J.* 14, 146–147.

Baron, J. A., Gridley, G., Weiderpass, E., Nyren, O., and Linet, M. (1998). Venous thromboembolism and cancer. *Lancet* 351, 1077–1080.

Barrowcliffe, T. W., Fabregas, P., Jardi, M., Cancelas, J., Rabaneda, M., and Felez, J. (2002). Procoagulant activity of T lymphoblastoid cells due to exposure of negatively charged phospholipid. *Thromb. Haemost.* 87, 442–449.

Baugh, R. J., Broze, G. J. Jr., and Krishnaswamy, S. (1998). Regulation of extrinsic pathway factor Xa formation by tissue factor pathway inhibitor. *J. Biol. Chem.* 273, 4378–4386.

Berny-Lang, M. A., Aslan, J. E., Tormoen, G. W., Patel, I. A., Bock, P. E., Gruber, A., and McCarty, O. J. (2011). Promotion of experimental thrombus formation by the procoagulant activity of breast cancer cells. *Phys. Biol.* 8, 015014.

Bock, P. E. (1992). Active-site-selective labeling of blood coagulation proteinases with fluorescence probes by the use of thioester peptide chloromethyl ketones. II. Properties of thrombin derivatives as reporters of prothrombin fragment 2 binding and specificity of the labeling approach for other proteinases. *J. Biol. Chem.* 267, 14974–14981.

Cohen, S. J., Punt, C. J., Iannotti, N., Saidman, B. H., Sabbath, K. D., Gabrail, N. Y., Picus, J., Morse, M., Mitchell, E., Miller, M. C., Doyle, G. V., Tissing, H., Terstappen, L. W., and Meropol, N. J. (2008). Relationship of circulating tumor cells to tumor response, progression-free survival, and overall survival in patients with metastatic colorectal cancer. *J. Clin. Oncol.* 26, 3213–3221.

Cristofanilli, M., Budd, G. T., Ellis, M. J., Stopeck, A., Matera, J., Miller, M. C., Reuben, J. M., Doyle, G. V., Allard, W. J., Terstappen, L. W., and Hayes, D. F. (2004). Circulating tumor cells, disease progression, and survival in metastatic breast cancer. *N. Engl. J. Med.* 351, 781–791.

Danila, D. C., Heller, G., Gignac, G. A., Gonzalez-Espinoza, R., Anand, A., Tanaka, E., Lilja, H., Schwartz, L., Larson, S., Fleisher, M., and Scher, H. I. (2007). Circulating tumor cell number and prognosis in progressive castration-resistant prostate cancer. *Clin. Cancer Res.* 13, 7053–7058.

de Bono, J. S., Scher, H. I., Montgomery, R. B., Parker, C., Miller, M. C., Tissing, H., Doyle, G. V., Terstappen, L. W., Pienta, K. J., and Raghavan, D. (2008). Circulating tumor cells predict survival benefit from treatment in metastatic castration-resistant prostate cancer. *Clin. Cancer Res.* 14, 6302–6309.

Falanga, A., and Marchetti, M. (2009). Venous thromboembolism in the hematologic malignancies. *J. Clin. Oncol.* 27, 4848–4857.

Gleghorn, J. P., Pratt, E. D., Denning, D., Liu, H., Bander, N. H., Tagawa, S. T., Nanus, D. M., Giannakakou, P. A., and Kirby, B. J. (2010). Capture of circulating tumor cells from whole blood of prostate cancer patients using geometrically enhanced differential immunocapture (GEDI) and a prostate-specific antibody. *Lab. Chip* 10, 27–29.

Itakura, A., Verbout, N. G., Phillips, K. G., Insall, R. H., Gailani, D., Tucker, E. I., Gruber, A., and McCarty, O. J. (2011). Activated factor XI inhibits chemotaxis of polymorphonuclear leukocytes. *J. Leukoc. Biol.* 90, 923–927.

Lu, G., Broze, G. J. Jr., and Krishnaswamy, S. (2004). Formation of factors IXa and Xa by the extrinsic pathway: differential regulation by tissue factor pathway inhibitor and antithrombin III. *J. Biol. Chem.* 279, 17241–17249.

Marrinucci, D., Bethel, K., Kolatkar, A., Luttgen, M. S., Malchiodi, M., Baehring, F., Voigt, K., Lazar, D., Nieva, J., Bazhenova, L., Ko, A. H., Korn, W. M., Schram, E., Coward, M., Yang, X., Metzner, T., Lamy, R., Honnatti, M., Yoshioka, C., Kunken, J., Petrova, Y., Sok, D., Nelson, D., and Kuhn, P. (2012). Fluid biopsy in patients with metastatic prostate, pancreatic and breast cancers. *Phys. Biol.* 9, 016003.

McCarty, O. J., Jadhav, S., Burdick, M. M., Bell, W. R., and Konstantopoulos, K. (2002). Fluid shear regulates the kinetics and molecular mechanisms of activation-dependent platelet binding to colon carcinoma cells. *Biophys. J.* 83, 836–848.

Morris, D. R., Ding, Y., Ricks, T. K., Gullapalli, A., Wolfe, B. L., and Trejo, J. (2006). Protease-activated receptor-2 is essential for factor VIIa and Xa-induced signaling, migration, and invasion of breast cancer cells. *Cancer Res.* 66, 307–314.

Nagrath, S., Sequist, L. V., Maheswaran, S., Bell, D. W., Irimia, D., Ulkus, L., Smith, M. R., Kwak, E. L., Digumarthy, S., Muzikansky, A., Ryan, P., Balis, U. J., Tompkins, R. G., Haber, D. A., and Toner, M. (2007). Isolation of rare circulating tumour cells in cancer patients by microchip technology. *Nature* 450, 1235–1239.

Panizzi, P., Friedrich, R., Fuentes-Prior, P., Kroh, H. K., Briggs, J., Tans, G., Bode, W., and Bock, P. E. (2006). Novel fluorescent prothrombin analogs as probes of staphylocoagulase-prothrombin interactions. *J. Biol. Chem.* 281, 1169–1178.

Pickering, W., Gray, E., Goodall, A. H., Ran, S., Thorpe, P. E., and Barrowcliffe, T. W. (2004). Characterization of the cell-surface procoagulant activity of T-lymphoblastoid cell lines. *J. Thromb. Haemost.* 2, 459–467.

Rickles, F. R., and Levine, M. N. (2001). Epidemiology of thrombosis in cancer. *Acta Haematol.* 106, 6–12.

Sampson-Johannes, A., Wang, W., and Shtivelman, E. (1996). Colonization of human lung grafts in SCID-hu mice by human colon carcinoma cells. *Int. J. Cancer* 65, 864–869.

Sorensen, H. T., Mellemkjaer, L., Olsen, J. H., and Baron, J. A. (2000). Prognosis of cancers associated with venous thromboembolism. *N. Engl. J. Med.* 343, 1846–1850.

Tormoen, G. W., Rugonyi, S., Gruber, A., and McCarty, O. J. (2011). The role of carrier number on the procoagulant activity of tissue factor in blood and plasma. *Phys. Biol.* 8, 066005.

Trousseau, A. (1865). *Phlegmasia Alba Dolens. Clinique Medicale de l'Hotel-Dieu de Paris.* Paris: The Syndenham Society, 654–712.

Tucker, E. I., Marzec, U. M., White, T. C., Hurst, S., Rugonyi, S., McCarty, O. J., Gailani, D., Gruber, A., and Hanson, S. R. (2009). Prevention of vascular graft occlusion and thrombus-associated thrombin generation by inhibition of factor XI. *Blood* 113, 936–944.

Welsh, J., Smith, J. D., Yates, K. R., Greenman, J., Maraveyas, A., and Madden, L. A. (2012). Tissue factor expression determines tumour cell coagulation kinetics. *Int. J. Lab. Hematol.* 34, 396–402.

White-Adams, T. C., Berny, M. A., Tucker, E. I., Gertz, J. M., Gailani, D., Urbanus, R. T., De Groot, P. G., Gruber, A., and McCarty, O. J. (2009). Identification of coagulation factor XI as a ligand for platelet apolipoprotein E receptor 2 (ApoER2). *Arterioscler. Thromb. Vasc. Biol.* 29, 1602–1607.

Yates, K. R., Welsh, J., Echrish, H. H., Greenman, J., Maraveyas, A., and Madden, L. A. (2011). Pancreatic cancer cell and microparticle procoagulant surface characterization: involvement of membrane-expressed tissue factor, phosphatidylserine and phosphatidylethanolamine. *Blood Coagul. Fibrinolysis* 22, 680–687.

Zhang, R. D., Fidler, I. J., and Price, J. E. (1991). Relative malignant potential of human breast carcinoma cell lines established from pleural effusions and a brain metastasis. *Invasion Metastasis* 11, 204–215.

Zhou, H., Hu, H., Shi, W., Ling, S., Wang, T., and Wang, H. (2008). The expression and the functional roles of tissue factor and protease-activated receptor-2 on SW620 cells. *Oncol. Rep.* 20, 1069–1076.

Conflict of Interest Statement: The authors declare that the research was conducted in the absence of any commercial or financial relationships that could be construed as a potential conflict of interest.

Received: 01 June 2012; accepted: 15 August 2012; published online: 06 September 2012.

Citation: Tormoen GW, Cianchetti FA, Bock PE and McCarty OJT (2012) Development of coagulation factor probes for the identification of procoagulant circulating tumor cells. Front. Oncol. ***2****:110. doi: 10.3389/fonc.2012.00110*

This article was submitted to Frontiers in Cancer Molecular Targets and Therapeutics, a specialty of Frontiers in Oncology.

frontiers in ONCOLOGY

REVIEW ARTICLE
published: 11 October 2012
doi: 10.3389/fonc.2012.00131

Isolation and characterization of circulating tumor cells in prostate cancer

Elan Diamond[1], Guang Yu Lee[1], Naveed H. Akhtar[1], Brian J. Kirby[1,2], Paraskevi Giannakakou[1], Scott T. Tagawa[1] and David M. Nanus[1]*

[1] Division of Hematology and Medical Oncology, Weill Cornell Medical College, New York, NY, USA
[2] Sibley School of Mechanical and Aerospace Engineering, Cornell University, Ithaca, NY, USA

Edited by:
Michael R. King, Cornell University, USA

Reviewed by:
Owen McCarty, Oregon Health and Science University, USA
Jeffrey Chalmers, The Ohio State University, USA
John A. Viator, University of Missouri, USA

***Correspondence:**
David M. Nanus, Division of Hematology and Medical Oncology, Weill Cornell Medical College, 1305 York Avenue, Room 741, New York, NY 10021, USA.
e-mail: dnanus@med.cornell.edu

Circulating tumor cells (CTCs) are tumor cells found in the peripheral blood that putatively originate from established sites of malignancy and likely have metastatic potential. Analysis of CTCs has demonstrated promise as a prognostic marker as well as a source of identifying potential targets for novel therapeutics. Isolation and characterization of these cells for study, however, remain challenging owing to their rarity in comparison with other cellular components of the peripheral blood. Several techniques that exploit the unique biochemical properties of CTCs have been developed to facilitate their isolation. Positive selection of CTCs has been achieved using microfluidic surfaces coated with antibodies against epithelial cell markers or tumor-specific antigens such as EpCAM or prostate-specific membrane antigen (PSMA). Following isolation, characterization of CTCs may help guide clinical decision making. For instance, molecular and genetic characterization may shed light on the development of chemotherapy resistance and mechanisms of metastasis without the need for a tissue biopsy. This paper will review novel isolation techniques to capture CTCs from patients with advanced prostate cancer, as well as efforts to characterize the CTCs. We will also review how these analyzes can assist in clinical decision making. **Conclusion:** The study of CTCs provides insight into the molecular biology of tumors of prostate origin that will eventually guide the development of tailored therapeutics. These advances are predicated on high yield and accurate isolation techniques that exploit the unique biochemical features of these cells.

Keywords: prostate cancer, circulating tumor cells (CTCs), prostate-specific membrane antigen (PSMA), microfluidic device, androgen receptor (AR)

INTRODUCTION

Tumor metastases are a major cause of cancer morbidity and mortality. The precise mechanisms underlying the development of metastases, however, remain poorly understood. Simply stated, this process requires the migration of malignant cells from a primary tumor to distant sites where these cells establish secondary tumors. Circulating tumor cells (CTCs), which were first detected in the blood of an autopsy patient who died from cancer in 1869, are thought to represent tumor cells in transit, some of which will result in metastases (Ashworth, 1869). These cells are capable of intravasation from a primary tumor, undergoing phenotypic alterations that enable intravascular survival, extravasation from the blood vessel, implantation in a target tissue, and proliferation to form a tumor metastasis. Attempts to study CTCs are limited by their rarity, with concentrations as low as one CTC per billion circulating hematopoietic cells. CTCs must therefore be enriched, isolated, and properly identified, in order to be clinically useful. Techniques that exploit the unique physical and biochemical features of CTCs are currently being developed and utilized in order to isolate and identify CTCs from whole blood samples obtained from cancer patients. Currently, there are numerous techniques available to detect and isolate CTCs (**Table 1**). With the exception of the CellSearch Circulating Tumor Cell Test, these techniques have not yet been approved by the Food and Drug Administration (FDA) for clinical use. CTC enumeration using the CellSearch device has already been shown to correlate with patient outcomes in a variety of malignancies, including prostate cancer (Danila et al., 2007). Capture technologies may also provide rare opportunities to perform molecular and genetic analyses of tumor-derived cells at sequential time points without invasive tissue biopsies. Thus, CTCs conceptually provide insight into the biology of a patient's tumor that may facilitate the development of new therapeutic options and enable clinicians to tailor therapy to an individual patient in a longitudinal fashion (van de Stolpe et al., 2011). It follows that CTC isolation can replace biopsies and noninvasively yield valuable information about the evolving status of a patient's disease.

Analyzing peripheral blood is an attractive alternative to currently available methods of obtaining tissue in prostate cancer owing to the unique challenges presented by this disease. A man with prostate cancer may not develop metastases until many years (5–15 years) after treatment of his original tumor in the prostate. Thus, performing a molecular analysis of archived prostate cancer tissue may be complicated by the inability to obtain old pathology specimens and by the possible irrelevance of that tissue sample to the current status of the patient's disease.

Table 1 | Summary of techniques used to isolate prostatic CTCs.

Method	Mechanism	Volume of blood used (ml)	Capture rate	References
Density gradient centrifugation	Differential migration of CTCs during centrifugation	Variable	70%	Rosenberg et al., 2002; Gertler et al., 2003; Kuhn and Bethel, 2012
Size-dependent selection	Separation based on cell diameter	6–7.5	90%	Vona et al., 2000; Lin et al., 2010; Farace et al., 2011
Immunomagnetic bead-based capture (CellSearch)	Positive selection using EpCAM coated magnetic beads	7.5	85%	Tibbe et al., 2002; Allard et al., 2004; Balic et al., 2005
Antibody-based negative selection	Depletion of normal blood cells using CD-45 coated magnetic beads	2.5 ml	52–88.4%	Wang et al., 2000; Zigeuner et al., 2000, 2003; Jatana et al., 2010; Liu et al., 2011; Schmidt et al., 2004
Flow cytometry	Cell sorting using fluorescently labeled epithelial antigens	NA	NA	Racila et al., 1998; He et al., 2008; Wu et al., 2011
Microfluidic device	Positive selection of CTCs using antibodies attached to microfluidic device	1–5.1	60–91.8%	Nagrath et al., 2007; Gleghorn et al., 2010; Stott et al., 2010a,b; Mayer et al., 2011; Kirby et al., 2012; Santana et al., 2012

Ideally, a tumor biopsy for molecular study would be obtained at the time of relapse, but as many men have only bone metastases, it is difficult to obtain adequate and representative tumor cells for study. In a disease for which a blood test measuring prostate specific antigen (PSA) is sufficiently specific to support the diagnosis of prostate cancer, it is difficult clinically to justify a biopsy. Consequently, analysis of peripheral blood overcomes these obstacles by easily providing clinically relevant tumor cells for study.

Ideally, a robust CTC capture technique would be highly sensitive, specific, reproducible, and automated (Doyen et al., 2012). It should have the ability to reliably capture a high percentage of CTCs present in a sample while minimizing the number of false positive events and contamination from non-malignant cells. The design of the test should be simple enough that it can be mass-produced and be performed in clinical laboratories with minimal inter-operator variability. It should also have the ability to both quantify and characterize CTCs in order to limit operator bias. Most importantly, in order to be clinically useful, a CTC capture technology should have proven clinical relevance confirmed in multiple prospective clinical trials. In this chapter, we will review the currently available CTC enrichment technologies with an emphasis on prostate cancer as well highlight current and future applications of these technologies.

CTC DETECTION METHODS

Accurate characterization of CTCs is essential to the development of these cells as a clinical biomarker and substrate for laboratory experimentation. There is currently, however, no "gold standard" approach for the specific identification of CTCs. This is essential, in part, because most available CTC enrichment technologies yield samples composed of hematopoietic cells, CTCs, and, in some cases, benign epithelial cells. Genomic analysis and surface antigen detection are the two most commonly used methods for CTC detection. Reverse transcription polymerase chain reaction (RT-PCR) and Fluorescence *in situ* hybridization (FISH) have been used to identify tumor-specific genetic and chromosomal features in order to differentiate CTCs from contaminating cells. Immunofluorescent microscopy is utilized to detect epithelial specific antigens such as epithelial cell adhesion molecule (EpCAM) or cytokeratin (CK), or prostatic antigens such as PSA and prostate-specific membrane antigen (PSMA).

POLYMERASE CHAIN REACTION

Reverse transcription-PCR is highly sensitive for identifying the presence of CTCs and is able to detect a single malignant cell among ten million peripheral blood mononuclear cells (PBMCs) (Gomella et al., 1997). In addition to its sensitivity, RT-PCR has the potential to detect mRNA from CTC fragments that may otherwise not be detected through direct visualization by immunohistochemistry (Sun et al., 2011). This technology has been used in various ways to detect CTCs. In early experiments, CTC capture was performed on whole blood samples to detect tumor-specific genes. Extracellular RNA is highly unstable and its presence in peripheral blood suggests the existence of circulating cells expressing tumor-specific transcripts (Seiden et al., 1994). For instance, detection of circulating prostate-specific RNA transcripts for PSA or PSMA is thought to indicate the presence of prostatic CTCs. The first study to detect CTCs from venous blood samples using RT-PCR was performed in 1992 by Moreno et al. (1992). They identified PSA mRNA in blood samples from 4 of 12 patients with metastatic prostate cancer and in none of the 17 controls, including subjects with benign prostatic hypertrophy (Moreno et al., 1992). Subsequent studies of PCR in prostate cancer have utilized PSMA, kallikrein-2 (hK2), and PTI-1, in addition to PSA, as prostate-specific markers (Olsson et al., 1997; Kurek et al., 2004).

There are several potential limitations to RT-PCR. It suffers from poor specificity, as it may detect target RNA shed by normal prostatic cells. Furthermore, "illegitimate transcripts," tissue-specific genes that are expressed such as spliced transcripts in non-specific tissues, may also lead to false positive results (Chelly et al., 1989; Zippelius and Pantel, 2000). For example, in a quality-control study, PSA and PSMA were detected in non-prostatic negative control cell lines and healthy donor blood, which upon further analysis were found to be perfectly homologous with the exception of specific sequence deletions or point mutations not found in RNA transcripts native to prostatic tissue (Gala et al., 1998).

This issue has been addressed in part by the introduction of quantitative PCR (Q-PCR), which increases the specificity of mRNA detection by use of transcript-specific probes and enables the determination of mRNA copy number such that above a specific threshold a transcript is thought to be of malignant origin (Pantel et al., 2008). In one study, PSA mRNA copy number used as a surrogate for CTC count was predictive of recurrence after radical prostatectomy (Yates et al., 2012). Several studies have shown significant differences in PSA and PSMA mRNA copy number among patients with benign prostatic hypertrophy, localized prostate cancer, and metastatic disease (Zhang et al., 2008; Kalfazade et al., 2009). A study using Q-PCR for Kallikrein-2 (klk-2), PSA, and prostate specific stem cell antigen (PSCA) mRNA, copy number was concordant with CellSearch Circulating Tumor Cell Test CTC counts, and were predictive of metastatic disease vs. localized prostate cancer. It should be noted that there was 95% concordance for patients with more than 15 CTCs but diminished significantly for CTC counts less than 5 cells per 7.5 ml of blood (Helo et al., 2009).

Nevertheless, the PCR approach has many potential drawbacks. Expression of target RNA markers varies significantly between patients and among different tumor cells derived from the same patient, complicating the interpretation of absolute RNA copy number. Additionally, false negative results may occur because of low levels of target RNA expression in patients who have CTCs and metastatic disease. Furthermore, this technique is not able to distinguish between viable and non-viable CTCs. Finally, PCR does not allow for the direct visualization of CTCs and further molecular analysis using other laboratory techniques (Sun et al., 2011).

SURFACE MARKER DETECTION

Immunofluorescent staining is one of the most widely used methods of identifying CTCs enriched from heterogeneous cell populations (**Figure 1**). This allows for direct visualization of cells by fluorescent microscopy and for discrimination of CTCs from surrounding leukocytes by differential antigen expression. Nuclei are identified using DAPI, a fluorescent molecule that binds to the adenine- and thymine-rich regions of DNA (Zink et al., 2003). Anti-EpCAM and anti-CK antibodies are then used to confirm the cells are of epithelial origin. Leukocytes are differentiated from epithelial cells by the presence of CD45, a tyrosine phosphatase that is expressed on hematopoietic cells. Using common platforms such as CellSearch, a cell is said to be a CTC if it is DAPI positive, stains positively for CK or EpCAM, and stains negatively for CD45 (Allard et al., 2004). Interestingly, cell populations co-expressing epithelial markers and CD45 have been detected using CellSearch and other CTC isolation technologies. The significance of these cells is poorly understood and these cells are currently excluded from enumeration (Yu et al., 2011).

Antibodies directed against PSA and PSMA provide additional specificity to immunofluorescent identification of prostatic CTCs (Wang et al., 2000; Stott et al., 2010b). As mentioned previously, PSMA is a non-secreted protein expressed in prostatic tissues and to a much lesser extent, non-prostatic cell types such as renal tubular cells and intestinal epithelial cells (Troyer et al., 1995; Bostwick et al., 1998; Sweat et al., 1998; Sokoloff et al., 2000). Its expression is significantly upregulated on prostate cancer cells and is also seen in the neovasculature of the majority of solid-organ malignancies. PSA is a kallikrein found in high concentrations in prostatic cells and seminal tissues, and to a lesser degree in non-prostatic tissue types such as mammary, lung, and uterine tissue (Wei et al., 1997; Fortier et al., 1999; Mannello and Gazzanelli, 2001). Other fluorescently labeled antibodies may also be employed to detect subcellular localization of proteins of interest. For example, antibodies that recognize androgen receptor (AR) and tubulin have been used in prostate cancer CTCs to determine changes in the distribution of these proteins in the presence of androgens before and after taxane treatment to determine susceptibility to these agents (Darshan et al., 2011).

Several different prostatic CTC morphologies have been identified using immunofluorescent microscopy. Large cells with irregularly shaped nuclei are the predominant CTC cell type. Other cell morphologies include very large fragile cells with loose chromatin, CK- and PSMA-positive enucleated cells, cellular debris, stem cell-like cells, and micro-clusters composed of 3–100 CTCs. The significance of these different morphologies is uncertain but may represent two distinct populations of cells; one which has no reproductive ability, and the other with growth potential and consequently metastatic potential (Wang et al., 2000). Of note, although the biological significance of CTC fragments is unknown, there is also evidence that enucleated CTCs and CTC fragments correlate with patient outcomes in prostate cancer (Coumans et al., 2010).

In addition to immunofluorescence, flow cytometry has been frequently used to detect prostatic CTCs on the basis of surface antigen expression (Racila et al., 1998; He et al., 2008). In one study, a fluorescently labeled phosphoramidate peptidomimetic PSMA inhibitor was used to detect PSMA positive cells with flow cytometry (Wu et al., 2011). The authors found that there was reasonable concordance between the number of cells spiked in a sample and the number determined by flow cytometry (Wu et al., 2011). Prostate cancer CTCs isolated by flow cytometry cell sorting can also be analyzed by multiplex RT-PCR for expression prostate-specific mRNAs such as PSA, AR, and the prostate cancer specific gene fusion TMPRSS2 (Danila et al., 2011).

FLUORESCENCE *in situ* HYBRIDIZATION

Visual detection of tumor-specific genomic material is an alternate means of detecting and characterizing CTCs after enrichment with the added benefit of providing potentially clinically useful information. FISH is technique that uses fluorescent

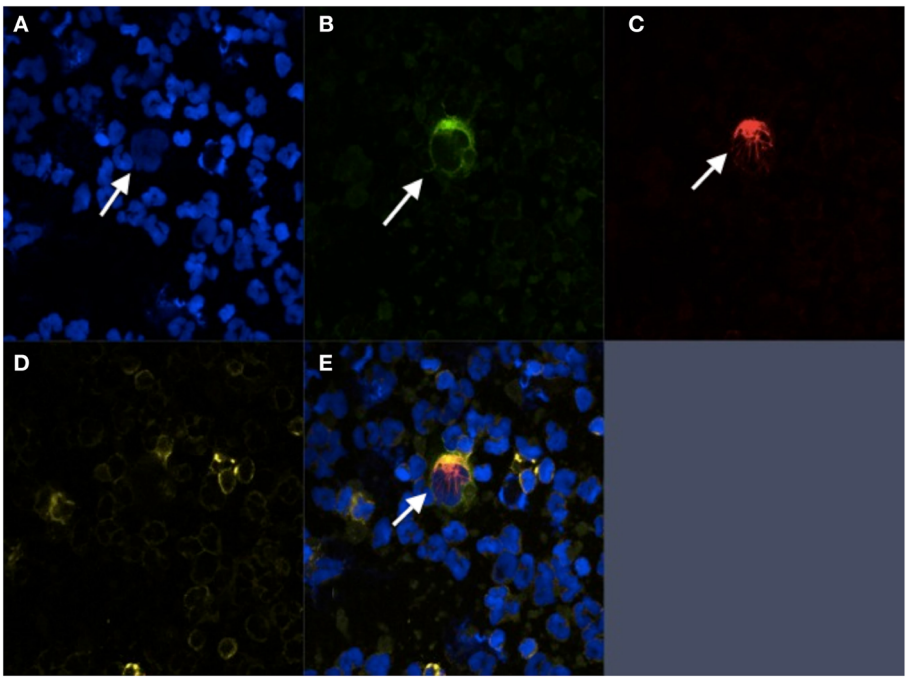

FIGURE 1 | Immunofluorescent staining of prostate cancer CTC. CTC isolated from patient with CRPC using negative selection. **(A)** DAPI; **(B)** PSMA; **(C)** Cytokeratin; **(D)** CD-45; **(E)** Composite image.

nucleic acid based probes that hybridize with genes of interest that are visualized using fluorescent microscopy. Several studies have successfully employed FISH to detect prostatic CTCs from enriched blood samples. In one study, enumerator probes designed to detect chromosomal aneusomy typical of prostatic malignancies identified prostatic CTCs in samples enriched using anti-EpCAM coated immunomagnetic beads. Interestingly, the authors found concordance between the chromosomal abnormalities detected in CTCs with those found in the primary tumor in a significant proportion of cases, supporting the theory that these cells are indeed tumor derived (Fehm et al., 2002). FISH probes have been used to detect AR amplification, gain of the MYC oncogene, and loss of the 8p gene locus in CTCs enriched using the CellSearch Circulating Tumor Cell Test. FISH using these probes also demonstrated that prostatic CTCs have similar cytogenetic profiles to advanced prostatic tumors, a finding that is consistent with data correlating higher CTC counts with poor clinical outcomes (Leversha et al., 2009).

CTC ENRICHMENT METHODS

DENSITY-DEPENDENT ENRICHMENT

Density-gradient centrifugation separates CTCs from whole blood based on the differential migration of cells through a fluid in a density-dependent manner during centrifugation. Whole blood centrifuged using a density gradient solution such as ficoll-paque™ separates blood into a layer of plasma, PBMCs, and an anucleate cell layer composed of erythrocytes and platelets. As mononuclear cells, CTCs migrate to the PBMC layer, which may be isolated for further processing. The advantages of this technique are that it is relatively inexpensive, easy to perform, and yields intact CTCs that can be subjected to further experimentation. Perhaps most importantly, it enables the capture of CTCs without relying on the expression of epithelial-specific surface markers commonly used in positive selection techniques (Sun et al., 2011). Under optimal conditions, density gradient centrifugation is able to capture ∼70% of CTCs present in a sample. The remaining cells are likely lost in the plasma or anucleate cell layer. The negative aspect of this approach is that samples obtained through this method are impure and are overwhelmingly composed of hematopoietic mononuclear cells. This makes the detection of CTCs using immunohistochemistry both difficult and time consuming. A newer density gradient solution, Oncoquick™, which employs a porous membrane, has been shown to prevent cross-contamination between layers and to improve sample purity (Rosenberg et al., 2002; Gertler et al., 2003). Nevertheless, because samples processed in this manner have significant leukocyte contamination, density gradient centrifugation is most often used as a precursor to other CTC enrichment procedures such as PCR-based and negative selection techniques.

A variation of density-gradient centrifugation is to use high-density imaging following isolation and immunostaining to identify CTCs using multiple fluorescent channels to produce high quality and high resolution digital images that retain fine cytologic details of nuclear contour and cytoplasmic distribution (Marrinucci et al., 2012). This enrichment-free strategy results in high sensitivity and high specificity, but still lacks the ability for further molecular analysis of identified CTCs.

SIZE-DEPENDENT SELECTION

In general, CTCs that emanate from solid tumors have a larger diameter and volume than other hematological cells found in the circulation. Consequently, many investigators have tried to exploit this characteristic in designing approaches to capture CTCs. The most common approach is to use a filtration-based device in which whole blood is passed through a filter with an 8 μm pore diameter, enabling the passage of most hematopoietic cells while retaining larger cells such as CTCs. Isolated cells are then stained for epithelial surface markers in order to identify the CTC population. This method, entitled ISET, has a high capture efficiency for cells >8 μm in diameter, which ranges between 86% and 100% of CTCs. It is sensitive enough to isolate a single micro-pipetted tumor cell added to one milliliter of blood and yields CTCs that are amenable to further experimentation such as PCR and flow cytometry (Vona et al., 2000; Zabaglo et al., 2003; Lin et al., 2010). In one study, a portable filter-based device achieved 90% capture efficiency from blood spiked with a prostate cancer cell line and found that it enriched more prostatic CTCs from more patient samples than did the FDA-approved CellSearch device (Lin et al., 2010). A prospective trial of 60 patients, 20 of whom had PC, further established ISET's sensitivity for detecting prostatic CTCs when compared with CellSearch (Farace et al., 2011). This approach has several practical advantages; it is relatively inexpensive and easy to perform (Lin et al., 2010). Furthermore, it does not rely on surface marker expression, which may vary widely, leading to inefficient cell capture. Filtration-based devices, however, may lack sensitivity when used to isolate CTCs from patient blood samples. Cell lines used to assess sensitivity and specificity of these devices tend to be composed of homogeneous, large tumor cells that may be consistently captured using this system. Patient-derived CTCs are heterogeneous and may not be large enough to be enriched. Thus, size-dependent filtration may underestimate the true number of CTCs in a given patient's blood (Wang et al., 2000; Stott et al., 2010b). Pore size may also limit the specificity of ISET-based devices, as certain classes of hematopoietic cells, such as neutrophils, plasma cells, and macrophages, are larger than 8 μm in diameter. Additionally, although most lymphocytes are 7–8 μm in diameter, larger lymphocytes may be captured, further limiting the specificity of this technology.

NEGATIVE SELECTION BY USE OF IMMUNOMAGNETIC BEADS

CTCs isolated from the mononuclear cell layer generated by density gradient centrifugation can be further purified using ferromagnetic anti-CD45 coated beads (Zigeuner et al., 2003). CD45 is a protein tyrosine phosphatase that is present on all hematopoietic cells with the exception of plasma cells and erythrocytes and is typically not expressed in epithelial cells (Stelzer et al., 1993). CTCs are negatively selected by depleting CD45-positive cells from a blood sample. Cells that bind to the beads are separated from the sample using a magnetic field. This technique has a reported capture efficiency ranging from 52% to 88%, but still has many of the limitations of density gradient centrifugation. The probability of isolating one cell spiked into one million leukocytes is 93.3% (Wang et al., 2000; Zigeuner et al., 2000). This technique has been used to detect cells in a variety of malignancies including prostate cancer (Wang et al., 2000; Schmidt et al., 2004; Yang et al., 2009). In one study, negative selection was used to isolate CTCs in patients with metastatic prostate cancer with a PSA decline while undergoing cytotoxic chemotherapy, demonstrating that CTCs may be present despite evidence of biochemical response to chemotherapy (Schmidt et al., 2004). A major advantage of this technique is that it does not rely on the expression of tumor-specific markers, enabling capture of cells that would otherwise be missed by positive selection methods (Liu et al., 2011). Negative selection also yields intact CTCs that are amenable to further experimentation. Samples isolated using this technique, however, still suffer from a lack of purity because not all CD45-positive cells are removed during sample processing. Because this process requires density gradient centrifugation, it also lacks sensitivity owing to the loss of cells in plasma or RBC layers. Additionally, negative selection by use of CD45-coated beads also adds several washing steps that may further contribute to low capture efficiencies.

POSITIVE SELECTION BY USE OF IMMUNOMAGNETIC BEADS

Ferromagnetic beads are also used to positively select for prostate cancer CTCs by exploiting their expression of epithelial cell-surface antigens. Cells isolated during density gradient centrifugation are incubated with anti-EpCAM and anti-CK coated magnetic beads, which bind to CTCs and remove them from the sample when a magnet is applied (Brandt et al., 1996; Jost et al., 2010). EpCAM is a type I membrane protein that functions as a cell adhesion molecule in epithelial and adenomatous cell types and is highly overexpressed in various carcinomas including prostate cancer (Litvinov et al., 1996; Mukherjee et al., 2009). CK is an intermediate filament component of the cytoplasm of epithelial cells and, to a lesser degree, in non-epithelial cell types including smooth muscle and endothelial cells (Franke et al., 1979; Mattey et al., 1993). In 2000, Wang et al. described isolation of CTCs from peripheral blood with centrifugation density gradients and magnetic cell sorting (Wang et al., 2000). This technology has evolved and today capture devices utilizing this approach are one of the most extensively studied methods of enriching CTCs. The CellSearch Circulating Tumor Cell Test device, which is the only FDA-approved test for CTC enrichment, positively selects CTCs from 7.5 ml of whole blood using EpCAM coated magnetic beads, separates them from other blood components using a magnetic field, and immunofluorescently labels them with 4′,6-diamidino-2-phenylindole (DAPI), anti-CD45 and anti-CK antibodies. A computer screen displays presents an operator with images of cells for review and enumeration (Tibbe et al., 2002). This method is 85% sensitive for the detection of cultured breast cancer cells spiked into whole blood (Riethdorf et al., 2007). This device has been shown to have a low false-positive rate in a series of 2,183 patients with metastatic cancers; CTCs were detected in 36% of patient samples and 0.3% of healthy controls (Allard et al., 2004). In the subset of patients with metastatic prostate cancer, more than two CTCs were detected in 37% of patients (Allard et al., 2004). It has also been shown to be more sensitive and specific than density-dependent centrifugation with Oncoquick™ (Balic et al., 2005). Cells captured from patients with metastatic prostate cancer by use of this device have also been

shown to possess other molecular features of prostate cancer cells such as AR gene amplification (Shaffer et al., 2007; Attard et al., 2009).

Despite multiple studies validating the CellSearch system's prognostic value as related to CTC enumeration, several important caveats limit its usefulness. It is both expensive and time consuming to perform. The CellSearch device fixes cells prior to staining them, significantly limiting the ability to perform subsequent functional assays and nucleic acid analysis (Stott et al., 2010b). Most importantly, the sensitivity of this device is limited by its use of EpCAM-based detection (Lara et al., 2004). CTCs express variable levels of EpCAM *in vivo*, due, in part, to downregulation of epithelial surface markers. This process, known as epithelial-to-mesenchymal transition (EMT), is a process in which epithelial CTCs assume a mesenchymal phenotype in preparation for extravasation and implantation in metastatic sites (He et al., 2010; Armstrong et al., 2011). These cells are more likely to metastasize and have been linked to more aggressive prostate cancers in a number of clinical studies (Tomita et al., 2000; Gravdal et al., 2007). Evidence for EMT has been found in CTCs that express both epithelial markers such as CK and EpCAM and mesenchymal markers such as vimentin, e-cadherin, and CD133 (Armstrong et al., 2011). The co-expression of these markers is thought to represent an intermediate state between the two cell types (Armstrong et al., 2011). CTCs that undergo EMT are less likely to express high levels of EpCAM and may therefore evade capture by anti-EpCAM antibodies (Santana et al., 2012). The superior capture efficiency of non-EpCAM based capture technologies such as ISET and PSMA microfluidic devices may, in part, be explained by this phenomenon.

MICROFLUIDIC DEVICES

Microfluidic devices have demonstrated high capability to enrich CTCs from whole blood. One example, the "CTC-chip" is composed of an array of antibody-coated microscopic posts arranged as equilateral triangles through which a blood sample is flowed. As described, the arrangement of the posts is designed to minimize the shear forces that cells are exposed to while within the device. CTCs within the sample collide with the posts and are specifically captured by the antibodies used to coat them (Nagrath et al., 2007). In 2007, Nagrath et al. successfully employed a CTC-chip functionalized with anti-EpCAM antibodies to isolate CTCs from whole blood taken from patients with a range of epithelial malignancies. Capture efficiency of approximately 60% was determined by spiking blood from healthy donors with a non-small cell lung cancer cell line. Interestingly, capture efficiency was not diminished by using cell lines with low levels of EpCAM expression. The authors were able to identify CTCs in 115 of 116 (99%) samples taken from patients with breast, colon, pancreatic, or prostate cancer with an average purity of 49–67%. Similar to the CellSearch Circulating Tumor Cell Test device, in a limited analysis, the authors were able to correlate patient outcomes and response to treatment with the number of CTCs captured (Nagrath et al., 2007).

The same investigators developed what they term a "herringbone chip" to use the vortical flow induced by anisotropic surface grooves to generate a device exhibiting chaotic advection (Stroock et al., 2002). The device consists of eight microchannels etched with periodically occurring herringbone-shaped grooves and functionalized with anti-EpCAM monoclonal antibodies. The herringbone device has a capture efficiency of 91.8% +/−5.2% in cell spiking experiments using PC-3 cells, and CTCs were detected in 93% of samples from patients with metastatic prostate cancer. The design of the herringbone device chip enabled cell capture at 50% more efficiency than the post-based anti-EpCAM device from the same investigators. Captured cells are again amenable to further experimentation such as PCR and on-chip immunofluorescent staining (Stott et al., 2010a).

Despite showing effective capture using cell lines with low levels of EpCAM expression, it is unclear whether chips functionalized with anti-EpCAM antibodies can efficiently capture cells that have undergone EMT in patient samples. CTCs may express lower levels of EpCAM than cultured cells used for these experiments and may evade capture. PSMA based CTC capture may be able overcome this limitation in prostate cancer patients and enable the capture of CTCs that have undergone EMT. PSMA, also known as glutamate carboxypeptidase II, is a type II transmembrane metallopeptidase that is universally expressed in prostatic tumors and may be conserved during EMT. Furthermore, levels of expression correlate with disease severity, suggesting utility as a prognostic marker (Bostwick et al., 1998; Sweat et al., 1998). Although it is normally expressed as a cytoplasmic protein in benign prostatic cells, alternative splicing of PSMA mRNA in prostatic carcinomas leads to its expression as a type II integral surface membrane protein, making it a suitable target for anti-PSMA antibody based capture (Israeli et al., 1993). Although this marker is not entirely specific to prostatic cells, expression in this population is 100–1000 times greater than cells in other tissue types such as cells of the small intestine, proximal renal tubules, and salivary glands (Troyer et al., 1995; Sokoloff et al., 2000). The J591 antibody is a deimmunized monoclonal antibody that specifically recognizes an extracellular epitope of PSMA. This antibody has been used successfully to capture CTCs from whole blood using a geometrically-enhanced differential immunocapture (GEDI) microfluidic device (**Figure 2**) (Gleghorn et al., 2010). The PSMA-GEDI "chip" is designed to maximally increase the frequency of CTC collisions with anti-PSMA immunocoated posts in a size and flow-dependent manner. Size-based selection is thought to increase capture efficiency and improve purity by limiting opportunities for non-target blood cells to interact with the immunocoated surfaces. The capture efficiency of the PSMA-coated GEDI chip is quite high, 97 ± 3% for cells spiked in PBS and 85 ± 5% for cells spiked in whole blood (Gleghorn et al., 2010).

CURRENT AND FUTURE APPLICATIONS OF CTC ENRICHMENT DEVICES

The FDA approved the CellSearch device for monitoring disease status in patients with metastatic prostate cancer (Wang et al., 2011). Studies using this device have demonstrated that prostate cancer patients with at least 5 CTCs in 7.5 ml of blood have an inferior overall survival compared with patients with less than 5

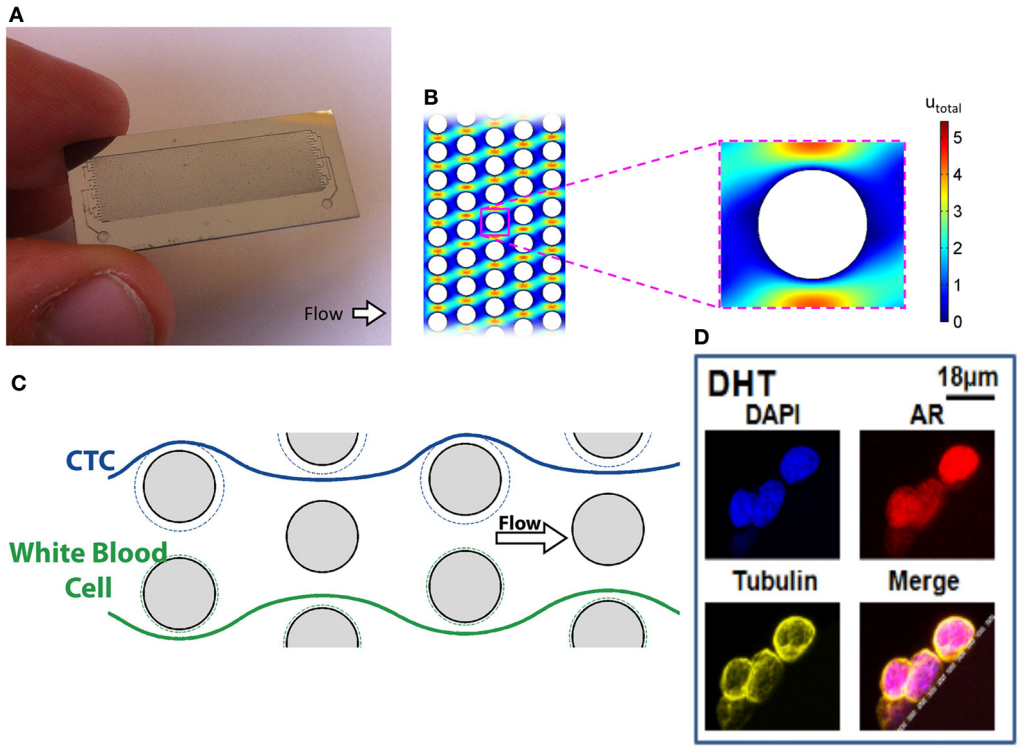

FIGURE 2 | Geometrically-enhanced differential immunocapture (GEDI) microfluidic device. (A) GEDI Chip **(B)** GEDI post-array **(C)** Illustration of laminar flow through GEDI device **(D)** Captured CTCs stained for AR and tubulin.

CTCs in 7.5 ml (Danila et al., 2007). The IMMC38 trial, which provided the basis of FDA clearance of the CellSearch device in prostate cancer, reported that a CTC count greater than 4 cells/7.5 ml is associated with unfavorable response to therapy in metastatic castrate-resistant prostate cancer patients (Scher et al., 2009). Several subsequent studies did not detect a threshold effect; suggesting the use of CTC counts as a continuous variable without a specific cutoff value (Danila et al., 2007). Nevertheless, chemotherapy-naïve patients with CTC counts greater than 4 cells/7.5 ml have a 45% decrease in overall survival when compared to those with fewer than 5 CTCs. The impact of CTC counts is even greater in patients who had undergone one or more chemotherapeutic regimens, where patients had a 60% decrease in overall survival (Danila et al., 2007). CTC counts are also useful in patients with hormone-sensitive PC. A CTC cut-off of three or more cells, detected using the CellSearch device was able to predict the magnitude and duration of response to androgen deprivation therapy in these patients (Goodman et al., 2011). Studies also compared CTC counts with traditional markers of disease progression and found that it is a more powerful predictor of survival and therapeutic response than currently used biomarkers such as PSA (de Bono et al., 2008; Scher et al., 2009).

The number of prostate cancer CTCs has also been studied as a secondary endpoint in a number of clinical trials. Two recent phase II trials examined the efficacy of abiraterone acetate, a CYP17 inhibitor that impairs androgen synthesis, in patients with castration resistant prostate cancer used CTCs as efficacy markers. In one study, CTCs were isolated from patient blood by use of the CellSearch Circulating Tumor Cell Test prior to treatment and every 4 weeks during treatment. The authors found significant declines in CTC counts of treated patients, with 63% of patients having a greater than 50% decrease in CTCs. This decline mirrored the PSA decline in a subset of patients with ERG gene mutations (Reid et al., 2010). A second study, which aimed at defining the efficacy of abiraterone combined with prednisone in metastatic castrate-resistant prostate cancer patients who failed first line chemotherapy used conversion from unfavorable to favorable CTC counts as a surrogate of clinical response. The authors reported that 34% of treated patients who had pre-treatment CTC counts greater than 5 cells/7.5 ml had a decrease in CTC counts to less than 5 cells/7.5 ml (Danila et al., 2010). Several recently reported and ongoing phase III studies are validating this biomarker as a potential surrogate marker of response and survival (Scher et al., 2011).

Although still in its early stages, molecular and genetic analyses of CTCs have also been used to correlate CTC characteristics with treatment outcomes. For example, a study using FISH to detect the fusion gene TMPRSS2-ERG demonstrated a significant association between expression of this marker and PSA response to abiraterone. Furthermore, this study also demonstrated a high

degree of concordance between the presence of the fusion gene in CTCs and in primary prostatic tumors, further supporting the utility of CTCs as a "liquid biopsy" (Attard et al., 2009). A second study examining TMPRSS2-ERG mRNA in CTCs showed no relationship to patient outcomes (Gopalan et al., 2009; Fine et al., 2010).

Studies have also examined the predictive value of nuclear and/or cytoplasmic localization of AR in CTCs. The AR plays a key role in the development and progression of prostate cancer. In hormone-sensitive prostate cancer, systemic androgens induce AR-mediated cellular proliferation, which is impaired by androgen deprivation therapy by preventing ligand-dependent nuclear AR translocation. AR signaling can continue to stimulate tumor growth in castrate patients via intra-tumoral androgen synthesis or constitutive AR activation-independent of ligand binding (Chen et al., 2004). Recent studies suggest that taxane chemotherapy in prostate cancer can impede AR translocation from the cytoplasm to the nucleus by disrupting microtubules that normally function to transport AR to the nucleus (Darshan et al., 2011). In a pilot study of patients receiving taxane chemotherapy, examination of AR nuclear localization and microtubule integrity in CTCs isolated using the CellSearch Circulating Tumor Cell Test device correlated with response to therapy (Darshan et al., 2011). In an unrelated study, PCR based analysis of prostate cancer CTCs detected several AR mutations some of which have been associated with therapeutic resistance to anti-androgen therapy (Jiang et al., 2010). Recent studies have also shown that AR splice variants may evolve with therapy and be a mechanism of treatment resistance (Sun et al., 2010; Guo and Qiu, 2011; Mostaghel et al., 2011). Studies are in progress to determine if these abnormalities in AR that could affect treatment decisions can be detected by examining CTCs.

CONCLUSION

The science of CTC capture and analysis is evolving and will certainly change as newer technologies are incorporated and validated. The only FDA-cleared device, CellSearch system, has been shown to be an important prognostic tool, providing valuable insights into treatment response and overall survival. Experiments with alternative enrichment methods highlight the poor sensitivity of the CellSearch technique, with multiple studies demonstrating significantly higher capture rates from patient with metastatic castrate-resistant prostate cancer. However, their clinical utility remains to be confirmed. Further studies are needed to improve and validate alternative enrichment in identification techniques.

The effect that CTC analysis will have on patient care remains to be determined. As discussed, genetic analysis of CTCs has enabled the detection of abnormalities that influence tumor sensitivity to a variety of prostate cancer therapies. Molecular analysis has helped elucidate the mechanism of taxane anti-tumor effect in prostate cancer, and provides a basis for an assay to assess the likely efficacy of this chemotherapeutic class. Future studies will be aimed at assessing additional markers of treatment sensitivity and resistance, and attempting to ascertain additional drug targets. Additional studies correlating the molecular features of CTCs with those of tissue specimens obtained from primary and metastatic sites are needed. The ultimate goal is to develop technology that will enable periodic monitoring of tumor biology in a way that will enable clinicians to effectively tailor therapy to the individual patient on an ongoing basis in order to maximize patient outcomes.

ACKNOWLEDGMENTS

This work was supported in part by National Cancer Institute (NCI) Grant CA062948, CA137020 and U54 CA143876.

REFERENCES

Allard, W. J., Matera, J., Miller, M. C., Repollet, M., Connelly, M. C., Rao, C., et al. (2004). Tumor cells circulate in the peripheral blood of all major carcinomas but not in healthy subjects or patients with nonmalignant diseases. *Clin. Cancer Res.* 10, 6897–6904.

Armstrong, A. J., Marengo, M. S., Oltean, S., Kemeny, G., Bitting, R. L., Turnbull, J. D., et al. (2011). Circulating tumor cells from patients with advanced prostate and breast cancer display both epithelial and mesenchymal markers. *Mol. Cancer Res.* 9, 997–1007.

Ashworth, T. R. (1869). A case of cancer in which cells similar to those in the tumors were seen in the blood after death. *Aus. Med. J.* 14, 146–149.

Attard, G., Swennenhuis, J. F., Olmos, D., Reid, A. H., Vickers, E., A'Hern, R., et al. (2009). Characterization of ERG, AR and PTEN gene status in circulating tumor cells from patients with castration-resistant prostate cancer. *Cancer Res.* 69, 2912–2918.

Balic, M., Dandachi, N., Hofmann, G., Samonigg, H., Loibner, H., Obwaller, A., et al. (2005). Comparison of two methods for enumerating circulating tumor cells in carcinoma patients. *Cytometry B Clin. Cytom.* 68, 25–30.

Bostwick, D. G., Pacelli, A., Blute, M., Roche, P., and Murphy, G. P. (1998). Prostate specific membrane antigen expression in prostatic intraepithelial neoplasia and adenocarcinoma: a study of 184 cases. *Cancer* 82, 2256–2261.

Brandt, B., Junker, R., Griwatz, C., Heidl, S., Brinkmann, O., Semjonow, A., et al. (1996). Isolation of prostate-derived single cells and cell clusters from human peripheral blood. *Cancer Res.* 56, 4556–4561.

Chelly, J., Concordet, J. P., Kaplan, J. C., and Kahn, A. (1989). Illegitimate transcription: transcription of any gene in any cell type. *Proc. Natl. Acad. Sci. U.S.A.* 86, 2617–2621.

Chen, C. D., Welsbie, D. S., Tran, C., Baek, S. H., Chen, R., Vessella, R., et al. (2004). Molecular determinants of resistance to antiandrogen therapy. *Nat. Med.* 10, 33–39.

Coumans, F. A., Doggen, C. J., Attard, G., de Bono, J. S., and Terstappen, L. W. (2010). All circulating EpCAM+CK+CD45- objects predict overall survival in castration-resistant prostate cancer. *Ann. Oncol.* 21, 1851–1857.

Danila, D. C., Fleisher, M., and Scher, H. I. (2011). Circulating tumor cells as biomarkers in prostate cancer. *Clin. Cancer Res.* 17, 3903–3912.

Danila, D. C., Heller, G., Gignac, G. A., Gonzalez-Espinoza, R., Anand, A., Tanaka, E., et al. (2007). Circulating tumor cell number and prognosis in progressive castration-resistant prostate cancer. *Clin. Cancer Res.* 13, 7053–7058.

Danila, D. C., Morris, M. J., de Bono, J. S., Ryan, C. J., Denmeade, S. R., Smith, M. R., et al. (2010). Phase II multicenter study of abiraterone acetate plus prednisone therapy in patients with docetaxel-treated castration-resistant prostate cancer. *J. Clin. Oncol.* 28, 1496–1501.

Darshan, M. S., Loftus, M. S., Thadani-Mulero, M., Levy, B. P., Escuin, D., Zhou, X. K., et al. (2011). Taxane-induced blockade to nuclear accumulation of the androgen receptor predicts clinical responses in metastatic prostate cancer. *Cancer Res.* 71, 6019–6029.

de Bono, J. S., Scher, H. I., Montgomery, R. B., Parker, C., Miller, M. C., Tissing, H., et al. (2008). Circulating tumor cells predict survival benefit from treatment

in metastatic castration-resistant prostate cancer. *Clin. Cancer Res.* 14, 6302–6309.

Doyen, J., Alix-Panabières, C., Hofman, P., Parks, S. K., Chamorey, E., Naman, H., et al. (2012). Circulating tumor cells in prostate cancer: a potential surrogate marker of survival. *Crit. Rev. Oncol. Hematol.* 81, 241–256.

Farace, F., Massard, C., Vimond, N., Drusch, F., Jacques, N., Billiot, F., et al. (2011). A direct comparison of CellSearch and ISET for circulating tumour-cell detection in patients with metastatic carcinomas. *Br. J. Cancer* 105, 847–853.

Fehm, T., Sagalowsky, A., Clifford, E., Beitsch, P., Saboorian, H., Euhus, D., et al. (2002). Cytogenetic evidence that circulating epithelial cells in patients with carcinoma are malignant. *Clin. Cancer Res.* 8, 2073–2084.

Fine, S. W., Gopalan, A., Leversha, M. A., Al-Ahmadie, H. A., Tickoo, S. K., Zhou, Q., et al. (2010). TMPRSS2-ERG gene fusion is associated with low Gleason scores and not with high-grade morphological features. *Mod. Pathol.* 23, 1325–1333.

Fortier, A. H., Nelson, B. J., Grella, D. K., and Holaday, J. W. (1999). Antiangiogenic activity of prostate-specific antigen. *J. Natl. Cancer Inst.* 91, 1635–1640.

Franke, W. W., Schmid, E., Osborn, M., and Weber, K. (1979). Intermediate-sized filaments of human endothelial cells. *J. Cell Biol.* 81, 570–580.

Gala, J. L., Heusterspreute, M., Loric, S., Hanon, F., Tombal, B., Van Cangh, P., et al. (1998). Expression of prostate-specific antigen and prostate-specific membrane antigen transcripts in blood cells: implications for the detection of hematogenous prostate cells and standardization. *Clin. Chem.* 44, 472–481.

Gertler, R., Rosenberg, R., Fuehrer, K., Dahm, M., Nekarda, H., and Siewert, J. R. (2003). Detection of circulating tumor cells in blood using an optimized density gradient centrifugation. *Recent Results Cancer Res.* 162, 149–155.

Gleghorn, J. P., Pratt, E. D., Denning, D., Liu, H., Bander, N. H., Tagawa, S. T., et al. (2010). Capture of circulating tumor cells from whole blood of prostate cancer patients using geometrically enhanced differential immunocapture (GEDI) and a prostate-specific antibody. *Lab Chip* 10, 27–29.

Gomella, L. G., Raj, G. V., and Moreno, J. G. (1997). Reverse transcriptase polymerase chain reaction for prostate specific antigen in the management of prostate cancer. *J. Urol.* 158, 326–337.

Goodman, O. B., Symanowski, J. T., Loudyi, A., Fink, L. M., Ward, D. C., and Vogelzang, N. J. (2011). Circulating tumor cells as a predictive biomarker in patients with hormone-sensitive prostate cancer. *Clin. Genitourin. Cancer* 9, 31–38.

Gopalan, A., Leversha, M. A., Satagopan, J. M., Zhou, Q., Al-Ahmadie, H. A., Fine, S. W., et al. (2009). TMPRSS2-ERG gene fusion is not associated with outcome in patients treated by prostatectomy. *Cancer Res.* 69, 1400–1406.

Gravdal, K., Halvorsen, O. J., Haukaas, S. A., and Akslen, L. A. (2007). A switch from E-cadherin to N-cadherin expression indicates epithelial to mesenchymal transition and is of strong and independent importance for the progress of prostate cancer. *Clin. Cancer Res.* 13, 7003–7011.

Guo, Z., and Qiu, Y. (2011). A new trick of an old molecule: androgen receptor splice variants taking the stage?! *Int. J. Biol. Sci.* 7, 815–822.

He, H., Yang, X., Davidson, A. J., Wu, D., Marshall, F. F., Chung, L. W., et al. (2010). Progressive epithelial to mesenchymal transitions in ARCaP E prostate cancer cells during xenograft tumor formation and metastasis. *Prostate* 70, 518–528.

Helo, P., Cronin, A. M., Danila, D. C., Wenske, S., Gonzalez-Espinoza, R., Anand, A., et al. (2009). Circulating prostate tumor cells detected by reverse transcription-PCR in men with localized or castration-refractory prostate cancer: concordance with CellSearch assay and association with bone metastases and with survival. *Clin. Chem.* 55, 765–773.

He, W., Kularatne, S. A., Kalli, K. R., Prendergast, F. G., Amato, R. J., Klee, G. G., et al. (2008). Quantitation of circulating tumor cells in blood samples from ovarian and prostate cancer patients using tumor-specific fluorescent ligands. *Int. J. Cancer* 123, 1968–1973.

Israeli, R. S., Powell, C. T., Fair, W. R., and Heston, W. D. (1993). Molecular cloning of a complementary DNA encoding a prostate-specific membrane antigen. *Cancer Res.* 53, 227–230.

Jatana, K. R., Balasubramanian, P., Lang, J. C., Yang, L., Jatana, C. A., White, E., et al. (2010). Significance of circulating tumor cells in patients with squamous cell carcinoma of the head and neck: initial results. *Arch. Otolaryngol. Head Neck Surg.* 136, 1274–1279.

Jiang, Y., Palma, J. F., Agus, D. B., Wang, Y., and Gross, M. E. (2010). Detection of androgen receptor mutations in circulating tumor cells in castration-resistant prostate cancer. *Clin. Chem.* 56, 1492–1495.

Jost, M., Day, J. R., Slaughter, R., Koreckij, T. D., Gonzales, D., Kinnunen, M., et al. (2010). Molecular assays for the detection of prostate tumor derived nucleic acids in peripheral blood. *Mol. Cancer* 9, 174.

Kalfazade, N., Kuskucu, A. M., Karadag, S., Sahin, S., Aras, B., Midilli, K., et al. (2009). Quantification of PSA mRNA levels in peripheral blood of patients with localized prostate adenocarcinoma before, during, and after radical prostatectomy by quantitative real-time PCR (qRT-PCR). *Int. Urol. Nephrol.* 41, 273–279.

Kirby, B. J., Jodari, M., Loftus, M. S., Gakhar, G., Pratt, E. D., Chanel-Vos, C., et al. (2012). Functional characterization of circulating tumor cells with a prostate-cancer-specific microfluidic device. *PLoS ONE* 7:e35976. doi: 10.1371/journal.pone.0035976

Kuhn, P., and Bethel, K. (2012). A fluid biopsy as investigating technology for the fluid phase of solid tumors. *Phys. Biol.* 9, 010301.

Kurek, R., Nunez, G., Tselis, N., Konrad, L., Martin, T., Roeddiger, S., et al. (2004). Prognostic value of combined "triple"-reverse transcription-PCR analysis for prostate-specific antigen, human kallikrein 2, and prostate-specific membrane antigen mRNA in peripheral blood and lymph nodes of prostate cancer patients. *Clin. Cancer Res.* 10, 5808–5814.

Lara, O., Tong, X., Zborowski, M., and Chalmers, J. J. (2004). Enrichment of rare cancer cells through depletion of normal cells using density and flow-through, immunomagnetic cell separation. *Exp. Hematol.* 32, 891–904.

Leversha, M. A., Han, J., Asgari, Z., Danila, D. C., Lin, O., Gonzalez-Espinoza, R., et al. (2009). Fluorescence *in situ* hybridization analysis of circulating tumor cells in metastatic prostate cancer. *Clin. Cancer Res.* 15, 2091–2097.

Lin, H. K., Zheng, S., Williams, A. J., Balic, M., Groshen, S., Scher, H. I., et al. (2010). Portable filter-based microdevice for detection and characterization of circulating tumor cells. *Clin. Cancer Res.* 16, 5011–5018.

Litvinov, S. V., van Driel, W., van Rhijn, C. M., Bakker, H. A., van Krieken, H., Fleuren, G. J., et al. (1996). Expression of Ep-CAM in cervical squamous epithelia correlates with an increased proliferation and the disappearance of markers for terminal differentiation. *Am. J. Pathol.* 148, 865–875.

Liu, Z., Fusi, A., Klopocki, E., Schmittel, A., Tinhofer, I., Nonnenmacher, A., et al. (2011). Negative enrichment by immunomagnetic nanobeads for unbiased characterization of circulating tumor cells from peripheral blood of cancer patients. *J. Transl. Med.* 9, 70.

Mannello, F., and Gazzanelli, G. (2001). Prostate-specific antigen (PSA/hK3): a further player in the field of breast cancer diagnostics? *Breast Cancer Res.* 3, 238–243.

Marrinucci, D., Bethel, K., Kolatkar, A., Luttgen, M. S., Malchiodi, M., Baehring, F., et al. (2012). Fluid biopsy in patients with metastatic prostate, pancreatic and breast cancers. *Phys. Biol.* 9, 016003.

Mattey, D. L., Nixon, N., Wynn-Jones, C., and Dawes, P. T. (1993). Demonstration of cytokeratin in endothelial cells of the synovial microvasculature *in situ* and *in vitro*. *Br. J. Rheumatol.* 32, 676–682.

Mayer, J. A., Pham, T., Wong, K. L., Scoggin, J., Sales, E. V., Clarin, T., et al. (2011). FISH-based determination of HER2 status in circulating tumor cells isolated with the microfluidic CEE™ platform. *Cancer Genet.* 204, 589–595.

Moreno, J. G., Croce, C. M., Fischer, R., Monne, M., Vihko, P., Mulholland, S. G., et al. (1992). Detection of hematogenous micrometastasis in patients with prostate cancer. *Cancer Res.* 52, 6110–6112.

Mostaghel, E. A., Marck, B. T., Plymate, S. R., Vessella, R. L., Balk, S., Matsumoto, A. M., et al. (2011). Resistance to CYP17A1 inhibition with abiraterone in castration-resistant prostate cancer: induction of steroidogenesis and androgen

receptor splice variants. *Clin. Cancer Res.* 17, 5913–5925.

Mukherjee, S., Richardson, A. M., Rodriguez-Canales, J., Ylaya, K., Erickson, H. S., Player, A., et al. (2009). Identification of EpCAM as a molecular target of prostate cancer stroma. *Am. J. Pathol.* 175, 2277–2287.

Nagrath, S., Sequist, L. V., Maheswaran, S., Bell, D. W., Irimia, D., Ulkus, L., et al. (2007). Isolation of rare circulating tumour cells in cancer patients by microchip technology. *Nature* 450, 1235–1239.

Olsson, C. A., de Vries, G. M., Buttyan, R., and Katz, A. E. (1997). Reverse transcriptase-polymerase chain reaction assays for prostate cancer. *Urol. Clin. North Am.* 24, 367–378.

Pantel, K., Brakenhoff, R. H., and Brandt, B. (2008). Detection, clinical relevance and specific biological properties of disseminating tumour cells. *Nat. Rev. Cancer* 8, 329–340.

Racila, E., Euhus, D., Weiss, A. J., Rao, C., McConnell, J., Terstappen, L. W., et al. (1998). Detection and characterization of carcinoma cells in the blood. *Proc. Natl. Acad. Sci. U.S.A.* 95, 4589–4594.

Reid, A. H., Attard, G., Danila, D. C., Oommen, N. B., Olmos, D., Fong, P. C., et al. (2010). Significant and sustained antitumor activity in post-docetaxel, castration-resistant prostate cancer with the CYP17 inhibitor abiraterone acetate. *J. Clin. Oncol.* 28, 1489–1495.

Riethdorf, S., Fritsche, H., Müller, V., Rau, T., Schindlbeck, C., Rack, B., et al. (2007). Detection of circulating tumor cells in peripheral blood of patients with metastatic breast cancer: a validation study of the CellSearch system. *Clin. Cancer Res.* 13, 920–928.

Rosenberg, R., Gertler, R., Friederichs, J., Fuehrer, K., Dahm, M., Phelps, R., et al. (2002). Comparison of two density gradient centrifugation systems for the enrichment of disseminated tumor cells in blood. *Cytometry* 49, 150–158.

Santana, S. M., Liu, H., Bander, N. H., Gleghorn, J. P., and Kirby, B. J. (2012). Immunocapture of prostate cancer cells by use of anti-PSMA antibodies in microdevices. *Biomed. Microdevices* 14, 401–407.

Scher, H. I., Heller, G., Molina, A., Kheoh, T. S., Attard, G., Moreira, J., et al. (2011). Evaluation of circulating tumor cell (CTC) enumeration as an efficacy response biomarker of overall survival (OS) in metastatic castration-resistant prostate cancer (mCRPC): planned final analysis (FA) of COU-AA-301, a randomized, double-blind, placebo-controlled, phase III study of abiraterone acetate (AA) plus low-dose prednisone (P) post docetaxel. *ASCO Meet. Abstr.* 29, LBA4517.

Scher, H. I., Jia, X., de Bono, J. S., Fleisher, M., Pienta, K. J., Raghavan, D., et al. (2009). Circulating tumour cells as prognostic markers in progressive, castration-resistant prostate cancer: a reanalysis of IMMC38 trial data. *Lancet Oncol.* 10, 233–239.

Schmidt, U., Bilkenroth, U., Linné, C., Fuessel, S., Kraemer, K., Froehner, M., et al. (2004). Quantification of disseminated tumor cells in the bloodstream of patients with hormone-refractory prostate carcinoma undergoing cytotoxic chemotherapy. *Int. J. Oncol.* 24, 1393–1399.

Seiden, M. V., Kantoff, P. W., Krithivas, K., Propert, K., Bryant, M., Haltom, E., et al. (1994). Detection of circulating tumor cells in men with localized prostate cancer. *J. Clin. Oncol.* 12, 2634–2639.

Shaffer, D. R., Leversha, M. A., Danila, D. C., Lin, O., Gonzalez-Espinoza, R., Gu, B., et al. (2007). Circulating tumor cell analysis in patients with progressive castration-resistant prostate cancer. *Clin. Cancer Res.* 13, 2023–2029.

Sokoloff, R. L., Norton, K. C., Gasior, C. L., Marker, K. M., and Grauer, L. S. (2000). A dual-monoclonal sandwich assay for prostate-specific membrane antigen: levels in tissues, seminal fluid and urine. *Prostate* 43, 150–157.

Stelzer, G. T., Shults, K. E., and Loken, M. R. (1993). CD45 gating for routine flow cytometric analysis of human bone marrow specimens. *Ann. N.Y. Acad. Sci.* 677, 265–280.

Stott, S. L., Hsu, C. H., Tsukrov, D. I., Yu, M., Miyamoto, D. T., Waltman, B. A., et al. (2010a). Isolation of circulating tumor cells using a microvortex-generating herringbone-chip. *Proc. Natl. Acad. Sci. U.S.A.* 107, 18392–18397.

Stott, S. L., Lee, R. J., Nagrath, S., Yu, M., Miyamoto, D. T., Ulkus, L., et al. (2010b). Isolation and characterization of circulating tumor cells from patients with localized and metastatic prostate cancer. *Sci. Transl. Med.* 2, 25ra23.

Stroock, A. D., Dertinger, S. K., Ajdari, A., Mezic, I., Stone, H. A., and Whitesides, G. M. (2002). Chaotic mixer for microchannels. *Science* 295, 647–651.

Sun, S., Sprenger, C. C., Vessella, R. L., Haugk, K., Soriano, K., Mostaghel, E. A., et al. (2010). Castration resistance in human prostate cancer is conferred by a frequently occurring androgen receptor splice variant. *J. Clin. Invest.* 120, 2715–2730.

Sun, Y. F., Yang, X. R., Zhou, J., Qiu, S. J., Fan, J., and Xu, Y. (2011). Circulating tumor cells: advances in detection methods, biological issues, and clinical relevance. *J. Cancer Res. Clin. Oncol.* 137, 1151–1173.

Sweat, S. D., Pacelli, A., Murphy, G. P., and Bostwick, D. G. (1998). Prostate-specific membrane antigen expression is greatest in prostate adenocarcinoma and lymph node metastases. *Urology* 52, 637–640.

Tibbe, A. G., de Grooth, B. G., Greve, J., Dolan, G. J., Rao, C., and Terstappen, L. W. (2002). Magnetic field design for selecting and aligning immunomagnetic labeled cells. *Cytometry* 47, 163–172.

Tomita, K., van Bokhoven, A., van Leenders, G. J., Ruijter, E. T., Jansen, C. F., Bussemakers, M. J., et al. (2000). Cadherin switching in human prostate cancer progression. *Cancer Res.* 60, 3650–3654.

Troyer, J. K., Beckett, M. L., and Wright, G. L. (1995). Detection and characterization of the prostate-specific membrane antigen (PSMA) in tissue extracts and body fluids. *Int. J. Cancer* 62, 552–558.

van de Stolpe, A., Pantel, K., Sleijfer, S., Terstappen, L. W., and den Toonder, J. M. (2011). Circulating tumor cell isolation and diagnostics: toward routine clinical use. *Cancer Res.* 71, 5955–5960.

Vona, G., Sabile, A., Louha, M., Sitruk, V., Romana, S., Schütze, K., et al. (2000). Isolation by size of epithelial tumor cells: a new method for the immunomorphological and molecular characterization of circulating-tumor cells. *Am. J. Pathol.* 156, 57–63.

Wang, F. B., Yang, X. Q., Yang, S., Wang, B. C., Feng, M. H., and Tu, J. C. (2011). A higher number of circulating tumor cells (CTC) in peripheral blood indicates poor prognosis in prostate cancer patients – a meta-analysis. *Asian Pac. J. Cancer Prev.* 12, 2629–2635.

Wang, Z. P., Eisenberger, M. A., Carducci, M. A., Partin, A. W., Scher, H. I., and Ts'o, P. O. (2000). Identification and characterization of circulating prostate carcinoma cells. *Cancer* 88, 2787–2795.

Wei, C., Willis, R. A., Tilton, B. R., Looney, R. J., Lord, E. M., Barth, R. K., et al. (1997). Tissue-specific expression of the human prostate-specific antigen gene in transgenic mice: implications for tolerance and immunotherapy. *Proc. Natl. Acad. Sci. U.S.A.* 94, 6369–6374.

Wu, L. Y., Liu, T., Grimm, A. L., Davis, W. C., and Berkman, C. E. (2011). Flow cytometric detection of prostate tumor cells using chemoaffinity labels. *Prostate* 71, 52–61.

Yang, L., Lang, J. C., Balasubramanian, P., Jatana, K. R., Schuller, D., Agrawal, A., et al. (2009). Optimization of an enrichment process for circulating tumor cells from the blood of head and neck cancer patients through depletion of normal cells. *Biotechnol. Bioeng.* 102, 521–534.

Yates, D. R., Rouprêt, M., Drouin, S. J., Comperat, E., Ricci, S., Lacave, R., et al. (2012). Quantitative RT-PCR analysis of PSA and prostate-specific membrane antigen mRNA to detect circulating tumor cells improves recurrence-free survival nomogram prediction after radical prostatectomy. *Prostate* 12, 1382–1388.

Yu, M., Stott, S., Toner, M., Maheswaran, S., and Haber, D. A. (2011). Circulating tumor cells: approaches to isolation and characterization. *J. Cell Biol.* 192, 373–382.

Zabaglo, L., Ormerod, M. G., Parton, M., Ring, A., Smith, I. E., and Dowsett, M. (2003). Cell filtration-laser scanning cytometry for the characterisation of circulating breast cancer cells. *Cytometry A* 55, 102–108.

Zhang, L., Wang, C. Y., Yang, R., Shi, J., Fu, R., Chen, L., et al. (2008). Real-time quantitative RT-PCR assay of prostate-specific antigen and prostate-specific membrane antigen in peripheral blood for detection of prostate cancer micrometastasis. *Urol. Oncol.* 26, 634–640.

Zigeuner, R. E., Riesenberg, R., Pohla, H., Hofstetter, A., and Oberneder, R. (2000). Immunomagnetic cell enrichment detects more disseminated cancer cells than immunocytochemistry *in vitro*. *J. Urol.* 164, 1834–1837.

Zigeuner, R. E., Riesenberg, R., Pohla, H., Hofstetter, A., and Oberneder,

R. (2003). Isolation of circulating cancer cells from whole blood by immunomagnetic cell enrichment and unenriched immunocytochemistry *in vitro*. *J. Urol.* 169, 701–705.

Zink, D., Sadoni, N., and Stelzer, E. (2003). Visualizing chromatin and chromosomes in living cells. *Methods* 29, 42–50.

Zippelius, A., and Pantel, K. (2000). RT-PCR-based detection of occult disseminated tumor cells in peripheral blood and bone marrow of patients with solid tumors. An overview. *Ann. N.Y. Acad. Sci.* 906, 110–123.

Conflict of Interest Statement: The authors declare that the research was conducted in the absence of any commercial or financial relationships that could be construed as a potential conflict of interest.

Received: 30 May 2012; paper pending published: 16 July 2012; accepted: 16 September 2012; published online: 11 October 2012.

Citation: Diamond E, Lee GY, Akhtar NH, Kirby BJ, Giannakakou P, Tagawa ST and Nanus DM (2012) Isolation and characterization of circulating tumor cells in prostate cancer. Front. Oncol. ***2****:131. doi: 10.3389/fonc.2012.00131*

This article was submitted to Frontiers in Cancer Molecular Targets and Therapeutics, a specialty of Frontiers in Oncology.

frontiers in
ONCOLOGY

METHODS ARTICLE
published: 25 October 2012
doi: 10.3389/fonc.2012.00128

Assessment of γ-H2AX levels in circulating tumor cells from patients receiving chemotherapy

Alejandra Garcia-Villa[1], Priya Balasubramanian[1], Brandon L. Miller[1], Maryam B. Lustberg[2], Bhuvaneswari Ramaswamy[2] and Jeffrey J. Chalmers[1]*

[1] *William G. Lowrie Department of Chemical and Biomolecular Engineering, The Ohio State University, Columbus, OH, USA*
[2] *Department of Internal Medicine, Breast Medical Oncology, James Cancer Hospital and Ohio State University Comprehensive Cancer Center, Columbus, OH, USA*

Edited by:
Michael R. King, Cornell University, USA

Reviewed by:
Kevin G. Phillips, Oregon Health & Science University, USA
Jong-Wei Hsu, Cornell University, USA

****Correspondence:***
Jeffrey J. Chalmers, William G. Lowrie Department of Chemical and Biomolecular Engineering, The Ohio State University, 140 West 19th Avenue, Columbus, OH 43210, USA.
e-mail: chalmers.1@osu.edu

Circulating tumor cells (CTCs) are prognostic markers in a variety of solid tumor malignancies. The potential of CTCs to be used as a "liquid biopsy" to monitor a patient's condition and predict drug response and resistance is currently under investigation. Using a negative depletion, enrichment methodology, CTCs isolated from the peripheral blood of breast cancer patients with stage IV breast cancer undergoing DNA damaging therapy with platinum-based therapy were enriched. The enriched cell suspensions were stained with an optimized labeling protocol targeting: nuclei, cytokeratins 8, 18, and 19, the surface marker CD45, and the presence of the protein γ-H2AX. As a direct or indirect result of platinum therapy, double-strand break of DNA initiates phosphorylation of the histone H2AX, at serine 139; this phosphorylated form is referred to as γ-H2AX. In addition to γ-H2AX staining in specific locations with the cell nuclei, consistent with previous reports and referred to as foci, more general staining in the cell cytoplasm was also observed in some cells suggesting the potential of cell apoptosis. Our study underscores the utility and the complexity of investigating CTCs as predictive markers of response to various therapies. Additional studies are ongoing to evaluate the diverse γ-H2AX staining patterns we report here which needs to be further correlated with patient outcomes.

Keywords: circulating tumor cells, metastatic breast cancer, γ-H2AX, chemotherapy, Her2neu

INTRODUCTION

Circulating tumor cells (CTCs) have been isolated in the peripheral blood samples of patients with various kinds of solid tumor malignancies, and elevated CTC numbers correlate with adverse clinical outcomes (Pantel and Alix-Panabieres, 2007). While there is an accumulating body of evidence supporting CTCs as prognostic biomarkers, their role as predictive markers of response to various chemotherapeutic agents is currently under investigation. One such area is whether measuring changes in specific markers on CTCs during chemotherapy can select the patients who are most likely to derive benefit from a specific chemotherapy regimen. One such marker of interest is γ-H2AX.

In higher eukaryotic cells, double-strand breaks (DSBs) in DNA within chromatin quickly (within minutes) initiate the phosphorylation of the histone H2AX, at serine 139 at its C-terminus, to generate γ-H2AX. It is further noted that a single strand break of DNA can elicit a cellular mechanism that will cut the other DNA strand resulting in, effectively, a DSB. The phosphorylated form of H2AX forms foci. All cells in the body contain background foci as a result of the presence of reactive oxygen species, collapsed replication forks, eroded telomeres and depending on cell type, and growth conditions. The foci can be visualized with antibodies to γ-H2AX with each DSB yielding one focus (Nakamura et al., 2006). H2AX phosphorylation and γ-H2AX foci formation are now generally accepted as consistent and quantitative markers of DSBs, applicable even under conditions where only a few DSBs are present (Rothkamm and Lobrich, 2003).

γ-H2AX focal growth was first studied in *Muntiacus muntjak* cells. Small foci appeared 3 min after exposure to ionizing radiation (IR). The foci became brighter and larger at 9 min after IR, and reached maximal brightness and size 30 min after IR. These findings suggest that H2AX molecules in a small region near the DSB site are phosphorylated first, and are followed by molecules at increasing distances from the break site. Thus, foci are sites of accumulation for many factors involved in DNA repair and chromatin remodeling (Nakamura et al., 2006; Bonner et al., 2008; Kinner et al., 2008). There is a close correlation between γ-H2AX foci and DNA DSB numbers and between the rate of foci loss and DSB repair, providing a potentially sensitive assay to monitor DNA damage.

It is this association between γ-H2AX foci and DNA DSB numbers that has lead researchers to suggest that the detection of γ-H2AX foci in CTCs as a rapid method to assess the effectiveness of chemotherapeutic agents that induce DSB (Wang et al., 2010). Such a use of CTCs is consistent with a general term being used to describe the collection of CTCs as a "liquid biopsies"; potentially allowing near real time analysis of the action of chemotherapy agents on the patient cancer cells.

The initial study of γ-H2AX expression in CTC by Wang et al. (2010), and further studies by Kummar et al. (2011, 2012) used the FDA approved, positive selection technology for CTCs,

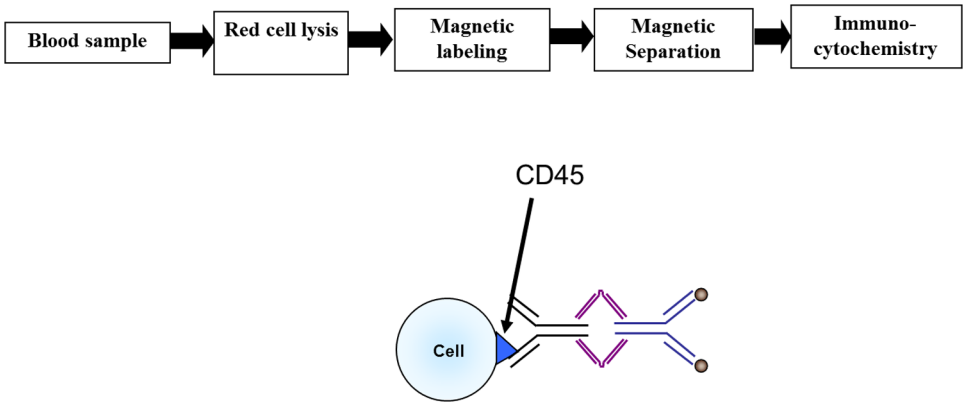

FIGURE 1 | Flow chart of the CTC enrichment methodology.

CellSearch^{TM}, for initial isolation of CTC prior to staining for γ-H2AX. While demonstrated to be effective in isolation of CTCs expressing the epithelial cells surface marker, EpCAM, significant experimental evidence is developing which suggests that potential CTCs are present in blood of cancer patients that do not express EpCAM (Sieuwerts et al., 2009; Konigsberg et al., 2011; Balasubramanian et al., 2012).

To address this bias in only selecting EpCAM positive cells, a purely negative depletion, enrichment approach was developed in which red blood cells are removed, and high expressing CD45 cells are removed in a flow through, high field magnetic quadrupole field (Lara et al., 2004; Yang et al., 2009). With this system, Jatana et al. (2010) presented results suggesting the prognostic significance of CTCs in squamous cell carcinoma of the head and neck (SCCHN) patients.

Given the initial success of this negative enrichment approach, we developed and optimized the staining protocol for evaluating γ-H2AX expression on CTCs stained using non-EpCAM positive selection which has not been previously described.

MATERIALS AND METHODS

CELL LINES

Two breast cancer cell lines, MCF-7 and MDA-MB-231, were procured from ATCC (Manassas, VA, USA) and grown to mid-log phase in Dulbecco's Modified Eagle Medium (DMEM; Cat#10-013, Mediatech, Manassas, VA, USA), supplemented with 10% fetal bovine serum (FBS; Cat#30-2020, ATCC, Manassas, VA, USA) and MEM nonessential amino acids (Cat#25-025, Mediatech, Manassas, VA, USA) at 37°C in a humidified atmosphere containing 5% CO_2. Cells were harvested by washing the adherent cells with PBS and subsequently incubating with Accutase^{TM} (Cat#AT104, Innovative Cell Technologies, Inc.) for 5 min at 37°C to remove the attached cells from the T-flask. The Accutase was then neutralized with the culture media before pelleting the cells at 350 × *g* for 5 min.

PATIENT SAMPLES

Representative samples of CTCs from the peripheral blood of breast cancer patients with stage IV breast cancer undergoing DNA damaging therapy with platinum-based therapy were selected (OSU IRB protocol 2008C0129).

REAGENTS USED FOR CELL SEPARATION

The blood cell suspension, after RBC lysis was labeled with tetrameric antibody complexes (TACs) from Stem Cell technologies (Cat.# 18259, Vancouver, BC, Canada). The specific TACs used in this study were a pan-leukocyte marker that targets different isoforms of the CD45 cell surface antigen and dextran coated magnetic nanoparticles.

SEPARATION/ENRICHMENT METHODOLOGY

The immunomagnetic separation was carried out as described in Yang et al. (2009) and will only be briefly summarized here. An overall view of the separation process is shown in **Figure 1**. Red blood cells in the samples were lysed by mixing the sample with

Table 1 | Antibodies and fluoroprobes used in this study.

Target	Antibody clone	Manufacturer/Cat#	Fluoroprobe	Secondary antibody	Manufacturer/Cat#	Fluoroprobe
Nucleus	–	–	DAPI	–	–	–
Cytokeratins 8, 18, and 19	CK3-6H5	Miltenyi Biotec (130-080-101)	AF488	–	–	–
CD45	Rabbit, polyclonal	Abcam (ab10558)	–	Donkey anti-rabbit	Invitrogen (A-31573)	AF647
Phospho-histone H2A.X (Ser139)	Clone JBW301	Millipore (05-636)	–	Goat anti-mouse IgG (H + L)	Invitrogen (A-11005)	Alexa Fluor 594

Table 2 | Optimized labeling protocol.

1. Prepare cytospin slide of enriched cell sample
2. Wash 1 × 5 min in PBST (PBS + 0.05% Tween 20)
3. Add permeabilization/blocking solution (PBS + 2% normal goat serum + 2% normal donkey serum + 1% BSA + 0.1% gelatin + 0.1% Triton X-100 + 0.05% Tween 20) for 30 min at room temperature
4. Add primary anti-CD45 (rabbit, polyclonal, 1:100) and primary anti-phospho-histone-H2A.X (Ser139; mouse, clone JBW301, 1:100) in antibody diluent, background reducing (Dako, Carpinteria, CA, USA) for 1 h at RT
5. Wash 3 × 5 min in PBST
6. Add secondary Alexa Fluor 647 donkey anti-rabbit IgG (H + L) and secondary Alexa Fluor 594 goat anti-mouse IgG (H + L) in PBST for 1 h at RT
7. Wash 2 × 5 min in PBST
8. Add custom-conjugated cytokeratin 8, 18, 19-Alexa Fluor 488 (clone CK3-6H5, 1:100) in 1% BSA/PBS for 1 h at RT
9. Wash 2 × 5 min in PBST
10. Mount with ProLong Gold antifade reagent with DAPI (Life Technologies, Grand Island, NY, USA)

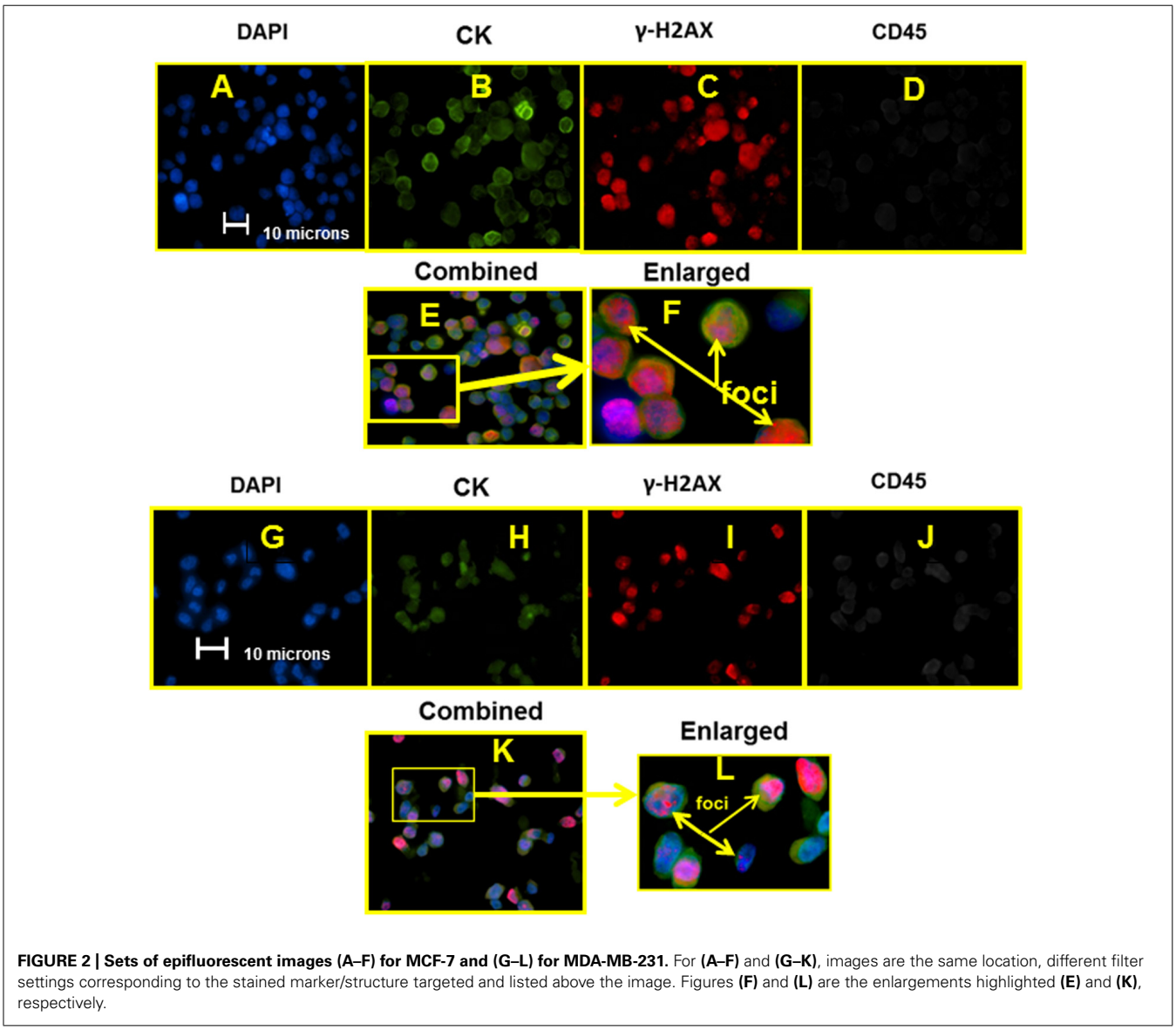

FIGURE 2 | Sets of epifluorescent images (A–F) for MCF-7 and (G–L) for MDA-MB-231. For **(A–F)** and **(G–K)**, images are the same location, different filter settings corresponding to the stained marker/structure targeted and listed above the image. Figures **(F)** and **(L)** are the enlargements highlighted **(E)** and **(K)**, respectively.

lysis buffer (154 mM NH_4Cl, 10 mM $NaHCO_3$, 0.1 mM EDTA) at a ratio of 1:20, incubating it for 5 min at room temperature, and then pelleting the remaining blood cells at 350 × *g* for 5 min. This cell pellet, consisting mostly of nucleated cells, was then labeled with 0.5 μl of anti-CD45 TAC per one million cells for 30 min at room temperature on a shaker. Without washing the cells, 1 μl per one million cells of the magnetic nanoparticles were added to the cell suspension and incubated for 15 min at room temperature on a shaker. The immunomagnetically labeled cell suspension was subsequently diluted with 10 ml of buffer and run through the our previously developed, and reported, magnetic deposition system (Lara et al., 2004; Yang et al., 2009; Balasubramanian et al., 2012).

The final cell suspension, which had passed through the magnetic sorter, was then measured for volume and the cell suspension was split into two aliquots; one of which was subsequently subjected to cell lysis and RNA preservation procedures and the other either directly cytospun for analysis or preserved with 10% neutral buffered formalin for later concentration and ICC analysis. Final cell numbers were obtained by diluting 10 μl of the enriched cell suspension in 3% acetic acid (1:10 dilution) and counting the number of total cells present using a hemocytometer.

REAGENTS, LABELING PROTOCOL, AND MICROSCOPIC IMAGING

Table 1 lists the antibodies used for immunocytochemistry in this study and **Table 2** lists the optimized labeling protocol. An epifluorescent microscope (Nikon Eclipse 80i; Melville, NY, USA) was used for image analysis using the manufacturer supplied NIS-Elements software.

RESULTS

POSITIVE CONTROLS: MCF-7 AND MDA-MB-213 CELLS EXPRESSING γ-H2AX FOCI

Figure 2 presents individual images, using appropriate excitation and emission, for each fluoroprobe as well as an electronically combined, and finally an electronically enlarged image of MCF-7 cells stained with the optimized labeling protocol (**Figures 2A–F**, respectively). **Figures 2G–L** presented DAPI stained and combined staining of MDA-MB-231 cell line.

NEGATIVE CONTROLS

For a negative control, images of buffy coat and fresh, normal, human blood is presented in **Figure 3**. Note the images presented are not truly a representative image; the vast majority of cells (greater than 1 in 1000) do not stain for peripheral or foci γ-H2AX.

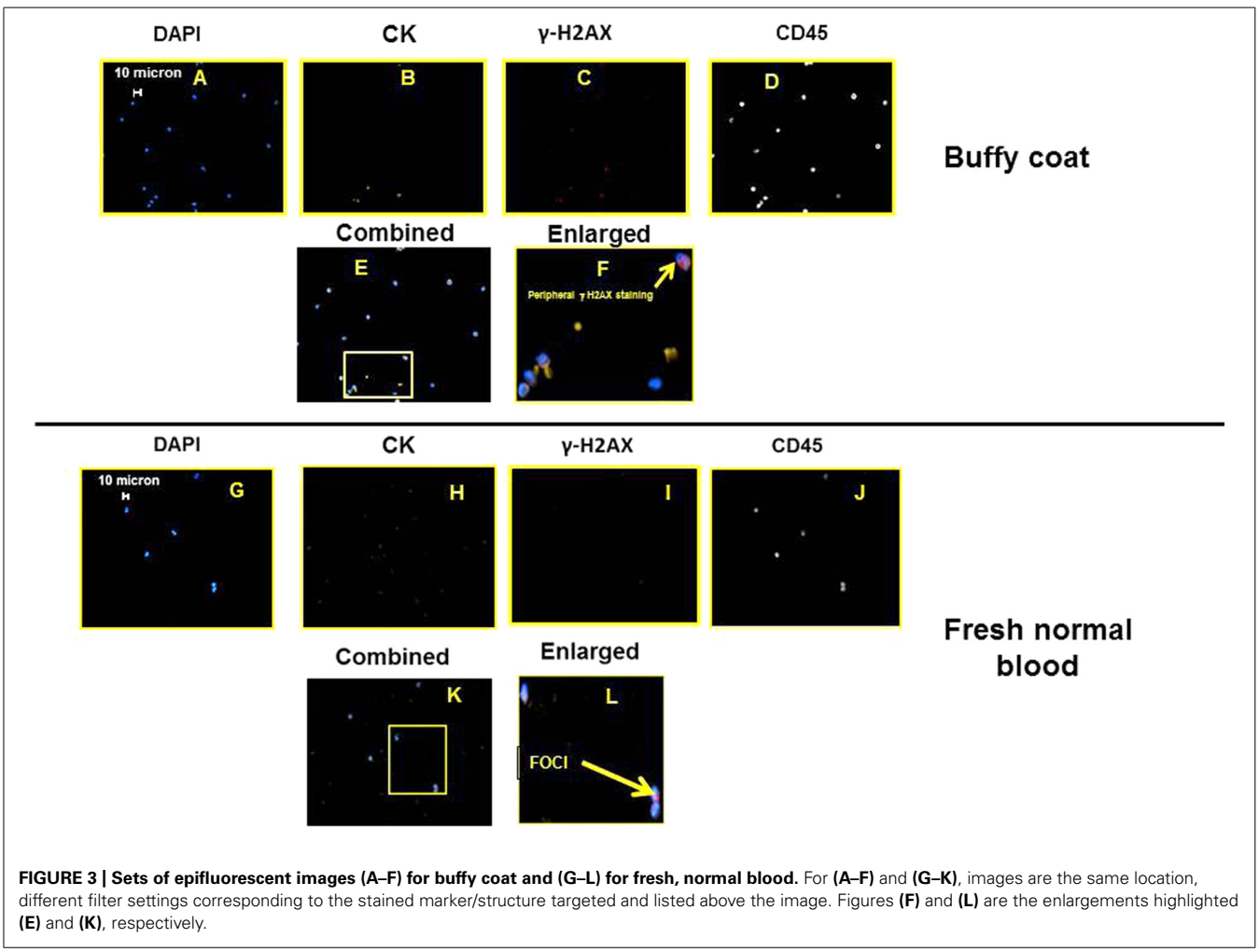

FIGURE 3 | Sets of epifluorescent images (A–F) for buffy coat and (G–L) for fresh, normal blood. For **(A–F)** and **(G–K)**, images are the same location, different filter settings corresponding to the stained marker/structure targeted and listed above the image. Figures **(F)** and **(L)** are the enlargements highlighted **(E)** and **(K)**, respectively.

The specific images were chosen to demonstrate that normal blood cells can have γ-H2AX staining; however, none of these γ-H2AX stained cells also co-stained for cytokeratins.

PATIENT SAMPLES

Figure 4 are representative images of the different types of cell staining observed, including: (1) a traditional CTC with γ-H2AX, nuclear, foci staining, (2) a traditional CTC with only peripheral γ-H2AX staining, (3) a CTC with γ-H2AX, nuclear, foci and peripheral staining, and (4) a cohesive cluster of cells suggestive of tumor embolus that exhibits traditional CTC characteristics and γ-H2AX, nuclear, foci staining. In addition, there exists in many patient samples cells which exhibit staining for all the markers, including CD45.

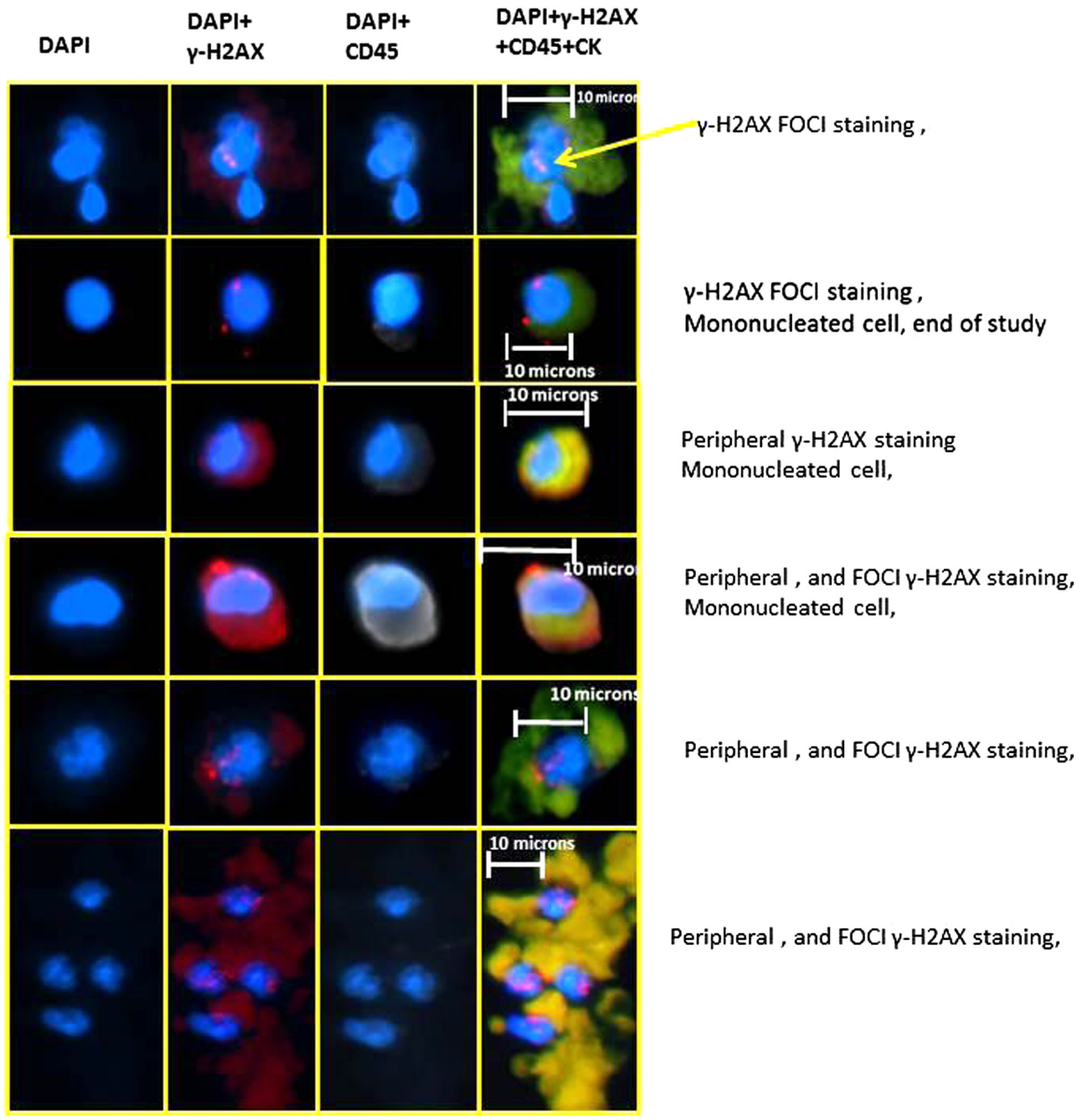

FIGURE 4 | Representative images of the different types of staining patterns observed in peripheral blood samples taken from metastatic breast cancer patients undergoing a phase I, two drug trail. Each sample was from a different patient; yet these images represent the range of types of cells seen in a majority of patients and time points.

DISCUSSION

Using our optimized staining protocol, on samples obtained using an enrichment methodology which depleted normal (RBCs and CD45 expressing) cells, we successfully illustrated the presence of γ-H2AX expression on CTCs in patients with metastatic breast cancer undergoing DNA damaging chemotherapy with platinums. Our multiparameter ICC staining targeted (a) the cell nuclei, (b) cytokeratins 8, 18, and 19, (c) γ-H2AX foci, and (d) CD45. Unlike many other ICC studies of CTCs, we only used specific Alexa Fluor dyes, which have a very low rate of photo bleaching and with very low crosstalk between channels. Using this protocol, we observed various staining patterns, represented by the six different sets of images presented in **Figure 4**.

Further, the distinction between peripheral versus nuclear foci, γ-H2AX staining of cells, as well as the presence of weak CD45 staining on some of the cells, demonstrate the complexity of this type of analysis. While it has been previously reported in the literature that the occurrence of γ-H2AX staining in cells from healthy patients can occur, and as we report in **Figure 3**, we did not see in normal cells positive staining for all four markers including cytokeratin staining. In addition, in these cells from healthy patients, we did not see γ-H2AX foci staining in the nuclei. However, **Figure 4** does indicate that in addition to seeing traditional CTC (i.e., nuclei, cytokeratin positive, and CD45 negative) with γ-H2AX foci, we also observed CTCs with significant peripheral γ-H2AX staining either with or without foci staining. Thus our work suggests that there may be more than just the presence or absence of γ-H2AX foci in CTCs and this may have clinical relevance. Also, unless high magnification is used, the distinction between peripheral staining, and nuclear, foci staining, is a challenge.

Several reports exist on the presence of not just specific "foci" of staining, but the presence of an "apoptotic ring" which looks very similar to some of the staining we have seen in the enriched patient samples (Solier and Pommier, 2009). As the name implies (apoptotic ring), Solier and Pommier (2009) associate a more diffuse staining pattern of γ-H2AX in the nucleus to the apoptotic process and suggest such γ-H2AX staining as another apoptosis marker. In a separate study, Mukherjee et al. (2006) present evidence that γ-H2AX is phosphorylated during apoptotic DNA fragmentation and provide images that are similar to ones we present here.

Finally, it is possible that the peripheral staining is the result of time/aging of cells that initially had nuclear foci. Most studies of γ-H2AX staining report a rapid (within hours) appearance of foci in cancer cell lines in cell culture. Both the lack of knowledge of the pharmacodynamics in actual patients, the practicality of obtaining blood samples at regular, short intervals, and our knowledge of the half-life of CTCs in patients blood, precludes our being able at this point to determine if peripheral staining can be considered a positive response in the same manner that clear foci are considered a positive result. For example, the cells that exhibit peripheral staining in our study could have been circulating in the patient for several days, or longer, and these same cells initially could have exhibited focal staining.

Our study underscores the utility and the complexity of investigating CTCs as predictive markers of response to various therapies. Additional studies are ongoing to evaluate the diverse γ-H2AX staining patterns we report here which needs to be further correlated with patient outcomes. The use of CTCs as a "liquid biopsy" hold great promise. However, systematic, methodological studies are needed to evaluate how to develop and test unbiased multiparameter assays to test markers of interest.

ACKNOWLEDGMENTS

We wish to acknowledge the financial support of the National Science Foundation (BES-0124897 to Jeffrey J. Chalmers and EEC 0425626) the National Cancer Institute (R01 CA97391-01A1 to Jeffrey J. Chalmers, 5 P30 CA16058-26) and the State of Ohio Third Frontier Program (ODOD 26140000: TECH 07-001). In addition, the work was partially supported by Award Number UL1RR025755 from the National Center For Research Resources. The content is solely the responsibility of the authors and does not necessarily represent the official views of the National Center For Research Resources or the National Institutes of Health.

REFERENCES

Balasubramanian, P., Lang, J. C., Jatana, K., Miller, B., Schuller, D., Agrawal, A., et al. (2012). Multiparameter analysis, including EMT markers, on negatively enriched blood samples from patients with squamous cell carcinoma of the head and neck. *PLoS ONE* 7, 1–11, e42048. doi: 10.1371/journal.pone.0042048

Bonner, W. M., Redon, C. E., Dickey, J. S., Nakamura, A. J., Sedelnikova, O. A., Solier, S., et al. (2008). γH2AX and cancer. *Nat. Rev.* 8, 957–967.

Jatana, K. R., Balasubramian, P., Lang, J. C., White, E., Agrwal, A., Ozer, E., et al. (2010). Significance of circulating tumor cells in patients with squamous cell carcinoma of the head and neck. *Arch. Otolaryngol. Head Neck Surg.* 136, 1274–1279.

Kinner, A., Wu, W., Staudt, C., and Iliakis, G. (2008). γ-H2AX in recognition and signaling of DNA double-strand breaks in the context of chromatin. *Nucleic Acids Res.* 36, 5678–5694.

Konigsberg, R., Obermayr, E., Bises, G., Pfeiler, G., Gneist, M., Wrba, F., et al. (2011). Detection of EpCAM positive and negative circulating tumor cells in metastatic breast cancer patients. *Acta Oncol.* 50, 700–710.

Kummar, S., Chen, A., and Ji, J. (2011). Phase I study of PARP inhibitor ABT-888 in combination with topotecan in adults with refractory solid tumors and lymphomas. *Cancer Res.* 71, 5626–5634.

Kummar, S., Ji, J., Morgan, R., Lenz, H., Puhalla, S. L., Belani, C. P., et al. (2012). A phase I study of veliparib in combination with metronomic cyclophosphamide in adults with refractory solid tumors and lymphomas. *Clin. Cancer Res.* 18, 1726–1734.

Lara, O., Tong, X., Zborowski, M., and Chalmers, J. J. (2004). Enrichment of rare cancer cells through depletion of normal cells using density and flow-through, immunomagnetic cell separation. *Exp. Hematol.* 32, 891–904.

Mukherjee, B., Kessinger, C., Kobayashi, J., Chen, B. P. C., Chen, D. J., Chatterjee, A., et al. (2006). DNA-PK phosphorylates histone H2AX during apoptotic DNA fragmentation in mammalian cells. *DNA Repair* 5, 575–590.

Nakamura, A., Sedelinkova, O. A., Rendon, C., Pilch, D. R., Sinogeeva, N. I., Shroff, R., et al. (2006). Techniques for γ-H2AX detection. *Methods Enzymol.* 409, 236–250.

Pantel, K., and Alix-Panabieres, C. (2007). The clinical significance of circulating tumor cells. *Nat. Clin. Pract. Oncol.* 4, 62–63.

Rothkamm, K., and Lobrich, M. (2003). Evidence for a lack of DNA double-strand break repair in human cells exposed to very low x-ray doses. *Proc. Natl. Acad. Sci. U.S.A.* 100, 5057–5062.

Sieuwerts, A. M., Kraan, J., Bolt, J., van der Spoel, P., Elstrodt, F., Schutte, M., et al. (2009). Anti-epithelial cell adhesion molecule antibodies and the

detection of circulating normal-like breast tumor cells. *J. Natl. Cancer Inst.* 101, 61–66.

Solier, S., and Pommier, Y. (2009). The apoptotic ring: a novel entity with phosphorylated histones H2AX and H2B and activated DNA damage response kinases. *Cell Cycle* 8, 1853–1859.

Wang, L. H., Pfister, T. D., Parchment, R. E., Kummar, S., Rubinstein, L., Evard, Y. A., et al. (2010). Monitoring drug-induced γH2AX as a pharmacodynamic biomarker in individual circulating tumor cells. *Clin. Cancer Res.* 16, 1073–1084.

Yang, L., Lang, J. C., Balasubramanian, P., Jantan, K. R., Schuller, D., Agrawal, A., et al. (2009). Optimization of an enrichment process for circulating tumor cells from the blood of head and neck cancer patients through depletion of normal cells. *Biotechnol. Bioeng.* 102, 521–534.

Conflict of Interest Statement: The authors declare that the research was conducted in the absence of any commercial or financial relationships that could be construed as a potential conflict of interest.

Received: 09 June 2012; accepted: 12 September 2012; published online: 25 October 2012.

Citation: Garcia-Villa A, Balasubramanian P, Miller BL, Lustberg MB, Ramaswamy B and Chalmers JJ (2012) Assessment of γ-H2AX levels in circulating tumor cells from patients receiving chemotherapy. Front. Oncol. ***2****:128. doi: 10.3389/fonc.2012.00128*

This article was submitted to Frontiers in Cancer Molecular Targets and Therapeutics, a specialty of Frontiers in Oncology.

frontiers in ONCOLOGY

ORIGINAL RESEARCH ARTICLE
published: 09 August 2012
doi: 10.3389/fonc.2012.00096

Quantification of cellular volume and sub-cellular density fluctuations: comparison of normal peripheral blood cells and circulating tumor cells identified in a breast cancer patient

Kevin G. Phillips[1]*, Anand Kolatkar[2], Kathleen J. Rees[1], Rachel Rigg[1], Dena Marrinucci[2†], Madelyn Luttgen[2], Kelly Bethel[3], Peter Kuhn[2] and Owen J. T. McCarty[1,4]

[1] Department of Biomedical Engineering, School of Medicine, Oregon Health and Science University, Portland, OR, USA
[2] Cell Biology Department, The Scripps Research Institute, La Jolla, CA, USA
[3] Scripps Clinic Medical Group, Scripps Clinic, La Jolla, CA, USA
[4] Department of Cell and Developmental Biology, School of Medicine, Oregon Health and Science University, Portland, OR, USA

Edited by:
Michael R. King, Cornell University, USA

Reviewed by:
Daniel Levy, University of Wyoming, USA
Susan N. Thomas, Georgia Institute of Technology, USA

***Correspondence:**
Kevin G. Phillips, Department of Biomedical Engineering, School of Medicine, Oregon Health and Science University, 3303 South West Bond Avenue, Portland, OR 97239, USA.
e-mail: phillkev@ohsu.edu

†Present address:
Dena Marrinucci, Epic Sciences, Inc., 3565 General Atomics Court, San Diego, CA 92121, USA.

Cancer metastasis, the leading cause of cancer-related deaths, is facilitated in part by the hematogenous transport of circulating tumor cells (CTCs) through the vasculature. Clinical studies have demonstrated that CTCs circulate in the blood of patients with metastatic disease across the major types of carcinomas, and that the number of CTCs in peripheral blood is correlated with overall survival in metastatic breast, colorectal, and prostate cancer. While the potential to monitor metastasis through CTC enumeration exists, the basic physical features of CTCs remain ill defined and moreover, the corresponding clinical utility of these physical parameters is unknown. To elucidate the basic physical features of CTCs we present a label-free imaging technique utilizing differential interference contrast (DIC) microscopy to measure cell volume and to quantify sub-cellular mass-density variations as well as the size of subcellular constituents from mass-density spatial correlations. DIC measurements were carried out on CTCs identified in a breast cancer patient using the high-definition (HD) CTC detection assay. We compared the biophysical features of HD-CTC to normal blood cell subpopulations including leukocytes, platelets (PLT), and red blood cells (RBCs). HD-CTCs were found to possess larger volumes, decreased mass-density fluctuations, and shorter-range spatial density correlations in comparison to leukocytes. Our results suggest that HD-CTCs exhibit biophysical signatures that might be used to potentially aid in their detection and to monitor responses to treatment in a label-free fashion. The biophysical parameters reported here can be incorporated into computational models of CTC-vascular interactions and *in vitro* flow models to better understand metastasis.

Keywords: circulating tumor cells, breast cancer, differential interference contrast microscopy, cellular volume, cellular density

INTRODUCTION

Cancer metastasis, the leading cause of cancer-related deaths, is facilitated in part by the hematogenous transport of circulating tumor cells (CTCs) from the primary tumor site to distant organs. Though CTCs circulate in exceedingly small quantities, approximately 1 CTC per 10^9 blood cells, clinical studies have demonstrated that CTCs circulate in the blood of patients with metastatic disease across all major types of carcinomas (Allard et al., 2004), and that the number of CTCs in peripheral blood is correlated with overall survival in metastatic breast (Cristofanilli et al., 2004), colorectal (Cohen et al., 2008) prostate (Scher et al., 2009) and non-small cell lung (Nieva et al., 2012) cancer, while case reports suggest that CTCs possess morphological features present in corresponding primary and/or metastatic lesions in breast (Marrinucci et al., 2007), colorectal (Marrinucci et al., 2009a), and lung (Marrinucci et al., 2009b) cancer. Together, these studies indicate that CTCs can be used to survey primary and metastatic lesions through minimally-invasive peripheral blood draws.

To date, label-based microscopy techniques have been instrumental in identifying CTCs and characterizing the CTC phenotype. Putative CTCs in existing purification assays are typically identified using immunofluorescent antibody labels to epithelial (EpCAM, CK) and leukocyte (CD45) cell surface markers as well as fluorescent nuclear (DAPI) staining to differentiate CTCs and leukocytes based on fluorescence expression profiles: CD45−CK+DAPI+ (CTC) vs. CD45+CK−DAPI+ (leukocyte) (Racila et al., 1998; Vona et al., 2000; Krivacic et al., 2004; Hsieha et al., 2006; Nagrath et al., 2007). The combined use of fluorescent antibodies to cell surface markers and bright field microscopy based stains (Papanicolau, Wright-Giemsa), for labeling of the nuclear and cytoplasmic cellular compartments, has been central

in establishing the pleomorphic similarity of CTCs to their corresponding primary and/or metastatic lesions (Marrinucci et al., 2007, 2009a,b). While there is great potential to monitor metastasis through CTC enumeration and qualitative investigations of their morphology using these label-based methods, the basic physical features (e.g., mass, volume, density, density fluctuations), discernable through label-free optical methods, of CTCs remain ill defined. Moreover, the corresponding clinical utility of these physical parameters is unknown.

To elucidate the basic physical features of CTCs we developed a label-free microscopy technique utilizing differential interference contrast (DIC) to quantitatively elucidate cell volume, sub-cellular mass-density variations, and the average size of subcellular constituents inferred from spatial mass density correlations. We report volume, mass density fluctuations, denoted $\sigma_A[-]$, and mass density spatial correlations, denoted L_C [μm], for CTCs isolated from a metastatic breast cancer patient using the HD-CTC assay (Marrinucci et al., 2012). The physical properties of HD-CTCs are compared across the normal cellular constituents of blood: platelets (PLT), red blood cells (RBCs), and leukocytes.

MATERIALS AND METHODS

HD-CTC AND LEUKOCYTE IDENTIFICATION AND CHARACTERIZATION

A 54-year-old breast cancer patient provided informed consent at Scripps Clinic (La Jolla, CA) as approved by the Institutional Review Board. The patient presented in October 2007 with bilateral invasive ductal mammary carcinoma and biopsy-proven metastatic disease to bone. The right breast was ER/PR+/HER-2−, while the left breast was ER/PR/HER-2+ with a positive axillary node by fine needle aspiration. A bony site biopsy was ER+, PR−, and HER-2+, all by immunohistochemistry. Blood was taken prior to a bilateral mastectomy in March 2010.

At each draw, 8 mL of peripheral blood was collected in a rare cell blood collection tube (Streck, Omaha, NE) and processed within 24 h after phlebotomy. CTCs were identified using the HD-CTC method, the sensitivity, and specificity of which has been previously reported in Marrinucci et al. (2012). Briefly, the HD-CTC isolation and characterization technique consists of a RBC lysis, after which nucleated cells are attached as a monolayer to custom-made glass slides. Slides are subsequently incubated with antibodies against cytokeratins (CK) 1, 4–8, 10, 13, 18, and 19; and CD45 with Alexa 647-conjugated secondary antibody, nuclei were counterstained with DAPI. For HD-CTC identification, an automated digital fluorescence microscopy technique was used to identify putative HD-CTCs. Fluorescence images of CTC candidates were then presented to a hematopathologist-trained technical analyst for interpretation. Cells are classified as HD-CTCs if they are CK-positive, CD45-negative, contained an intact DAPI nucleus without identifiable apoptotic changes or a disrupted appearance and were morphologically distinct from surrounding leukocytes. Leukocytes were classified according to a CK-negatiave, CD45-positive, DAPI-positive fluorescence status. Cartesian coordinates for each HD-CTC on a slide are generated from a fixed fiduciary marking and used to relocate the cells of interest for DIC measurements. Leukocytes located in the same field of view of HD-CTCs were selected at random to be quantitatively compared to the HD-CTC population.

PREPARATION OF HUMAN PLATELETS

Human venous blood was drawn from healthy donors into citrate-phosphate-dextrose (1:7 vol/vol). PLT rich plasma (PRP) was prepared by centrifugation of anticoagulated blood at 200 g for 10 min. PLTs were further purified from PRP by centrifugation at 1000 g in the presence of prostacyclin (0.1 μg/mL). Purified PLTs were resuspended in modified HEPES/Tyrode buffer (129 mM NaCl, 0.34 mM Na_2HPO_4, 2.9 mM KCl, 12 mM $NaHCO_3$, 20 mM HEPES, 5 mM glucose, 1 mM $MgCl_2$; pH 7.3) containing 0.1 μg/mL prostacyclin. PLTs were washed once by centrifugation and resuspended in modified HEPES/tyrode buffer at indicated concentrations. Purified PLTs were fixed and immobilized on poly-L-lysine coated coverslips.

OPTICAL MEASUREMENT OF CELLULAR VOLUME AND AREA

DIC microscopy is carried out by illuminating the sample of interest with orthogonally polarized co-propagating wave fronts separated by a distance approximately equal to half the wavelength of the light source. These distinct wave fronts are generated by a Wollaston prism in combination with a polarizer placed in the illumination optics of the microscope. Image contrast is produced by specimen mass density variations that give rise to relative phase distortions in the transmitted orthogonally polarized wave fronts exiting the sample. A second Wollason prism and polarizer are used to carry out polarization-dependent common path interferometry; to interfere the exiting orthogonally polarized fronts from the diffraction limited imaging volume of the objective lens. This process converts sample induced phase perturbations in the orthogonal polarization modes into a detectable intensity (Preza et al., 2011). High numerical aperture (NA = 0.9) Köhler illumination enables the visualization of distinct transverse planes of the specimen along the optical axis.

HD-CTCs were relocated and through-focus DIC imagery at ×63 magnification, NA = 1.4, of each cell type was performed on a Zeiss Axio Imager 2 microscope (Carl Zeiss MicroImaging GmbH, Germany) under software control by SlideBook (Intelligent Imaging Innovations, Denver, CO), **Figures 1A,B**. Images were post-processed using a custom program written in MATLAB (The MathWorks, Inc., USA). Post-processing consisted of the application of a Hilbert transform to each *en face* DIC image to ensure optimal contrast in image cube construction (Arinson et al., 2000), **Figure 1C**. This process enables thresholding of DIC images at the cost of introducing image blur along the axial direction. Image blur is eliminated using a high-pass filter applied to each cross-sectional image of the image cube, **Figure 1D**.

The cross sectional areas of the cell in distinct sagittal planes separated by 0.5 [μm] were added together to obtain cellular volume. Each voxel in the analysis corresponds to a diffraction limited volume of 0.28 [μm] × 0.28 [μm] × 0.35 [μm] = 0.029 [fL]. No thresholding of the high-pass filtered Hilbert transformed sagittal images was required. Further details on the method and validation of the Hilbert DIC method for volume are reported in Baker et al. (2012). Cellular area was determined by outlining each cell in *en face* DIC images.

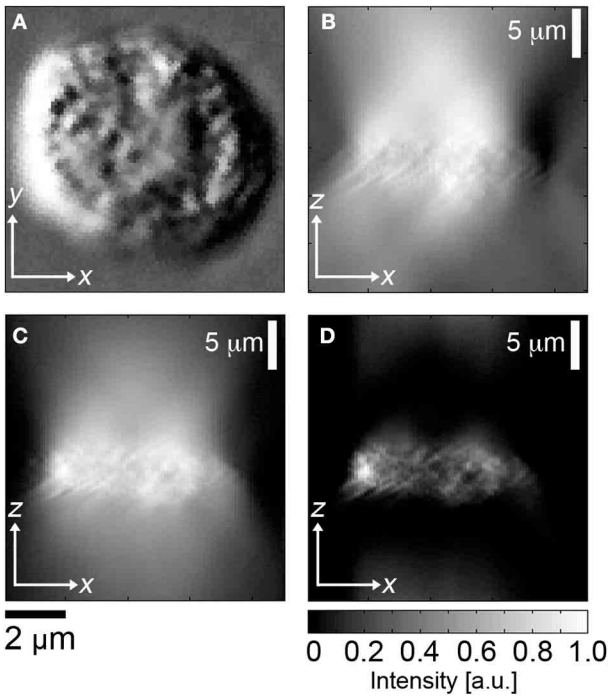

FIGURE 1 | Image segmentation of DIC image cubes. (A) *En face* DIC image, leukocyte, **(B)** corresponding cross sectional image through center of cell, **(C)** Hilbert transform of **(B)**, **(D)** high pass filter applied to **(C)**.

THE DIC IMAGE CONTRAST ARISES FROM SUB-CELLULAR DENSITY GRADIENTS ALONG THE SHEAR DIRECTION OF THE WOLLASTON PRISMS

Following (Preza et al., 1999) we demonstrate that the DIC contrast is dominated by mass-density gradients inside the focal volume of the objective lens. This provides the rationale to adapt the language of "mass density variations" as opposed to "pathlength changes" in describing the origin of DIC image contrast.

We begin with Equation 20 of Preza et al. (1999); a three dimensional DIC imaging model that presumes temporal coherence of the waves interacting with the sample. The temporal coherence assumption is appropriate as the coherence length of the mercury lamp is on the order of cm while the thickness of the sample times the refractive index is on the order of μm. To determine the form of the fields interfering at the detector plane the amplitudes of the waves must be added together.

Referring to Figure 7 of Preza et al. (1999) we define our notation: Let $\mathbb{A}$ denote the area of the front focal plane of the condenser lens, $\vec{\xi}$ denote a point in the front focal plane of the condenser lens, $s(\vec{\xi})$ denotes the intensity of the light source in the focal plane of the of the condenser lens. x, y, z are coordinates in the image plane; x', y', z' are coordinates in the object plane. The transmitted field of the specimen is denoted as $f(x, y, z)$. The point spread function (PSF) of the DIC microscope is denoted $h(x-x', y-y', z-z')$. Lastly, the Köhler illumination plane wave fields are denoted $U_k(\vec{\xi}, x, y)$; see the definition of these waves just after Equation 3 of Preza et al. (1999).

The three dimensional DIC imaging model is Equation 20 of Preza et al. (1999).

$$i(x,y,z) = \int_{\mathbb{A}} s(\vec{\xi}) \left| \int_{\mathbb{R}^3} f(x',y',z')\, h(x-x', y-y', z-z') \right. \\ \left. U_k(\vec{\xi}, x', y') dz' dx' dy' \right|^2 d\vec{\xi} \quad (1)$$

We make the following simplifying assumptions:

1. We assume the DIC PSF is a delta function in x and y coordinates but we retain broadening along the optical axis. The DIC PSF is given in Equation 1 of Preza et al. (1999). The axial PSF is denoted $P(z-z')$. $\Delta\theta$ is the bias retardation introduced by the translation of the Wollaston prism. Δx is the lateral shear introduced by the Wollaston prism. The DIC PSF is then

$$h(x-x', y-y', z-z') = \left(\frac{1}{2} e^{-i\Delta\theta} \delta(x-x'-\Delta x, y) \right. \\ \left. - \frac{1}{2} e^{i\Delta\theta} \delta(x-x'+\Delta x, y) \right) P(z-z') \quad (2)$$

2. The specimen is a "phase" object. The transmitted field is of the form

$$f(x',y',z') = exp(-i\phi(x',y',z')) \quad (3)$$

Plugging in Equation 2 and 3 into Equation 1, we carry out the integration in the x', y' variables to obtain:

$$i(x,y,z) = \frac{1}{4} \int_{\mathbb{A}} s(\vec{\xi}) \left| \int_{\mathbb{R}} P(z-z') \left\{ U_k^- e^{-i\phi^- - i\Delta\theta} \right. \right. \\ \left. \left. - U_k^+ e^{-i\phi^+ + i\Delta\theta} \right\} dz' \right|^2 d\vec{\xi} \quad (4)$$

In this expression we have utilized a shorthand notation in which $U_k^{\pm} = U_k(\vec{\xi}, x \pm \Delta x, y, z')$, and $\phi^{\pm} = \phi(x \pm \Delta x, y, z')$.

We next linearize the phase terms in Equation 4 by taking the small angle approximation of the complex exponentials; appropriate for weak index contrast specimens.

$$i(x,y,z) = \frac{1}{4} \int_{\mathbb{A}} s(\vec{\xi}) \left| \int_{\mathbb{R}} P(z-z') \left\{ (U_k^- - U_k^+) \right. \right. \\ \left. \left. + i(\phi^+ U_k^+ - \phi^- U_k^-) - i\Delta\theta(U_k^- + U_k^+) \right\} dz' \right|^2 d\vec{\xi} \quad (5)$$

Next, we assume that for fixed $\vec{\xi}$ that $U_k \approx U_k^-, U_k \approx U_k^+$, as these fields are separated along the shear direction by approximately $\lambda/2$. This enables the simplification of

Equation 5 to:

$$i\left(x,y,z\right)=\frac{1}{4}\int_{\mathbb{A}}s(\overrightarrow{\xi})\left|\int_{\mathbb{R}}P\left(z-z'\right)\left\{(\phi^{+}-\phi^{-}-2\Delta\theta)U_k\right\}dz'\right|^2 d\overrightarrow{\xi} \quad (6)$$

Multiplying and dividing the phase difference by the magnitude of the shear, $\triangle x = s$ we obtain:

$$i\left(x,y,z\right)=\frac{1}{4}\int_{\mathbb{A}}s(\overrightarrow{\xi})\left|U_k\int_{\mathbb{R}}P\left(z-z'\right)\left\{(s\hat{x}\cdot\nabla\phi-2\Delta\theta)\right\}dz'\right|^2 d\overrightarrow{\xi} \quad (7)$$

We now develop an expression for the phase in terms of the mass-density of the sample.

Let $\overrightarrow{p}(z',\overrightarrow{\xi})$ denote the parameterized path of the wave. We utilize the variable dependence of the Kohler waves on $\overrightarrow{\xi}$ as described in Figure 7 of Preza et al. (1999). We presume that waves traverse the sample in straight-line trajectories—an assumption that is appropriate to weak index contrast samples such as cells. Let f_c denote the focal length of the condenser lens.

$$\overrightarrow{p}(z',\overrightarrow{\xi})=z'\left(\frac{\xi_x}{f_c}\sqrt{1-\frac{\xi_y^2}{f_c^2}}\hat{x}+\frac{\xi_x\xi_y}{f_c^2}\hat{y}+\sqrt{1-\frac{\xi_x^2}{f_c^2}}\hat{z}\right)=z'\widehat{\xi} \quad (8)$$

Letting k denote the wave number, ϕ the phase of waves traversing a specimen, and n the refractive index of the sample, under the paraxial approximation for weak index contrast specimens the phase of plane waves traversing the sample is given by:

$$\phi\left(\overrightarrow{p}(z',\overrightarrow{\xi})\right)=k\int_0^{z'}n\left(\overrightarrow{p}(z'',\overrightarrow{\xi})\right)dz''. \quad (9)$$

The refractive index, as shown in Barer (1952) is related to the mass-density, denoted C [pg/fL], according to:

$$n\left(x,y,z\right)=n_o+\alpha C\left(x,y,z\right). \quad (10)$$

Where n_o is the background index of the cell within a diffraction limited volume, α is the refractive increment ~ 0.2 [fl/pg]. We substitute Equation 10 into Equation 9 and then substitute the resulting expression into Equation 7 to obtain:

$$i(x,y,z)=\frac{1}{4}\int_{\mathbb{A}}s(\overrightarrow{\xi})\left|U_k\alpha ks\hat{x}\cdot\nabla\int_{\mathbb{R}}P\left(z-z'\right)\int_0^{z'}C\left(z''\widehat{\xi}\right)dz''dz'-2\Delta\theta U_k\int_{\mathbb{R}}P\left(z-z'\right)dz'\right|^2 d\overrightarrow{\xi}. \quad (11)$$

Lastly, we note that the PSF limits the axial contributions of the mass density to axial locations near the focal position given by z. Without loss of generality, we presume an axial PSF with a square function shape with width $2\Delta z$ about the focal point z. We find that:

$$\int_{\mathbb{R}}P\left(z-z'\right)\int_0^{z'}C\left(z''\widehat{\xi}\right)dz''dz'\approx\int_{z-\Delta z}^{z+\Delta z}C\left(z''\widehat{\xi}\right)dz''. \quad (12)$$

Substituting Equation 12 into Equation 11 we arrive at the main result

$$i(x,y,z)=\frac{1}{4}\int_{\mathbb{A}}s(\overrightarrow{\xi})\left|U_k\alpha ks\int_{z-\Delta z}^{z+\Delta z}\hat{x}\cdot\nabla C\left(z''\widehat{\xi}\right)dz''-4\Delta\theta\Delta zU_k\right|^2 d\overrightarrow{\xi}. \quad (13)$$

This formula demonstrates that the DIC intensity contrast at a particular z location *inside* the sample is dominated by the spatial gradient of the concentration of cellular mass in that plane (the integral over dz'').

The "pathlength" point of view of DIC microscopy—while entirely valid—does not speak to the main contribution of contrast inside the cell. The axial distance over which the phase is being compared (the limits of integration of the axial variable z'') among the sheared trajectories is held fixed by the objective lens. Hence the height of the sample has been decoupled from the refractive index due to optical sectioning by the objective lens.

This point of view breaks down when the axial extent of the sample changes inside the focal volume: a situation that might arise as the focal volume first encounters the top of the cell.

OPTICAL DETERMINATION OF SUB-CELLULAR DENSITY FLUCTUATION AND SPATIAL CORRELATION

The DIC intensity is a non-linear function of the mass density gradient of the sample along the shear direction of the Wollaston prisms (Preza et al., 2011). Furthermore, the DIC intensity depends on the bias settings of the Wollaston prisms and illumination conditions (Preza et al., 2011). These complications often limit the use of DIC microscopy to qualitative investigations of morphology as the DIC intensity is difficult to relate to physical properties (e.g., density) of the sample. DIC microscopy images do, however, have a simple physical interpretation: they visualize edges of sub-cellular features. The variations of the DIC intensity in space can then be utilized, by analogy with time series analysis of random processes (Wainstein and Zubakov, 1962; Ishimaru, 1978; Subramanian et al., 2009), to quantify the average size of sub-cellular constituents, through spatial correlation, and the average magnitude of density fluctuations, through the analysis of DIC intensity amplitude variations. This heuristic analysis is able to probe the organization of cellular features ranging from the diffraction limit up to multiple microns in scale.

For each pixel location (x, y) in the image of a cell (**Figure 2A**), the axial profile of the DIC intensity was recorded using a charge coupled device camera (CCD), (**Figure 2B**). The DIC signal was then normalized by the background glass signal to eliminate the effects of exposure time and gain settings (**Figure 2C**). A smooth fit to the normalized DIC axial profile was then performed, (**Figure 2C**), and subtracted from the normalized DIC intensity to determine the fluctuating part of the DIC axial profile,

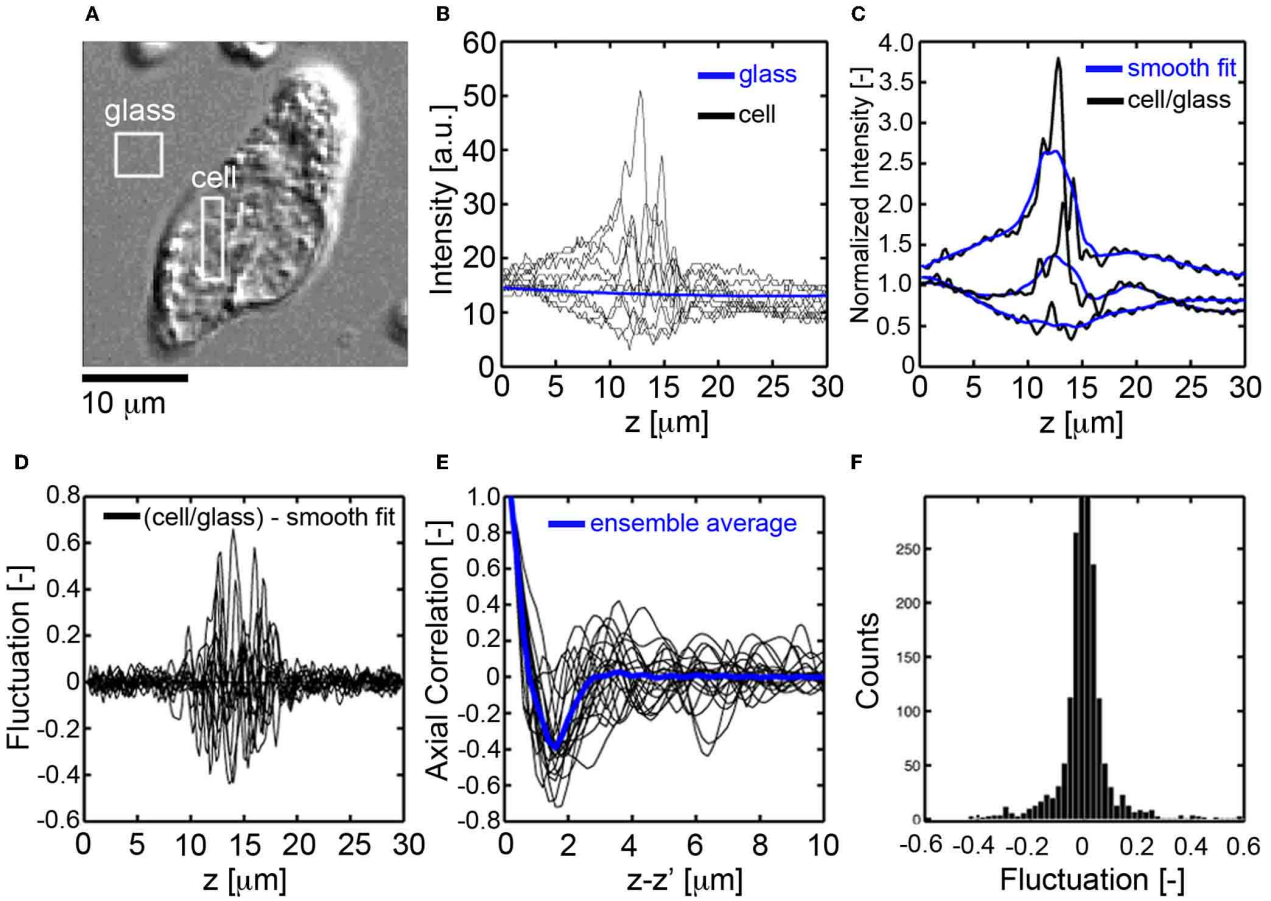

FIGURE 2 | Fluctuation and spatial correlation analysis of axial DIC intensity profiles. (A) *En face* DIC image CTC. **(B)** Axial profiles of DIC intensity for pixels in the cell (black) and glass substrate (blue), **(C)** normalized DIC intensity profile (black, cell signal divided by glass signal) for pixels inside the cell and corresponding smooth fit (blue), **(D)** fluctuating part of the DIC intensity (normalized signal minus smooth fit), **(E)** autocorrelation function of the fluctuating part of the DIC signal, the correlation length L_c[μm] is defined as the first zero crossing, **(F)** histogram of the fluctuating part of the DIC intensity, the mass-density fluctuations are quantified through the standard deviation, σ_A[−], of the histogram.

(**Figure 2D**). The autocorrelation of the fluctuating part of the DIC signal was then numerically computed, (**Figure 2E**). The correlation length, L_C [μm], for each axial profile within a cell was defined as the first zero-crossing of the autocorrelation function. The average magnitude of sub-cellular density fluctuations was assessed by binning the fluctuating part of the DIC intensity into a histogram, (**Figure 2F**). The standard deviation of the fluctuations, σ_A[−], was determined and recorded for each pixel location within the cell. Example L_C and σ_A maps are presented for CTCs and leukocytes in **Figures 4C,D**, respectively.

STATISTICAL ANALYSIS

The Jarque–Bera test was used to evaluate normality of all parameters. One-Way analysis of variance with Bonferonni *post-hoc* analysis was used to assess statistical significance among parameters across multiple normally distributed cell parameters. The Kruskal–Wallis test was used to assess significance among non-normally distributed parameters. *P*-values of 0.05 or less were considered significant. All quantities presented as mean ± standard deviation unless otherwise noted.

RESULTS

BREAST CANCER ASSOCIATED HD-CTCs HAVE LARGER VOLUMES AND AREAS THAN NORMAL BLOOD CELL SUBPOPULATIONS

To investigate the validity of the optical volume measurement technique, we performed measurements on polystyrene spheres and found the measured volumes to coincide with the manufacturers specifications (Baker et al., 2012). To establish the ability of the technique to work with biological specimens, we purified populations of PLTs ($N = 30$) and RBCs ($N = 20$) from healthy volunteers. PLTs and RBCs were measured to have volumes (mean ± standard error of the mean) of 10.5 ± 0.5 fL, 100.6 ± 4.0 fL, within physiological norms determined by the Coulter method (Paulus, 1975; Lichtman, 2005). See **Table 1**.

After this initial validation of the technique, we set out to determine if HD-CTCs had distinct volumes from leukocytes. We measured the volumes of HD-CTCs ($N = 42$, using four slides from the different blood draws of one patient) and leukocytes ($N = 100$) identified in the peripheral blood of a breast cancer patient with known metastatic disease, (**Figure 3**). Leukocytes

Table 1 | Biophysical properties of normal peripheral blood cells and breast cancer associated HD-CTCs.

Cell type	Area [μm^2]	Volume [fL]	L_C [μm]	σ_A[−]	*N*
PLT	7.5 ± 0.3	10.5 ± 0.5	0.42 ± 0.03	0.06 ± 0.01	30
RBC	42.0 ± 1.0	100.6 ± 4.0	1.19 ± 0.05	0.06 ± 0.01	20
Leukocyte	48.0 ± 0.6	234.1 ± 4.1	0.87 ± 0.03	0.17 ± 0.05	100
HD-CTC	135.6 ± 6.0*	851.6 ± 45.8*	0.80 ± 0.04*	0.12 ± 0.04*	42

**Denotes $p < 0.001$ with respect to leukocytes. Leukocytes and HD-CTCs are from the same patient while PLTs and RBCs were collected from healthy donors.*

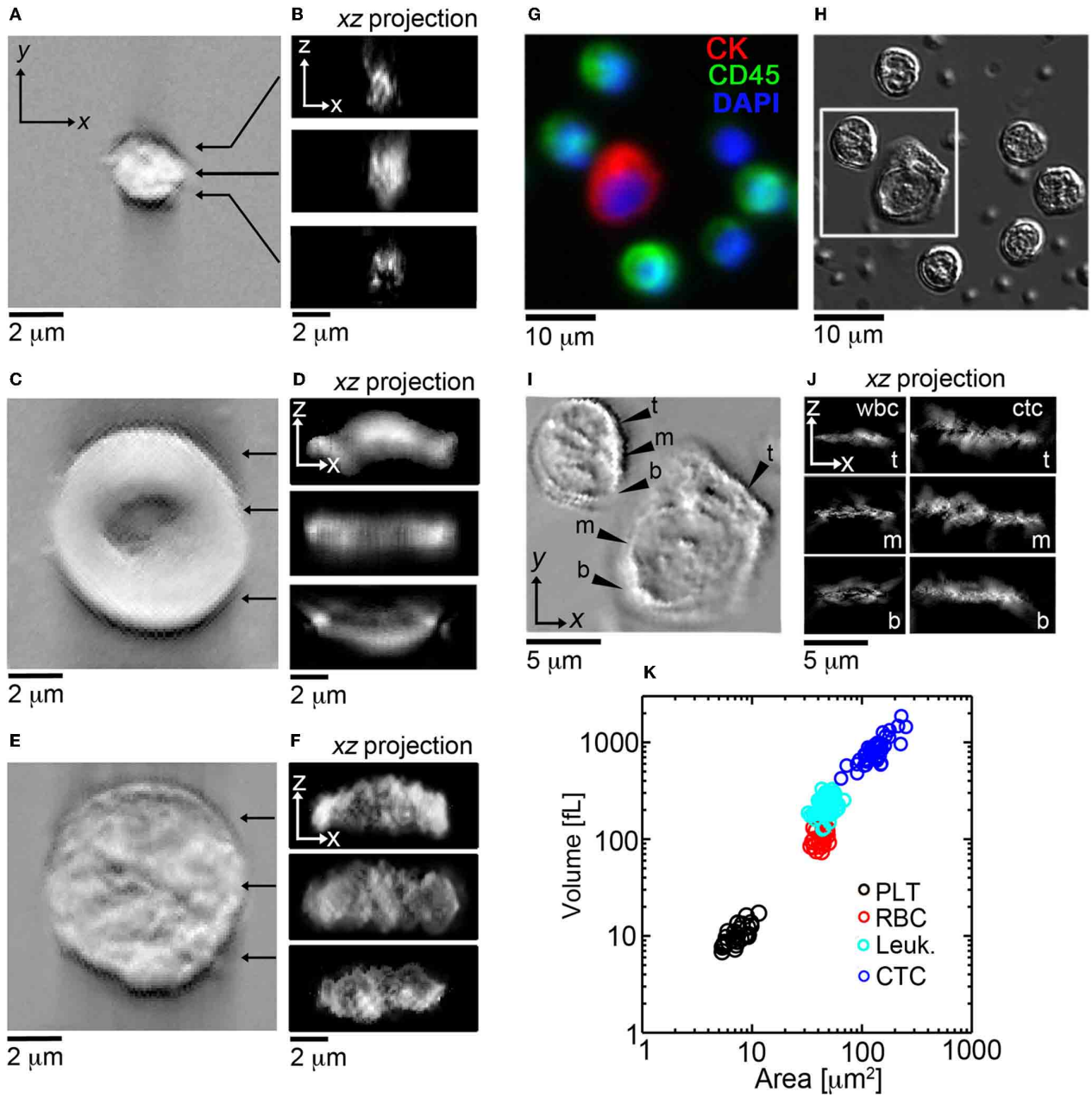

FIGURE 3 | ***En face*** **and cross sectional post-processed DIC images of normal blood cell populations and HD-CTCs.** Representative *en face* and sagittal Hilbert transformed DIC images of **(A,B)** PLT, **(C,D)** RBC, **(E,F)** leukocytes. **(G)** Merged fluorescence image of HD-CTCs and leukocytes from breast cancer patient, **(H)** corresponding DIC image, **(I)** corresponding Hilbert transformed DIC image, **(J)** corresponding cross sectional images at the t, top; m, middle; b, bottom locations denoted in **(I)**. **(K)** Scatter plot of cell areas vs. corresponding volume for each cell type.

were chosen at random in the field of view containing the HD-CTC. HD-CTCs were determined to have significantly larger volumes (mean ± standard error of the mean), 851.6 ± 45.8 [fL], than leukocytes, 234.1 ± 4.1 fL, $p < 0.0001$ (**Table 1**).

Next, we measured the area of each cell type to test for overlap of this parameter among HD-CTCs and leukocytes as previously observed in colorectal cancer (Marrinucci et al., 2009a) and prostate cancer (Stott et al., 2010). The area for normal cell types was measured to be 7.5 ± 0.3 [μm^2] (PLT), 42.0 ± 1.0 [μm^2] (RBC), 48.0 ± 0.6 [μm^2] (leukocytes). CTCs were found to have a mean area of 135.1 ± 6.0 [μm^2], significantly larger than leukocytes, $p < 0.0001$ (**Table 1**).

HD-CTCs EXHIBIT SMALLER MASS-DENSITY FLUCTUATIONS AND SHORTER-RANGE MASS-DENSITY SPATIAL CORRELATIONS IN COMPARISON TO LEUKOCYTES

Previously, we determined by Wright-Giemsa staining that CTCs have a high degree of pleomorphism, exhibit a range of high and low nuclear-to-cytoplasmic ratios, and possess morphological features similar to the primary and/or metastatic lesions in breast (Marrinucci et al., 2007), colorectal (Marrinucci et al., 2009a), and lung (Marrinucci et al., 2009b) cancer.

As the organization of cellular mass density is central in determining the absorption properties exhibited by stained cells and thus central to the qualitative evaluation of CTCs by pathologists, we sought to quantify the heterogeneity of sub-cellular mass density using the optical sectioning and edge detection capabilities of DIC microscopy. DIC intensity variations along the optical axis were used to infer the relative magnitude of sub-cellular density fluctuations, σ_A[−], and spatial correlations along the axial direction can be used to assess the average size of sub-cellular constituents, L_C [μm].

First, we established the utility of the (σ_A, L_C) parameters in distinguishing purified populations of normal blood cells, (**Figures 5B,C**). L_C was found to be unique to each blood cell type: 0.42 ± 0.03 [μm] (PLT), 1.19 ± 0.05 [μm] (RBC), 0.87 ± 0.03 [μm] (leukocyte), $p < 0.001$, while σ_A values were identical for PLTs and RBCs: 0.06 ± 0.01 [−], though distinct for leukocytes: 0.17 ± 0.05 [−], $p < 0.001$, (**Table 1**).

Next, we explored the (σ_A, L_C) properties of HD-CTCs and compared these to leukocytes. Mapping of the σ_A and L_C parameters over the nuclear and cytoplasmic compartments of the cell revealed that CTCs had reduced nuclear density fluctuations and reduced nuclear spatial correlation lengths in comparison to leukocytes, (**Figures 4C,D**). Upon binning the (σ_A, L_C) values corresponding to each cell type into histograms, systematic decreases in both of these parameters were observed cell-wide for CTCs in comparison to leukocytes, (**Figures 4F,G**). No differences between HD-CTCs and leukocytes were observed in histograms of the DIC image alone, (**Figure 4E**).

To determine the ability of the (σ_A, L_C) parameters to quantitatively characterize CTCs and leukocytes, we computed the mean values of σ_A and L_C for CTCs ($N = 42$) and compared these to leukocytes and found statistically significant decreases in both parameters among HD-CTCs in comparison to leukocytes, (**Figure 5**, **Table 1**). The mean subcellular constituent size, L_C, for HD-CTCs was 0.80 ± 0.04 [μm] compared to 0.87 ± 0.03 [μm] for leukocytes, $p < 0.001$; density fluctuations for HD-CTCs, σ_A, were found to be 0.12 ± 0.04 compared to 0.17 ± 0.05 for leukocytes, $p < 0.001$, **Table 1**.

DISCUSSION

Clinical studies have demonstrated that metastatic cancer is accompanied by the presence of CTCs in the peripheral circulation across the major carcinomas (Allard et al., 2004) and that CTCs possess morphologic similarities to primary and/or metastatic lesions (Marrinucci et al., 2007, 2009a,b) and are morphologically distinct from the surrounding white blood cell population (Marrinucci et al., 2012).

To date, the biophysical characterization of CTCs has been restricted to two-dimensional investigations of morphology, area, and nuclear to cytoplasmic ratio. Here we quantified basic three-dimensional biophysical properties of CTCs associated with metastatic disease of the breast: volume and mass density variations. We find that HD-CTCs are characterized by larger volumes, decreased mass-density fluctuations, and possess shorter-range spatial density correlations in comparison to leukocytes. We attribute this basic difference in HD-CTCs and leukocytes to the high nuclear content of leukocytes, giving rise to increased amplitude fluctuations, and the increased amount of compaction of nuclear material in leukocytes, giving rise to larger spatial correlations (sub-cellular constituent sizes). These results mirror the qualitative observation that HD-CTCs in this study had large, spread out nuclei, that were homogenous in comparison to the surrounding leukocytes, **Figure 4B**. Future studies linking DIC based measurements of mass density variations with nano-scopic tools (Subramanian et al., 2008) will provide insight into nuclear architecture over the nano-to-micro scale divide (Zink et al., 2004).

The optical sectioning capability of DIC microscopy provides a means to account for structural information that is normally out of focus or not detectable in fluorescence and stain based imaging, thus yielding a complementary characterization of CTC cellular structure. Indeed, we found that in some instances the cell bodies of CTCs were spread across multiple planes perpendicular to the optical axis, spanning up to 10 μm, while the cell bodies of the leukocyte population were consistently confined to a 3–4 μm range about the central focal plane. As previous reports (Marrinucci et al., 2009a; Stott et al., 2010) utilizing fluorescence microscopy have documented the general separation but partial overlap of CTC area with leukocyte area and the similarity of nuclear to cytoplasmic ratio among breast cancer associated CTCs and leukoctyes (Marrinucci et al., 2007) the future measurement of CTC volume across tumor type and disease stage will provide further insight into the geometric similarities and differences of CTCs and the corresponding leukocyte population.

Physical parameters independent of volume and area, such as density amplitude fluctuations and spatial correlations introduced in this study, provide a complementary measurement of cellular structure that attempt to quantify the qualitative observations of pathologists using stain based analysis under light microscopy. Investigations on transformed human cell lines utilizing label-free optical scattering and spectroscopic reflection microscopy measurements have demonstrated the presence of

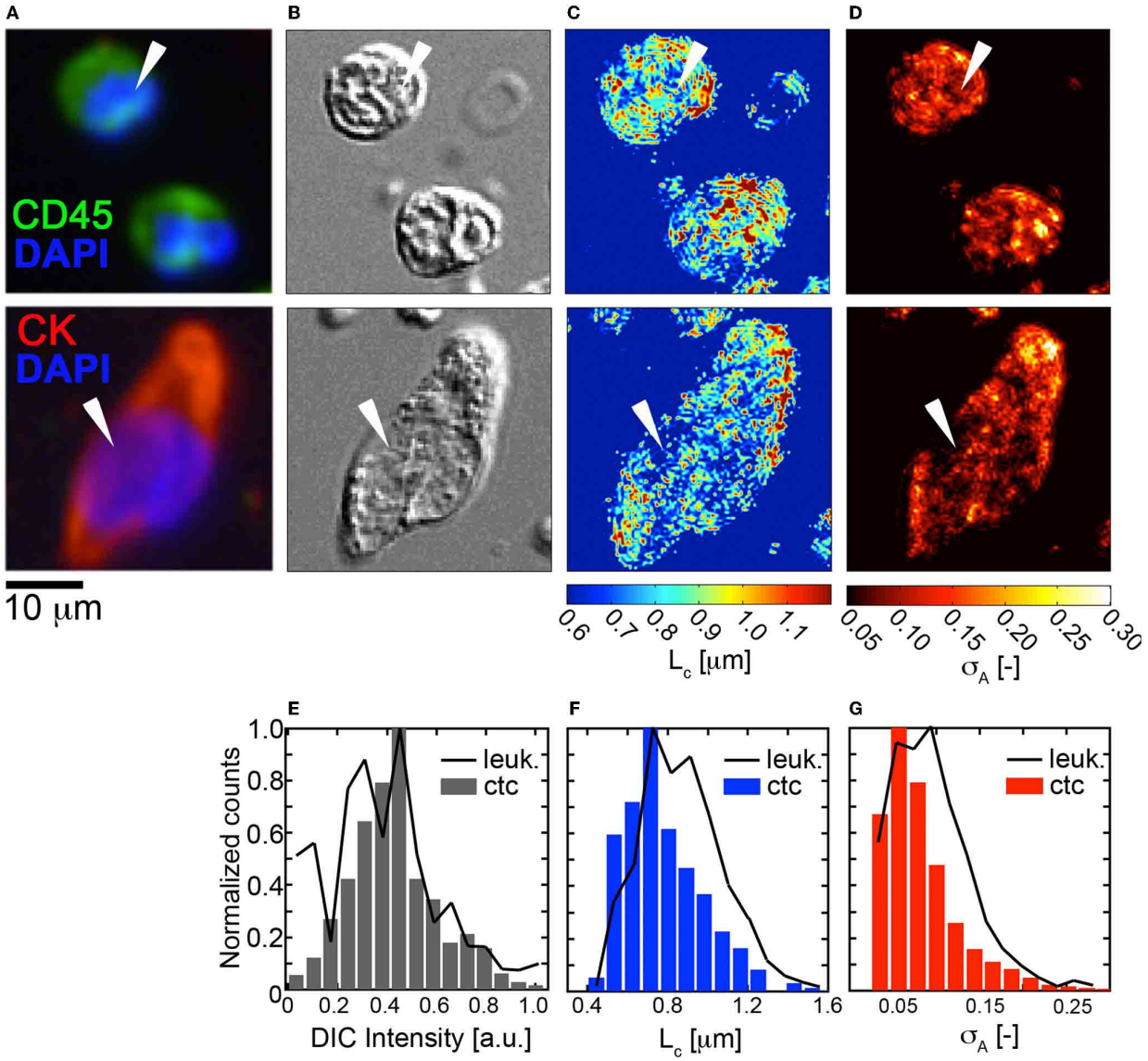

FIGURE 4 | Fluctuation and spatial correlation maps: comparison of HD-CTCs and leukocytes. (A) Merged fluorescence image of HD-CTCs and leukocytes, **(B)** corresponding DIC images, **(C)** spatial correlation length map, **(D)** density amplitude fluctuation map, **(E)** histogram of DIC intensity of cells indicated with white arrows in **(B)**. **(F)** HD-CTC and leukocyte L_c histograms of cells indicated in **(C)**. **(G)** HD-CTC and leukocyte σ_A histograms of cells indicated in **(D)**.

distinct optical signatures from cancer cells: increased sub-cellular constituent size (Mourant et al., 1998), and an increased amount of structural "disorder" at the nanoscale (Subramanian et al., 2008). These observations suggest that cancer at the cellular level is characterized by unique structural features that can be utilized to detect, monitor, and potentially understand cancer.

The DIC method presented is utilized subsequent to molecular based identification of CTCs using the HD-CTC assay. Future validation studies are required to assess the sensitivity and specificity of the biophysical metrics in relation to the HD-CTC inclusion criteria. To be competitive with the HD-CTC assay, the DIC method would need to be drastically sped up. Currently, the DIC method requires two minutes to complete image cube acquisition of a single field using a Zeiss Axio Imager 2 with a moveable stage. This time could be reduced by a factor of 10 with a piezo-driven objective lens holder. Post-processing of image cubes in MATLAB currently takes 5–7 min on a Dell TerraStation using the full resolution image cubes. Down sampling of the cubes to courser grids could speed up computation time at the possible expense of losing information. Future optimization studies are required to make the label-free DIC method competitive with label-based approaches.

Probing the "fluid phase" of cancer has been technologically challenging owing to the minute concentration of CTCs in the peripheral blood of cancer patients with metastatic disease. The advent of modern CTC isolation and characterization

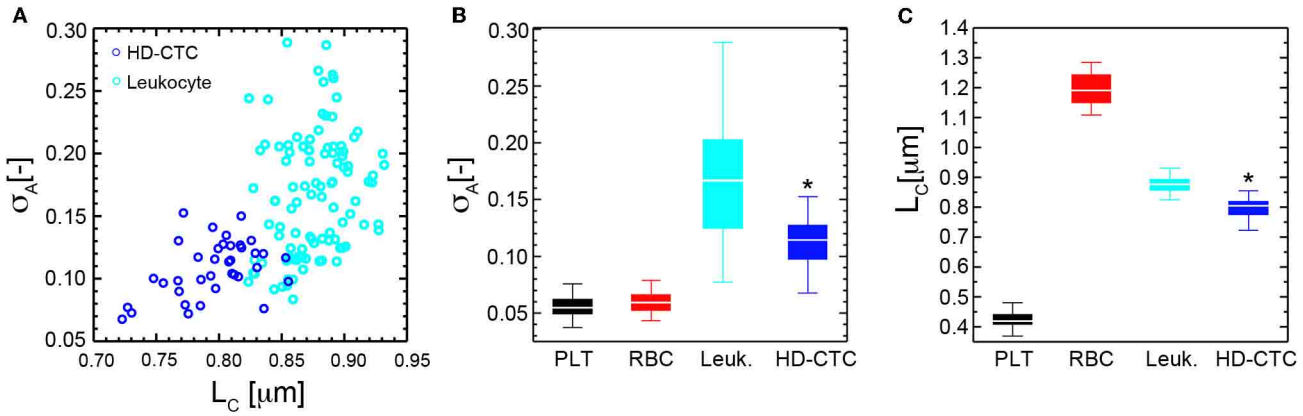

FIGURE 5 | Mass density fluctuation and spatial correlation metrics for normal blood cell subpopulations and HD-CTCs. (A) Scatter plot of spatial correlation length vs. amplitude fluctuations for HD-CTCs and leukocytes from breast cancer patient. **(B)** Box plot comparing population averages of the axial resolved DIC amplitude fluctuations averages of the axial resolved DIC intensity spatial correlation length among PLTs, RBCs, leukocytes, and HD-CTCs. **(C)** Box plot comparing population averages of the axial resolved DIC intensity spatial correlation length among PLTs, RBCs, leukocytes, and HD-CTCs. *Denotes $p < 0.001$ in comparison to leukocytes.

methods has recently enabled the use of these rare cells to survey primary and metastatic tumors through non-invasive blood draws. This study suggests that CTCs may possess a distinct set of physical parameters in comparison to the white blood cell populations in the same patient. However, these parameters have yet to be developed completely to demonstrate their utility for clinical applications. Further studies will be required across multiple patients and disease types to determine whether the physical parameters observed in this study are conserved across patient populations, time, treatment, and cancer type. Measurement of the basic biophysical characteristics of CTCs is critical to both understanding the physical characteristics and chemical kinetics of metastasis and aiding in future detection of CTCs in non-perturbative ways to maintain the viability of these enigmatic cells.

ACKNOWLEDGMENTS

We thank the patients and clinical staff at Scripps Health and the Scripps Clinic Medical Group for their participation and help in this ongoing project. We thank Dr. Steven L. Jacques for insightful discussions. We thank Asako Itakura, Garth Tormoen, Joseph Aslan, Cassandra Loren, Allison McClain, and Kristina Haley for preparing purified blood cell subpopulations. This work was supported by the National Institutes of Health under grant no. 1U54CA143906, and a Physical Sciences in Oncology Young Investigator Award (Kevin G. Phillips). We thank the reviewers for their constructive comments.

REFERENCES

Allard, W. J., Mater, J., Miller, M. C., Repollet, M., Connelly, M. C., Rao, C., Tibbe, A. G. J., Uhr, J. W., and Terstappen, L. W. M. M. (2004). Tumor cells circulate in the peripheral blood of all major carcinomas but not in healthy subjects or patients with nonmalignant diseases. *Clin. Cancer Res.* 10, 6897–6904.

Arinson, M. R., Cogswell, C. J., Smith, N. I., Fekete, P. W., and Larkin, K. G. (2000). Using the Hilbert transform for 3D visualization of differential interference contrast microscope images. *J. Microsc.* 199, 79–84.

Baker, S. M., Phillips, K. G., and McCarty, O. J. T. M. (2012). Development of a label-free imaging technique for the quantification of thrombus formation. *Cell. Mol. Bioeng.* (in press).

Barer, R. (1952). Interference microscopy and mass determination. *Nature* 169, 366–367.

Cohen, S. J., Punt, C. J. A., Iannotti, N., Saidman, B. H., Sabbath, K. D., Gabrail, N. Y., Picus, J., Morse, M., Mitchell, E., Miller, M. C., Doyle, G. V., Tissing, H., Terstappen, L. W. M. M., and Meropol, N. J. (2008). Relationship of circulating tumor cells to tumor response, progression-free survival, and overall survival in patients with metastatic colorectal cancer. *JCO* 26, 3213–3221.

Cristofanilli, M., Budd, G. T., Ellis, M. J., Stopeck, A., Matera, J., Miller, M. C., Reuben, J. M., Doyle, G. V., Allard, W. J., Terstappen, L. W. M. M., and Hayes, D. F. (2004). Circulating tumor cells, disease progression, and survival in metastatic breast cancer. *N. Engl. J. Med.* 351, 781–791.

Hsieha, H. B., Marrinucci, D., Bethel, K., Currya, D. N., Humphreya, M., Krivacica, R. T., Kroenerc, J., Kroenerb, L., Ladanyia, A., Lazarusa, N., Kuhn, P., Bruce, R. H., and Nieva, J. (2006). High-speed detection of circulating tumor cells. *Biosens. Bioelectron.* 21, 1893–1899.

Ishimaru, A. (1978). *Wave Propagation and Scattering in Random Media.* Vol. 2, Chapter 16, New York, NY: Academic Press.

Krivacic, R. T., Ladanyi, A., Curry, D. N., Hsieh, H. B., Kuhn, P., Bergsrud, D. E., Kepros, J. F., Barbera, T., Ho, M. Y., Chen, L. B., Lerner, R. A., and Bruce, R. H. (2004). A rare-cell detector for cancer. *Proc. Natl. Acad. Sci. U.S.A.* 101, 10501–10504.

Lichtman, M. (2005). *Williams Hematology*. New York, NY: McGraw-Hill Professional.

Marrinucci, D., Bethel, K., Bruce, R. H., Curry, D. N., Hsieh, H. B., Humphrey, M., Krivacic, B., Kroener, J., Kroener, L., Ladanyi, A., Lazarus, N., Nieva, J., and Kuhn, P. (2007). Case study of the morphologic variation of circulating tumor cells. *Hum. Pathol.* 38, 514–519.

Marrinucci, D., Bethel, K., Lazar, D., Fisher, J., Huynh, E., Clark, P., Bruce, R., Nieva, J., and Kuhn, P. (2009a). Cytomorphology of circulating colorectal tumor cells: a small case series. *J. Oncol.* 10, Article ID 861341.

Marrinucci, D., Bethel, K., Luttgen, M., Bruce, R. H., Nieva, J., and Kuhn, P. (2009b). Circulating tumor cells from well-differentiated lung adenocarcinoma retain cytomorphologic features of primary tumor type. *Arch. Pathol. Lab. Med.* 133, 1468–1471.

Marrinucci, D., Bethel, K., Kolatkar, A., Luttgen, M., Malchiodi, M.,

Baehring, F., Voigt, K., Lazar, D., Nieva, J., Bazhenova, L., Ko, A. H., Korn, W. M., Schram, E., Coward, M., Yang, X., Metzner, T., Lamy, R., Honnatti, M., Yoshioka, C., Kunken, J., Petrova, Y., Sok, D., Nelson, D., and Kuhn, P. (2012). Fluid biopsy in patients with metastatic prostate, pancreatic and breast cancers. *Phys. Biol.* 9, 016003.

Mourant, J. R., Hielscher, A. H., Eick, A. A., Johnson, T. M., and Freyer, J. P. (1998). Evidence of intrinsic differences in the light scattering properties of tumorigenic and nontumorigenic cells. *Cancer Cytopathol.* 84, 366–374.

Nagrath, S., Sequist, L. V., Maheswaran, S., Bell, D. W., Irimia, D., Ulkus, L., Smith, M. R., Kwak, E. L., Digumarthy, S., Muzikansky, A., Ryan, P., Balis, U. J., Tompkins, R. G., Haber, D. A., and Toner, M. (2007). Isolation of rare circulating tumour cells in cancer patients by microchip technology. *Nature* 450, 1235–1239.

Nieva, J., Wendel, M., Luttgen, M. S., Marrinucci, D., Bazhenova, L., Kolatkar, A., Santala, R., Whittenberger, B., Burke, J., Torrey, M., Bethel, K., and Kuhn, P. (2012). High-definition imaging of circulating tumor cells and associated cellular events in non-small cell lung cancer patients: a longitudinal analysis. *Phys. Biol.* 9, 016004.

Paulus, J. M. (1975). Platelet size in man. *Blood* 46, 321–336.

Preza, C., King, S., Dragomir, N., and Cogswell, C. (2011). "Phase imaging microscopy: beyond dark-field, phase contrast, and differential interference contrast microscopy," in *Handbook of Biomedical Optics*, eds D. Boas, C. Pitris, and N. Ramanujam (New York, NY: Taylor and Francis Books), 483–517.

Preza, C., Snyder, D. L., and Conchello, J. A. (1999). Theoretical development and experimental evaluation of imaging models for differential interference contrast microscopy. *J. Opt. Soc. Am. A* 16, 2185–2199.

Racila, E., Euhus, D., Weiss, A. J., Rao, C., McConnell, J., Terstappen, L. W. M. M., and Uhr, J. W. (1998). Detection and characterization of carcinoma cells in the blood. *Proc. Natl. Acad. Sci. U.S.A.* 95, 4589–4594.

Scher, H. I., Jia, X., de Bono, J. S., Fleisher, M., Pienta, K. J., Raghavan, D., and Heller, G. (2009). Circulating tumour cells as prognostic markers in progressive, castration-resistant prostate cancer: a reanalysis of IMMC38 trial data. *Lancet Oncol.* 10, 233–239.

Stott, S. L., Hsu, C. H., Tsukrov, D. I., Yu, M., Miyamoto, D. T., Waltman, B. A., Rothenberg, S. M., Shah, A. M., Smas, M. E., Korir, G. K., Floyd, F. P., Gilman, A. J., Lord, J. B., Winokur, D., Springer, S., Irimia, D., Nagrath, S., Sequist, L. V., Lee, R. J., Isselbacher, K. J., Maheswaran, S., Haber, D. A., and Tonera, M. (2010). Isolation of circulating tumor cells using a microvortex-generating herringbone-chip. *Proc. Natl. Acad. Sci. U.S.A.* 107, 18392–18397.

Subramanian, H., Pradhan, P., Liu, Y., Capoglu, I. R., Lia, X., Rogers, J. D., Heifetz, A., Kunte, D., Roy, H. K., Taflove, A., and Backman, V. (2008). Optical methodology for detecting histologically unapparent nanoscale consequences of genetic alterations in biological cells. *Proc. Natl. Acad. Sci. U.S.A.* 105, 20118–20123.

Subramanian, S., Pradhan, P., Liu, Y., Capoglu, I. R., Rogers, J. D., Roy, H. K., Brand, R. E., and Backman1, V. (2009). Partial-wave microscopic spectroscopy detects subwavelength refractive index fluctuations: an application to cancer diagnosis. *Opt. Lett.* 34, 518–520.

Vona, G., Sabile, A., Louha, M., Sitruck, V., Romana, S., Schütze, K., Capron, F. D., Pazzagli, M., Vekemans, M., Lacour, B., Bréchot, C., and Paterlini-Bréchot, P. (2000). Isolation by size of epithelial tumor cells: a new method for the immunopharmological and molecular characterization of circulating tumor cells. *Am. J. Pathol.* 156, 57–63.

Wainstein, L. A., and Zubakov, V. D. (1962). *Extraction of Signals from Noise.* (New York, NY: Dover Publications, Inc.).

Zink, D., Fischer, A. H., and Nickerson, J. A. (2004). Nuclear structure in cancer cells. *Nat. Rev. Cancer* 4, 677–687.

Conflict of Interest Statement: The HD-CTC technology has been licensed to Epic Sciences. Authors of this manuscript have ownership in Epic Sciences.

Received: 01 June 2012; accepted: 23 July 2012; published online: 09 August 2012.
Citation: Phillips KG, Kolatkar A, Rees KJ, Rigg R, Marrinucci D, Luttgen M, Bethel K, Kuhn P and McCarty OJT (2012) Quantification of cellular volume and sub-cellular density fluctuations: comparison of normal peripheral blood cells and circulating tumor cells identified in a breast cancer patient. Front. Oncol. ***2****:96. doi: 10.3389/fonc.2012.00096*
This article was submitted to Frontiers in Cancer Molecular Targets and Therapeutics, a specialty of Frontiers in Oncology.

frontiers in ONCOLOGY

ORIGINAL RESEARCH ARTICLE
published: 18 July 2012
doi: 10.3389/fonc.2012.00072

Optical quantification of cellular mass, volume, and density of circulating tumor cells identified in an ovarian cancer patient

Kevin G. Phillips[1]*, Carmen Ruiz Velasco[2], Julia Li[2], Anand Kolatkar[2], Madelyn Luttgen[2], Kelly Bethel[3], Bridgette Duggan[3], Peter Kuhn[2] and Owen J. T. McCarty[1,4]

[1] Department of Biomedical Engineering, School of Medicine, Oregon Health & Science University, Portland, OR, USA
[2] Department of Cell Biology, The Scripps Research Institute, La Jolla, CA, USA
[3] Scripps Clinic Medical Group, Scripps Clinic, La Jolla, CA, USA
[4] Department of Cell and Developmental Biology, School of Medicine, Oregon Health & Science University, Portland, OR, USA

Edited by:
Michael R. King, Cornell University, USA

Reviewed by:
Bryan Greene, BioCytics, Inc., USA
Andrew Hughes, Cornell University, USA

***Correspondence:**
Kevin G. Phillips, Department of Biomedical Engineering, School of Medicine, Oregon Health & Science University, 3303 South West Bond Avenue, Portland, OR 97239, USA.
e-mail: phillkev@ohsu.edu

Clinical studies have demonstrated that circulating tumor cells (CTCs) are present in the blood of cancer patients with known metastatic disease across the major types of epithelial malignancies. Recent studies have shown that the concentration of CTCs in the blood is prognostic of overall survival in breast, prostate, colorectal, and non-small cell lung cancer. This study characterizes CTCs identified using the high-definition (HD)-CTC assay in an ovarian cancer patient with stage IIIC disease. We characterized the physical properties of 31 HD-CTCs and 50 normal leukocytes from a single blood draw taken just prior to the initial debulking surgery. We utilized a non-interferometric quantitative phase microscopy technique using brightfield imagery to measure cellular dry mass. Next we used a quantitative differential interference contrast microscopy technique to measure cellular volume. These techniques were combined to determine cellular dry mass density. We found that HD-CTCs were more massive than leukocytes: 33.6 ± 3.2 pg (HD-CTC) compared to 18.7 ± 0.6 pg (leukocytes), $p < 0.001$; had greater volumes: 518.3 ± 24.5 fL (HD-CTC) compared to 230.9 ± 78.5 fL (leukocyte), $p < 0.001$; and possessed a decreased dry mass density with respect to leukocytes: 0.065 ± 0.006 pg/fL (HD-CTC) compared to 0.085 ± 0.004 pg/fL (leukocyte), $p < 0.006$. Quantification of HD-CTC dry mass content and volume provide key insights into the fluid dynamics of cancer, and may provide the rationale for strategies to isolate, monitor or target CTCs based on their physical properties. The parameters reported here can also be incorporated into blood cell flow models to better understand metastasis.

Keywords: circulating tumor cell, ovarian cancer, differential interference contrast, quantitative phase microscopy, cellular mass, cellular volume, cellular density

INTRODUCTION

Ovarian cancer is the most lethal gynecological cancer and the fifth leading cause of cancer death among women in the United States. Over 90% of stage I patients with ovarian cancer can be cured with the current standard of care: tumor resection followed by platinum and taxane based chemotherapy. However, only 20% of ovarian cancers are detected in stage I (Bast et al., 2009). This is due in part to the anatomic location of the ovaries deep within the pelvis, the absence of tumor-specific symptoms (Lim et al., 2012) and a lack of effective serum markers that correlate with early disease progression (Anderson et al., 2010; Urban et al., 2011). The development of sensitive and specific diagnostic techniques for ovarian cancer is thus imperative to enhance the treatment outcomes of this disease. The enumeration and physical characterization of circulating tumor cells (CTCs) represents a new strategy to monitor the dynamics of tumor burden and potentially gain insight into the hematogenous transport of CTCs to other locations in the body.

Clinical studies have demonstrated that CTCs are present in the blood of cancer patients with known metastatic disease across the major types of epithelial malignancies (Allard et al., 2004). The concentration of CTCs in the blood is prognostic of overall survival in ovarian (Poveda et al., 2011), breast (Cristofanilli et al., 2004), prostate (Scher et al., 2009), colorectal (Cohen et al., 2008), and non-small cell lung cancer (Nieva et al., 2012) and is predictive of radiological response in some instances (Hayes et al., 2006; Cristofanilli et al., 2004). Further, case reports suggest that CTCs possess morphological features resembling the corresponding primary and/or metastatic lesions in breast (Marrinucci et al., 2007), colorectal (Marrinucci et al., 2009a), and lung (Marrinucci et al., 2009b) cancer. Together, these studies indicate that CTCs can be used to survey primary and metastatic lesions through minimally invasive peripheral blood draws or "fluid biopsies."

While the morphology of CTCs is understood from the perspective of hematopathology, the physical properties of CTCs and their potential correlation to disease progression, the physics of hematogenous dissemination, and the processes governing arrest in distant organs are ill-defined. The observation that epithelial cells are less dense than red blood cells (RBCs) and tend to be

large in comparison to hematopoetic cells has inspired the use of density dependent enrichment via centrifugation (Rosenberg et al., 2002) and size dependent selection through isolation by size filtration (Vona et al., 2000). In this study, we sought to measure the physical properties of CTCs without any fundamental assumptions regarding the value of these parameters. Hence, the detection technique is independent of these parameters. We utilized the high-definition (HD) CTC assay (Marrinucci et al., 2012) which retains all nucleated cells from peripheral blood and employs a rapid surface marker based fluorescence technique utilizing laser scanning microscopy to identify cytokeratin positive, CD45-negative, DAPI positive cells.

We analyzed 31 CTCs in a 66-year-old ovarian cancer patient with stage IIIC disease. The cells were isolated from a blood draw taken just prior to a debulking surgery. The HD-CTC assay is compatible with high magnification optical microscopy, enabling the use of non-interferometric quantitative phase microscopy (NI-QPM) techniques to measure cellular dry mass and density; as well as the use of differential interference contrast (DIC) microscopy to measure cellular volume. We present a comparison of these biophysical metrics among CTCs and normal leukocyte populations ($N = 50$) with the goal of understanding the cytophysical properties of cancer cells in the circulation. This study may provide the rationale for future strategies to isolate, target, and monitor CTCs using their physical properties.

MATERIALS AND METHODS

HD-CTC ENUMERATION AND CHARACTERIZATION

An ovarian cancer patient provided informed consent at Scripps Clinic (La Jolla, CA, USA) as approved by the Institutional Review Board. Eight milliliters of peripheral blood was collected in a rare cell blood collection tube (Streck, Omaha, NE, USA) and processed within 24 h after phlebotomy. HD-CTCs were identified according to the published protocol, the sensitivity and specificity of which is documented in Marrinucci et al. (2012). The technique consists of a red blood cell lysis, after which nucleated cells are attached as a monolayer to custom-made glass slides. These slides are the same size as standard microscope slides and possess a proprietary coating to ensure maximal retention of live cells. Slides were subsequently incubated with antibodies against cytokeratins (CK) 1, 4–8, 10, 13, 18, and 19 (Sigma); and CD45 with *Alexa* 647-conjugated secondary antibody (Serotec), nuclei were counterstained with DAPI (Serotec). For HD-CTC identification, an automated digital microscopy technique was used for fluorescence imaging. Potential CTCs were located and identified by computational analysis of the resulting image data. Fluorescence images of CTC candidates were then presented to a hematopathologist-trained technical analyst for interpretation. Cells were classified as HD-CTCs if they were CK-positive, CD45-negative, contained an intact DAPI nucleus without identifiable apoptotic changes or a disrupted appearance, and were morphologically distinct from surrounding leukocytes. Cartesian coordinates for each HD-CTC on a slide were generated from a fixed origin on that slide and used to relocate the cells of interest for NI-QPM and DIC measurements. Leukocytes located in the same field of view of HD-CTCs were chosen at random to be quantitatively compared to the HD-CTC population.

NON-INTERFEROMETRIC QUANTITATIVE PHASE MICROSCOPY TO DETERMINE CELLULAR DRY MASS CONTENT

Due to their weak scattering and absorption properties over the optical spectrum, cells appear semi-transparent when imaged with standard brightfield microscopes. This low endogenous contrast under brightfield is a result of the amplitude of the waves traveling through the cell remaining relatively unchanged. The thickness and spatially variable density of the cell however, contributes to appreciable phase lags of the transmitted waves. This fact has inspired the utilization of phase as a contrast mechanism in cellular imaging in modalities such as phase contrast microscopy and DIC microscopy (Preza et al., 2011).

Under the paraxial approximation, appropriate to weak index contrast specimens such as cells, the phase, denoted ϕ (radian), is defined as the sum of the relative refractive index of the sample along the (typically unknown) height of the specimen, denoted $h(x, y)$ (μm) (Barer, 1952; Popescu, 2008)

$$\phi(x,y) = \frac{2\pi}{\lambda}\int_0^{h(x,y)} \left[n_{\text{cell}}(x,y,z) - n_0\right] \text{dz} \tag{1}$$

λ is the wavelength of light used when determining phase. Interestingly, Barer (1952) demonstrated that the dry mass content of a cell could be extracted from quantitative measurements of phase as a result of the cellular refractive index being linearly proportional to the dry mass content of a cell. This technique has been applied to the measurement cellular mass changes through the cell cycle (Mir et al., 2011).

Denoting by C (g/mL) the dry mass density of a cell, and α the specific refraction increment of the cell solids (~0.2 mL/g), the refractive index is dependent on the dry mass density as given by

$$n_{\text{cell}}(x,y,z) = n_0 + \alpha C(x,y,z). \tag{2}$$

Defining the "projected" mass density as $\rho(x,y) = \int_0^{h(x,y)} C(x,y,z)\,\text{dz}$ (g/μm^2), we can obtain ρ from phase by substituting Eq. 2 into Eq. 1 to find

$$\rho = \frac{\lambda\phi}{2\pi\alpha}\,[g/\mu\text{m}^2] \tag{3}$$

Cell mass is then determined by integrating ρ over the area of the cell. Equation 3 requires no assumptions regarding the uniformity of the refractive index or mass density along height of the cell.

In the present investigation we utilize a computational technique based on the transport of intensity equation (TIE; Paganin and Nugent, 1998) that relates axial intensity, denoted $I(x, y, z)$, variations to transverse phase variations

$$-\frac{2\pi}{\lambda}\frac{\partial I(x,y,z)}{\partial z} = \nabla_{x,y}.\left[I(x,y,z)\,\nabla_{x,y}\phi(x,y,z)\right]. \tag{4}$$

$\nabla_{x,y}$ denotes the two-dimensional gradient operator in the transverse x, y (perpendicular to optical, z-axis) coordinates. The

TIE enables the determination of phase from standard brightfield intensity measurements acquired on a traditional microscope employing a charge coupled device (CCD) camera.

The TIE phase measurement consists of an image acquisition step and a post-processing procedure to determine phase. Low numerical aperture (NA) ∼0.3 Köhler illumination of the sample is carried out on a Zeiss Axio Imager 2 microscope (Carl Zeiss MicroImaging GmbH, Germany) with a green, $\lambda = 540 \pm 20$ nm, filter (Chroma Technology Corp., Bellows Falls, VT, USA). Three-hundred through-focus brightfield intensity images of the sample are obtained with a 0.1-μm axial step size under software control by SlideBook 5.5 (Intelligent Imaging Innovations, Denver, CO, USA). The measured intensity is used to approximate the axial derivative of the intensity, left hand side of Eq. 4. A Green function technique is then utilized to solve for phase numerically (Frank et al., 2010) using a two-dimensional Fourier spectral method. Lastly, Eq. 3 is used to determine the projected mass density, ρ, from which the total cellular mass is determined by integration over the area of the cell.

PREPARATION OF POLYSTYRENE SPHERES FOR NI-QPM VALIDATION

To explore the validity of the NI-QPM technique we prepared polystyrene spheres whose phase properties are readily calculable. Twenty microlitres of a 10% solution of polystyrene spheres (Polysciences, Inc.) of diameter 0.11, 0.95, and 4.8 μm were pipetted separately on glass microscope slides (Fischer Scientific). Slides

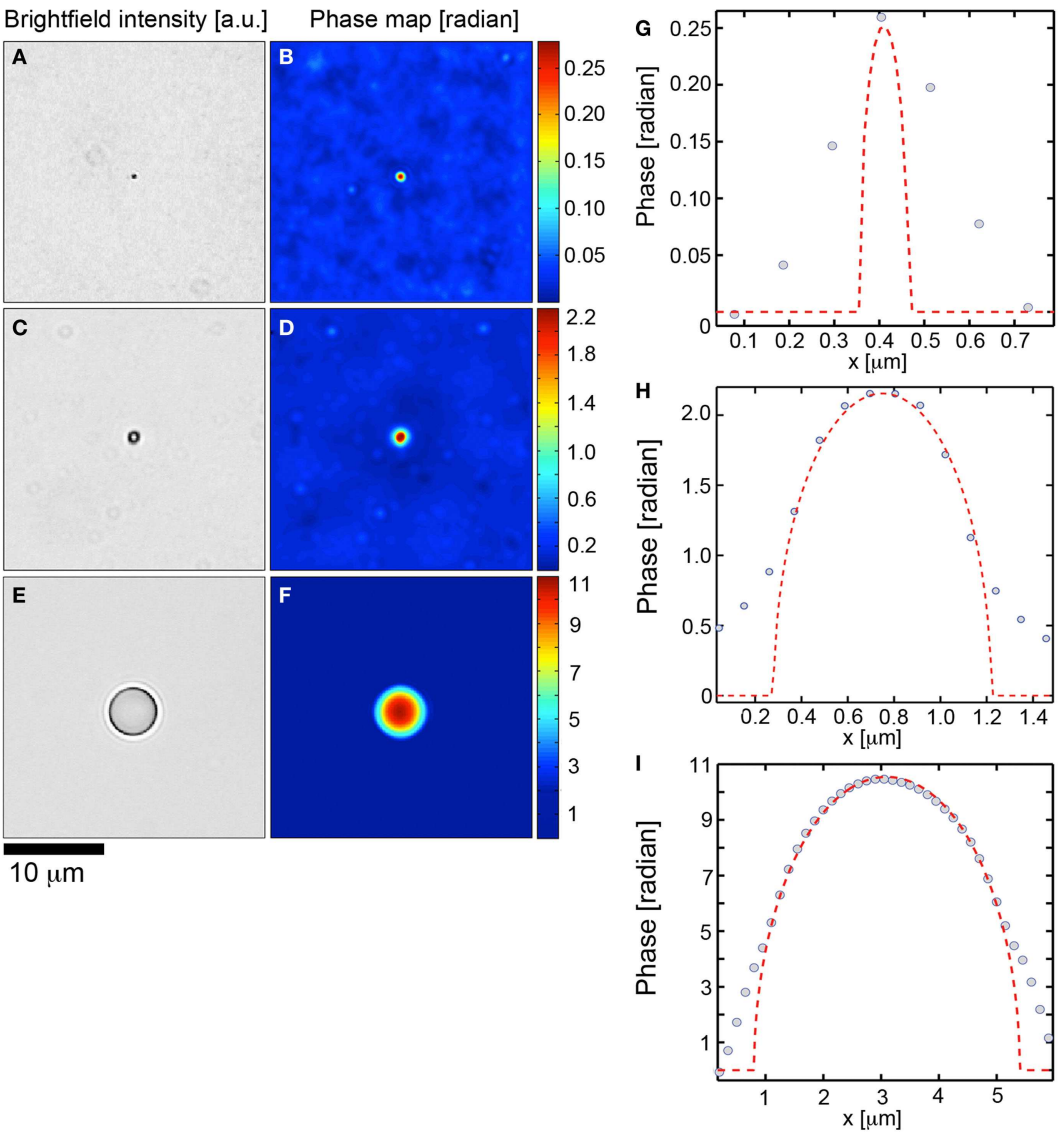

FIGURE 1 | Transport of intensity based quantitative phase microscopy validation over two orders of magnitude. (A,C,E) Brightfield imagery of polystyrene spheres ($n = 1.597$, $\lambda = 540$ nm) suspended in fluoromount G ($n = 1.4$) with diameters of 0.11, 0.95, and 4.8 tm, respectively. **(B,D,F)** Corresponding transport of intensity based quantitative phase maps. **(G,H,I)** demonstrate theoretical phase profiles (dashed) for each polystyrene sphere with corresponding data (circles) overlaid.

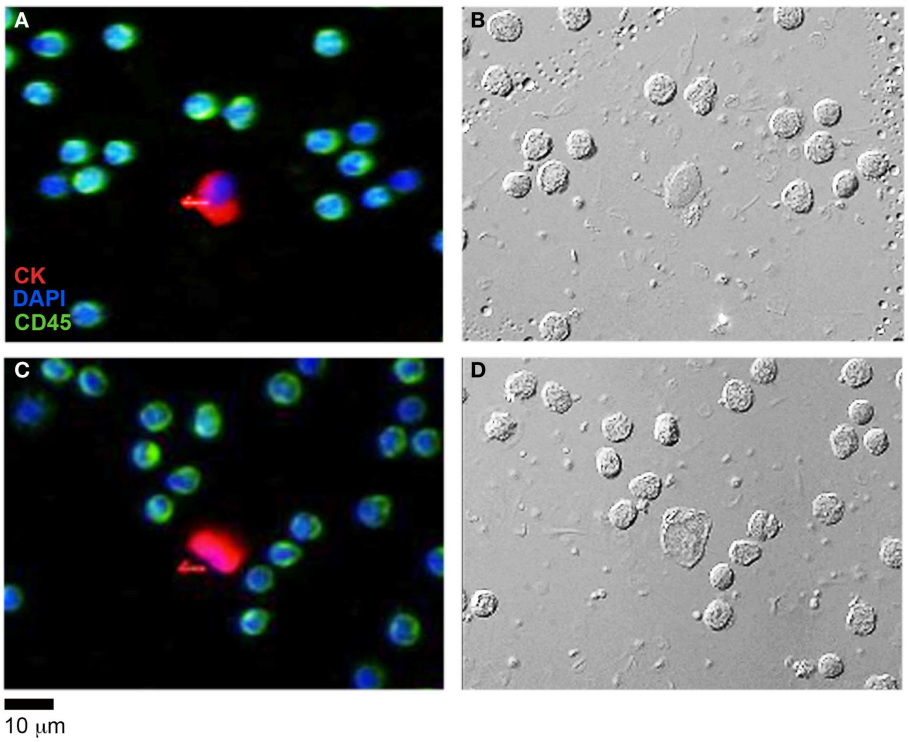

FIGURE 2 | HD-CTC identification of ovarian cancer CTCs and corresponding differential interference contrast (DIC) imagery. (A,C) Immunofluorescent identification of HD-CTCs: CK+CD45−DAPI+ and peripheral leukocytes: CK−CD45+DAPI+ **(B,D)** corresponding differential interference contrast images of the same fields.

were air dried over night and then covered in Fluoromount G (Southern Biotech) whereupon a number 1.5 glass coverslip (Carl Zeiss MicroImaging) was placed overtop of the spheres. The sphere samples were stored overnight at 4°C to allow the Fluoromount G to cure. Prior to imaging, the samples were allowed to return to room temperature for 15 min.

DIFFERENTIAL INTERFERENCE CONTRAST BASED CELLULAR VOLUME DETERMINATION

HD-CTCs were relocated and through-focus DIC imagery at ×63 magnification, NA = 1.4, of each cell type was performed using a Zeiss Axio Imager 2 microscope (Carl Zeiss MicroImaging GmbH, Germany) with a green, $\lambda = 540 \pm 20$ nm, filter (Chroma Technology Corp., Bellows Falls, VT, USA). Three-hundred planes through the sample were acquired with an axial increment of 0.1 μm. The microscope was under software control by SlideBook (Intelligent Imaging Innovations, Denver, CO, USA). Images were post-processed using a custom written program in MATLAB (The MathWorks, Inc., MA, USA). Post-processing consisted of the application of a Hilbert transform to each *en face* DIC image to ensure optimal contrast in image cube construction (Arinson et al., 2000). This process enables thresholding of DIC images at the cost of introducing some image blur along the axial direction. This low frequency noise was eliminated with the application of a high-pass filter to each sagittal plane of the image volume. The relative refractive index of the mounting media and immersion media (matching the cover glass) is low enough to prevent appreciable elongation of images along the optical axis (Rajadhyaksha et al., 1999). The cross sectional area of the cell in distinct sagittal planes was determined using a Sobel-based edge detection algorithm. Outlined sagittal planes of the cell separated by 0.6 μm were added together to obtain cellular volume. Each voxel in the analysis corresponds to a diffraction limited volume of $0.28\,\mu m \times 0.28\,\mu m \times 0.35\,\mu m = 0.029$ fL. Cellular area was determined by outlining each cell in *en face* DIC images.

STATISTICAL ANALYSIS

The Jarque–Bera test was used to evaluate normality of all parameters. One-way analysis of variance with Bonferonni *post hoc* analysis was used to assess statistical significance among parameters across multiple normally distributed cell parameters. The Kruskal–Wallis test was used to assess significance among non-normally distributed parameters. *P*-values of 0.05 or less were considered significant. All quantities presented as mean ± standard error of the mean unless otherwise noted.

RESULTS

TRANSPORT OF INTENSITY BASED QUANTITATIVE PHASE RETRIEVAL METHOD MAINTAINS THE RESOLUTION OF THE DIFFRACTION LIMIT AND IS STABLE OVER TWO ORDERS OF MAGNITUDE OF PHASE

To establish the accuracy of the TIE based phase retrieval algorithm employed in this study, we performed phase retrieval on polystyrene spheres (Polysciences, Inc., Warrington, PA, USA; $n_{sphere} = 1.597$, $\lambda = 0.54\,\mu m$) mounted in Fluoromount G

(Southern Biotech, Birmingham, AL, USA; $n_{\mathrm{Fl.G}} = 1.4$) on glass slides. The reconstructed phase profile was compared to the theoretical phase profile for transmitted waves through a sphere of radius r, given by

$$\phi = \frac{4\pi\left(n_{\mathrm{sphere}} - n_{\mathrm{Fl.G}}\right)}{\lambda}\sqrt{r^2 - (x - x_0)^2}. \quad (5)$$

First we investigated the ability of the TIE to perform phase retrieval at the diffraction limit of the microscope by evaluating the algorithm on 0.11 μm diameter spheres subject to Köhler illumination at an NA = 0.33. The measured resolution (×63, NA = 1.4) was 0.38 μm which agreed with the theoretical resolution for a system: $1.22\lambda/(1.4 + 0.33)$. A higher illumination NA could be used but at the expense of the validity of the TIE which is posed under the paraxial approximation. In **Figures 1A,B** we demonstrate the brightfield intensity and corresponding phase map. **Figure 1G** compares the phase profile through the center of the sphere to the theoretical profile. The TIE based phase had a full-width at half maximum spatial resolution of 0.39 μm. The maximal phase shift of the sphere is 0.25 ± 0.03 radians, given the manufacturer's diameter variation of 0.012 μm, and was measured to be 0.26 by the TIE algorithm, within the manufacturing limits of the sphere. The diffraction limit of the microscope prevented any further information regarding the spatial dependence of the phase profile (**Figure 1G**).

We next investigated the phase retrieval over two orders of magnitude of the phase. Spheres of diameter 0.95 (**Figures 1C,D,H**) and 4.75 μm (**Figures 1E,F,I**) were investigated. The maximum theoretical phase shifts induced by the spheres were 2.18 ± 0.18, 10.9 ± 1.06 rad. In all cases, the TIE phase retrieval was able to recapitulate the theoretical values to within the manufacturing constrains of the spheres (**Figures 1D,F**). As well, the TIE method recapitulated the correct spatial phase profile inside the spheres (**Figures 1H,I**). Deviations of the TIE phase measurement at the edges of the spheres are to be expected from the discontinuity of the refractive index at these locations.

HD-CTCs IDENTIFIED IN AN OVARIAN CANCER PATIENT HAVE DECREASED DENSITIES, DECREASED MASS, INCREASED VOLUME AND INCREASED AREA IN COMPARISON TO NORMAL PERIPHERAL LEUKOCYTES

Having determined the validity of the TIE based NI-QPM algorithm, we performed phase imaging on 31 HD-CTCs. The HD-CTCs were identified in a single blood draw taken just prior to a debulking surgery from a 66-year-old ovarian cancer patient with stage IIIC disease. HD-CTCs were first identified by immunofluorescence staining and subsequently relocated for label-free analysis (**Figure 2**). Separate 25 μm × 25 μm × 30 μm image cubes of

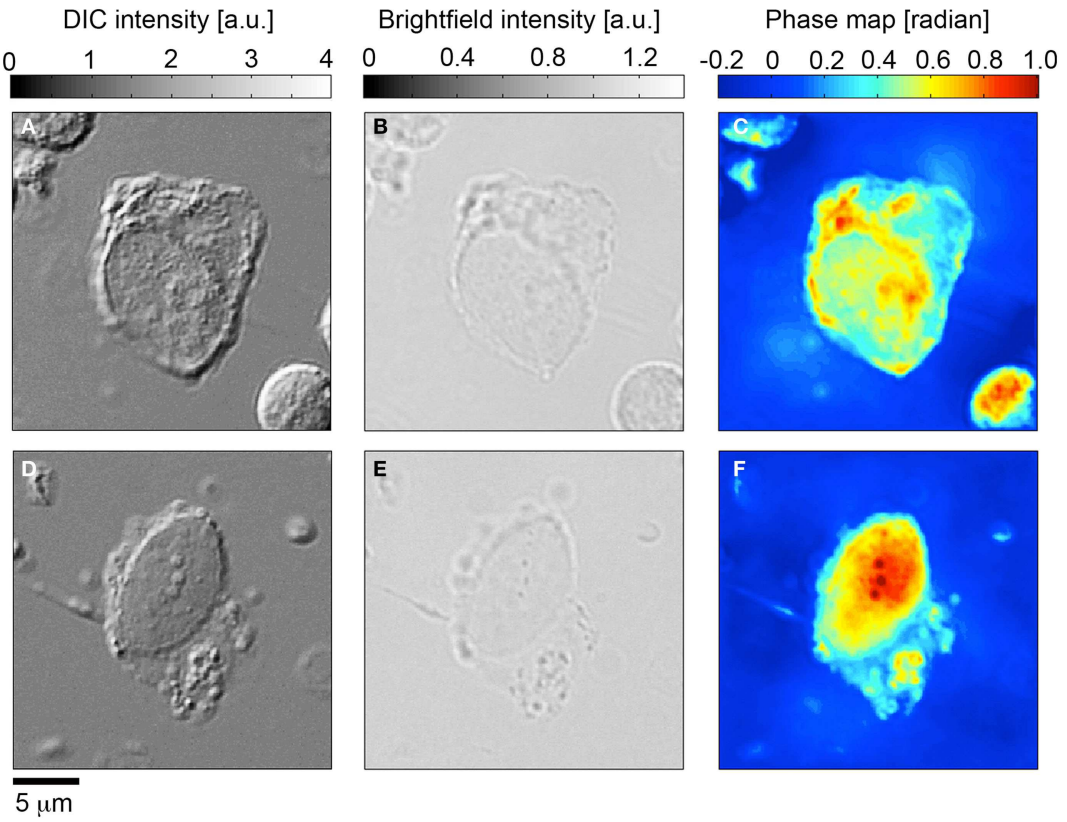

FIGURE 3 | Quantitative phase microscopy of circulating tumor cells; comparison to differential interference contrast (DIC) and brightfield microscopy. (A,D) Differential interference contrast imagery of CK+CD45-DAPI+ HD-CTC5. **(B,E)** Corresponding bright field images. **(C,F)** Quantitative phase microscopy images determined from the transport of intensity equation analysis applied to brightfield through-focus imagery.

individual cells comprised of 18,750,000 voxels were created under brightfield and DIC settings (**Figures 3A,B,D,E**).

Brightfield image cubes were inputted into the TIE phase algorithm to determine phase profiles for each cell (**Figures 3C,F**). DIC image cubes were post-processed using a Hilbert transform technique to enable Sobel-based edge detection to quantify cellular volume.

HD-CTCs and leukocytes separated into distinct populations in the mass-volume parameter space (**Figure 4A**) under the current sampling condition of similar numbers of leukocytes and HD-CTCs analyzed. We found that HD-CTCs were more massive than leukocytes (**Table 1**): 33.6 ± 3.2 pg (HD-CTC) compared to 18.7 ± 0.6 pg (leukocytes), $p < 0.001$ (**Figure 4C**) and had greater volumes (**Table 1**): 518.3 ± 24.5 fL (HD-CTC) compared to 230.9 ± 78.5 fL (leukocyte), $p < 0.001$ (**Figure 4D**). HD-CTCs were found to possess a decreased dry mass density with respect to leukocytes (**Table 1**): 0.065 ± 0.006 pg/fL (HD-CTC) compared to 0.085 ± 0.004 pg/fL (leukocyte), $p < 0.006$ (**Figure 4B**). CTC areas were larger than those of leukocytes (**Table 1**): $138.6 \pm 8.1\ \mu m^2$ (CTC) compared to $51.8 \pm 1.5\ \mu m^2$, $p < 0.001$ (**Figure 4E**).

DISCUSSION

Quantification of the biophysical properties of CTCs provides insight into the physics of the fluid phase of cancer. Flow-dependent interactions with RBCs in the vessels of the microcirculation give rise to the prevalence of less dense cells along the periphery of the vessel wall (e.g., platelets, leukocytes), a phenomenon known as margination (Goldsmith and Spain, 1984). Oxygenated RBCs have a dry mass density of 0.3 pg/fL (Park et al., 2008) by contrast, the leukocytes and HD-CTCs analyzed in this study are roughly 3.5–4.5 times less dense than RBCs, respectively (**Table 1**). The reduced dry mass density of leukocytes and HD-CTCs in comparison to RBCs suggests that these less dense cells may be physically trafficked to the vessel periphery through margination in a similar manner. Proximity of CTCs to the endothelium coupled with a large surface area could enhance the kinetics for interactions with endothelial cells and aid in promoting metastasis.

The label-free optical measurement of dry mass density and volume of HD-CTCs and leukocytes quantifies the density overlap and volumetric differences among these cells. Area and volume

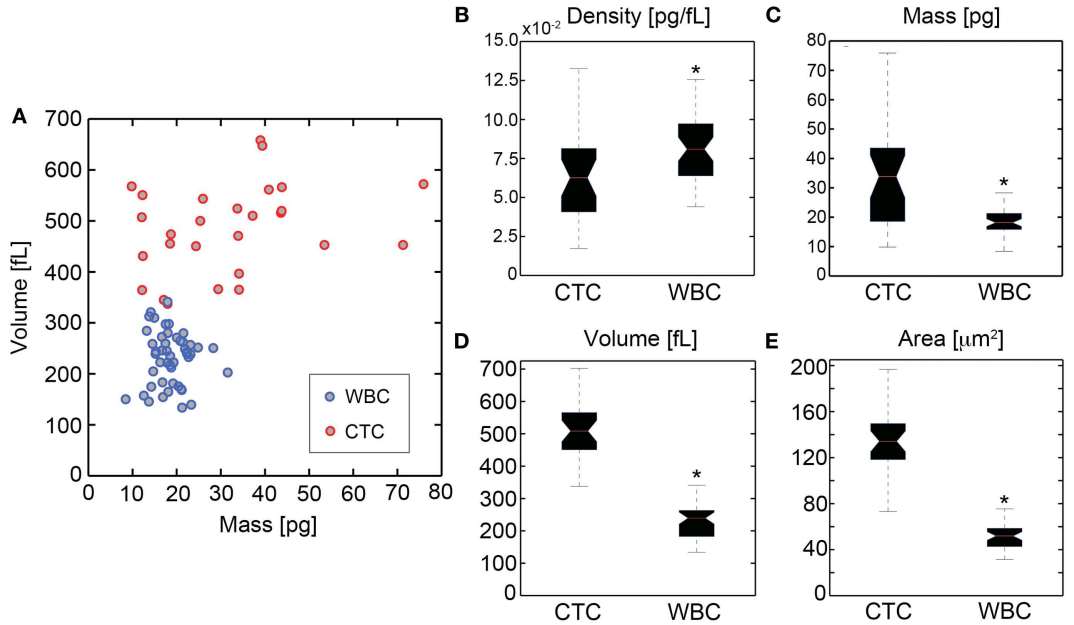

FIGURE 4 | Quantification of biophysical properties of ovarian cancer HD-CTCs. (A) Scatter plot of cellular dry mass in pg (abscissa) versus cellular volume in fL (ordinate). Quantitative phase microscopy based mass measurements and differential interference contrast based volume measurements were uncorrelated. **(B)** Density box and whisker plot, **(C)** mass box and whisker, **(D)** volume box and whisker, **(E)** area box whisker. *Denotes $p < 0.05$ with respect to CTCs.

Table 1 | Biophysical properties of normal peripheral leukocytes and ovarian cancer associated HD-CTCs.

Cell type	Area (mm^2)	Volume (fL)	Mass (pg)	Density (pg/fL)	*N*
Leukocyte (WBC)	51.8 ± 1.5	230.9 ± 78.5	18.7 ± 0.6	0.085 ± 0.004	50
HD-CTC	138.6 ± 8.1*	518.3 ± 24.5*	33.6 ± 3.2*	0.065 ± 0.006*	31

*Area was determined from outlining the boarder of cells using DIC imaging. Volume was determined using a Hilbert transform post-processing algorithm on through-focus DIC image cubes. A non-interferometric quantitative phase microscopy method was used to determine cellular dry mass content. Cellular density was determined by dividing cellular mass by cellular volume. *Denotes $p < 0.05$ with respect to leukocytes.*

were the most statistically significant features that separated the populations from a physical standpoint. The dry mass density values reported here (**Table 1**) demonstrate why CTC enrichment using a density-based method is prone to leukocyte contamination (Rosenberg et al., 2002): the overlap of leukocytes and HD-CTCs makes the use of this parameter an unlikely means to separate the two cell populations (**Figure 4B**). Volumetric differences among these cell types demonstrate that isolation by size methods would omit a fraction of leukocytes (assuming an 8 μm diameter filter) but again, at the cost of leukocyte contamination. One may be tempted to make the filter size larger, allowing more leukocytes to pass through the filter. This should result in reduced leukocyte contamination but at the cost of omitting the potential CTC subpopulation that could overlap volumetrically with leukocytes. This preliminary study in an Ovarian cancer patient demonstrated that volume could separate the CTCs from the leukocyte population. However, more investigations across patients, tumor types, and treatment regimens are required to ensure members of the CTC population would not be lost in the use of larger filter sizes in filtration enrichment approaches. The HD-CTC assay, an enrichment free method, is an optimal tool to investigate the rationale for biophysical based enrichment strategies for CTC detection and lab-on-a-chip type characterizations.

The biophysical properties of HD-CTCs offer quantitative metrics with which to document potential changes in the CTC population in response to therapeutics, disease progression, or interventional surgeries. This label-free biophysical characterization can be carried out in parallel with current efforts to understand the genetic and proteomic composition of both the solid and fluid phase of caner. Together, these complementary approaches might aid in the search for targeted therapies.

ACKNOWLEDGMENTS

We thank the patients and clinical staff at Scripps Health and the Scripps Clinic Medical Group for their participation and help in this ongoing project. We thank Drs. Paul Newton and Steven L. Jacques for enlightening conversations. This work was supported by the National Institutes of Health under grant no. 1U54CA143906, and a Physical Sciences in Oncology Young Investigator Award (Kevin G. Phillips).

REFERENCES

Allard, W. J., Mater, J., Miller, M. C., Repollet, M., Connelly, M. C., Rao, C., Tibbe, A. G. J., Uhr, J. W., and Terstappen, L. W. M. M. (2004). Tumor cells circulate in the peripheral blood of all major carcinomas but not in healthy subjects of patients with nonmalignant disease. *Clin. Cancer Res.* 10, 6897–6904.

Anderson, G. L., McIntosh, M., Wu, L., Thorpe, J. D., Bergan, L., Thornquist, M. D., Scholler, N., Kim, N., O'Briant, K., Drescher, C., and Urban, N. (2010). Assessing lead time of selected ovarian cancer biomarkers: a nested case-control study. *J. Natl. Cancer Inst.* 102, 26–38.

Arinson, M. R., Cogswell, C. J., Smith, N. I., Fekete, P. W., and Larkin, K. G. (2000). Using the Hilbert transform for 3D visualization of differential interference contrast microscope images. *J. Microsc.* 199, 79–84.

Barer, R. (1952). Interference microscopy and mass determination. *Nature* 169, 366–367.

Bast, R. C. Jr., Hennessy, B., and Mills, G. B. (2009). The biology of ovarian cancer: new opportunities for translation. *Nat. Rev. Cancer.* 9, 415–428.

Cohen, S. J., Punt, C. J. A., Iannotti, N., Saidman, B. H., Sabbath, K. D., Gabrail, N. Y., Picus, J., Morse, M., Mitchell, E., Miller, M. C., Doyle, G. V., Tissing, H., Terstappen, L. W. M. M., and Meropol, N. J. (2008). Relationship of circulating tumor cells to tumor response, progression-free survival, and overall survival in patients with metastatic colorectal cancer. *J. Clin. Oncol.* 26, 3213–3221.

Cristofanilli, M., Budd, G. T., Ellis, M. J., Stopeck, A., Matera, J., Miller, M. C., Reuben, J. M., Doyle, G. V., Allard, W. J., Terstappen, L. W. M. M., and Hayes, D. F. (2004). Circulating tumor cells, disease progression, and survival in metastatic breast cancer. *N. Engl. J. Med.* 351, 781–791.

Frank, J., Altmeyer, S., and Wernicke, G. (2010). Non-interferometric, non-iterative phase retrieval by green's functions. *J. Opt. Soc. Am. A Opt. Image Sci. Vis.* 27, 2244–2251.

Goldsmith, H. L., and Spain, S. (1984). Margination of leukocytes in blood flow through small tubes. *Microvasc. Res.* 27, 204–222.

Hayes, D. F., Cristofanilli, M., Budd, G. T., Ellis, M. J., Stopeck, A., Miller, M. C., Matera, J., Allard, W. J., and Doyle, G. V. (2006). Circulating tumor cells at each follow-up time point during therapy of metastatic breast cancer patients predict progression-free and overall survival. *Clin. Cancer Res.* 12, 4218–4224.

Lim, A. W. W., Mesher, D., Gentry-Maharaj, A., and Balogun, N., Jacobs, I., Menon, U., and Sasieni, P. (2012). Predictive value of symptoms for ovarian cancer: comparison of symptoms reported by questionnaire, interview, and general practitioner notes. *J. Natl. Cancer Inst.* 104, 114–124.

Marrinucci, D., Bethel, K., Bruce, R. H., Curry, D. N., Hsieh, H. B., Humphrey, M., Krivacic, B., Kroener, J., Kroener, L., Ladanyi, A., Lazarus, N., Nieva, J., and Kuhn, P. (2007). Case study of the morphologic variation of circulating tumor cells. *Hum. Pathol.* 38, 514–519.

Marrinucci, D., Bethel, K., Kolatkar, A., Luttgen, M., Malchiodi, M., Baehring, F., Voigt, K., Lazar, D., Nieva, J., Bazhenova, L., Ko, A. H., Korn, W. M., Schram, E., Coward, M., Yang, X., Metzner, T., Lamy, R., Honnatti, M., Yoshioka, C., Kunken, J., Petrova, Y., Sok, D., Nelson, D., and Kuhn, P. (2012). Fluid biopsy in patients with metastatic prostate, pancreatic and breast cancers. *Phys. Biol.* 9, 016003.

Marrinucci, D., Bethel, K., Lazar, D., Fisher, J., Huynh, E., Clark, P., Bruce, R., Nieva, J., and Kuhn, P. (2009a). Cytomorphology of circulating colorectal tumor cells: a small case series. *J. Oncol.* 10. [Article ID 861341], 7.

Marrinucci, D., Bethel, K., Luttgen, M., Bruce, R. H., Nieva, J., and Kuhn, P. (2009b). Circulating tumor cells from well-differentiated lung adenocarcinoma retain cytomorphologic features of primary tumor type. *Arch. Pathol. Lab. Med.* 133, 1468–1471.

Mir, M., Wang, Z., Shen, Z., Bednarz, M., Bashir, R., Golding, I., Prasanth, S. G., and Popescu, G. (2011). Optical measurement of cycle-dependent cell growth. *Proc. Natl. Acad. Sci. U.S.A.* 108, 13124–13129.

Nieva, J., Wendel, M., Luttgen, M. S., Marrinucci, D., Bazhenova, L., Kolatkar, A., Santala, R., Whittenberger, B., Burke, J., Torrey, M., Bethel, K., and Kuhn, P. (2012). High-definition imaging of circulating tumor cells and associated cellular events in non-small cell lung cancer patients: a longitudinal analysis. *Phys. Biol.* 9, 016004.

Paganin, D., and Nugent, K. A. (1998). Noninterferometric phase imaging with partially coherent light. *Phys. Rev. Lett.* 80, 2586–2589.

Park, Y. K., Diez-Silva, M., Popescu, G., Lykotrafitis, G., Choi, W., Feld, M. S., and Suresh, S. (2008). Refractive index maps and membrane dynamics of human red blood cells parasitized by *Plasmodium falciparum*. *Proc. Natl. Acad. Sci. U.S.A.* 105, 13730–13735.

Popescu, G. (2008). "Quantitative phase imaging of nanoscale cell structure and dynamics," in *Methods in Cell Biology*, Vol. 90, ed. B. Jena (Burlington: Elsevier), 87–115.

Poveda, A., Kaye, S. B., McCormack, R., Wang, S., Parekh, T., Ricci, D., Lebedinsky, C. A., Tercero, J. C., Zintl, P., and Monk, B. J. (2011). Circulating tumor cells predict progression free survival and overall survival in patients with relapsed/recurrent advanced ovarian cancer. *Gynecol. Oncol.* 122, 567–572.

Preza, C., King, S., Dragomir, N., and Cogswell, C. (2011). "Phase imaging microscopy: beyond dark-field, phase contrast, and differential interference contrast microscopy," in *Handbook of Biomedical Optics*, ed. D. Boas, C. Pitris, and N. Ramanujam (New York: Taylor and Francis Books), 483–517.

Rajadhyaksha, M., Gonzalez, S., Zavislan, J. M., and Anderson, R. R. (1999). In vivo confocal scanning laser microscopy of human skin II: advances in instrumentation and comparison with histology. *J. Invest. Dermatol.* 113, 293–303.

Rosenberg, R., Gertler, R., Friederichs, J., Fuehrer, K., Dahm, M., Phelps, R., Thorban, S., Nekarda, H., and Siewert, J. R. (2002). Comparison of two density gradient centrifugation systems for the enrichment of disseminated tumor cells in blood. *Cytometry* 49, 150–158.

Scher, H. I., Jia, X., de Bono, J. S., Fleisher, M., Pienta, K. J., Raghavan, D., and Heller, G. (2009). Circulating tumor cells as prognostic markers in progressive, castration-resistant prostate cancer: a reanalysis of IMMC38 trial data. *Lancet Oncol.* 10, 233–239.

Urban, N., Thorpe, J. D., Bergan, L., Kampani, A. V., Scholler, N., O'Briant, K. C., Anderson, G. L., Cramer, D. W., Berg, C. D., McIntosh, M. W., Hartge, P., and Drescher, C. W. (2011). Potential role of HE4 in multimodal screening for epithelial ovarian cancer. *J. Natl. Cancer Inst.* 103, 1630–1634.

Vona, G., Sabile, A., Louha, M., Sitruk, V., Romana, S., Schütze, K., Capron, F., Franco, D., Pazzagli, M., Vekemans, M., Lacour, B., Bréchot, C., and Paterlini-Bréchot, P. (2000). Isolation by size of epithelial tumor cells: a new method for the immunomorphological and molecular characterization of circulating tumor cells. *Am. J. Pathol.* 156, 57–63.

Conflict of Interest Statement: The HD-CTC technology has been licensed to Epic Sciences. Authors of this manuscript have ownership in Epic Sciences.

Received: 14 May 2012; paper pending published: 21 May 2012; accepted: 26 June 2012; published online: 18 July 2012. Citation: Phillips KG, Velasco CR, Li J, Kolatkar A, Luttgen M, Bethel K, Duggan B, Kuhn P and McCarty OJT (2012) Optical quantification of cellular mass, volume, and density of circulating tumor cells identified in an ovarian cancer patient. Front. Oncol. ***2****:72. doi: 10.3389/fonc.2012.00072*
This article was submitted to Frontiers in Cancer Molecular Targets and Therapeutics, a specialty of Frontiers in Oncology.